Dark matter and detectors

Laura Baudis
University of Zurich

EDIT school
Frascati, October 27, 2015

Content

- **Overview: dark matter and candidates**
- **Direct WIMP detection**
  - Principles, input from astrophysics, particle physics, nuclear physics
  - Expected signatures and rates in a terrestrial detector
  - Backgrounds
  - Overview of experimental techniques
- **Cryogenic experiments at mK temperatures**
  - Principles of phonon mediated detectors, temperature measurement
  - Current and future experiments
- **Liquid Noble Element Experiments**
  - Principles, the scintillation and ionization process in noble liquids
  - Challenges for dark matter detectors
  - The single and double phase detector concept
  - Current and future experiments
- **Conclusions**

Some (very brief) history

- **1922:** J.C. Kapteyn coined the name *'dark matter'*, in studies of the stellar motion in our galaxy *(he found that no dark matter is needed in the solar neighbourhood)*

- **1932:** J. Oort suggested that there would be more dark than visible matter in the vicinity of the Sun *(later the result turned out to be wrong)*

- **1933: F. Zwicky found *'dunkle Materie'* in the Coma cluster *(the redshift of galaxies were much larger than the escape velocity due to luminous matter alone)***

- **1970s:** V.C. Rubin & W. Ford: flat optical rotation curves of spiral galaxies, 1978: Bosma, radio

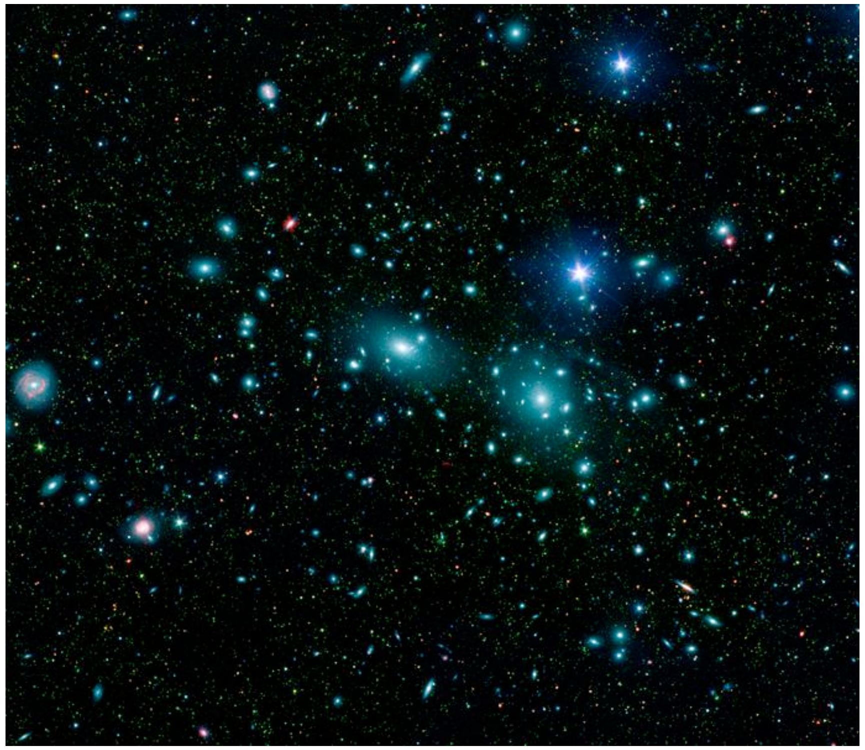

from "Fritz Zwicky, Astrophysiker", Verlag NZZ

Our Universe today: apparently consistent picture from an impressive number of observations

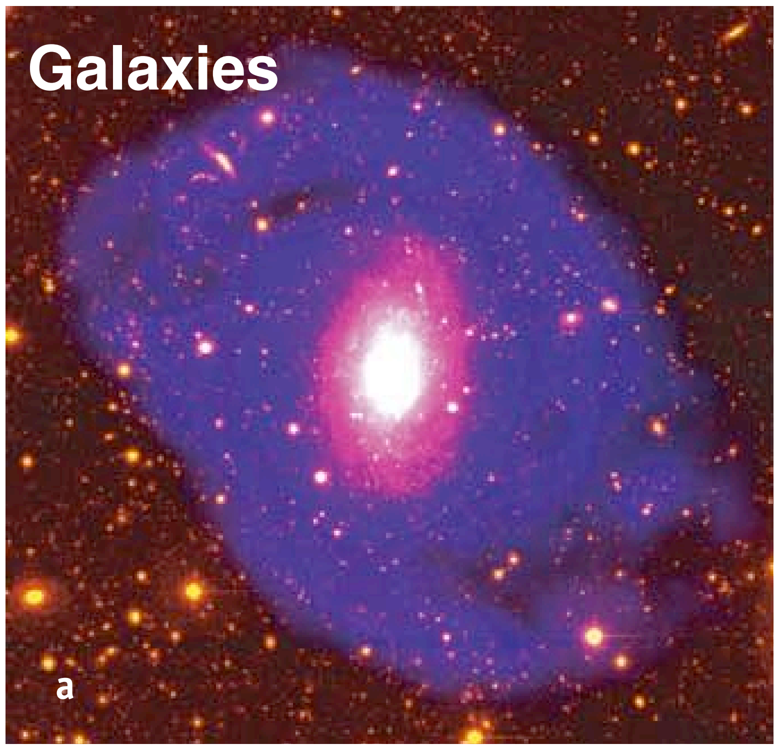

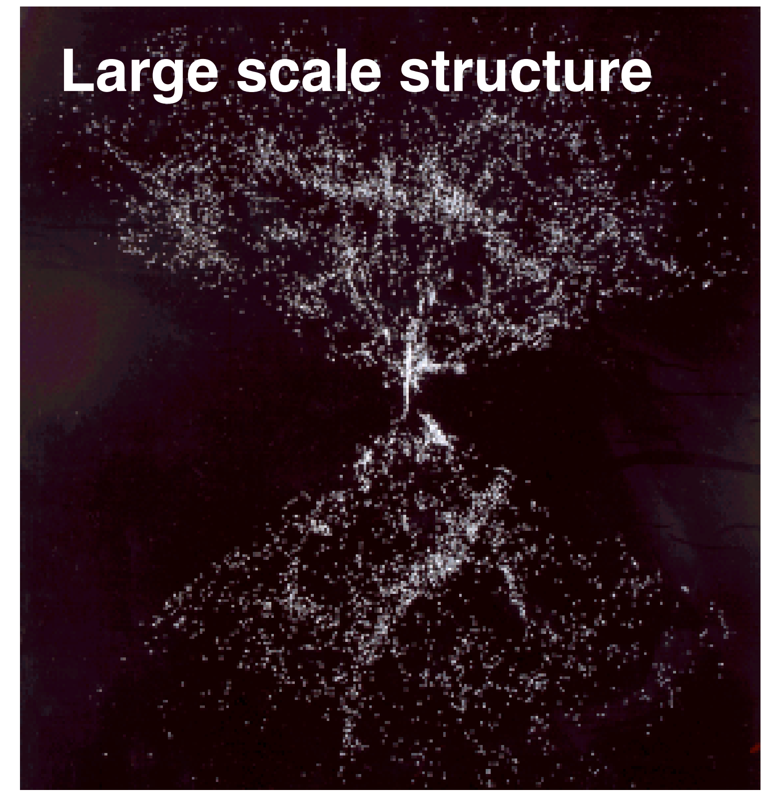

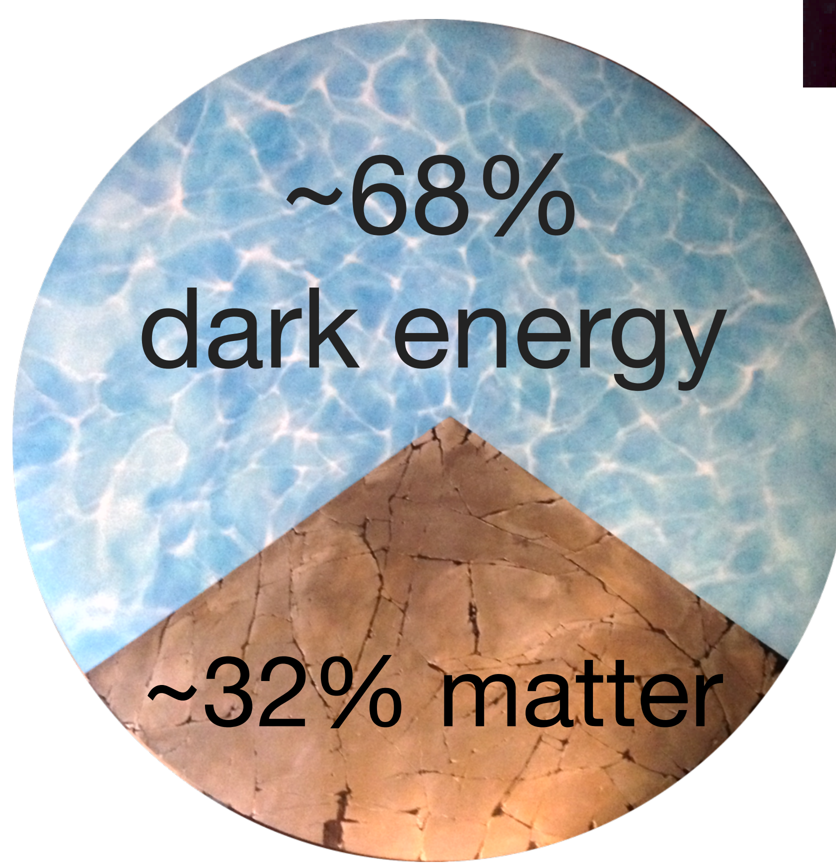

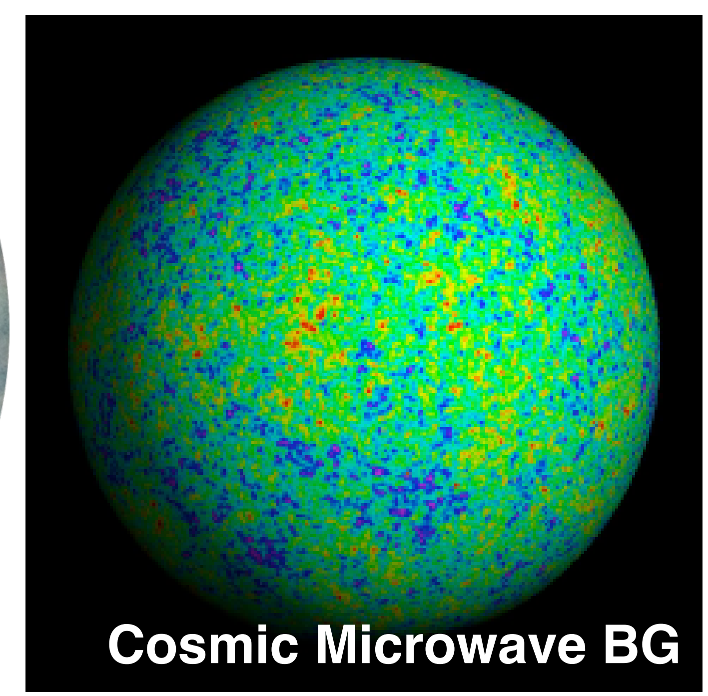

The dark matter puzzle

The dark matter puzzle remains *fundamental*: dark matter leads to the formation of structure and galaxies in our universe

We have a standard model of CDM, from ‘precision cosmology’ (CMB, LSS): however, *measurement ≠ understanding*

For ~85% of matter in the universe is of unknown nature

Large scale distribution of dark matter, probed through gravitational lensing

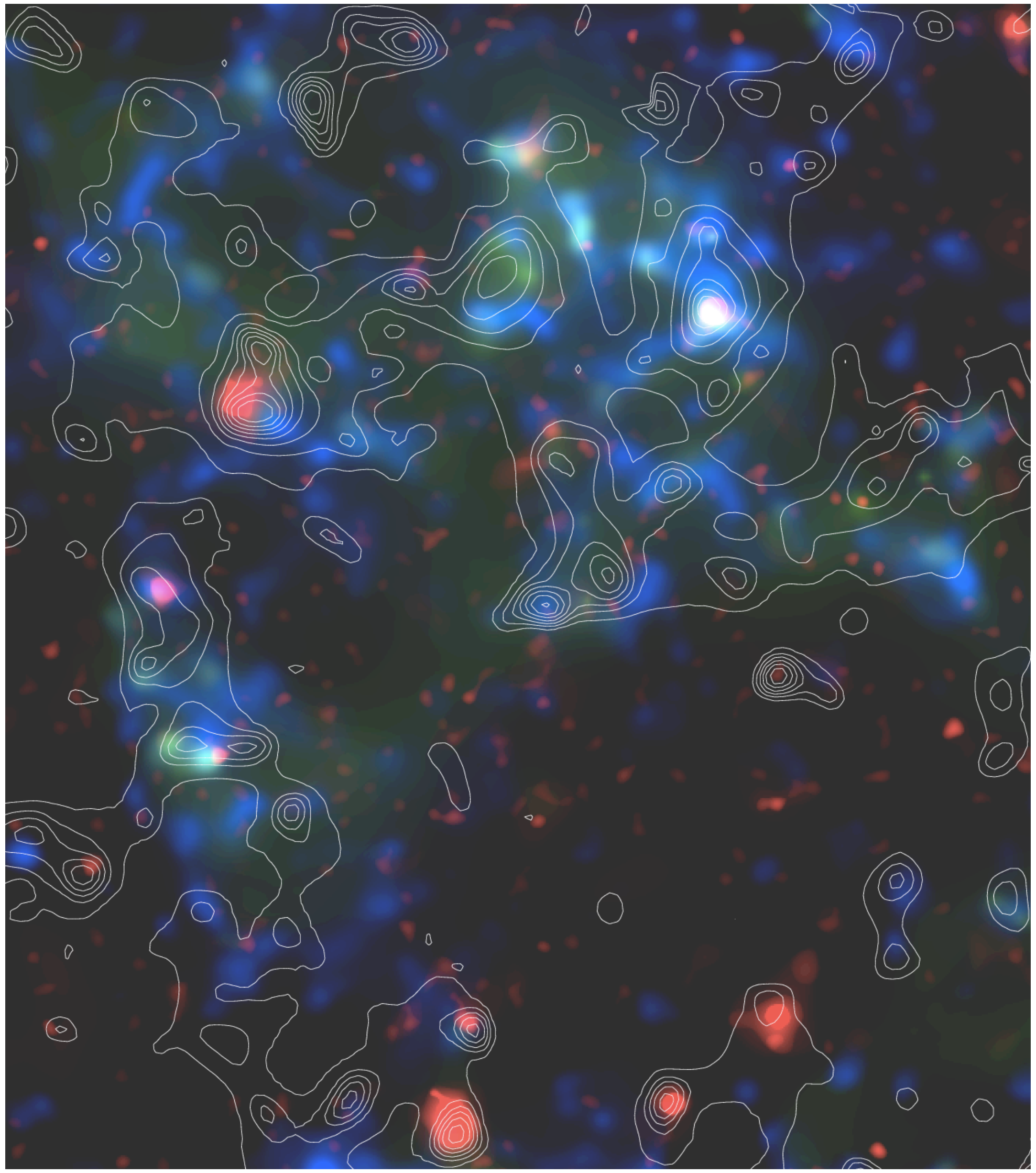

HST COSMOS survey; Nature 445 (2007), 268

What do we know about the dark matter?

So far, we mostly have “negative” information

Constraints from astrophysics and searches for new particles:

No colour charge

No electric charge

No strong self-interaction

Stable, or very long-lived

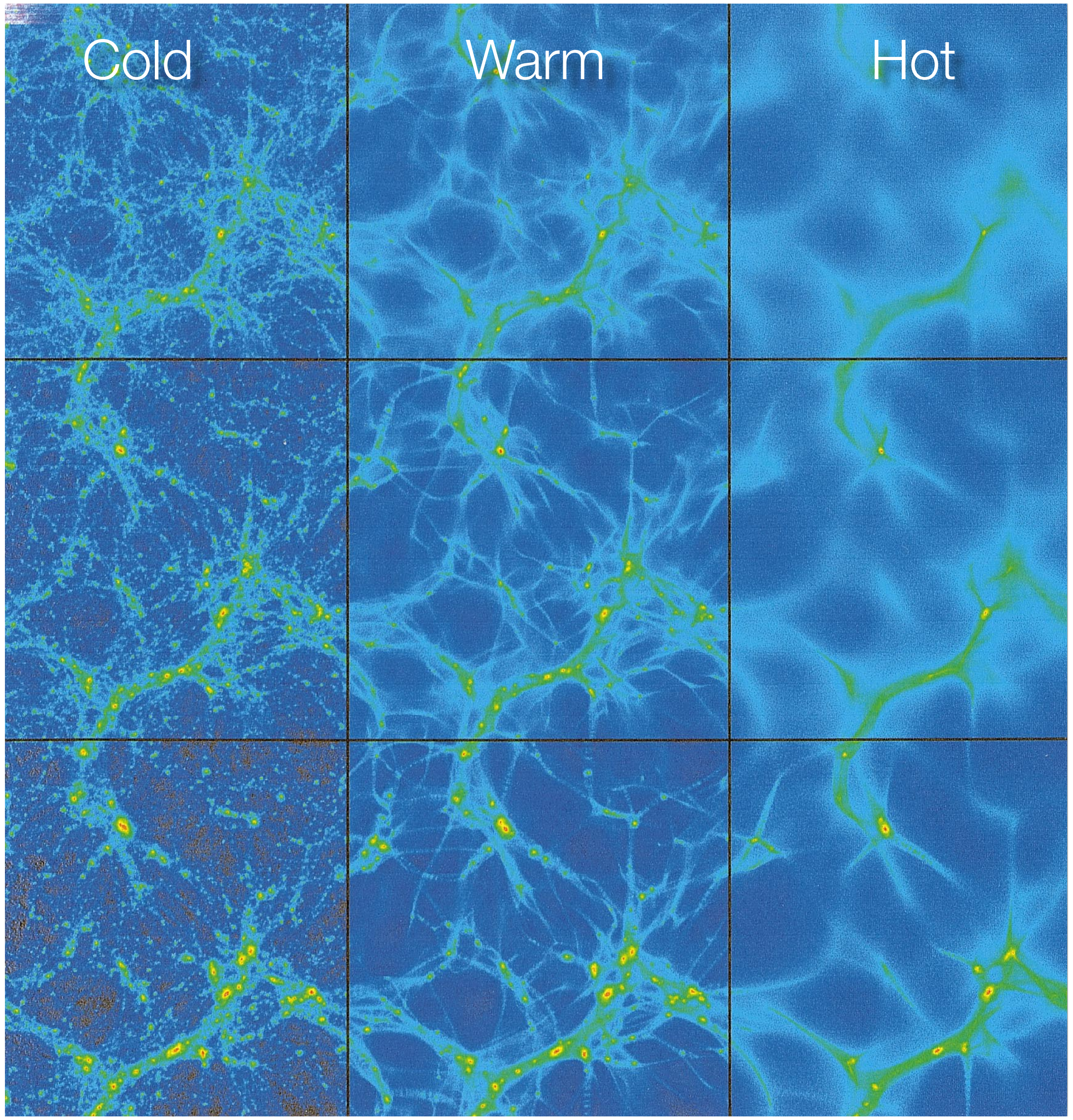

Probing dark matter through gravity

Parameter space for searches

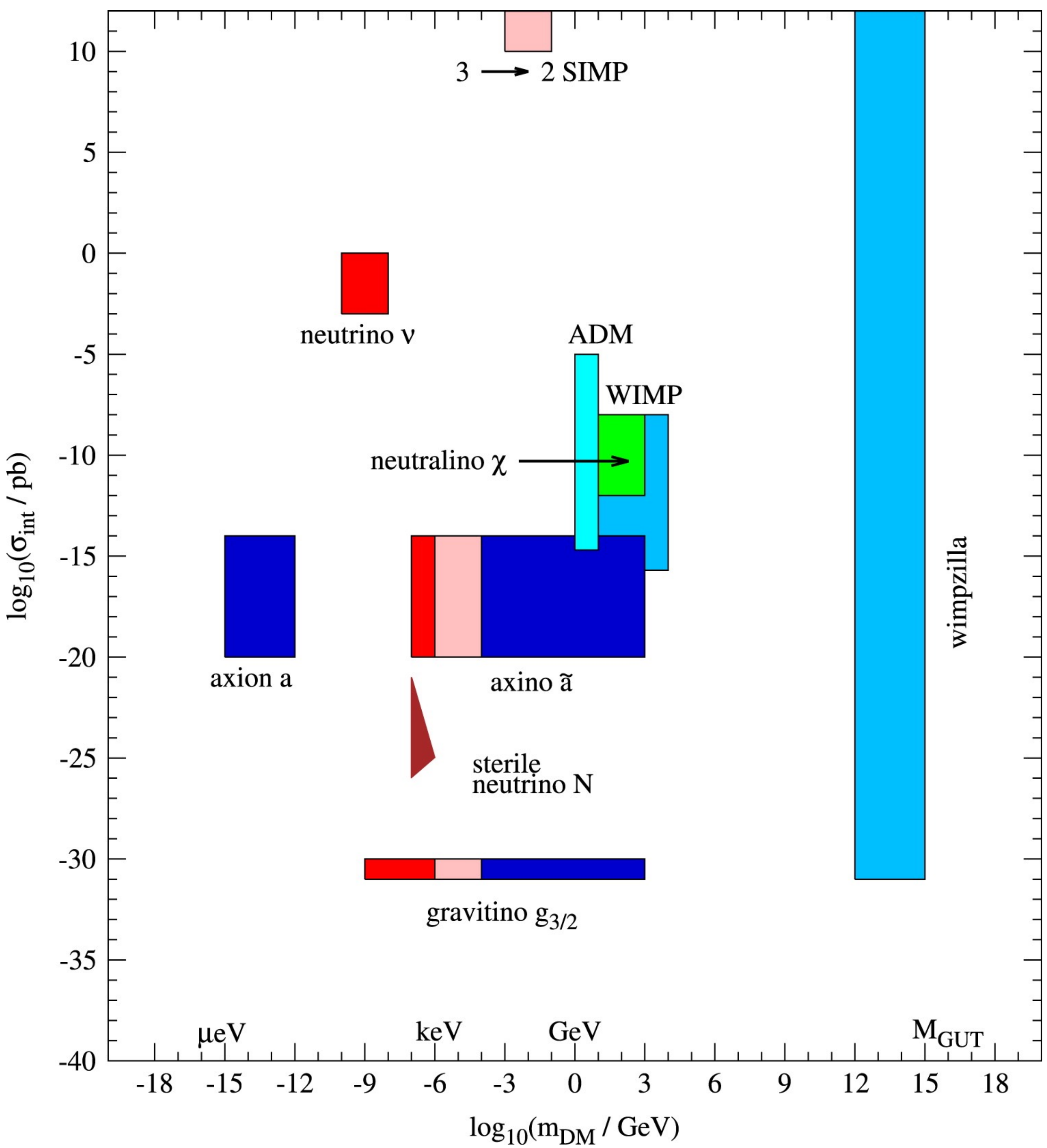

- **Masses & interaction cross sections span an enormous range**
- Most dark matter experiments optimised to search for WIMPs
- However also searches for axions, ALPs, SuperWIMPs, etc

H. Baer et al., Phys. Rept. 555, 2014

Parameter space for searches

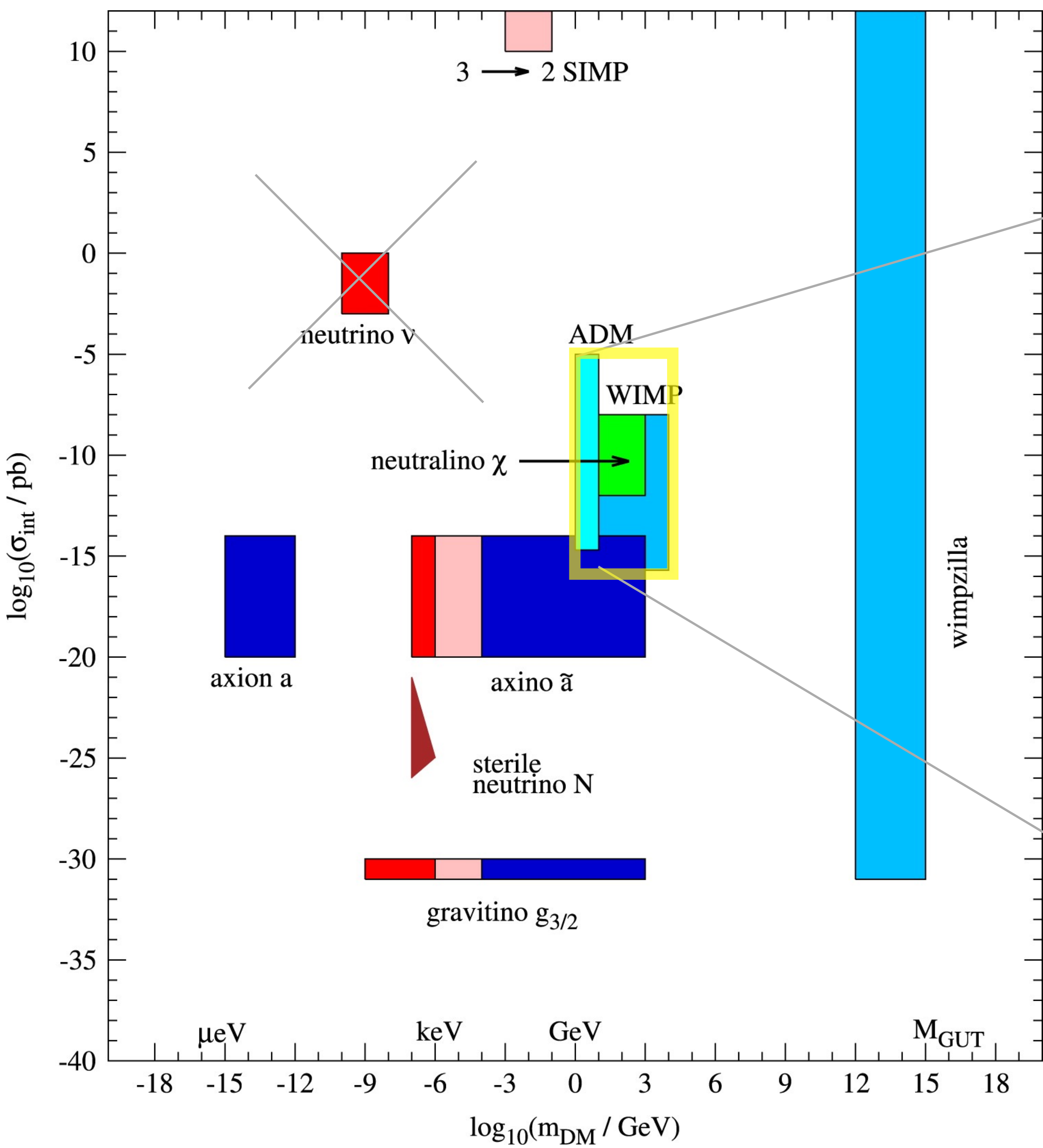

WIMP direct searches

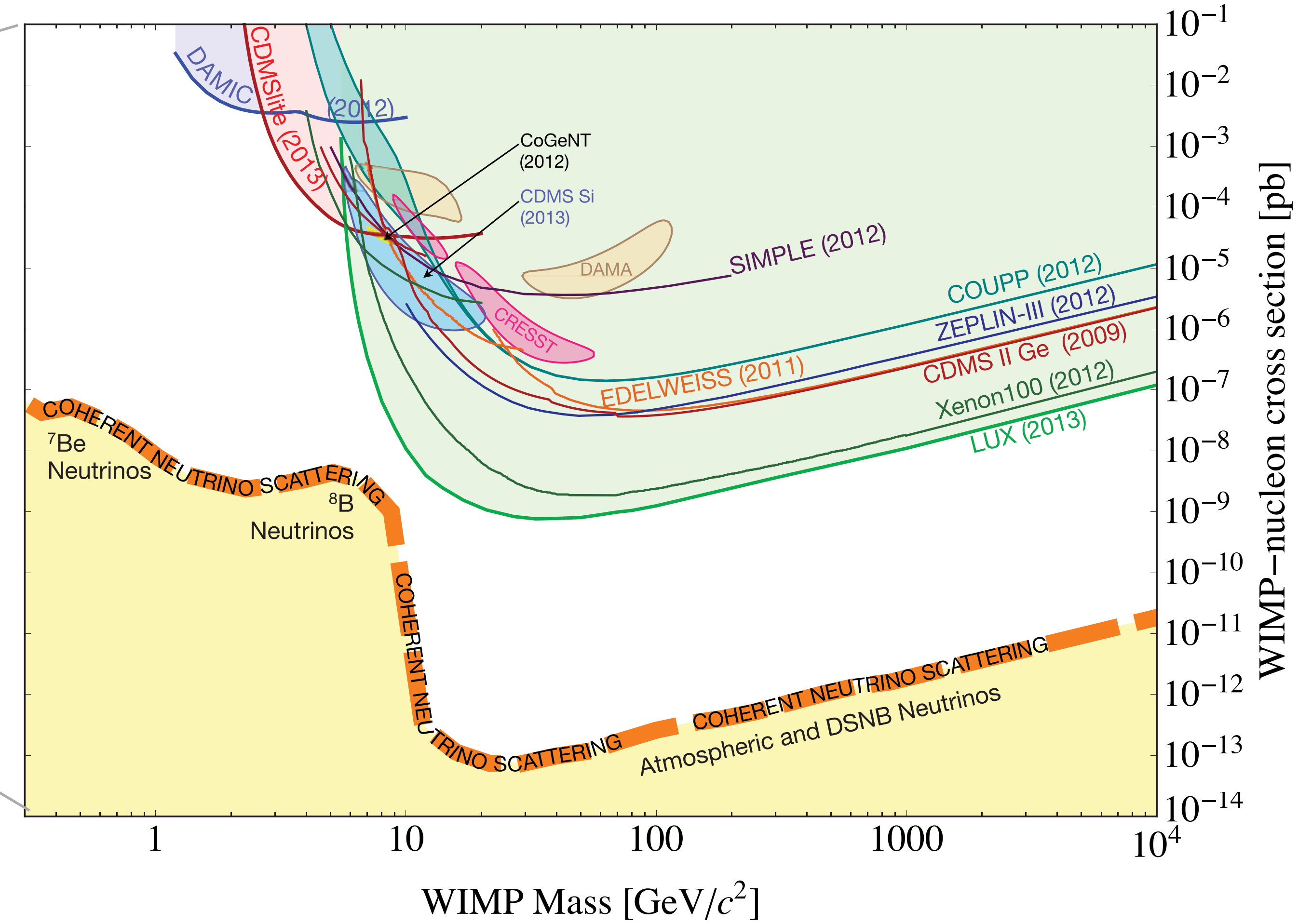

H. Baer et al., Phys. Rept. 555, 2014

Parameter space for searches

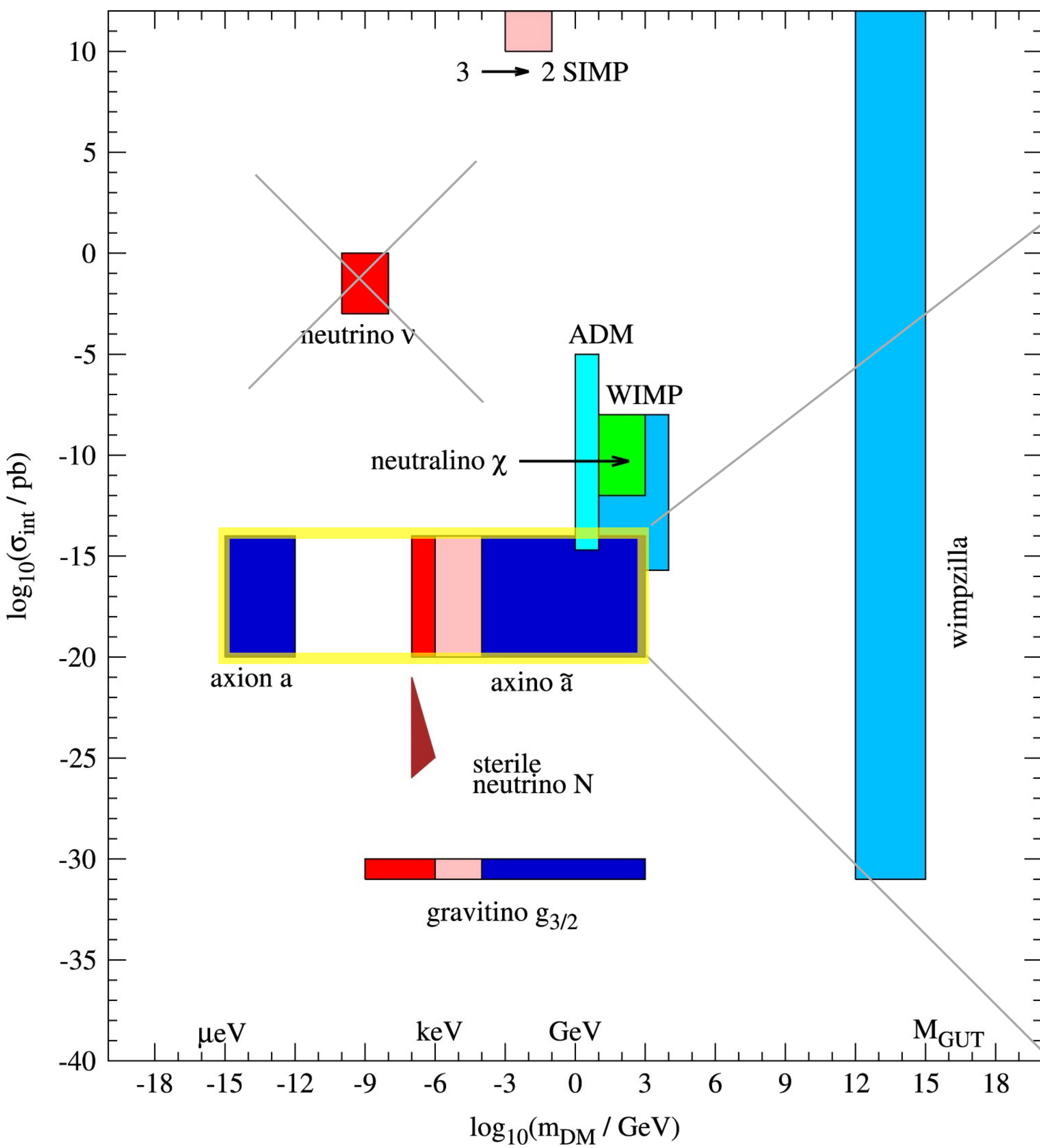

H. Baer et al., Phys. Rept. 555, 2014

Axion searches

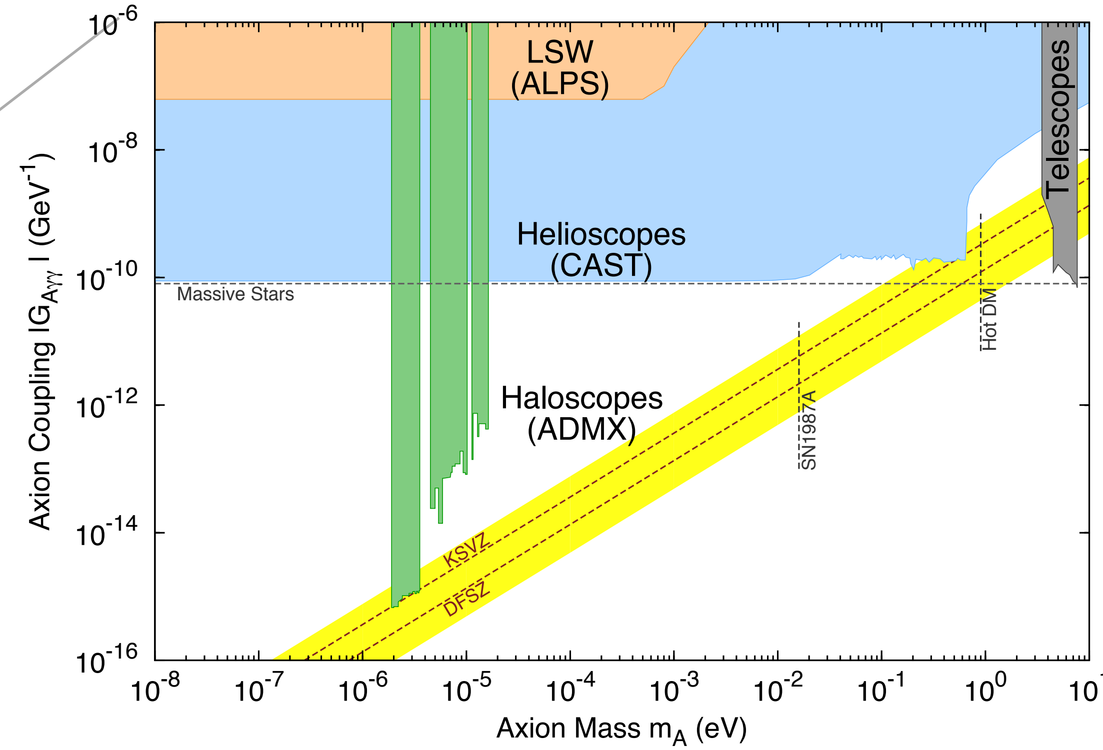

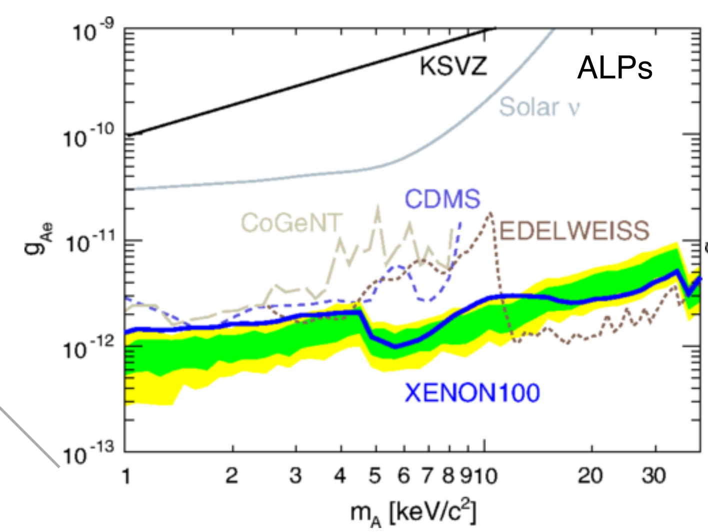

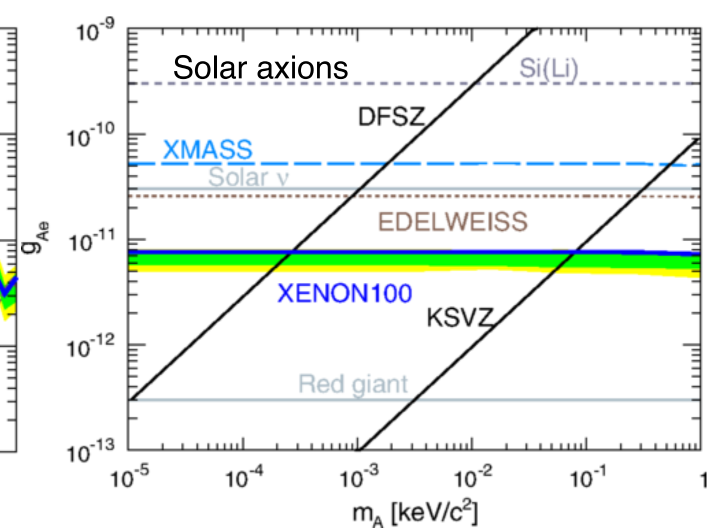

XENON, Phys. Rev. D 90, 062009 (2014)

How to detect Weakly Interacting Massive Particles

Direct detection

nuclear recoils from elastic scattering

dependance on A, J; annual modulation, directionality

local density and v-distribution

Indirect detection

high-energy neutrinos, gammas, charged CRs

look at over-dense regions in the sky

astrophysics backgrounds difficult

Accelerator searches

missing E_T, mono-‘objects’, etc

can it establish that the new particle is the DM?

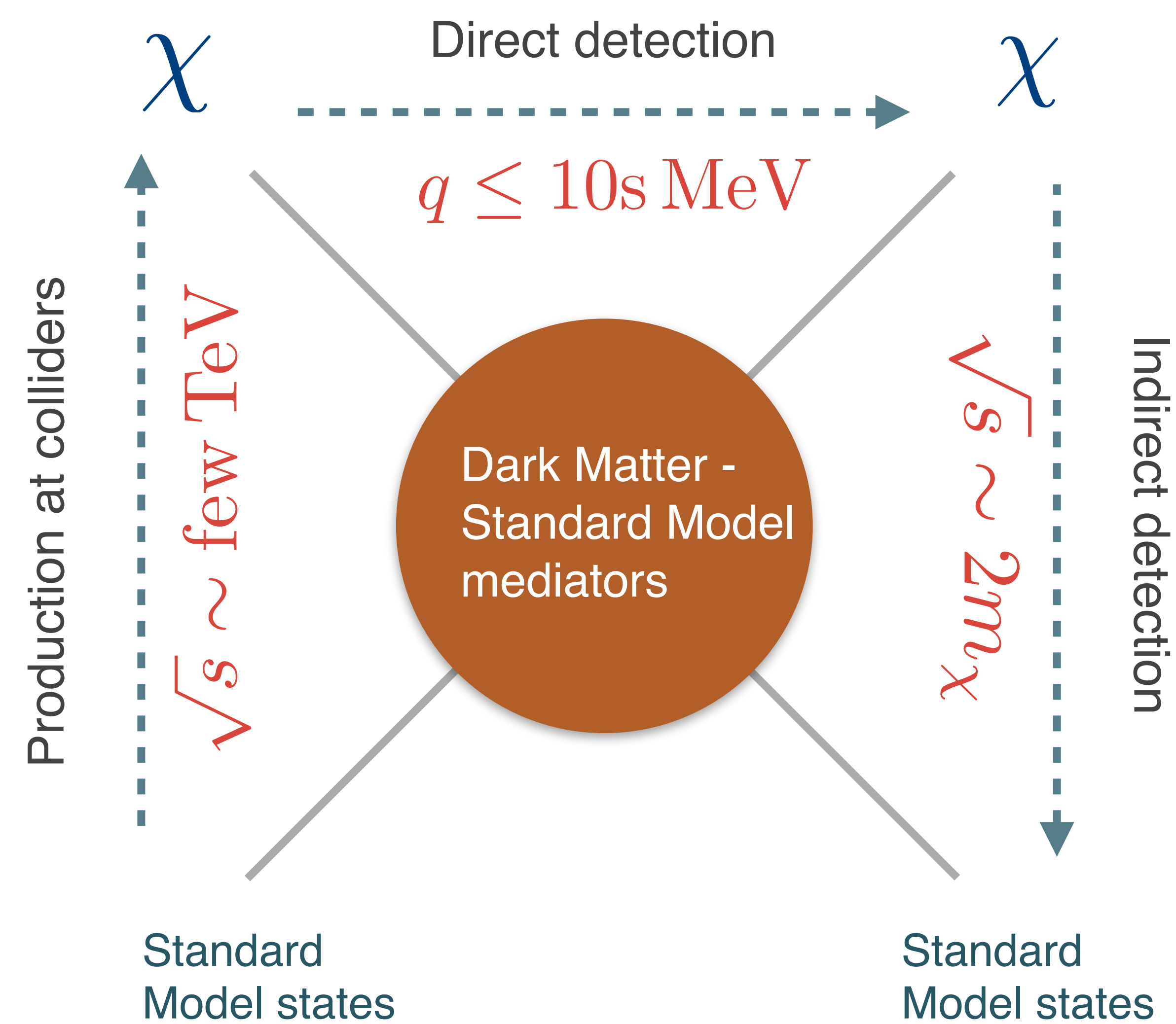

Direct detection

Collisions of invisibles particles with atomic nuclei

=> E_{vis} (q ~ tens of MeV):

$v/c \sim 0.75 \times 10^{-3}$

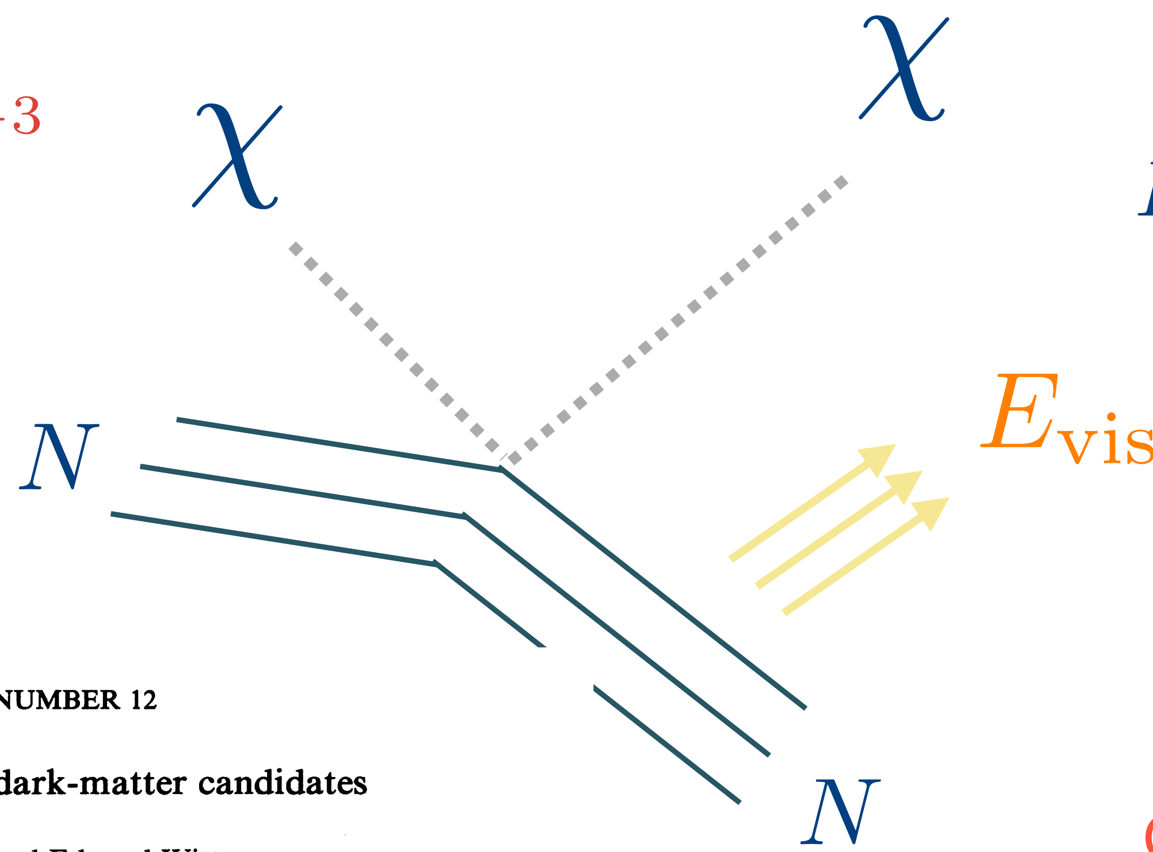

$$E_R = \frac{q^2}{2m_N} < 30\,\mathrm{keV}$$

Observable: kinetic energy of the recoiling nucleus

REVIEW D VOLUME 31, NUMBER 12

Detectability of certain dark-matter candidates

Mark W. Goodman and Edward Witten
Joseph Henry Laboratories, Princeton University, Princeton, New Jersey 08544
(Received 7 January 1985)

We consider the possibility that the neutral-current neutrino detector recently proposed by Drukier and Stodolsky could be used to detect some possible candidates for the dark matter in galactic halos. This may be feasible if the galactic halos are made of particles with coherent weak interactions and masses $1-10^6$ GeV; particles with spin-dependent interactions of typical weak strength and masses $1-10^2$ GeV; or strongly interacting particles of masses $1-10^{13}$ GeV.

What to expect in a terrestrial detector?

$$\frac{dR}{dE_R} = N_N \frac{\rho_0}{m_W} \int_{\sqrt{(m_N E_{th})/(2\mu^2)}}^{v_{max}} dv f(v) v \frac{d\sigma}{dE_R}$$

Detector physics

N_N, E_{th}

Particle/nuclear physics

$m_W, d\sigma/dE_R$

Astrophysics

$\rho_0, f(v)$

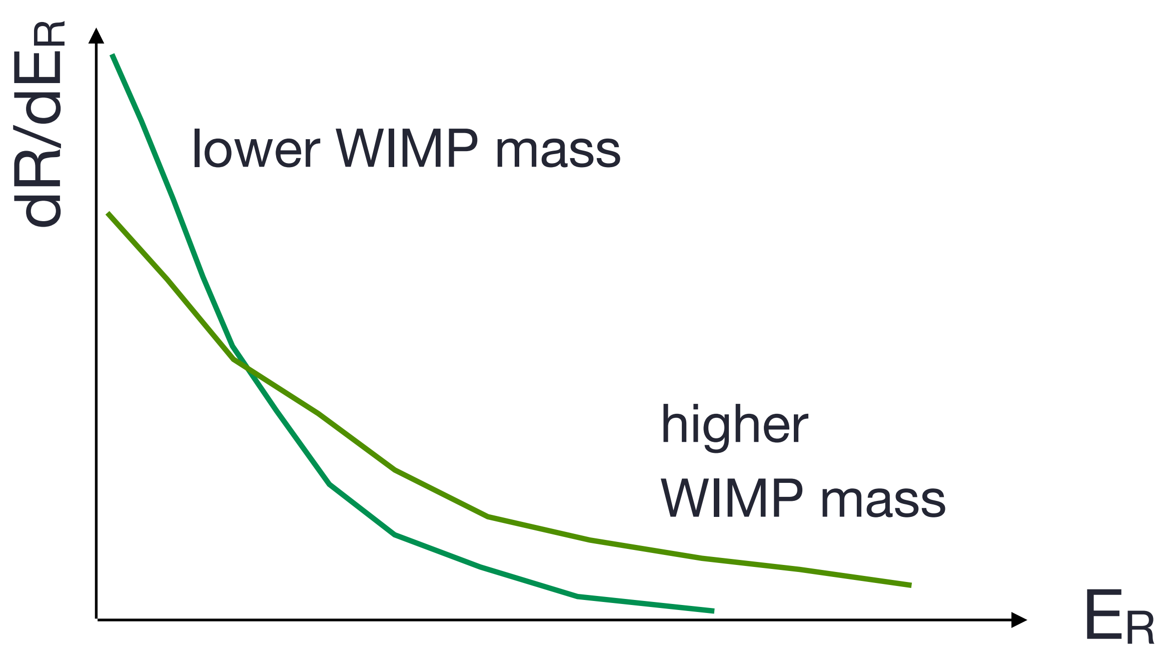

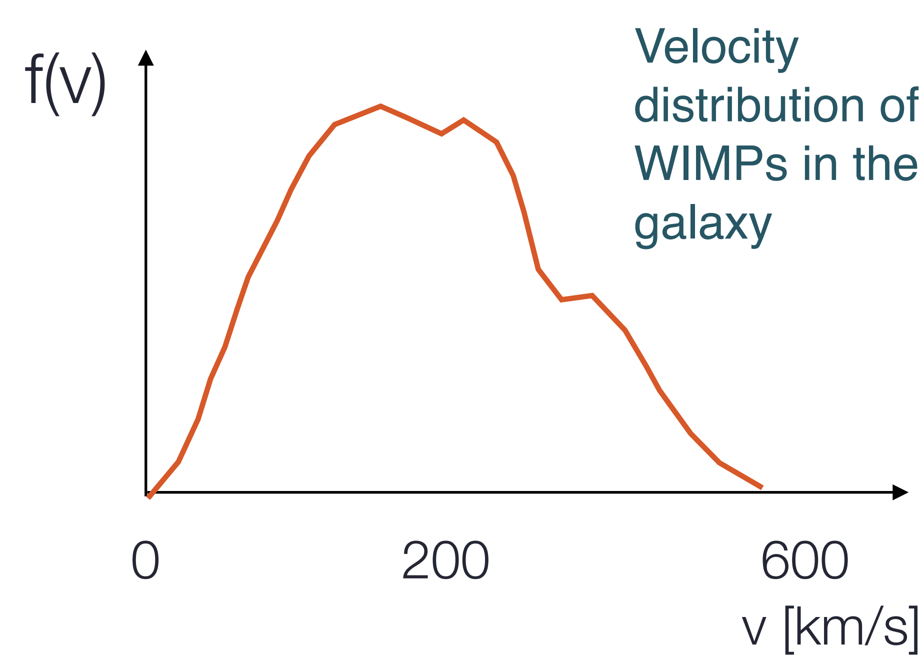

Astrophysics

Local density (at R_0 ~ 8 kpc)

local measures use the vertical kinematics of stars near the Sun as ‘tracers’ (smaller error bars, but stronger assumptions about the halo shape)

global measures extrapolate the density from the rotation curve (larger errors, but fewer assumptions)

Density map of the dark matter halo
rho = [0.1, 0.3, 1.0, 3.0] GeV cm^{-3}

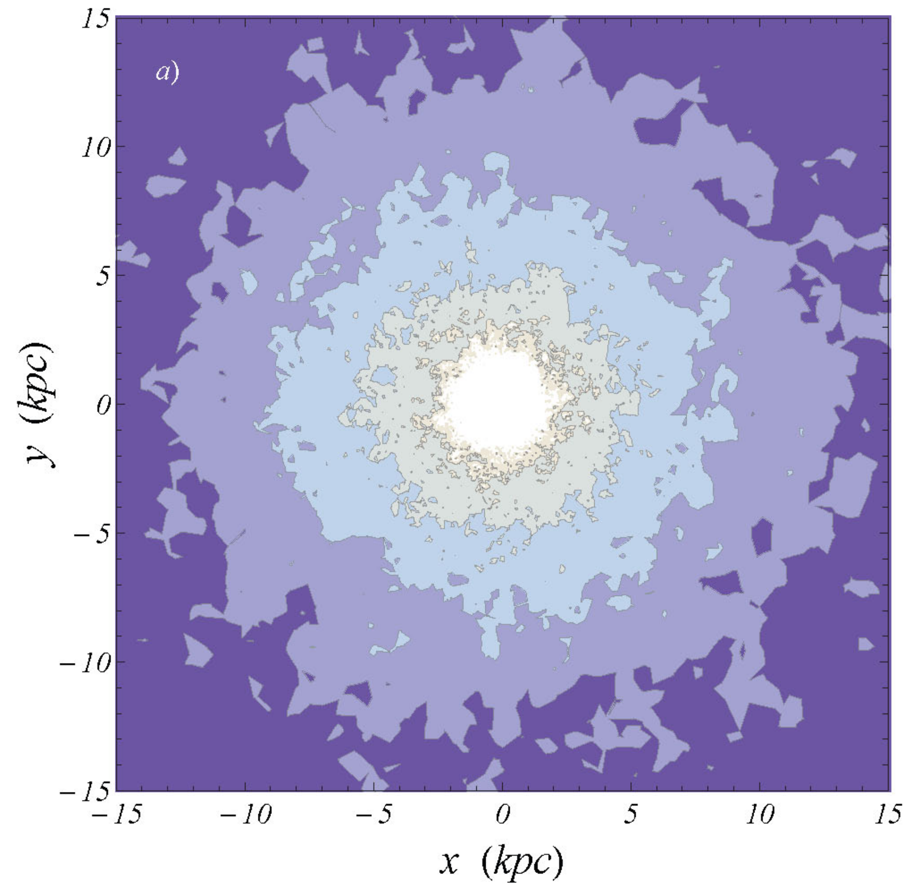

High-resolution cosmological simulation with baryons: F.S. Ling et al, JCAP02 (2010) 012

$$\rho(R_0) = 0.2 - 0.56\,\mathrm{GeV\,cm^{-3}} = 0.005 - 0.015\,\mathrm{M_\odot\,pc^{-3}}$$

J. Read, Journal of Phys. G41 (2014) 063101

=> **WIMP flux on Earth: ~10^5 cm^{-2}s^{-1}** (M_W=100 GeV, for 0.3 GeV cm^{-3})

Particle physics

- Use *effective operators* to describe WIMP-quark interactions
- Example: vector mediator

$$\mathcal{L}_\chi^{\text{eff}} = \frac{1}{\Lambda^2}\bar{\chi}\gamma_\mu\chi\bar{q}\gamma^\mu q$$

- The effective operator arises from "integrating out" the mediator with mass M and couplings g_q and g_χ to the quark and the WIMP

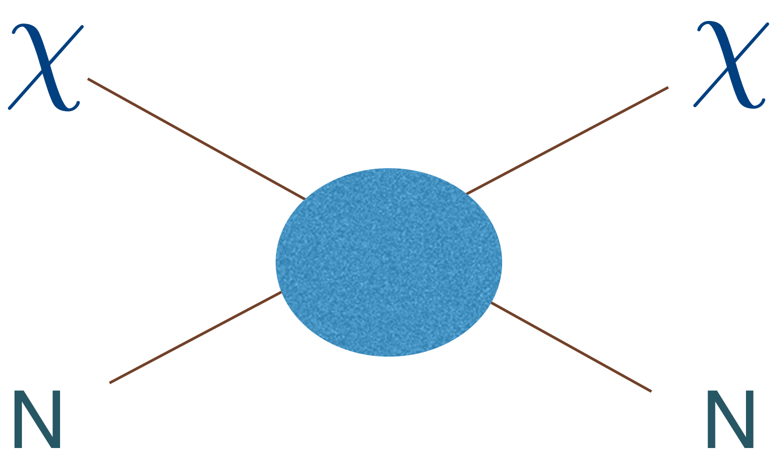

$$\Lambda = \frac{M}{\sqrt{g_q g_\chi}} \quad \Rightarrow \sigma_{\text{tot}} \propto \Lambda^{-4}$$

contact interaction scale

Example cross sections

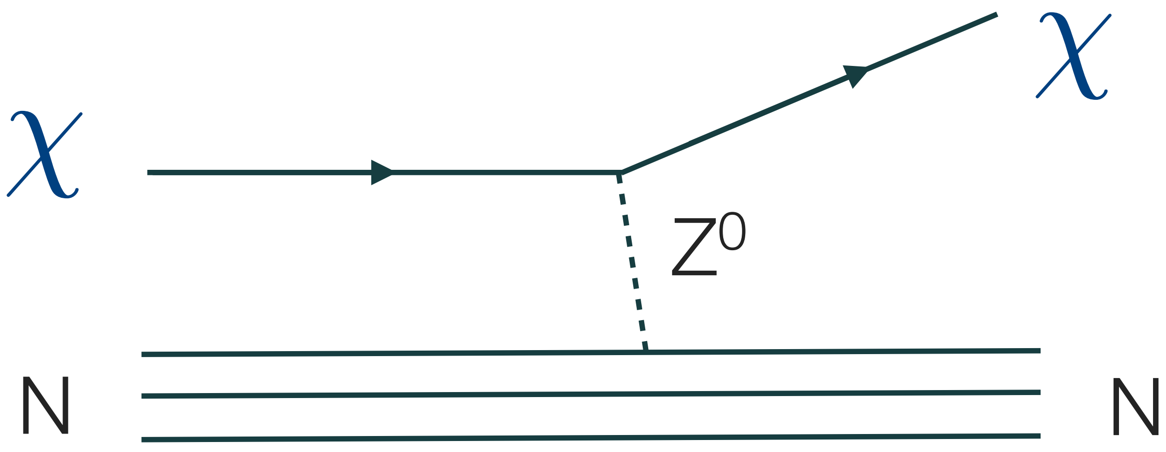

$$\sigma_0 \sim 10^{-39}\mathrm{cm}^2$$

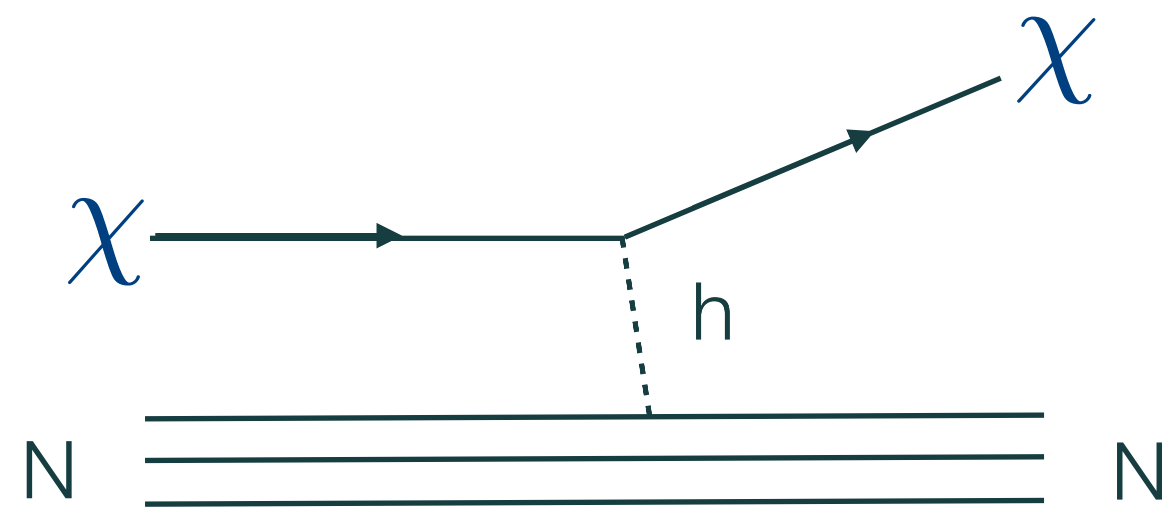

$$\sigma_0 \sim 10^{-44} - 10^{-47}\,\mathrm{cm}^2$$

Scattering cross section on nuclei

- In general, interactions leading to WIMP-nucleus scattering are parameterized as:
  - **scalar interactions** (coupling to WIMP mass, from scalar, vector, tensor part of L)

$$\sigma_{SI} \sim \frac{\mu^2}{m_\chi^2}[Z f_p + (A - Z) f_n]^2$$

f_p, f_n: scalar 4-fermion couplings to p and n

=> nuclei with large A favourable (but nuclear form factor corrections)

  - **spin-spin interactions** (coupling to the nuclear spin J_N, from axial-vector part of L)

$$\sigma_{SD} \sim \mu^2 \frac{J_N + 1}{J_N}(a_p \langle S_p \rangle + a_n \langle S_n \rangle)^2$$

a_p, a_n: effective couplings to p and n; $\langle S_p \rangle$ and $\langle S_n \rangle$ expectation values of the p and n spins within the nucleus

=> nuclei with non-zero angular momentum (corrections due to spin structure functions)

Form factor corrections

- With the WIMP-nucleus speed being of the order of 100 km s^{-1}, the average momentum transfer

$$\langle p \rangle \simeq \mu \langle v \rangle$$

- will be in the range between 3 MeV/c - 30 MeV/c for WIMP and nucleus masses in the range 10 GeV/c^2 - 100 GeV/c^2. Thus the elastic scattering occurs in the extreme non-relativistic limit and the scattering will be isotropic in the center of mass frame

- The de Broglie wavelength corresponding to a momentum transfer of p = 10 MeV/c

$$\lambda = \frac{h}{p} \simeq 20\,\mathrm{fm} > r_0 A^{1/3}\mathrm{fm} = 1.25\,\mathrm{fm}\,A^{1/3}$$

- is larger than the size of most nuclei, thus the scattering amplitudes on individual nucleons will add coherently

- **coherence loss will be important for heavy nuclei and/or WIMPs, and WIMPs in the tail of the velocity distribution**

Form factor corrections: spin-independent

- Important for heavy WIMPs and/or nuclei and for WIMPs in the tail of the velocity distribution

$$\frac{d\sigma_{SI}}{dq^2} = \sigma_{0,SI} \times S_s(q)$$

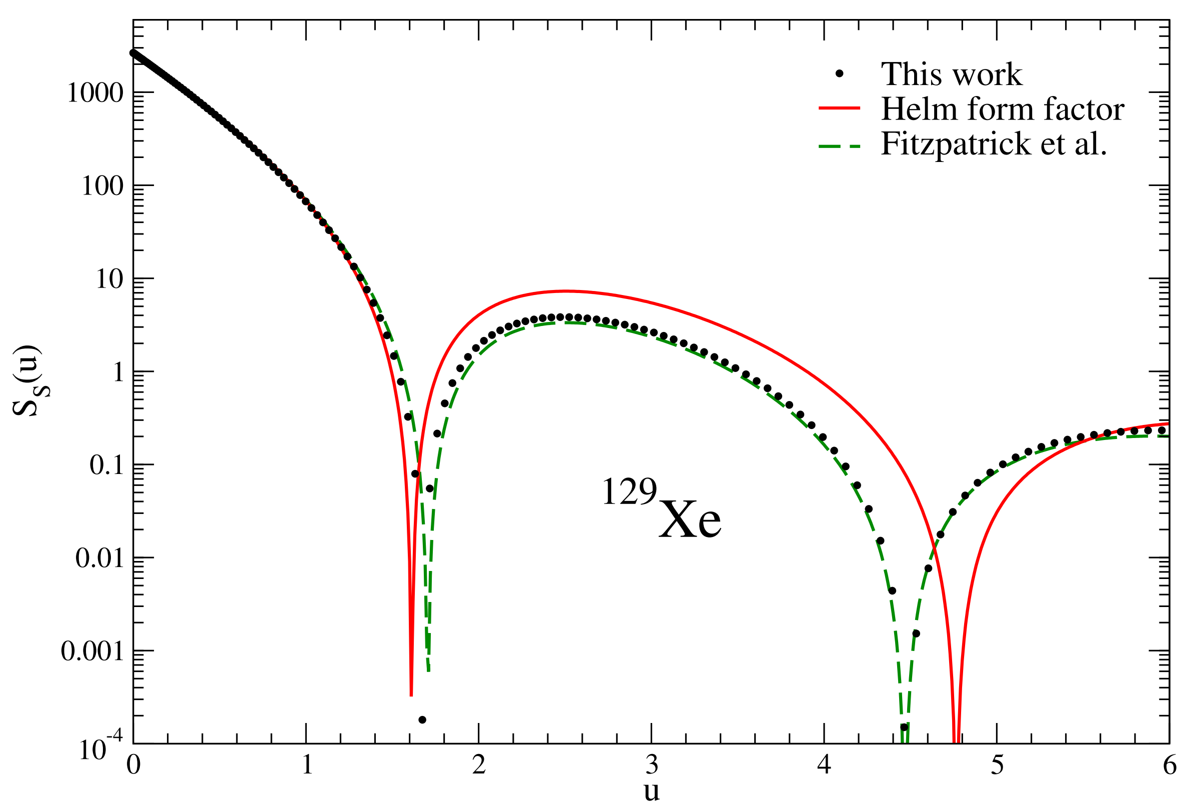

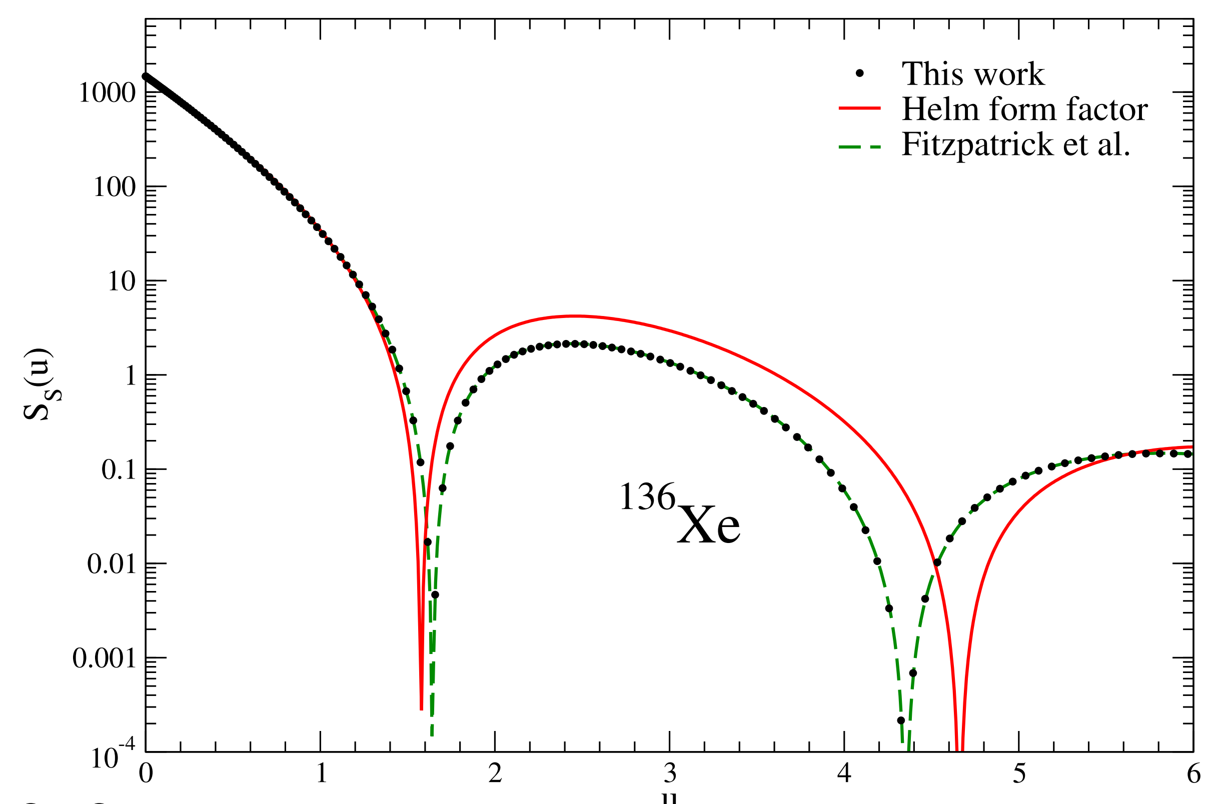

$$u = q^2 b^2 / 2$$

L. Vietze et al., Phys.Rev. D91 (2015) 4, 043520

Form factor corrections: spin-dependent

- WIMP-nucleus response (based on detailed nuclear structure calculations) especially important for spin-dependent interactions

$$\frac{d\sigma_{SD}}{dq^2} = \sigma_{0,SD} \times S_A(q)$$

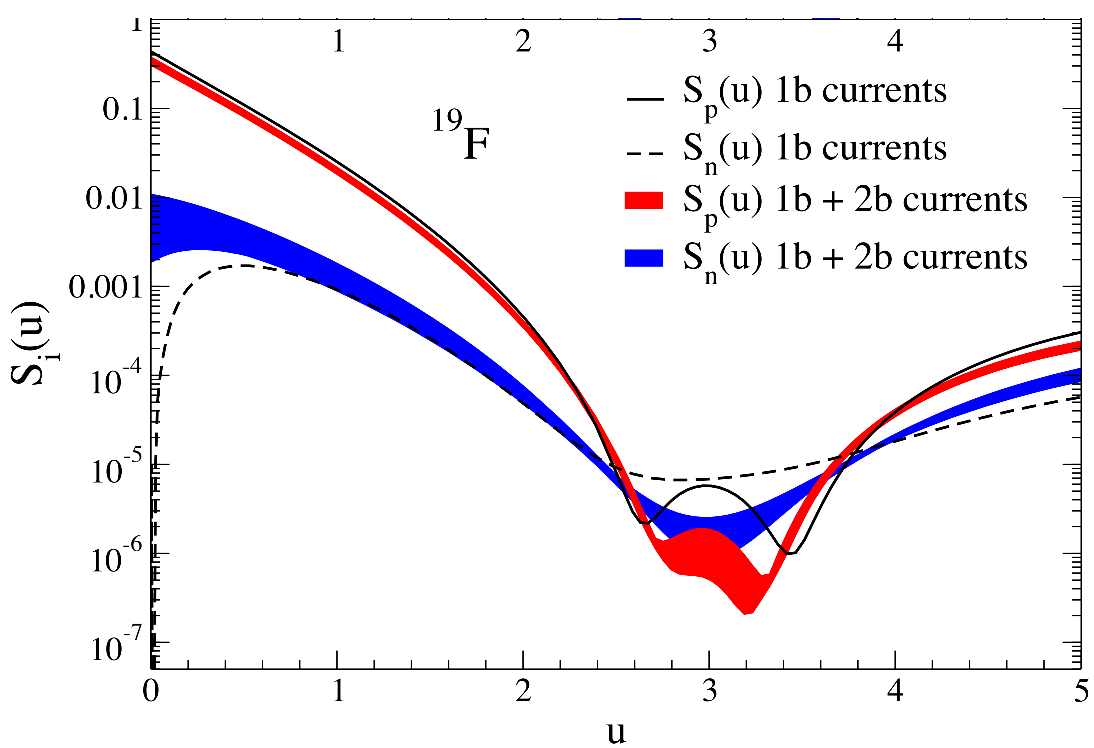

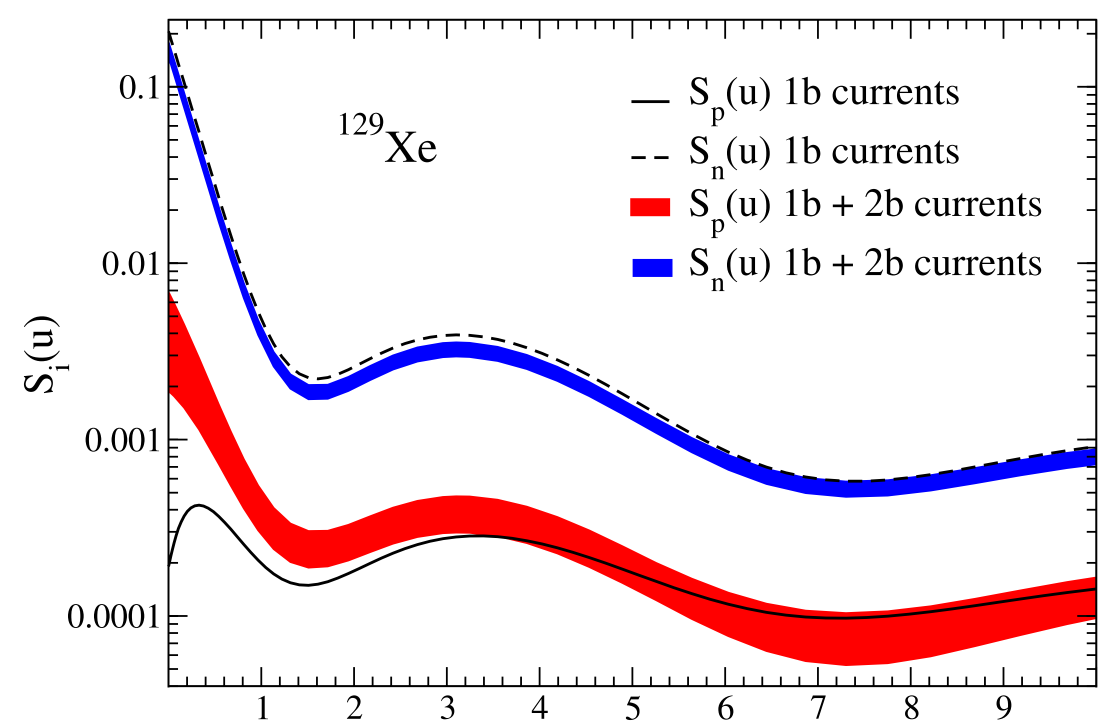

$$u = q^2 b^2 / 2$$

P. Klos et al., PRD 88 (2013)

Expected interaction rates

- For a typical WIMP mass of 100 GeV/c^2, the expected WIMP flux on Earth (for the 'standard local density' value) is:

$$\phi_\chi = \frac{\rho_\chi}{m_\chi} \times \langle v \rangle = 6.6 \times 10^4\,\mathrm{cm}^{-2}\mathrm{s}^{-1}$$

- This flux is sufficiently large that, even though WIMPs are weakly interacting, a small but potentially measurable fraction will elastically scatter off nuclei in an Earth-bound detector
- Direct dark matter detection experiments aim to detect WIMPs via nuclear recoils which are caused by WIMP-nucleus elastic scattering
- Assuming a scattering cross section of 10^{-38} cm^2, the expected rate (for a nucleus with atomic mass A = 100) would be:

$$R = \frac{N_A}{A} \times \phi_\chi \times \sigma \sim 0.13\,\mathrm{events\,kg^{-1}yr^{-1}}$$

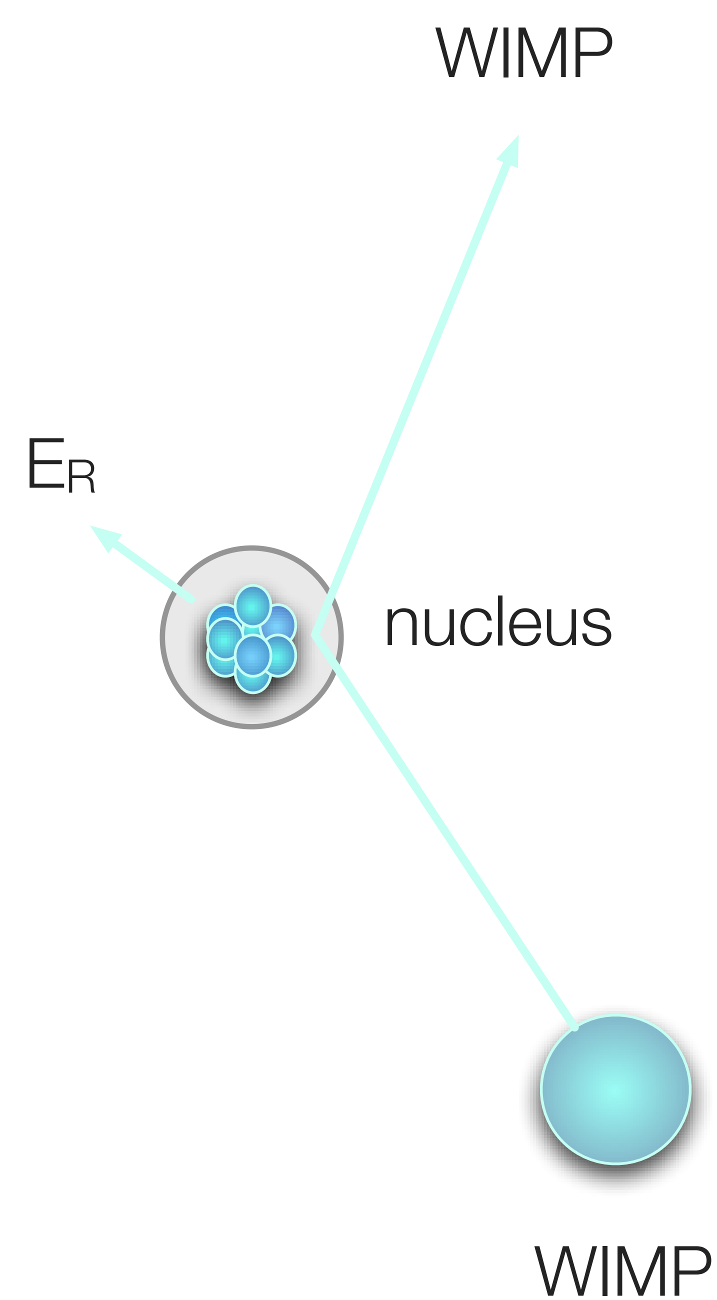

Expected interaction rates

$$R \sim 0.13\ \frac{\text{events}}{\text{kg year}}\left[\frac{A}{100}\times\frac{\sigma_{WN}}{10^{-38}\,\mathrm{cm}^2}\times\frac{\langle v\rangle}{220\,\mathrm{km\,s}^{-1}}\times\frac{\rho_0}{0.3\,\mathrm{GeV cm}^{-3}}\right]$$

$$v_{min} = \sqrt{\frac{m_N E_{th}}{2\mu^2}}$$

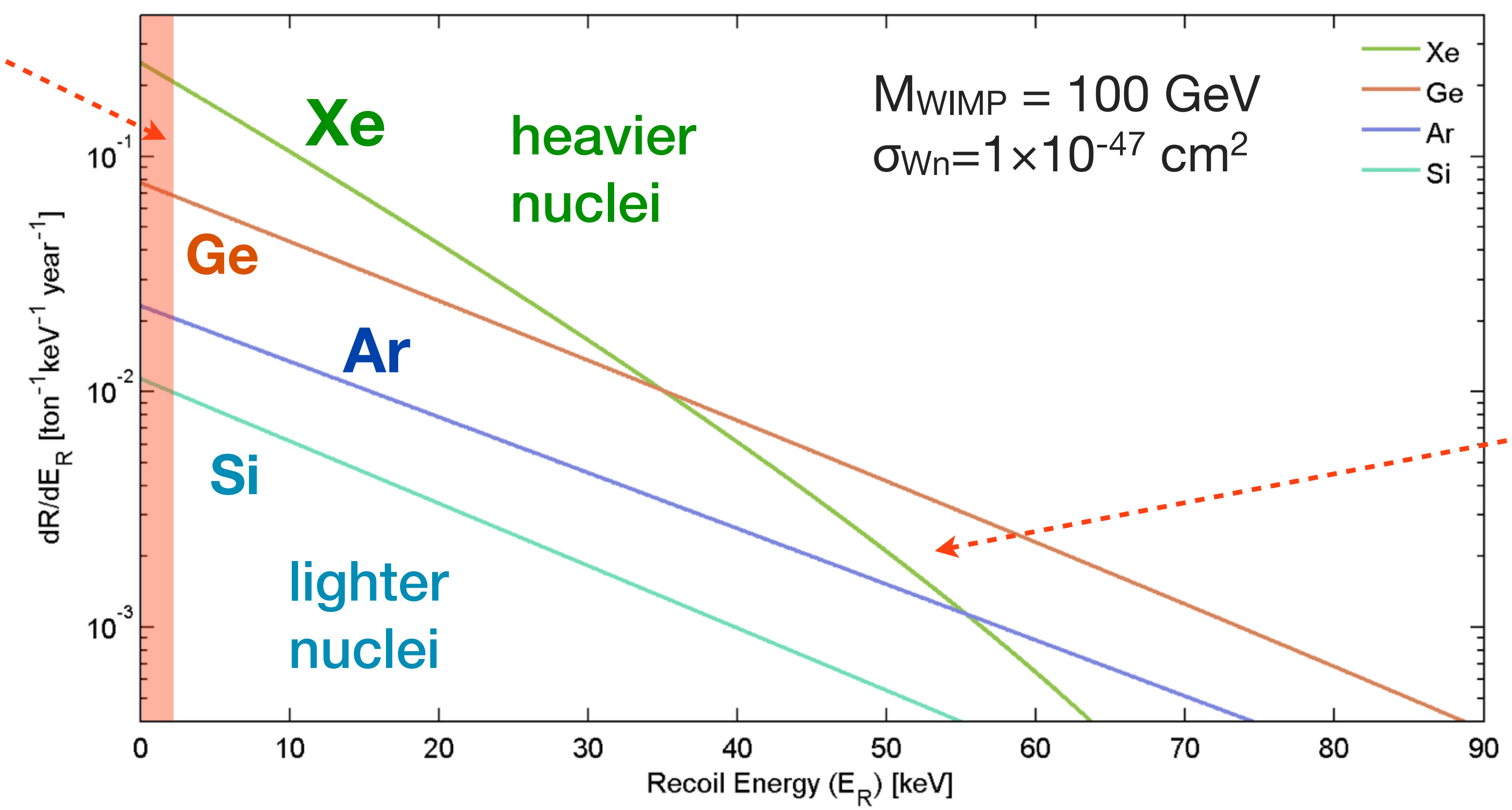

$F^2(E_R)$

Example: spectral dependance on the WIMP mass

- Recoil spectrum gets shifted to low energies for low WIMP masses
- One needs a light target and/or a low threshold to see low-mass WIMPs

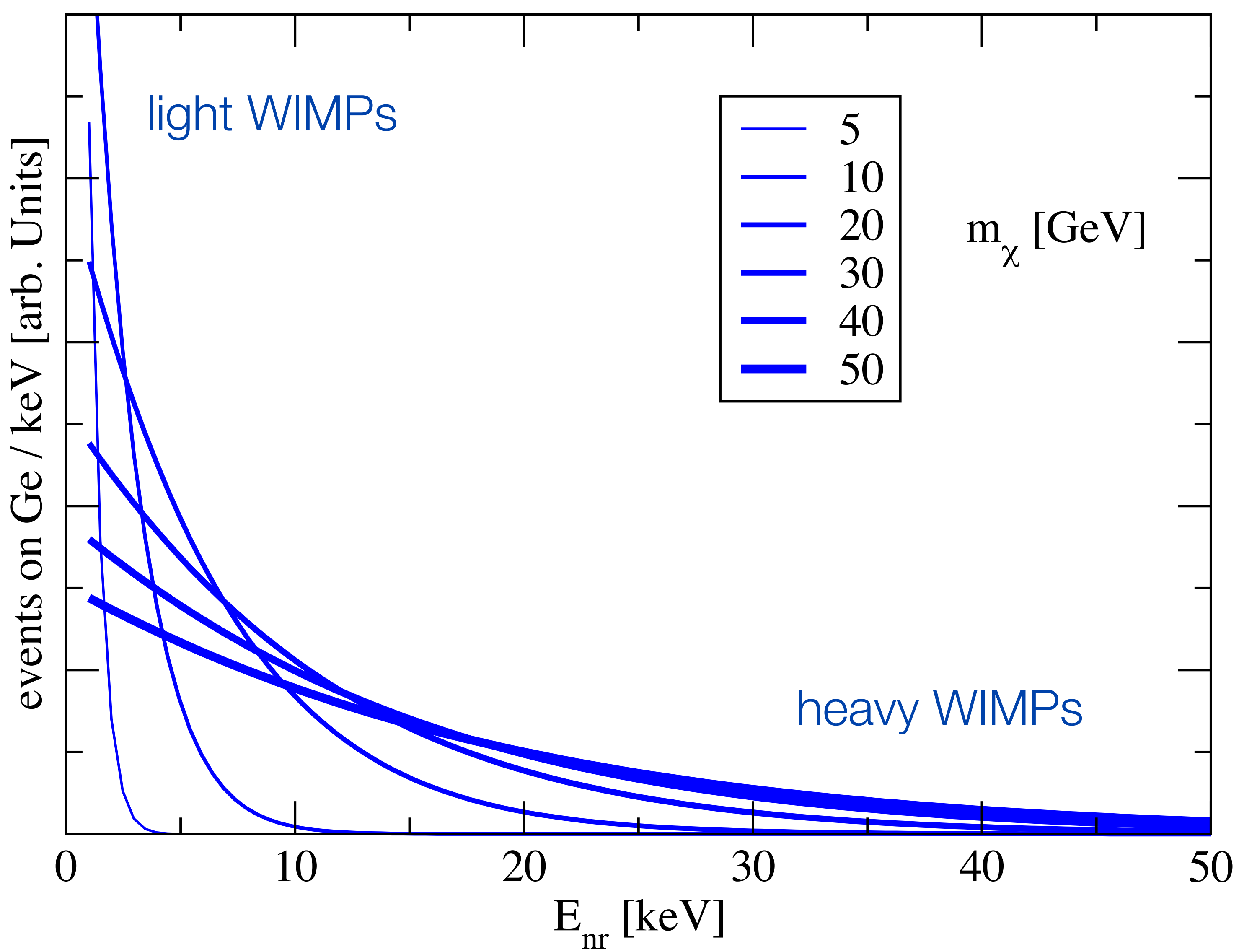

Dark matter signatures

- **Rate and shape of recoil spectrum depend on target material**
- **Motion of the Earth causes:**
  - annual event rate modulation: June - December asymmetry ~ 2-10%
  - sidereal directional modulation: asymmetry ~20-100% in forward-backward event rate

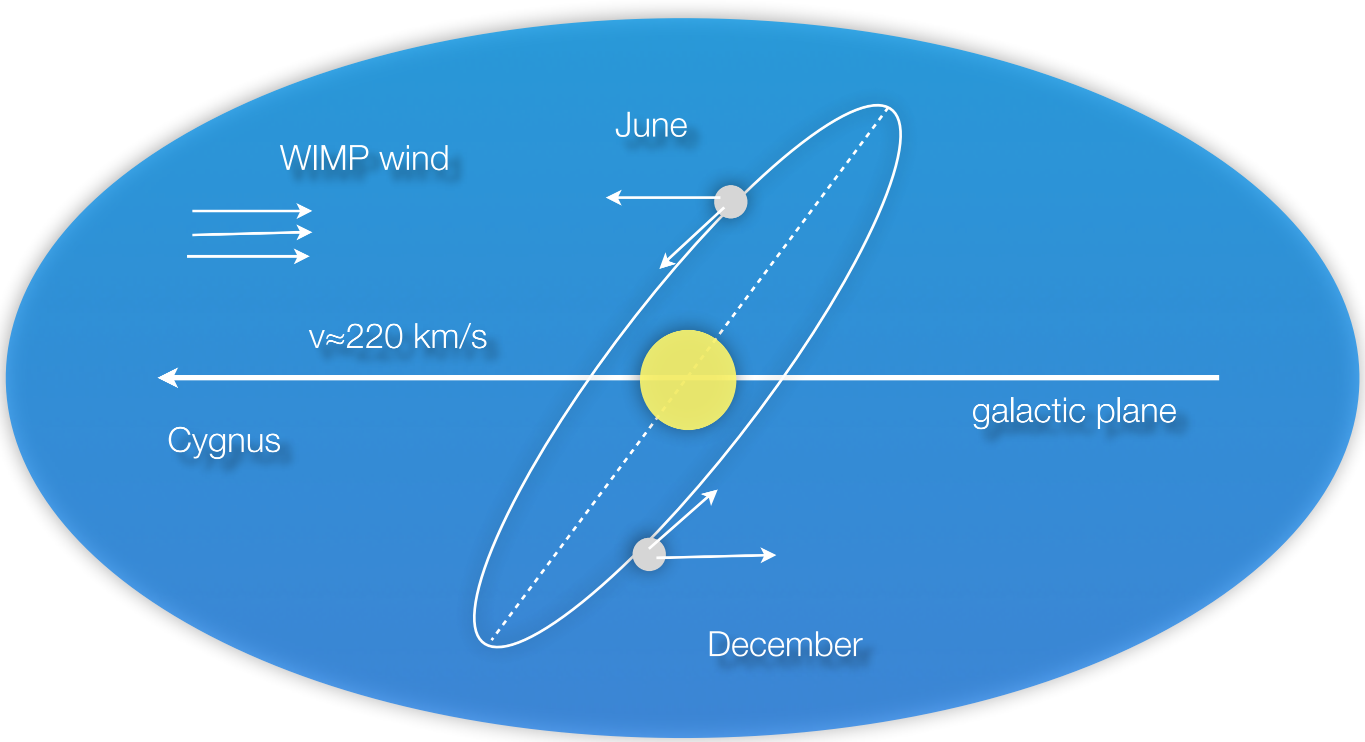

Drukier, Freese, Spergel, PRD 33,1986

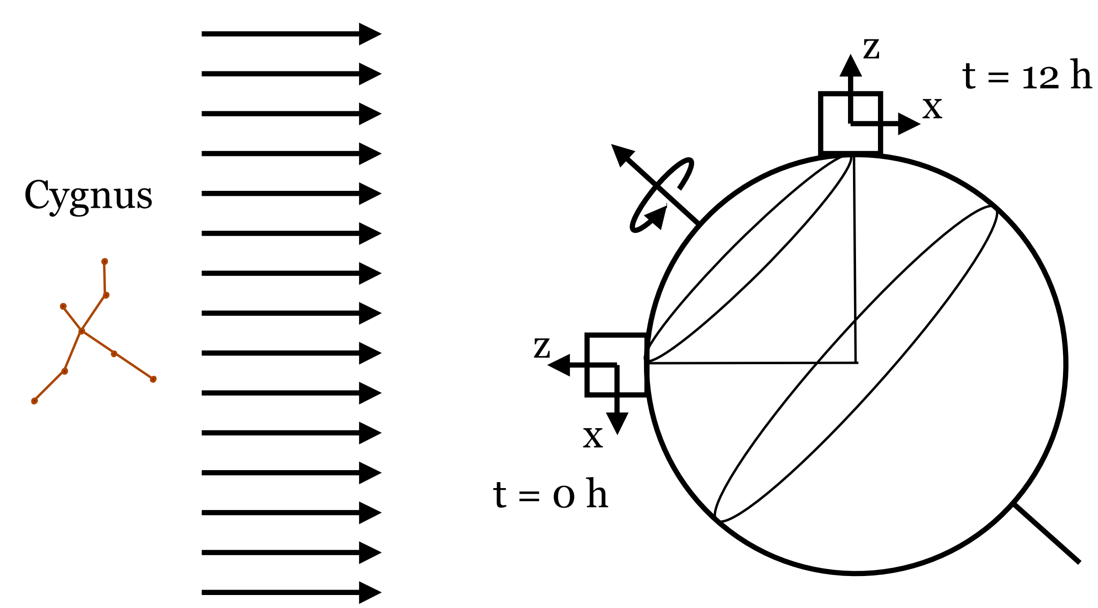

D. Spergel, PRD 36, 1988

Backgrounds

- Cosmic rays & cosmic activation of detector materials
- Natural (^{238}U, ^{232}Th, ^{40}K) & anthropogenic (^{85}Kr, ^{137}Cs) radioactivity: γ, e^-, n, α
- Ultimately: **neutrino-nucleus scattering (solar, atmospheric and supernovae neutrinos)**

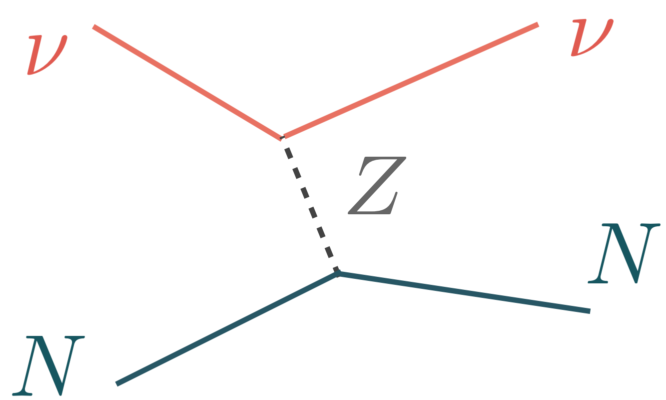

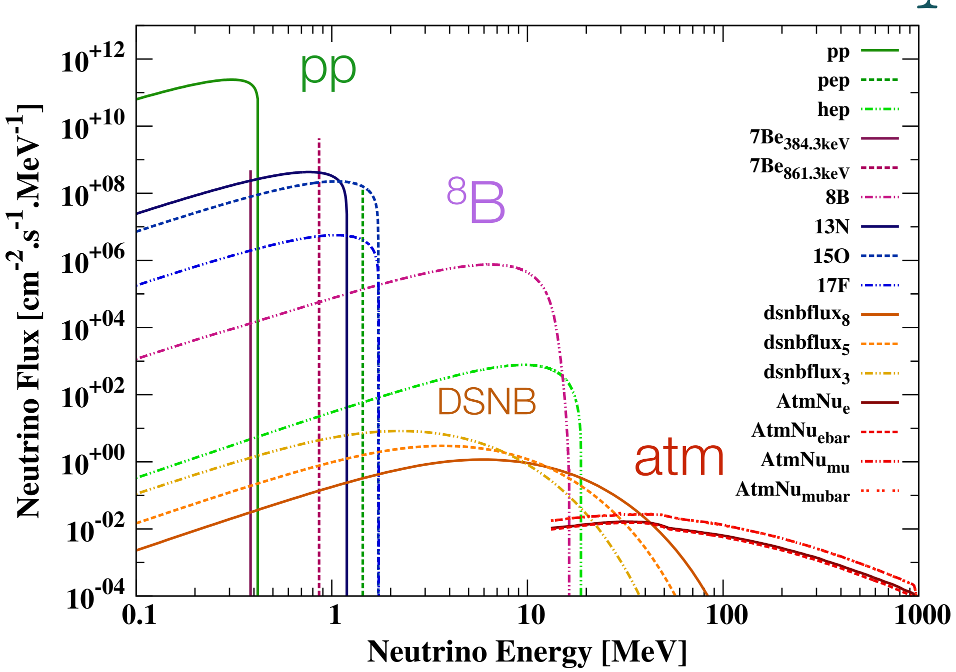

F. Ruppin et al., 1408.3581

$\nu + N \longrightarrow \nu + N$

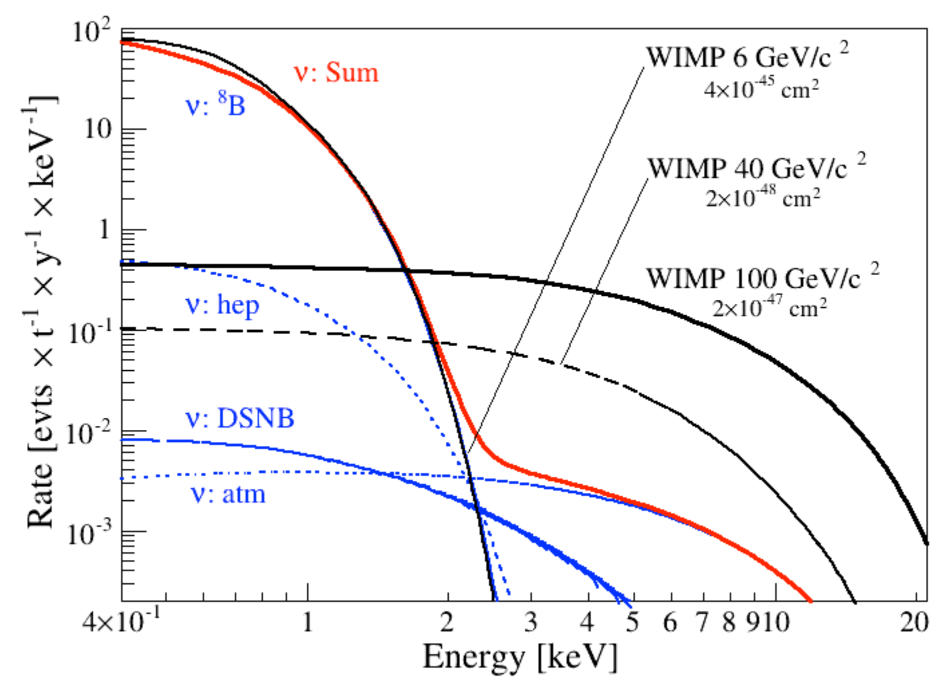

LB et al., JCAP01 (2014) 044

How to deal with backgrounds?

- Go deep underground
- Use active shields
- HPGe material screening

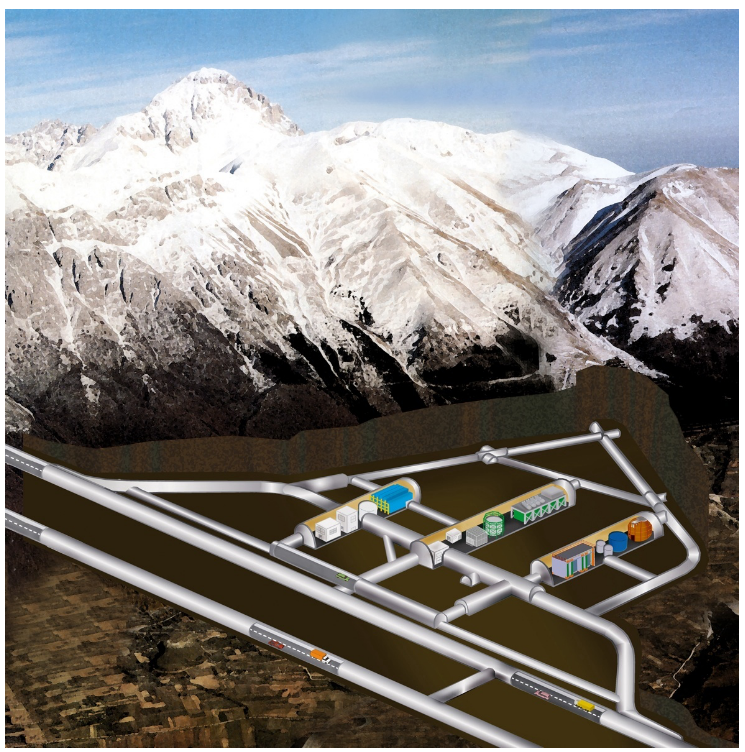

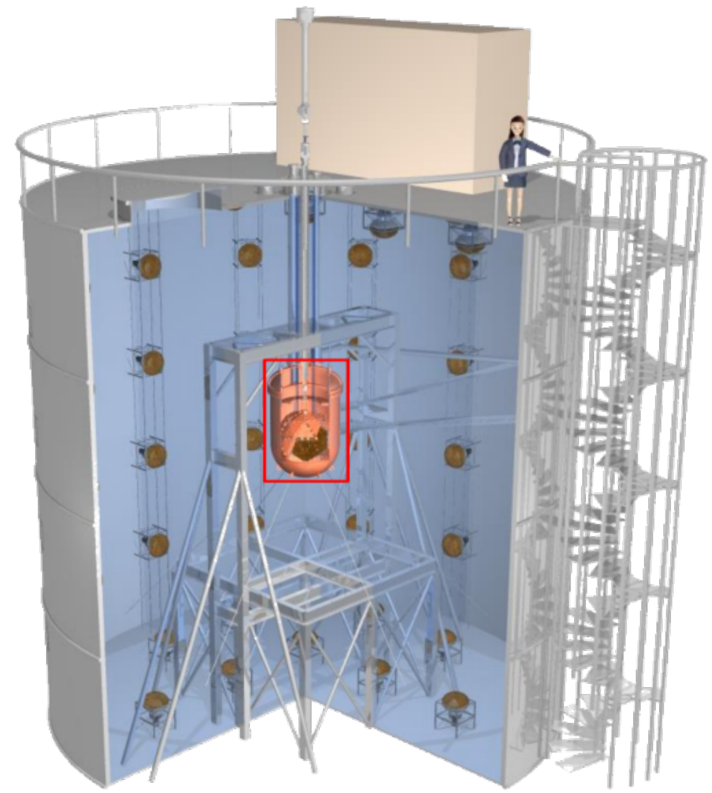

- Select low-background materials

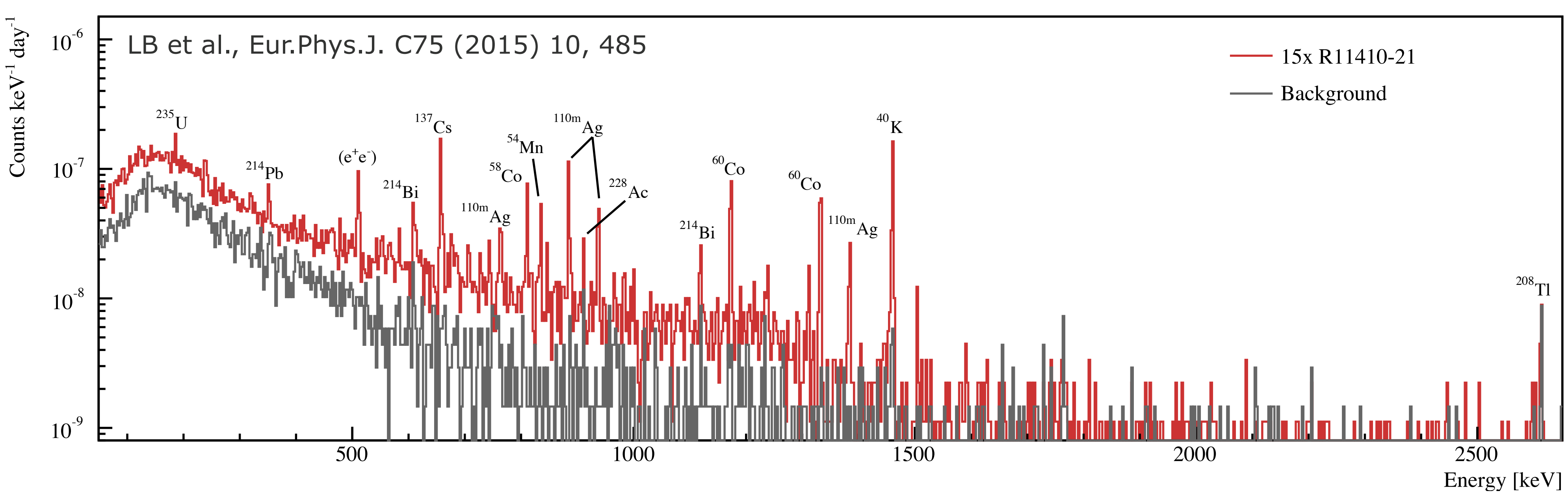

How to deal with backgrounds?

- Fiducialization

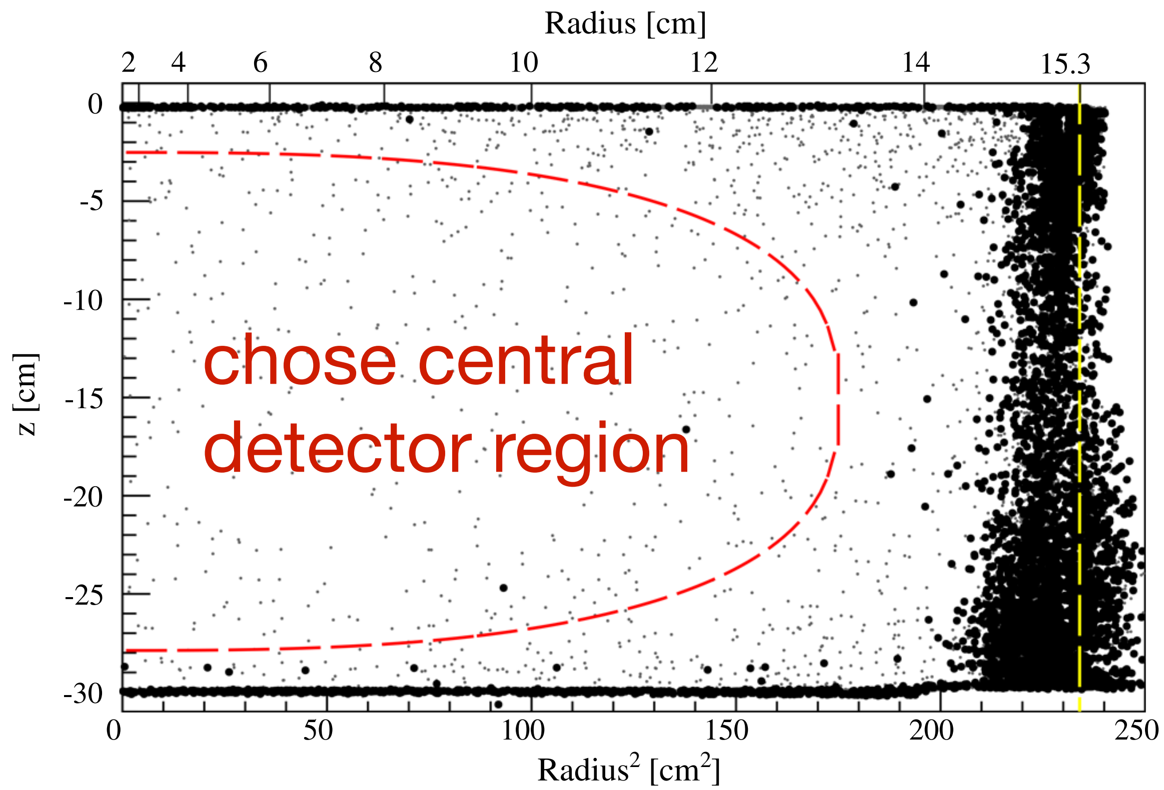

- Discrimination

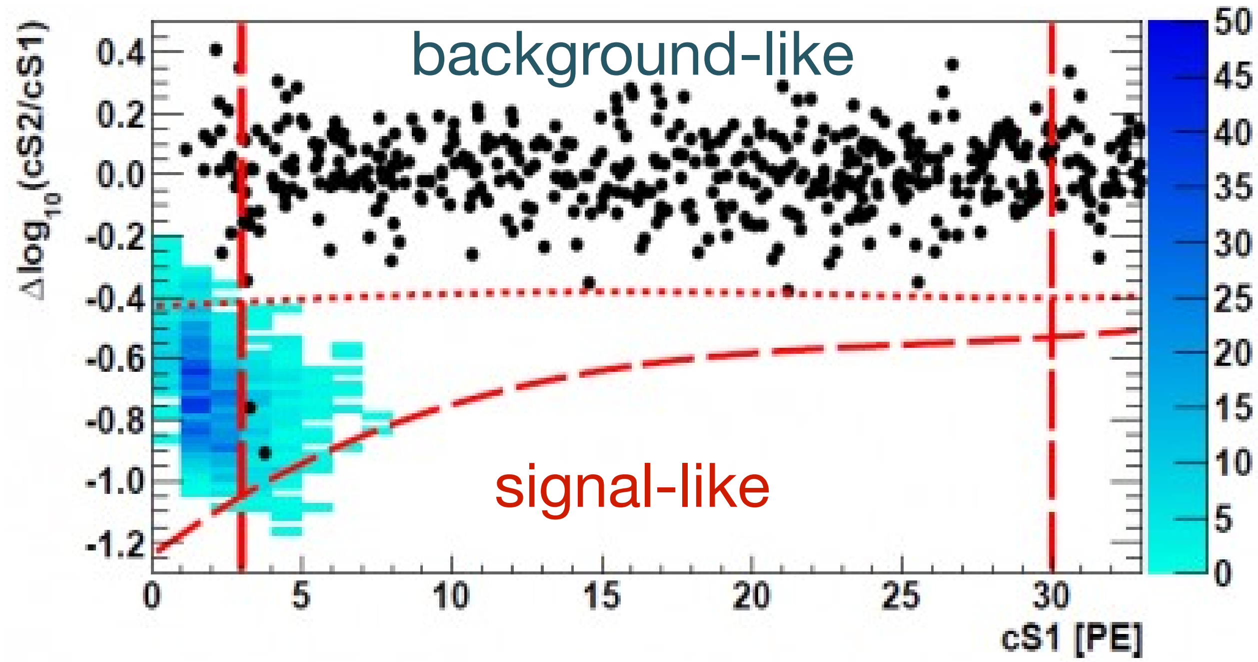

- Avoid exposure to cosmic rays

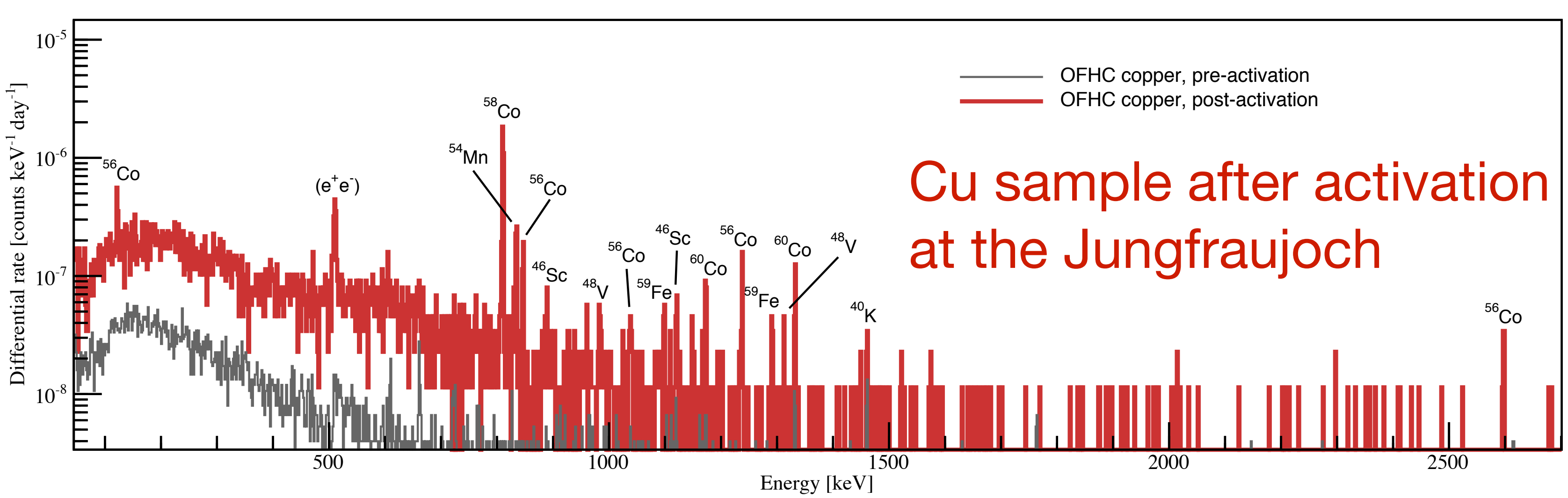

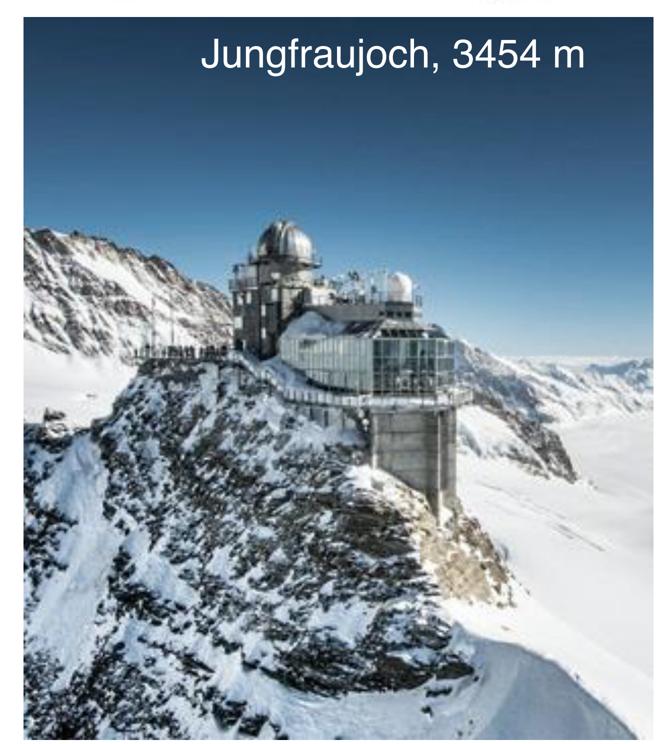

Direct dark matter detection techniques

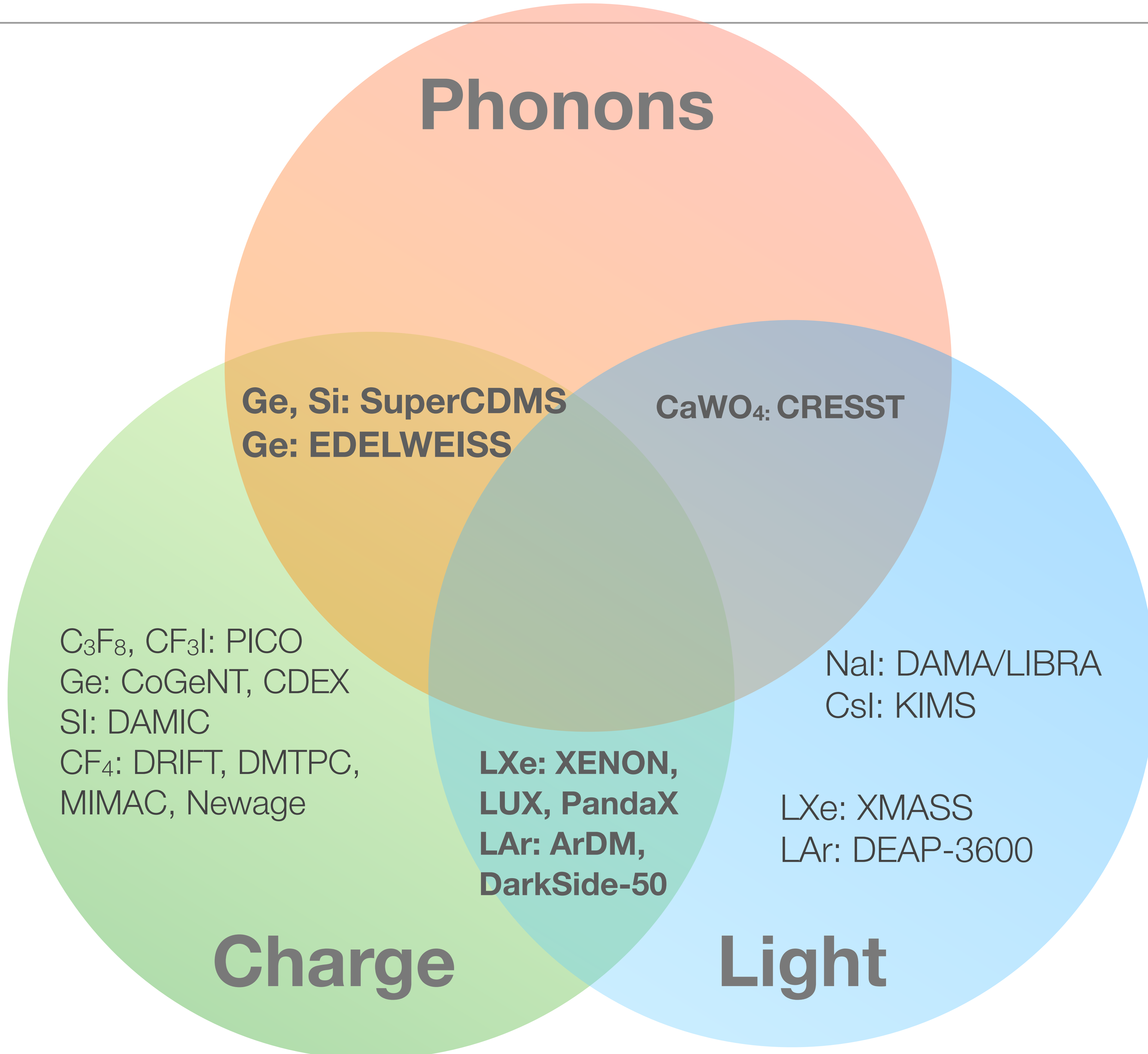

The WIMP landscape in 2015

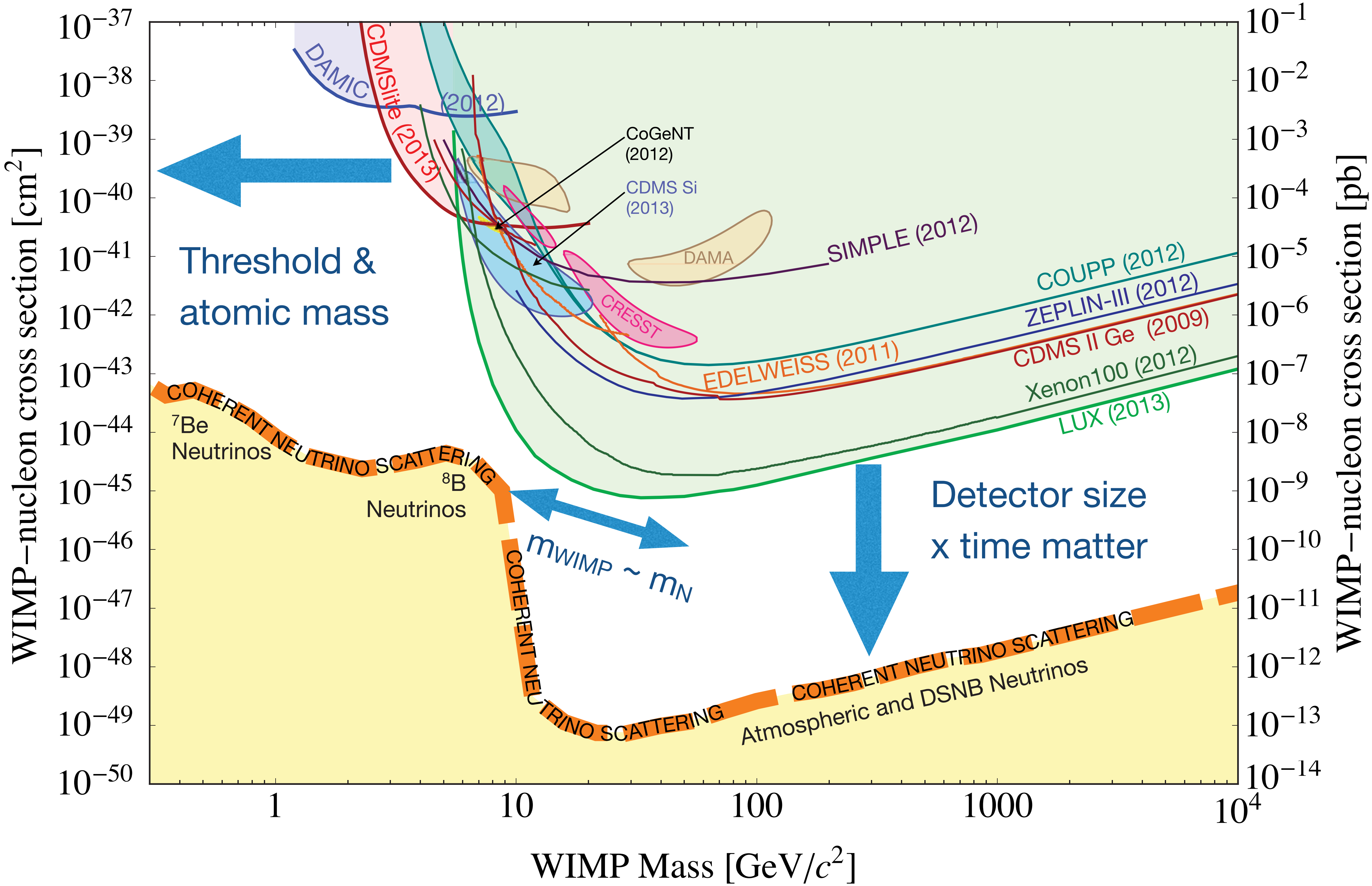

SUSY Predictions: 2 examples

CMSSM

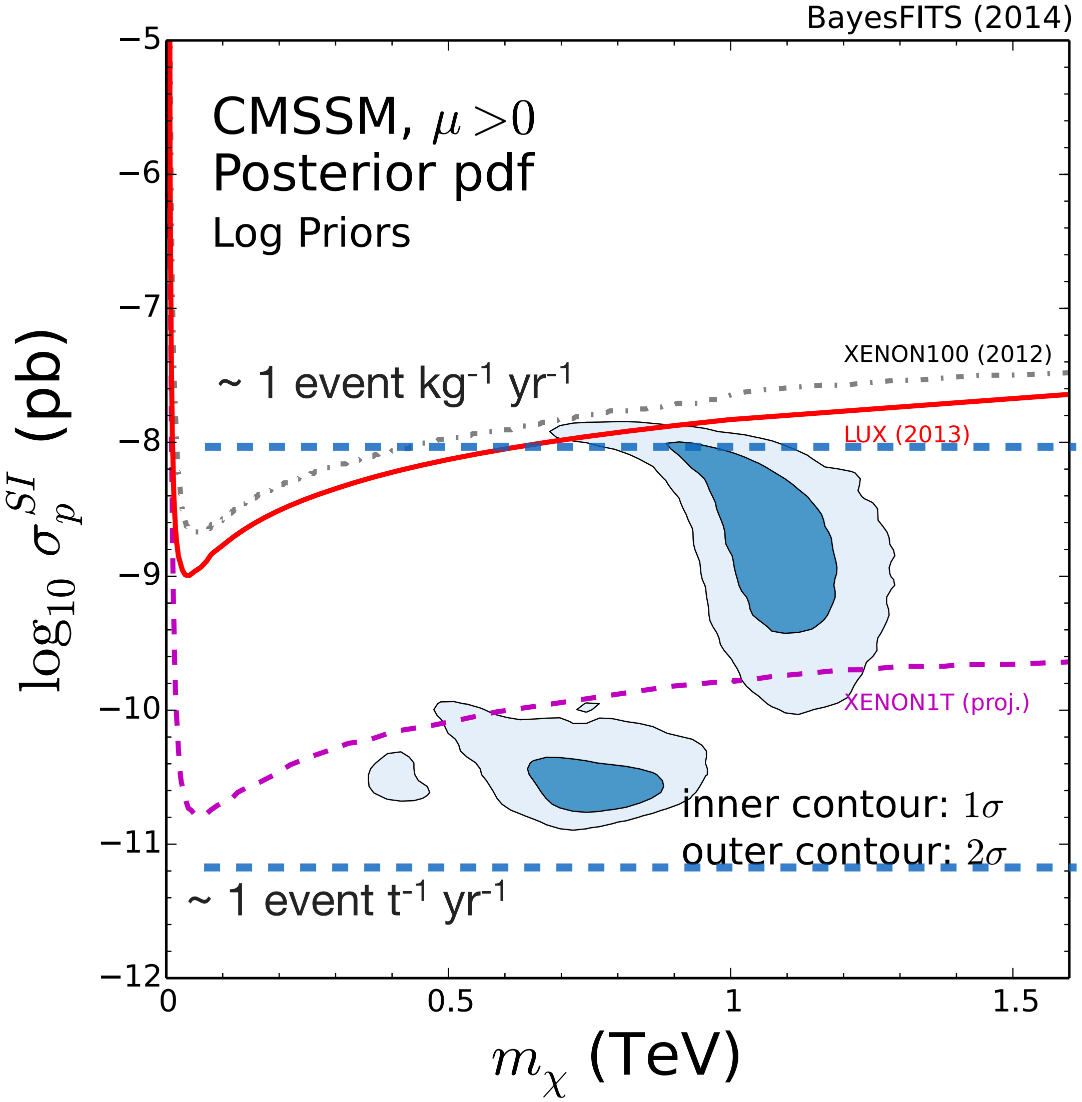

L. Rozkowski, Stockholm 2015

pMSSM

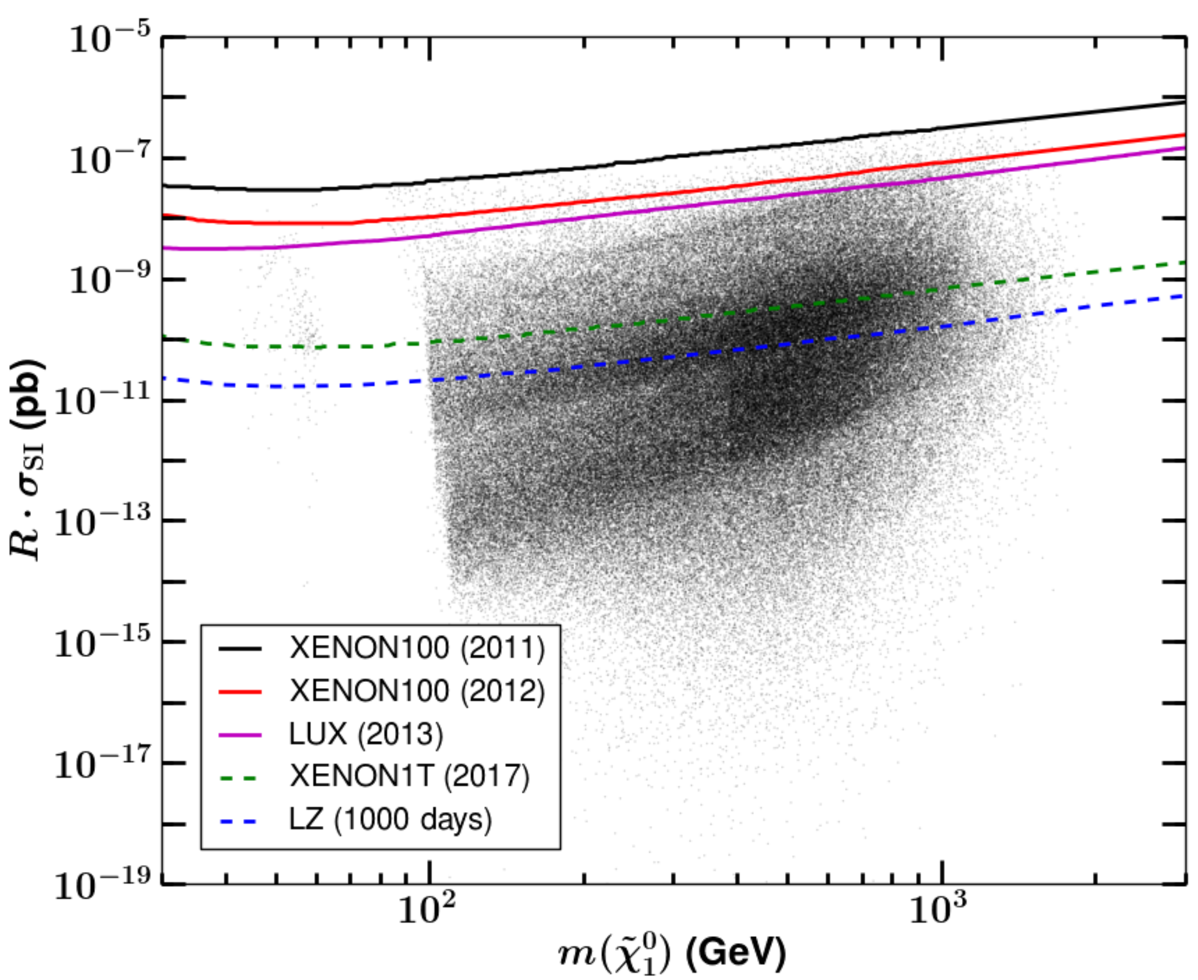

M. Cahill-Rowley, Phys.Rev. D91 (2015) 055011

DAMA/LIBRA annual modulation signal

- Period = 1 year, phase = June 2 ± 7 days; 9.3-sigma
- Results in tension with many WIMP searches
- Several experiments to *directly probe the modulation signal* with similar detectors (NaI, CsI): **SABRE, ANAIS, DM-Ice, KIMS**
- **"Leptophilic" models viable (until a few weeks ago…)**

DAMA/LIBRA NaI: 2% annual modulation

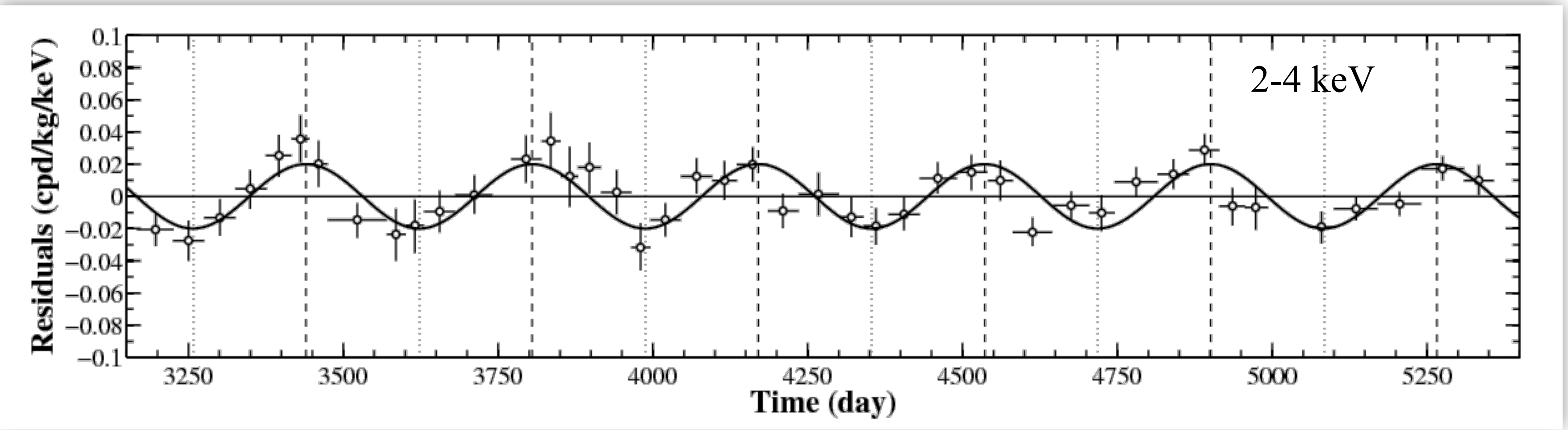

R. Bernabei et al, EPJ-C67 (2010)

Emily Shields et al. / Physics Procedia 61 (2015) 169 – 178

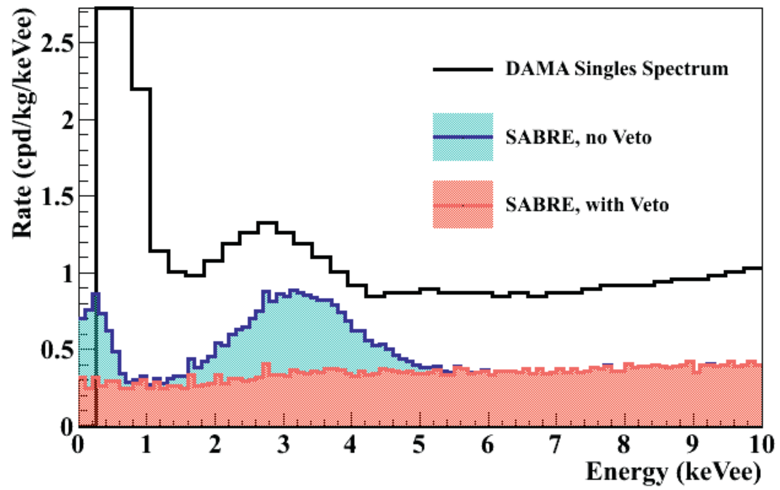

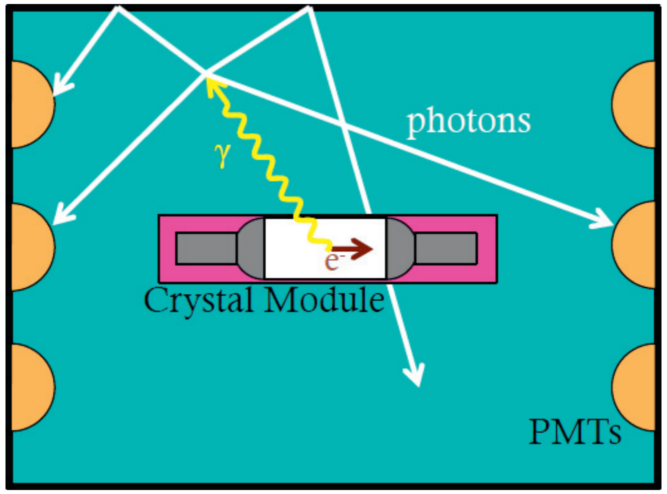

SABRE, 50 kg NaI detectors

Cryogenic Experiments at mK Temperatures

Cryogenic Experiments at mK Temperatures

- Principle: phonon (quanta of lattice vibrations) mediated detectors
- **Motivation:** increase the energy resolution + detect smaller energy depositions (lower the threshold); use a variety of absorber materials (not only Ge and Si)
- The energy resolution (W = FWHM) of a semiconductor detector (N = nr. of e^--h excitations)

$$W_{stat} = 2.35\sqrt{F\epsilon E} \qquad \frac{\sigma(E)}{E} = \sqrt{\frac{F}{N}} = \sqrt{\frac{F\epsilon}{E}} \qquad W_{stat} = 2.35\,\sigma(E)$$

- E = deposited energy; F = Fano factor; N = E/ε; in Si: ε = 3.6 eV/e^--h pair (band gap is 1.2 eV! - where does 70% of the energy go?). F-> the energy loss in a collision is not purely statistical (=0.13 in Ge; 0.11 in Si)
- Maximum phonon energy in Si: 60 meV
  - ➡ **many more phonons are created than e^--h pairs!**
- For dark matter searches:
  - ➡ **thermal phonon detectors (measure an increase in temperature)**
  - ➡ **athermal phonon detectors (detect fast, non-equilibrium phonons)**
- Detector made from superconductors: the superconducting energy gap 2Δ~ 1 meV
  - ➡ binding energy of a Cooper pair (equiv. of band gap in semiconductors); 2 quasi-particles for every unbound Cooper pair; these can be detected -> in principle large improvement in energy resolution

Basic Principles of mK Cryogenic Detectors

- **A deposited energy E (ER or NR) will produce a temperature rise ΔT given by:**

$$\Delta T = \frac{E}{C(T)} e^{-\frac{t}{\tau}} \qquad \tau = \frac{C(T)}{G(T)}$$

C(T) = heat capacity of absorber

G(T) = thermal conductance of the link between the absorber and the reservoir at temperature T_0

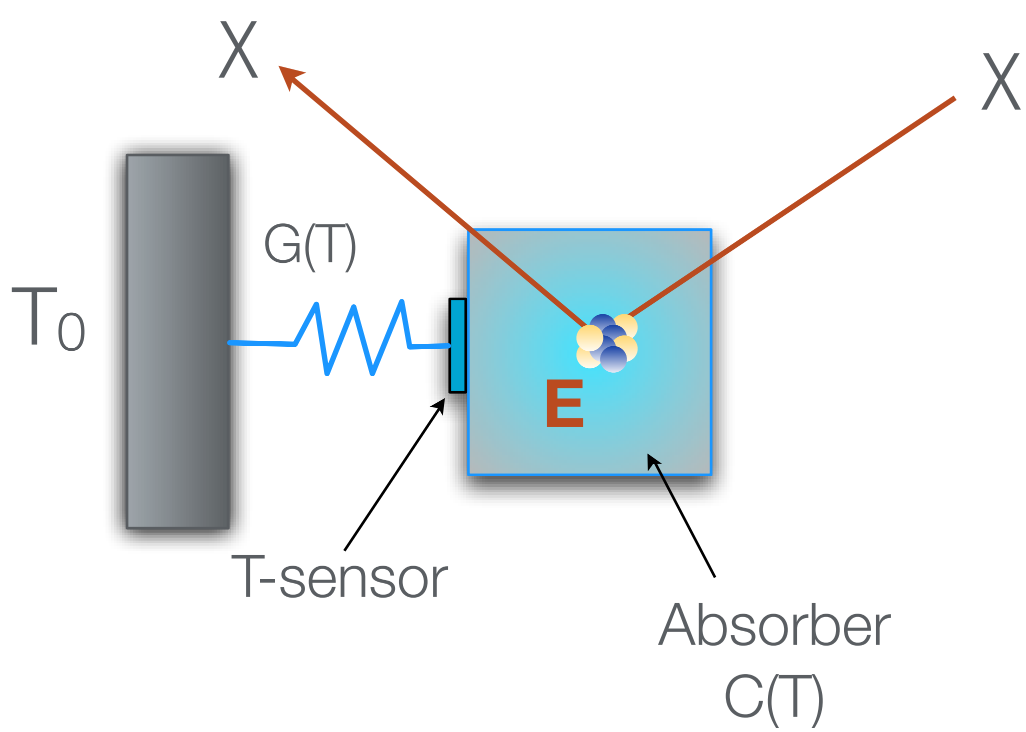

Normal metals:
the electronic part of C(T) ~ T, and dominates the heat capacity at low temperatures

Superconductors:
the electronic part is proportional to $\exp(-T_c/T)$ (T_c = superconducting transition temperature) and is negligible compared to lattice contributions for $T \ll T_c$

Basic Principles of mK Cryogenic Detectors

- **For pure dielectric crystals and superconductors at T << T_c, the heat capacity is given by:**

$$C(T) \sim \frac{m}{M}\left(\frac{T}{\theta_D}\right)^3 \ \mathrm{J\,K^{-1}}$$

m = absorber mass

M = molecular weight of absorber

Θ_D = Debye temperature (at which the highest frequency gets excited) $\theta_D = \frac{h\nu_m}{k}$

➡ the lower the T, the larger the ΔT per unit of absorbed energy

➡ in thermal detectors E is measured as the temperature rise ΔT

- **Example:** at T = 10 mK, a 1 keV energy deposition in a 100 g detector increases the temperature by:

$$\Delta T \approx 1\,\mu K$$

- this can be measured!

Thermal Detectors

- The intrinsic energy resolution (as FWHM) of such a calorimeter is given by (k_B is the Boltzmann constant):

$$W = 2.35\xi\sqrt{k_B T^2 C(T)}$$

$$\frac{C(T)}{k_B} = \text{number of phonon modes}$$

$$k_B T = \text{mean energy per mode}$$

$$\xi = 1.5 - 2$$

Info about the sensor. the thermal link and the T-dependance of C(T)

- **Example for the theoretical expectation of the intrinsic energy resolution:**
  - ➡ a 1 kg Ge crystal operated at 10 mK could achieve an energy resolution of about 10 eV => two orders of magnitude better than Ge ionization detectors
  - ➡ a 1 mg of Si at 50 mK could achieve an energy resolution of 1 eV => two orders of magnitude better than conventional Si detectors

Temperature Sensors

- **Semiconductor thermistor**: a highly doped semiconductor such that the resistance R is a strong function of temperature (NTD = neutron-transmutation-doped Ge - uniformly dope the crystal by neutron irradiation)
- **Superconducting (SC) transition sensor (TES/SPT):** thin film of superconductor biased near the middle of its normal/SC transition

- For both NTDs and TESs/SPTs, an energy deposition produces a change in the electrical resistance R(T). The response can be expressed in terms of the logarithmic sensitivity:

$$\alpha \equiv \frac{d\log(R(T))}{d\log(T)}$$

Typical values:

α = -10 to -1 for semiconductor thermistors

$\alpha \sim +10^3$ for TES/SPT devices

→ the sensitivity of TES/SPTs can be extremely high (depending on the width of the SC/normal transition)

→ however, the temperature of the detector system must be kept very stable

Example: Thermal Detector with SPT-sensor

- **The change of resistance due to a particle interaction in the absorber is detected by a superconducting quantum interference device (SQUID)** *(by the change in current induced in the input coil of the SQUID)*

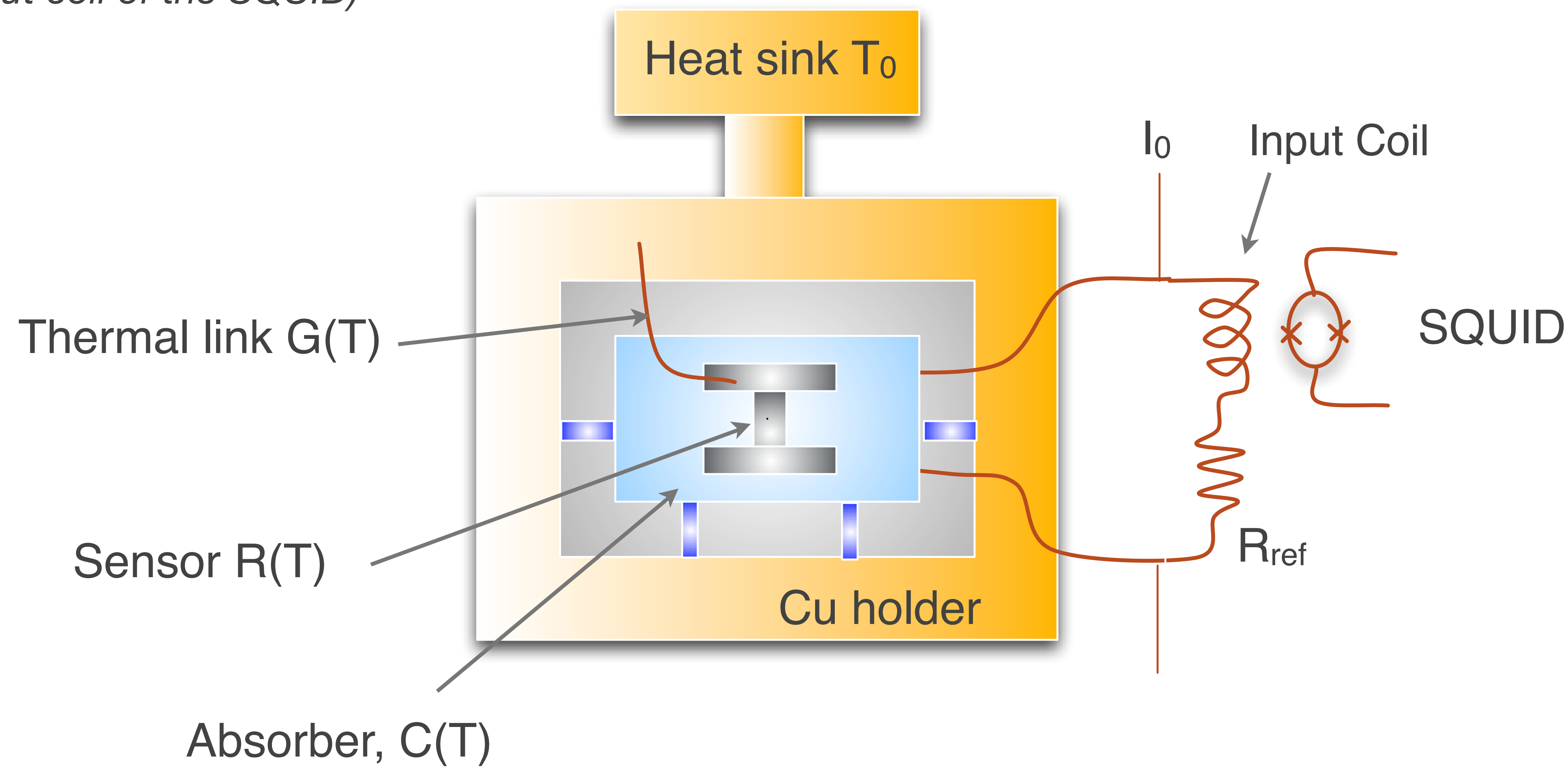

- Thermal detectors: slow -> ms for the phonons to relax to a thermal distribution
- TES: can be used to detect fast, athermal phonons -> how are these kept stable?

TES with Electrothermal-Feedback

- $T_0 << T_C$: substrate is cooled well below the SC transition temperature T_C

- **A voltage V_B is placed across the film (TES)**

  and equilibrium is reached when ohmic heating of the TES by its bias current is balanced by the heat flow into the absorber

  When an excitation reaches the TES

  → the resistance R increases

  → the current decreases by ΔI

  ⇒ this results in a reduction in the Joule heating

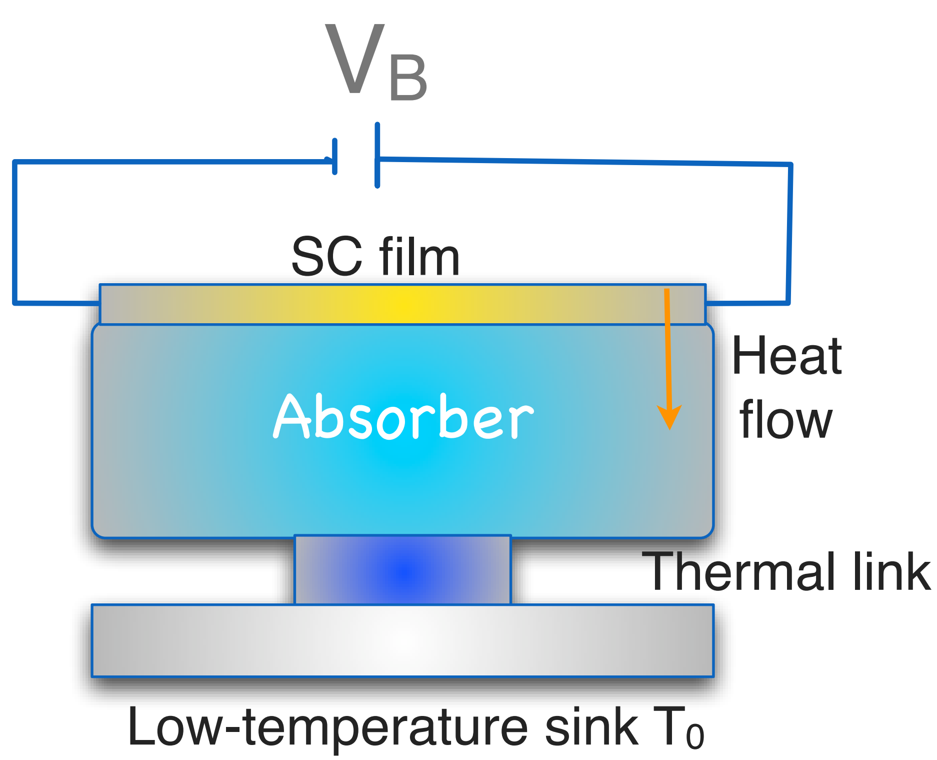

The feedback signal = the change in Joule power heating the film $P = IV_B = V_B^2/R$

The energy deposited is then given by:

$$E = -V_B \int \Delta I(t) \mathrm{d}t$$

=> the device is self-calibrating

TES with Electrothermal-Feedback

- **By choosing the voltage V_B and the film resistivity properly**

=> one achieves a stable operating T on the steep portion of the transition edge

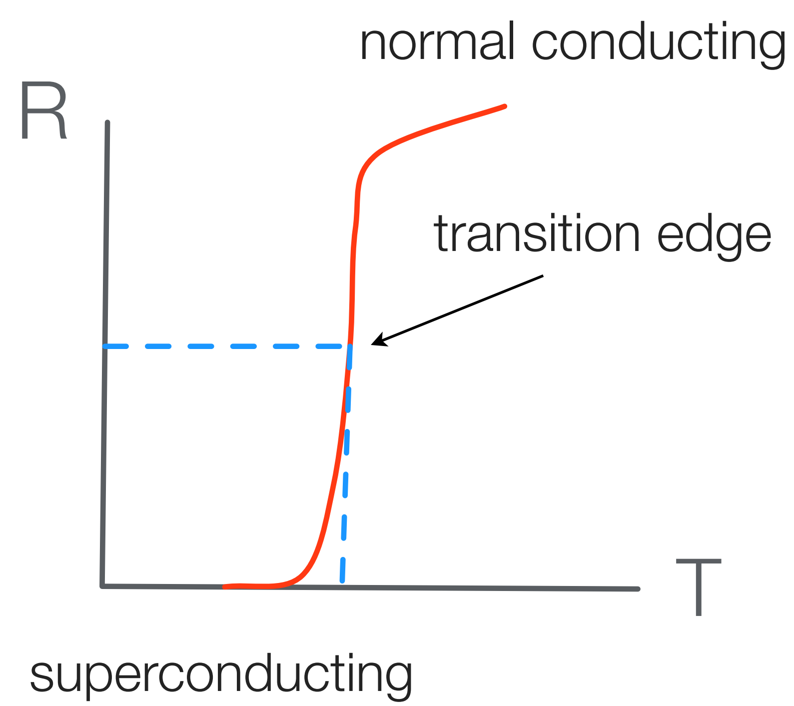

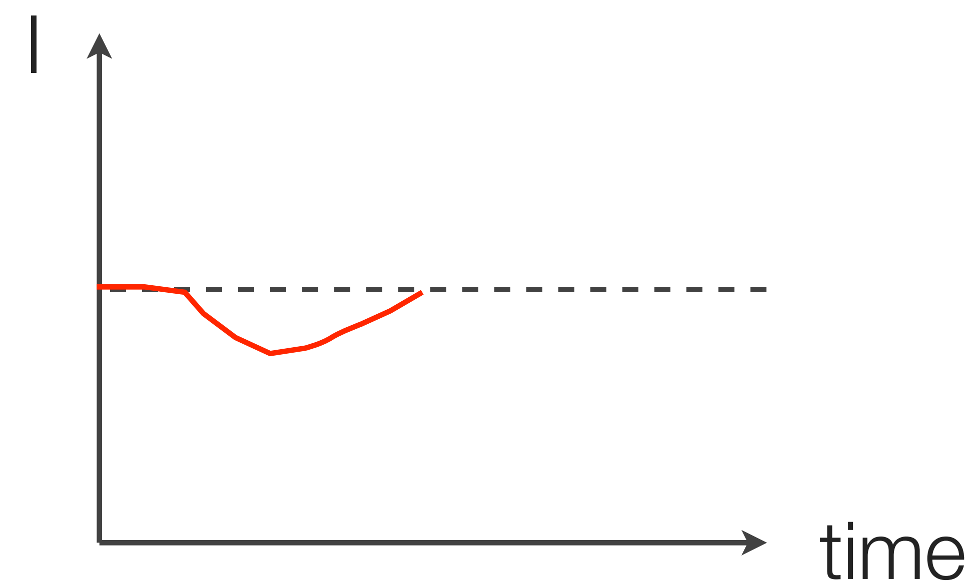

ET-feedback: leads to a thermal response time 10^2 faster than the thermal relaxation time
+ a large variety of absorbers can be used with the transition edge sensor

Experiments at ~mK temperatures

CDMS at Soudan
SuperCDMS at SNOlab
Ge/Si detectors at 30 mK
Detect phonons and charge

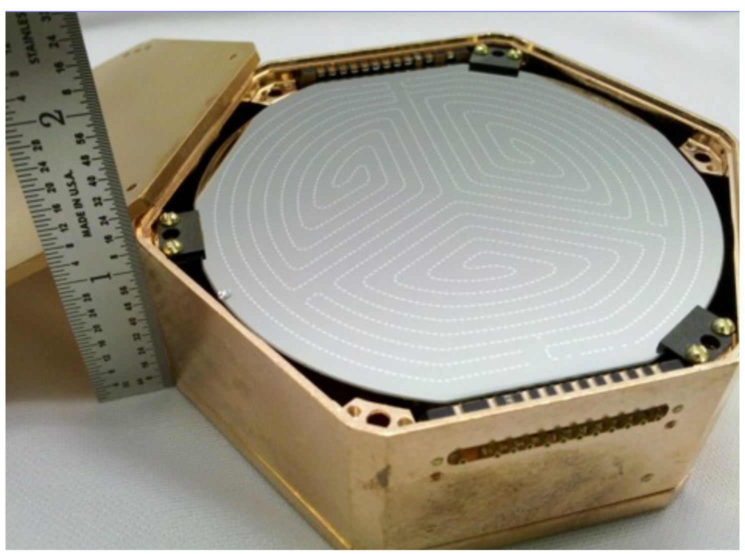

EDELWEISS at Modane
Ge detectors at 18 mK
Detect phonons and charge

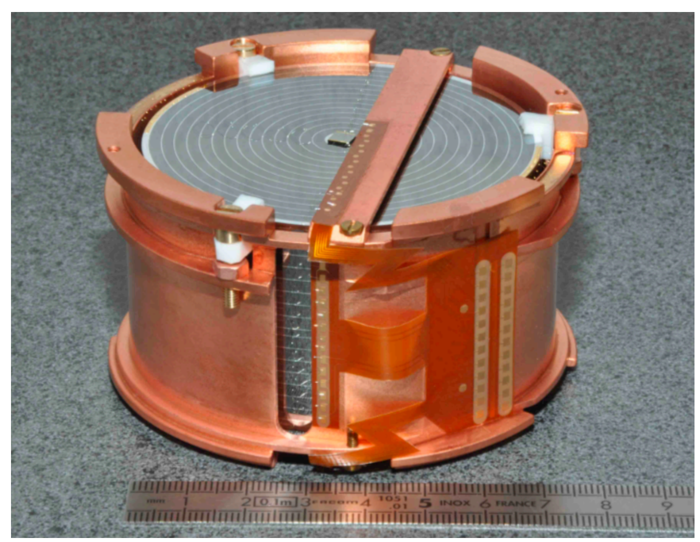

CRESST at LNGS
$CaWO_3$ detectors at 10 mK
Detect phonons and light

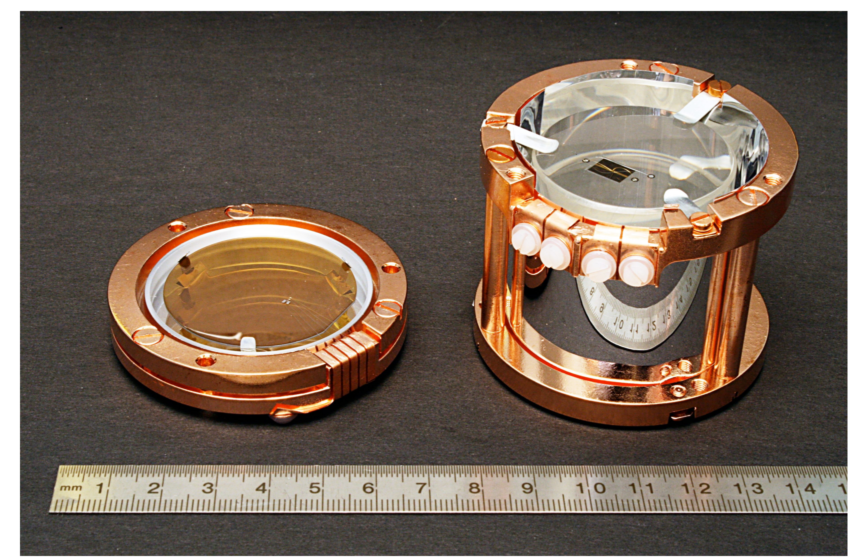

Background rejection in CDMS

- Ratio of the charge/phonon-signal and time difference between charge and phonon signals => distinguish signal (WIMPs) from background of electromagnetic origin

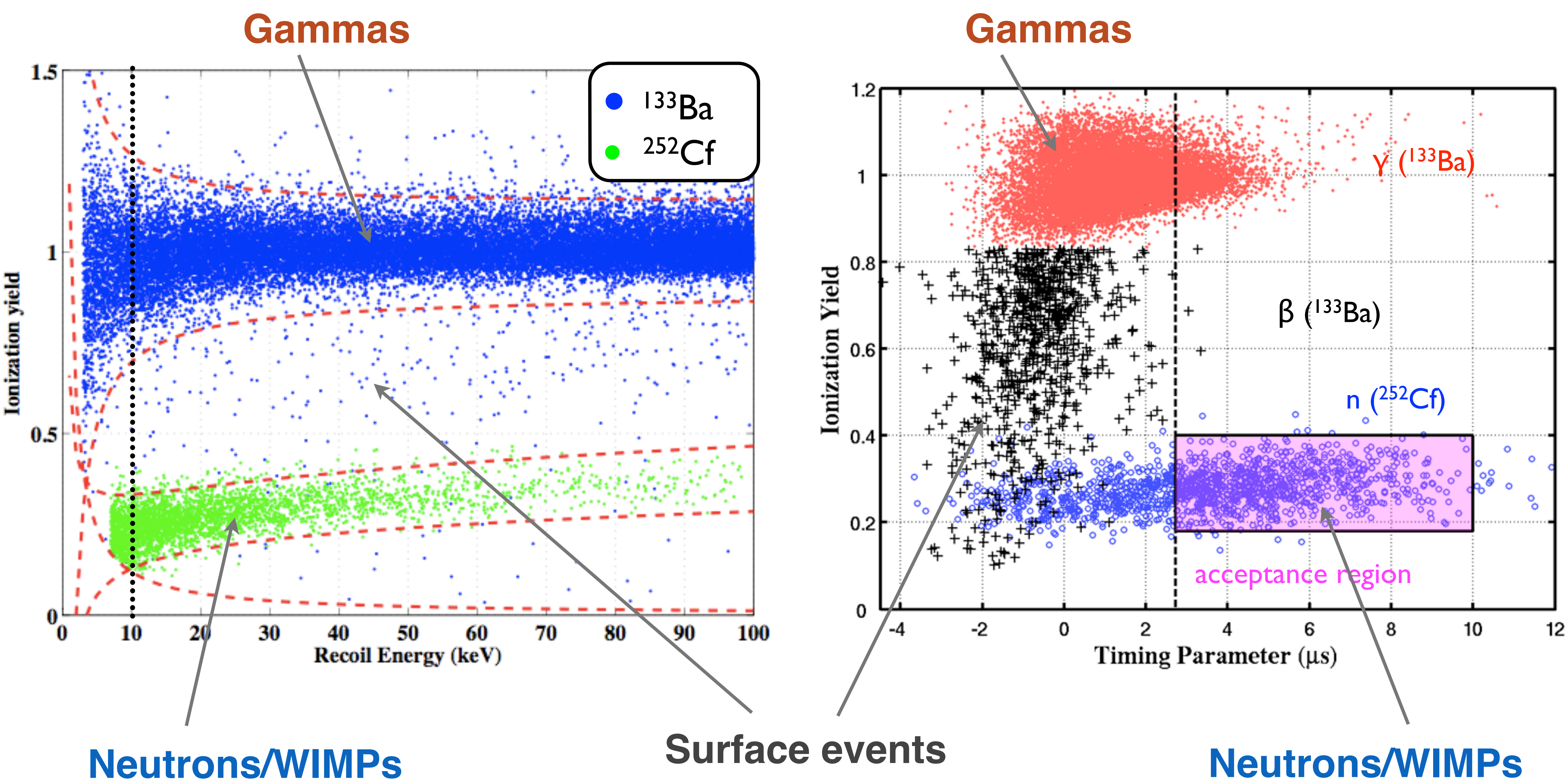

EDELWEISS and CRESST (example, older runs)

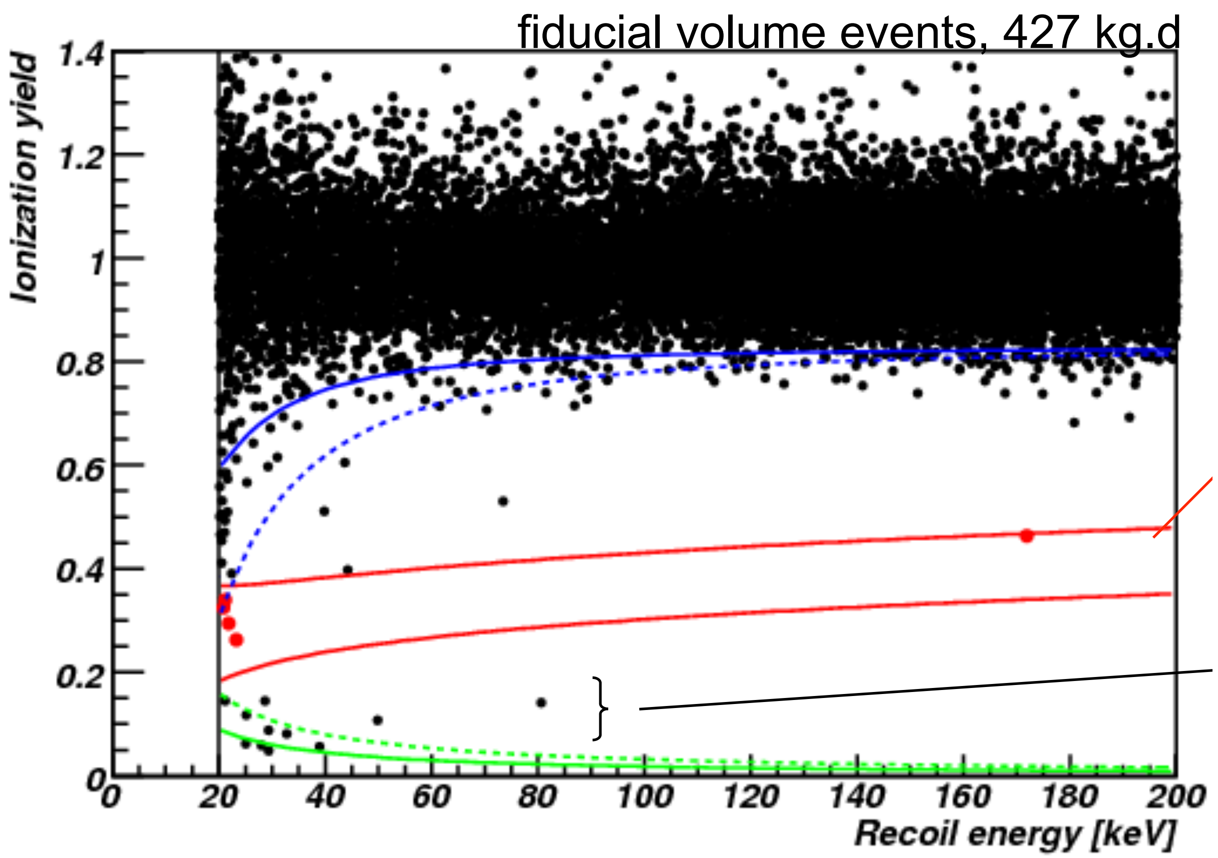

Phys. Lett. B 702 (2011)

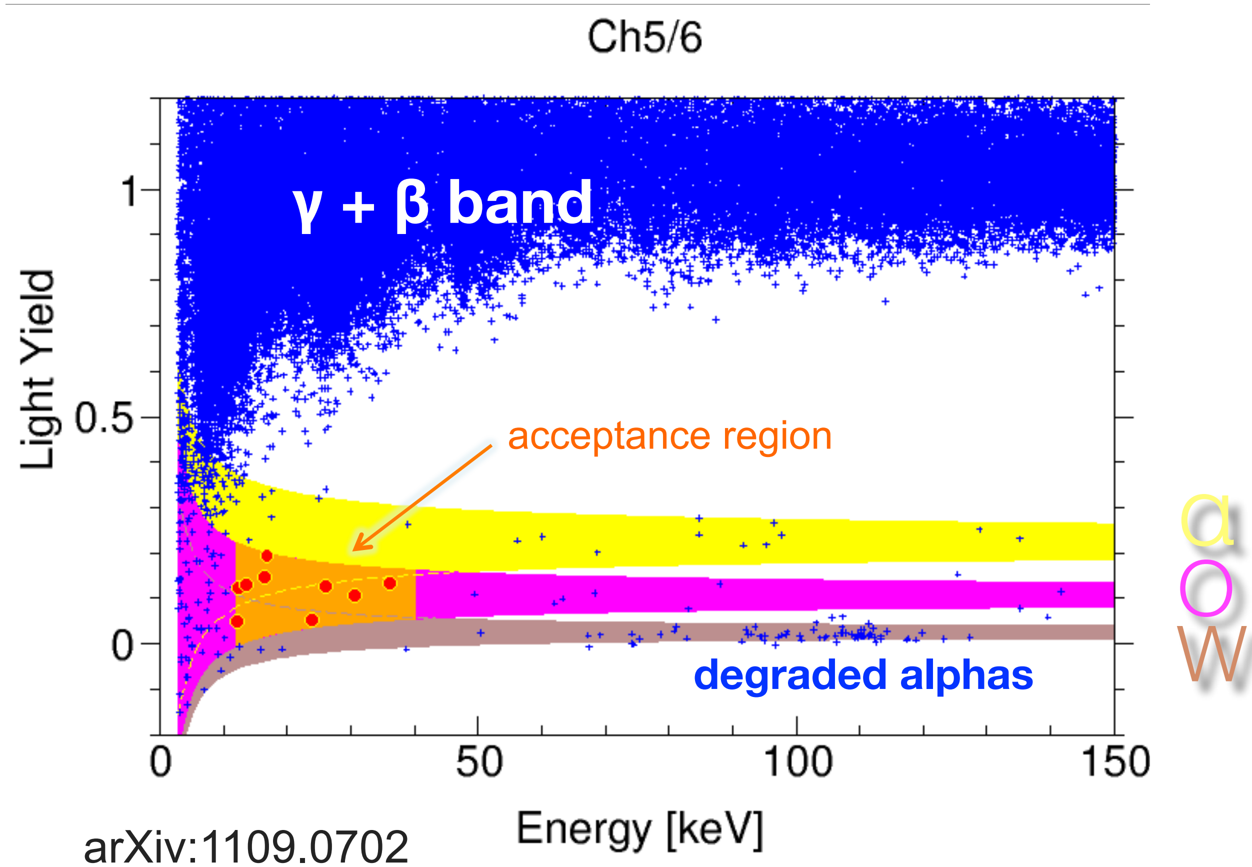

arXiv:1109.0702

Ge detectors at 18 mK

5 events (427 kg-day)

3 expected from backgrounds

operates 36 new, 800 g crystals with improved background rejection

$CaWO_3$ detectors at 10 mK

67 events observed (730 kg-day)

~ 37 expected from backgrounds

there was room for a signal…

later focussed on reducing backgrounds

New CRESST data

- Exposure of 29.35 kg days, one upgraded detector module (data August 2013 - January 2014)
- New design with fully scintillating inner housing (past: metal clamps holding crystals were not scintillating, ^{206}Pb recoils from alpha-decays of ^{210}Po were source of background)
- The past excess over background found in previous runs is not confirmed

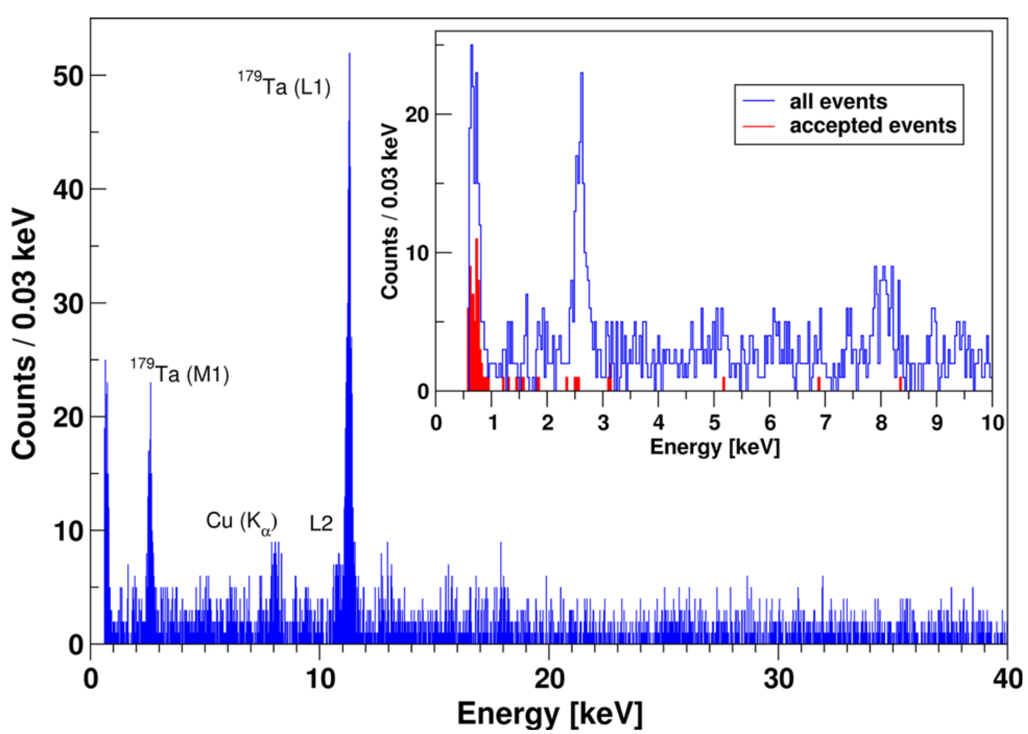

Visible lines: cosmogenic activation of crystals

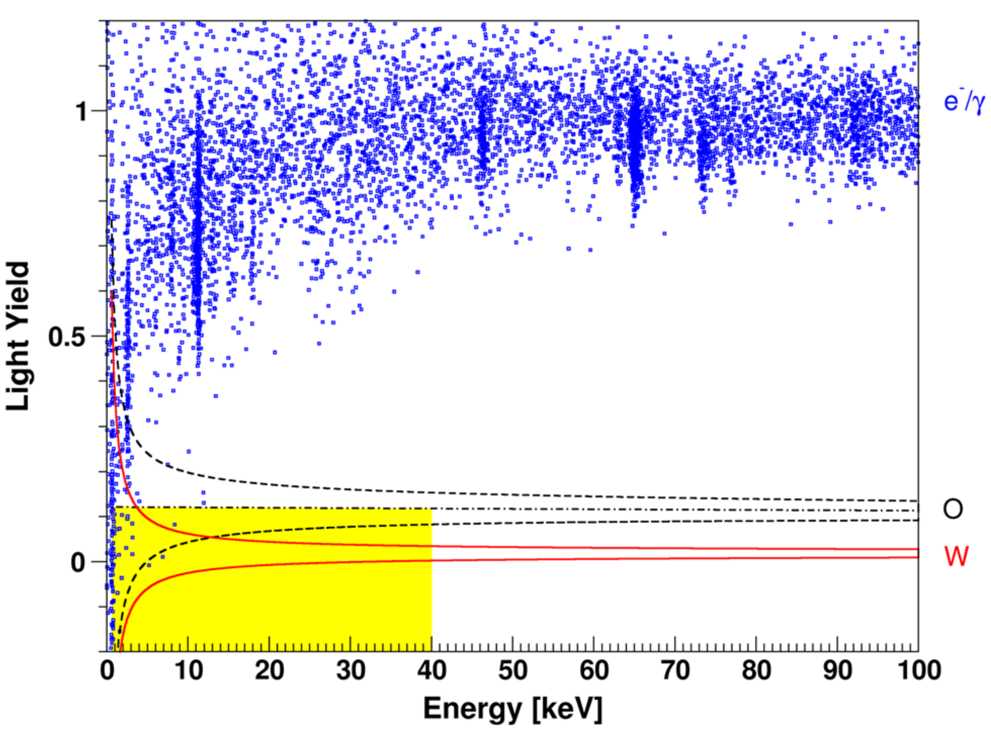

Red: tungsten NR band; black: oxygen NR band

Eur. Phys. J-C 74, 2014

New phase of EDELWEISS

- Operate 36 new, fully inter-digitized detectors, 800 g each (~ 600 g fiducial mass)
- With 150 live days => 3000 kg days of exposure
- The cryostat was redesigned, and an additional neutron shield added
- 2015-2016: installation of new detectors with reduced threshold

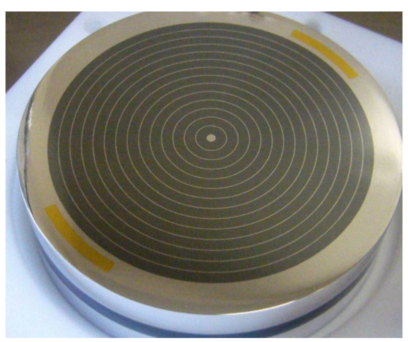

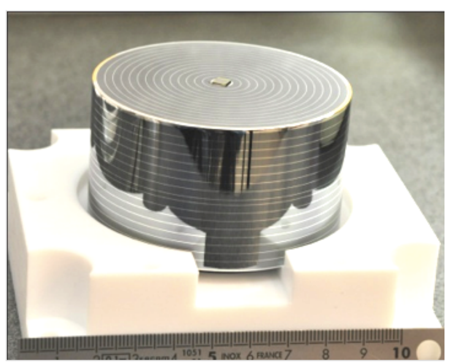

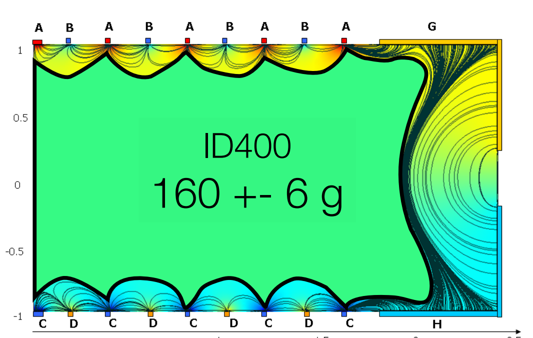

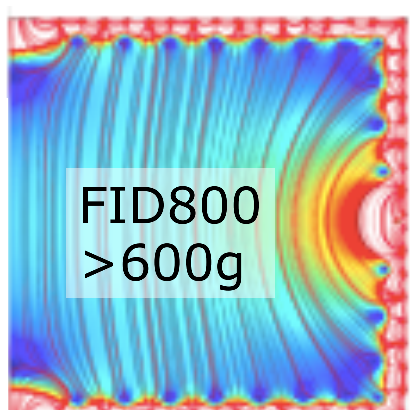

neutrons

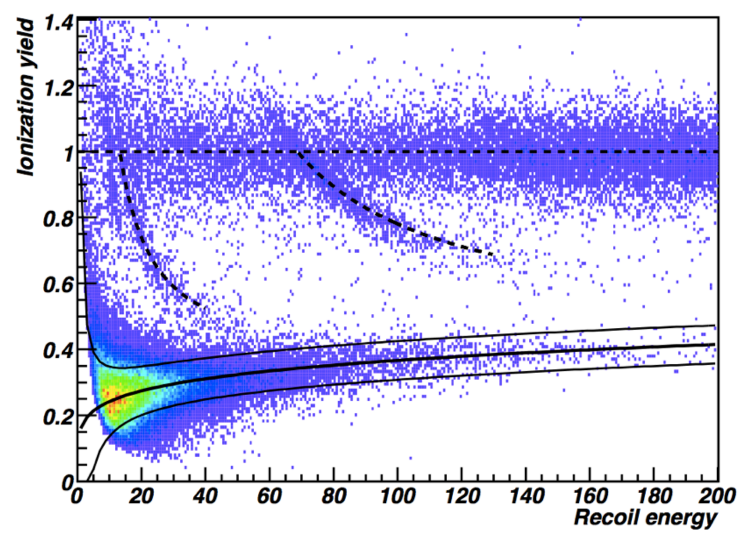

Ge recoil Ion yield = $0.16\ E_{rec}^{0.18}$

^{133}Ba (347k events)

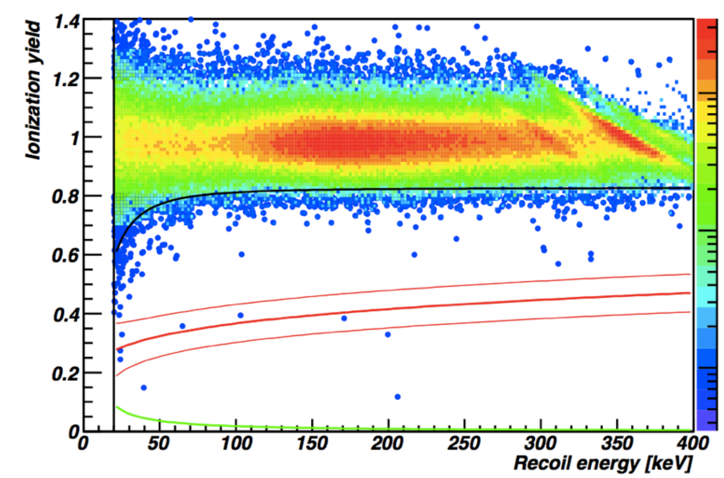

1 NR for every 30k gammas between 20 and 200 keV

Bolometers: recent results

Phys. Rev. Lett. 112 (2014) 24, 241302

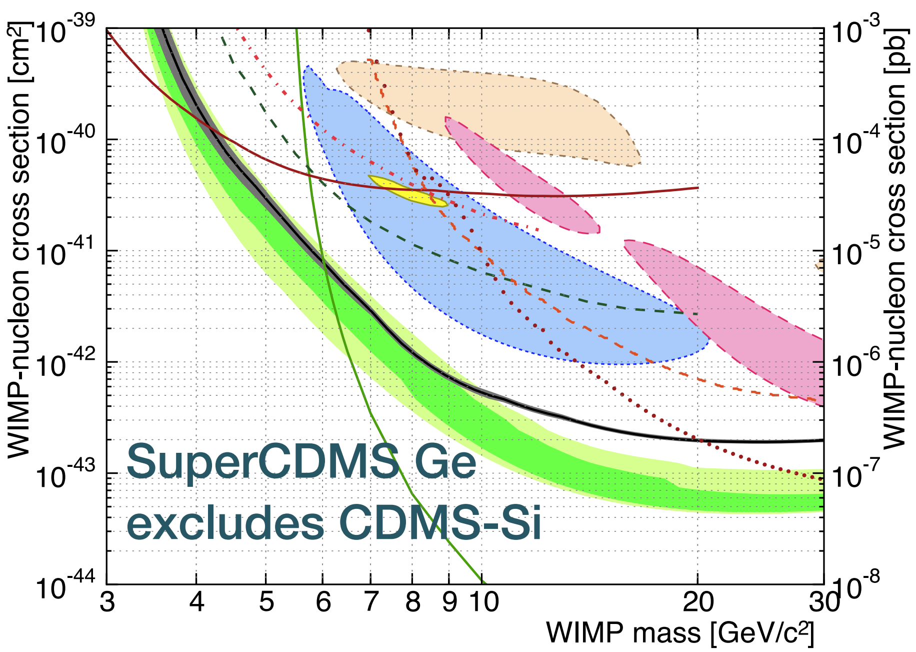

arXiv: 1504.00820

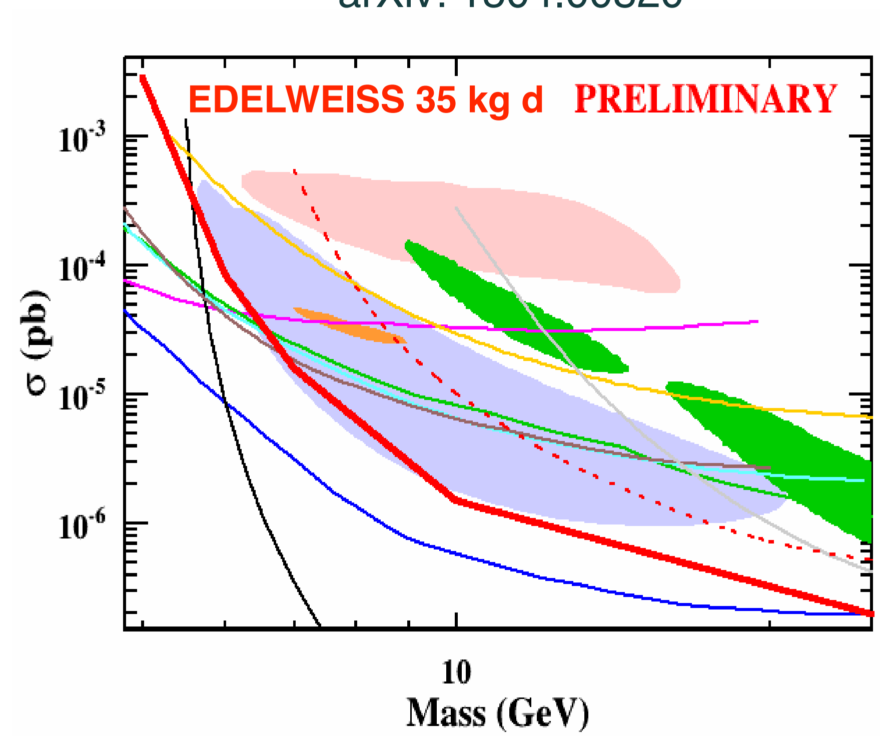

Plan to use several detectors, and decrease the analysis threshold (< 5 GeV WIMP mass)

F. Reindl, EPS-HEP 2015

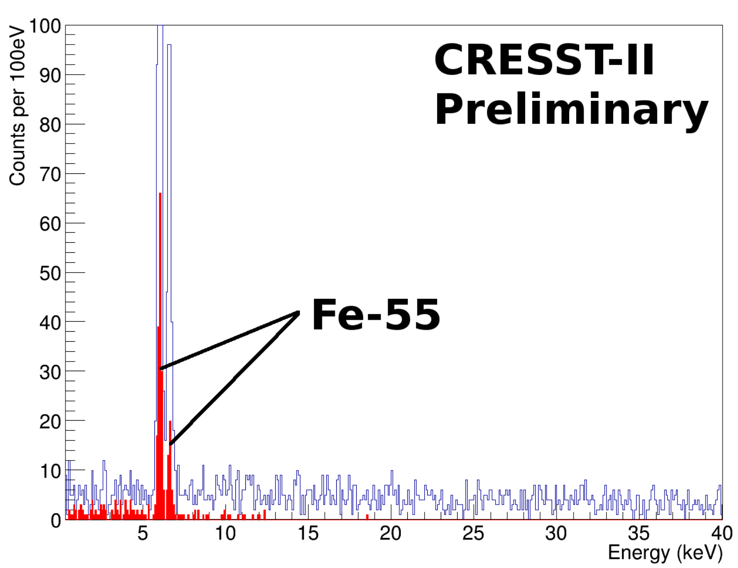

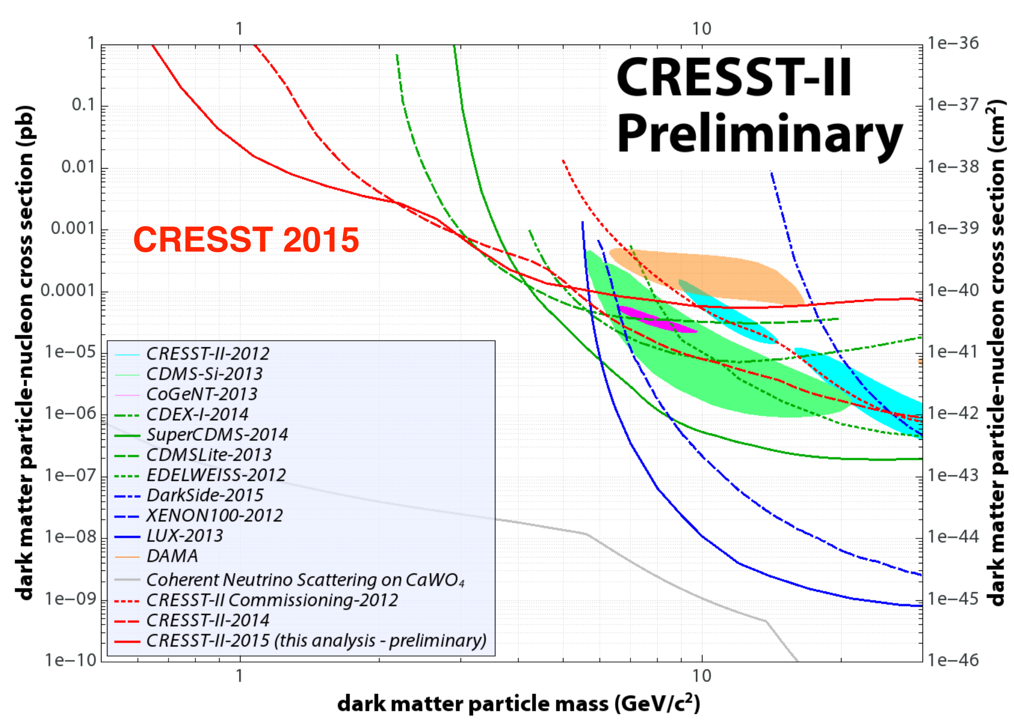

Final, blind analysis in autumn 2015
+ start of CRESST-III at the end of this year (new detector modules, 24 g each, 100 eV E_{th})

Future: SuperCDMS/EURECA at SNOLAB

- Cooperation between **SuperCDM and EURECA** (CRESST+EDELWEISS) at SNOLAB
- SuperCDMS cryostat payload
  - **initially 50 kg, up to 400 kg**

➡ multi-target approach (Si, Ge, $CaWO_3$) to low-mass WIMP region

Start data taking in 2018

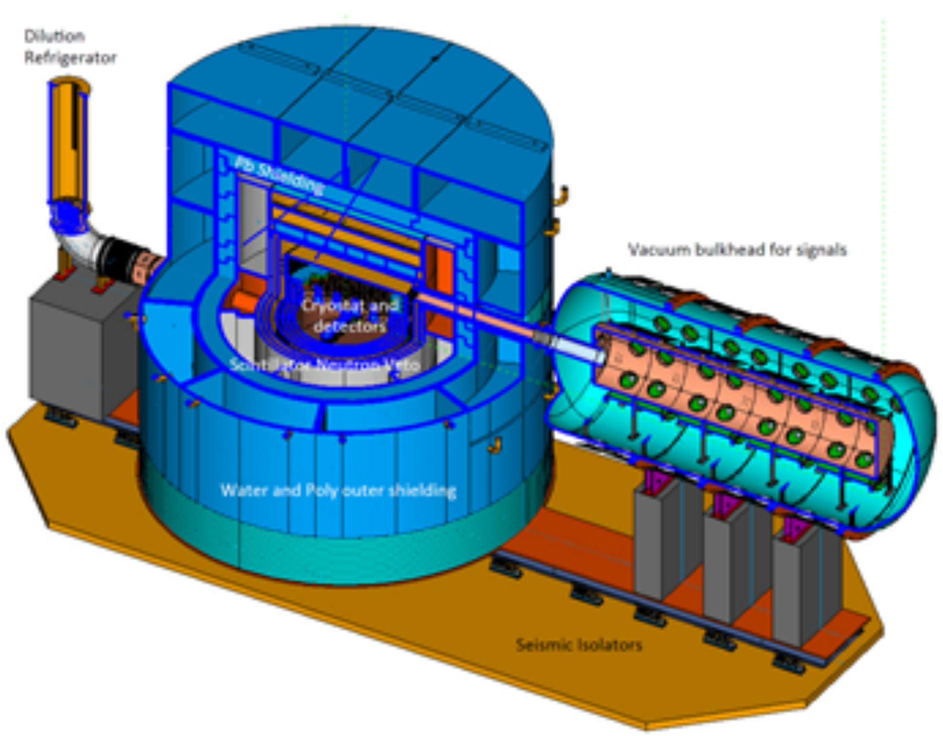

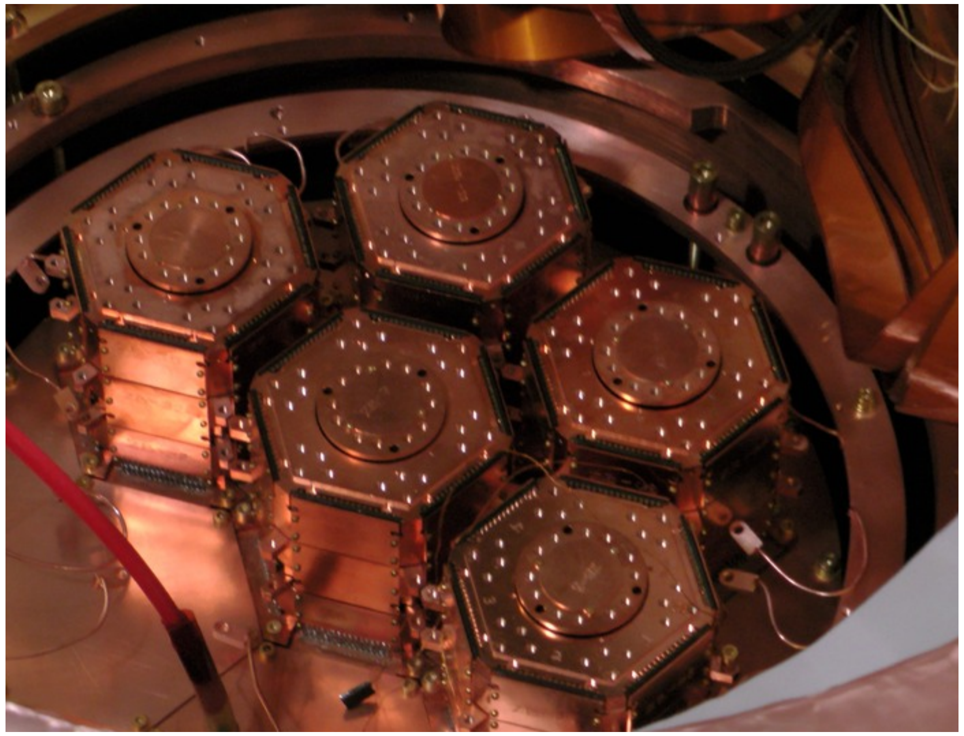

Cryogenic detectors at mK temperatures

Probe low WIMP mass region

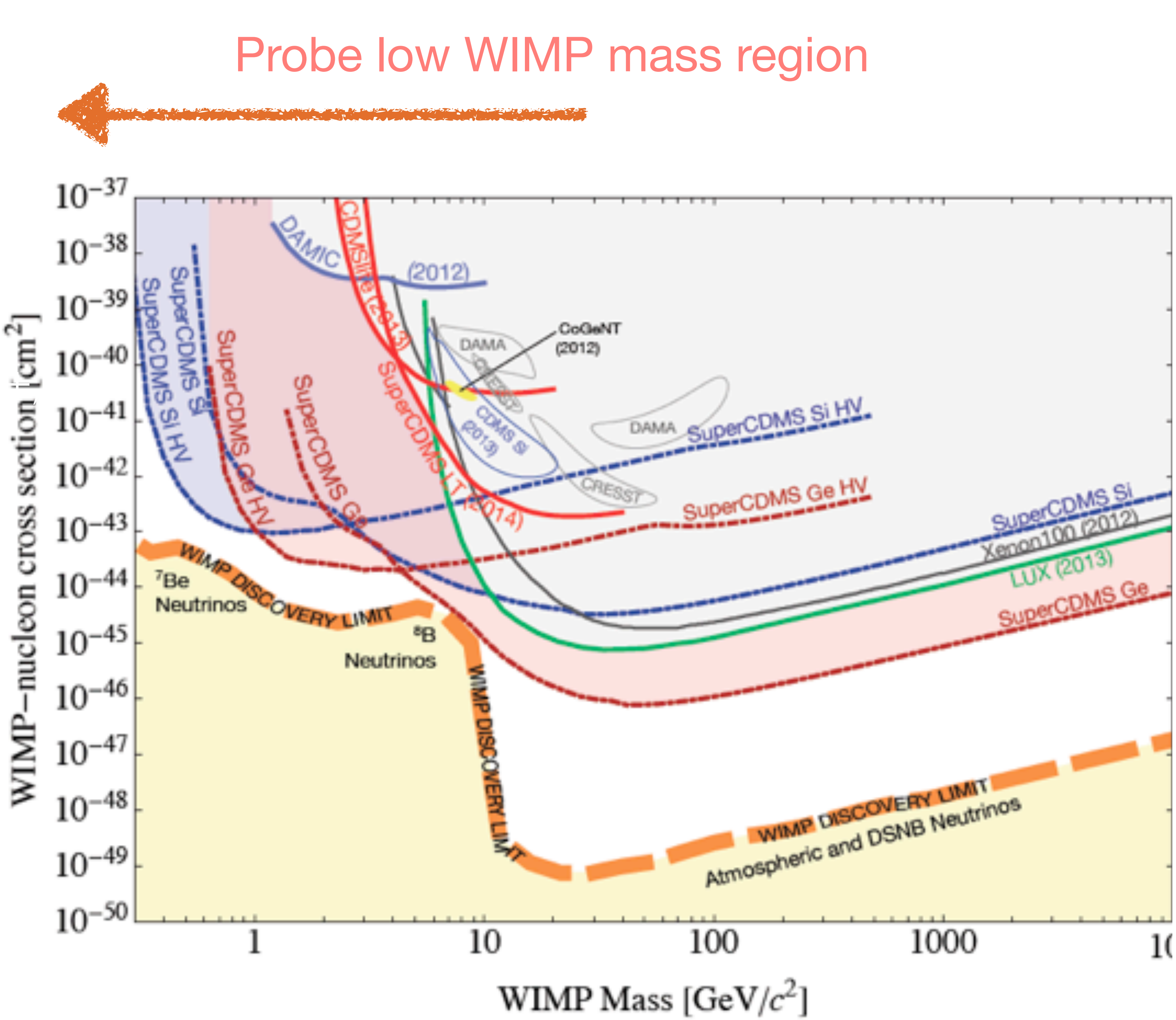

Liquefied noble gases

Cryogenic noble liquids: some properties

- **Xenon ("the strange one")** and **argon ("the inactive one")** used in dark matter detectors
- Dense, homogeneous targets with self-shielding; fiducialization
- Large detector masses feasible at moderate costs
- High light (~40 photons/keV) and charge (W_{LAr} = 24 eV, W_{LXe} = 15 eV) yields

Properties [unit]	**Xe**	**Ar**	**Ne**
Atomic number:	54	18	10
Mean relative atomic mass:	131.3	40.0	20.2
Boiling point T_b at 1 atm [K]	165.0	87.3	27.1
Melting point T_m at 1 atm [K]	161.4	83.8	24.6
Gas density at 1 atm & 298 K [$\mathrm{g\,l^{-1}}$]	5.40	1.63	0.82
Gas density at 1 atm & T_b [$\mathrm{g\,l^{-1}}$]	9.99	5.77	9.56
Liquid density at T_b [$\mathrm{g\,cm^{-3}}$]	2.94	1.40	1.21
Dielectric constant of liquid	1.95	1.51	1.53
Volume fraction in Earth's atmosphere [ppm]	0.09	9340	18.2

W. Ramsay: "These gases occur in the air but sparingly as a rule, for while argon forms nearly 1 hundredth of the volume of the air, neon occurs only as 1 to 2 hundred-thousandth, helium as 1 to 2 millionth, krypton as 1 millionth and xenon only as about 1 twenty-millionth part per volume. *This more than anything else will enable us to form an idea of the vast difficulties which attend these investigations*. "

Ionization in noble liquids

- The energy loss of an incident particle in noble liquids is shared between: *excitation, ionization and sub-excitation electrons liberated in the ionization process*
- The average energy loss in ionization is slightly larger than the ionization potential or the gap energy, because it includes multiple ionization processes

➡ the ratio of the W-value (= average energy required to produce an electron-ion pair) to the ionization potential or gap energy = 1.6 - 1.7

Material	Ar	Kr	Xe
Gas			
Ionization potential I (eV)	15.75	14.00	12.13
W values (eV)	26.4[a]	24.2[a]	22.0[a]
Liquid			
Gap energy (eV)	14.3	11.7	9.28
W value (eV)	23.6 ± 0.3[b]	18.4 ± 0.3[c]	15.6 ± 0.3[d]

- the W-value in the liquid phase is smaller than in the gaseous phase

- the W-value in xenon is smaller than the one in liquid argon, and krypton (and neon)

=> the ionization yield is highest in liquid xenon (of all noble liquids)

The scintillation process in noble liquids

- Scintillation in noble liquids arises in two distinct processes: *excited atoms R* (excitons) and ions R⁺*, both produced by ionizing radiation:

$$\mathrm{R}^* + \mathrm{R} + \mathrm{R} \rightarrow \mathrm{R}_2^* + \mathrm{R}$$

$$\mathrm{R}_2^* \rightarrow 2\mathrm{R} + h\nu$$

$$\mathrm{R}^+ + \mathrm{R} \rightarrow \mathrm{R}_2^+$$

$$\mathrm{R}_2^+ + e^- \rightarrow \mathrm{R}^{**} + \mathrm{R}$$

$$\mathrm{R}^{**} \rightarrow \mathrm{R}^* + \mathrm{heat}$$

$$\mathrm{R}^* + \mathrm{R} + \mathrm{R} \rightarrow \mathrm{R}_2^* + \mathrm{R}$$

$$\mathrm{R}_2^* \rightarrow 2\mathrm{R} + h\nu$$

Excitons (R^*) will rapidly form excited dimers (R^*_2) with neighbouring atoms

The excited dimer R^*_2, at its lowest excited level, is de-excited to the dissociative ground state by the emission of a single UV photon

This comes from the large energy gap between the lowest excitation and the ground level, forbidding other decay channels such as non-radiative transitions

hν = UV photon emitted in the process

The scintillation process in noble liquids

Kubota et al., PRB 20, 1979

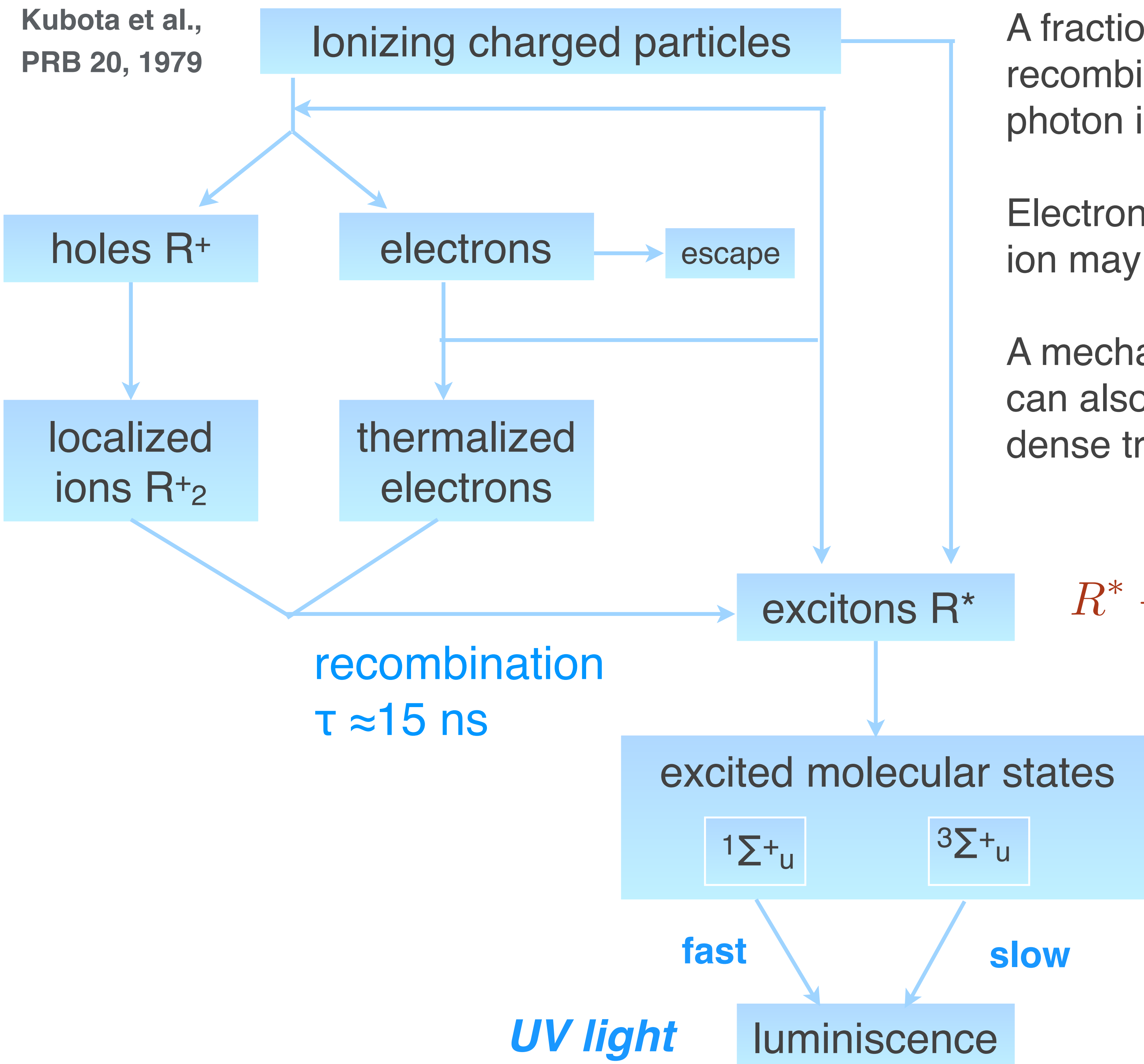

A fraction of the ionization electrons will recombine with ions and produce a scintillation photon in the process called recombination

Electrons that thermalize far from their parent ion may escape recombination

A mechanism called "bi-excitonic quenching" can also reduce the scintillation yield in very dense tracks:

$$R^* + R^* \longrightarrow R_2^{**} \longrightarrow R + R^+ + e^-$$

The energy of the UV photons

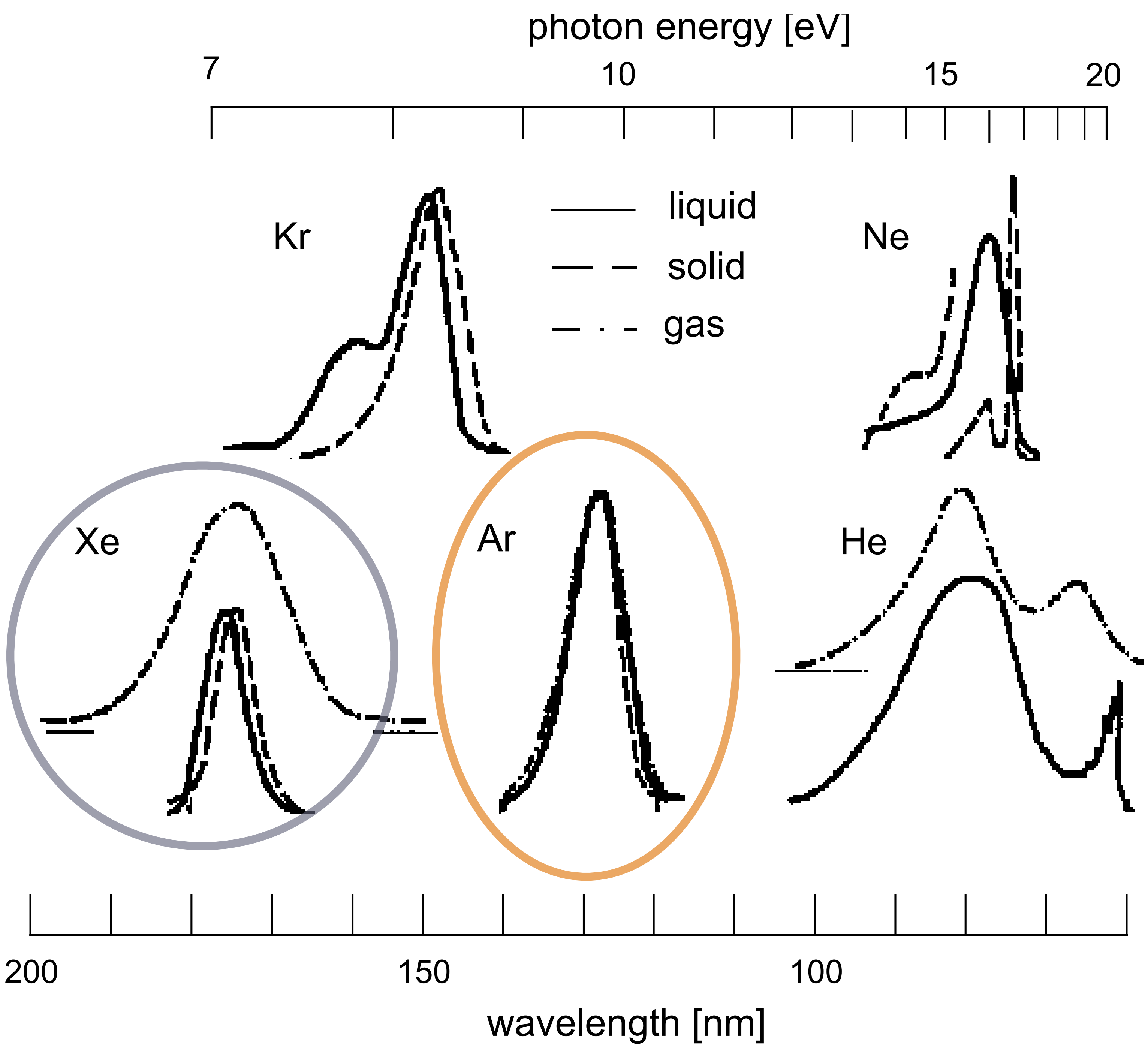

$\lambda_{LNe} \sim 78nm$

$\lambda_{LAr} \sim 128nm$

$\lambda_{LXe} \sim 178nm$

Light yield in noble liquids (nuclear recoils)

- In general, two methods are used:
  - ➡ a direct method using mono-energetic neutrons scatters which are tagged with a n-detector
  - ➡ an indirect method by comparing measured energy spectra in LXe from n-sources (AmBe) with Monte Carlo predictions

$$\mathcal{L}_{\mathrm{eff}}(E_{\mathrm{nr}}) = \frac{L_{y,er}(E_{\mathrm{nr}})}{L_{y,er}(E_{\mathrm{ee}} = 122\,\mathrm{keV})}$$

Direct method example, liquid xenon

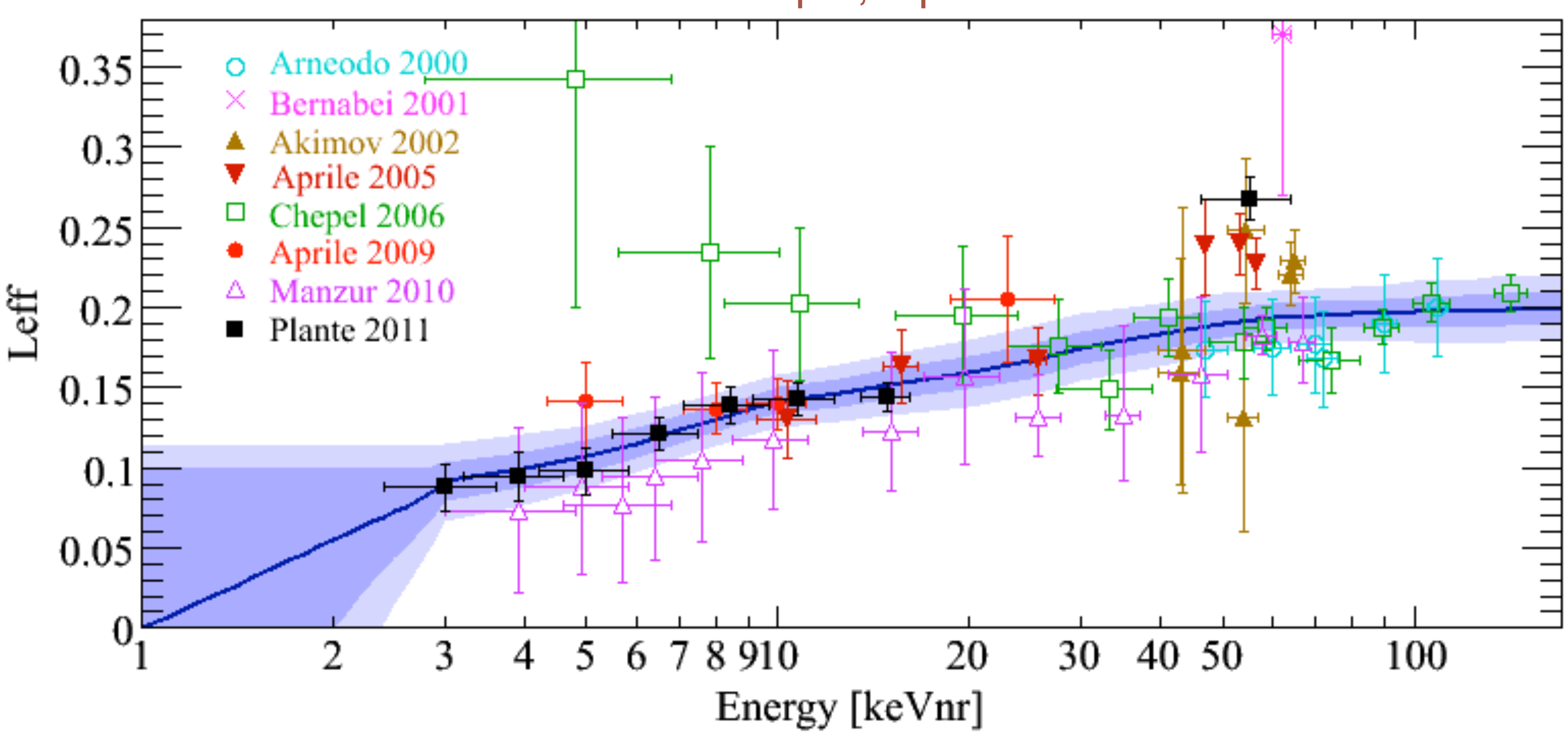

Plante *et al.*, Phys. Rev. C **84**, 045805, 2011

mean (solid) and 1-, 2-sigma uncertainties (blue bands)

Light yield in noble liquids (electronic recoils)

- The light yield decreases with lower deposited energies in the LXe; field quenching is ~ 75%, only weak field-dependance
- The energy threshold of XENON100 is 2.3 keV => can test DAMA/LIBRA

Relative light yield to 32.1 keV of ^{83m}Kr

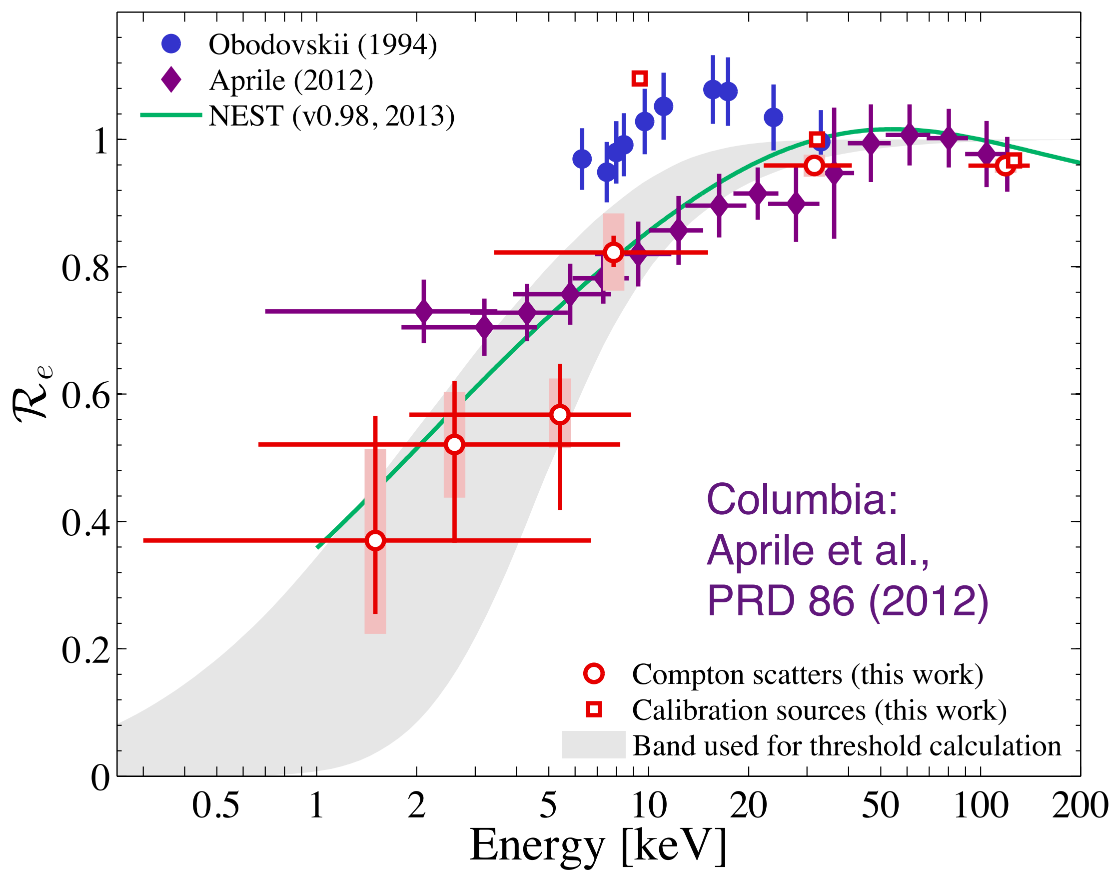

LB et al., PRD 87, 2013; arXiv:1303.6891

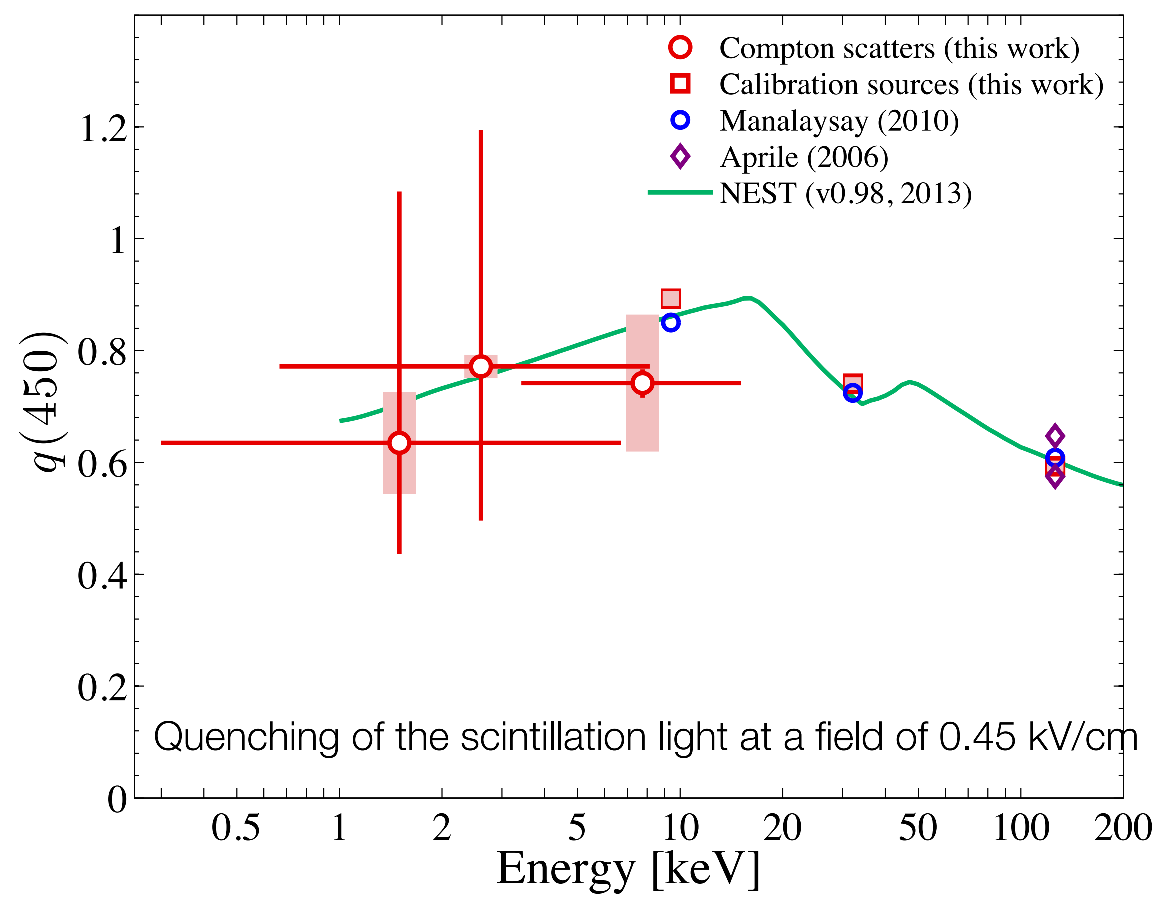

17.3 MBq

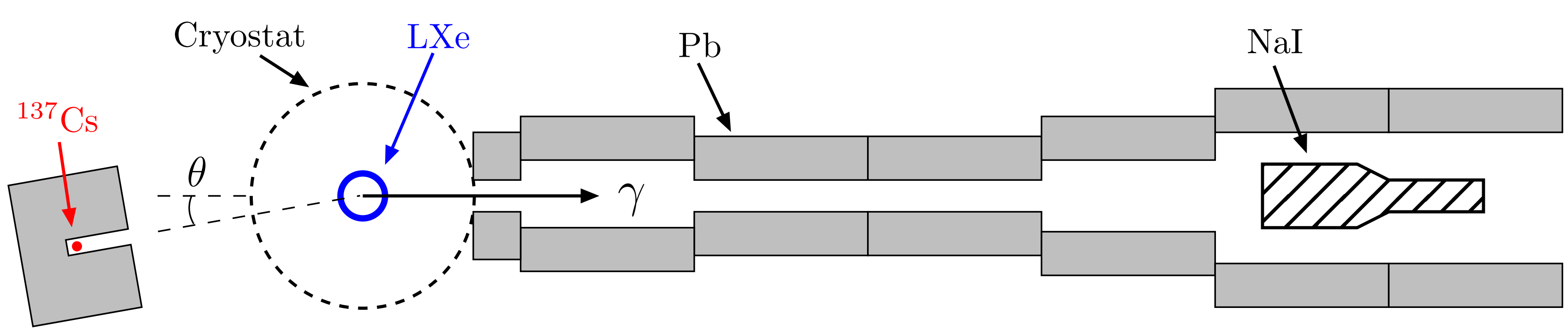

Ionization Yield of Nuclear Recoils in Noble Liquids

- Nuclear recoils have denser tracks, and are assumed to have *larger electron-ion recombination than electronic recoils*

  ➡ in consequence, the collection of ionization electrons becomes more difficult for nuclear than electronic recoils

- The ionization yield of nuclear recoils is defined as the number of observed electrons per unit recoil energy:

$$Q_{y,nr} = \frac{n_{e,nr}}{E_{nr}}$$

- It has been measured mostly in LXe, with two-phase detectors

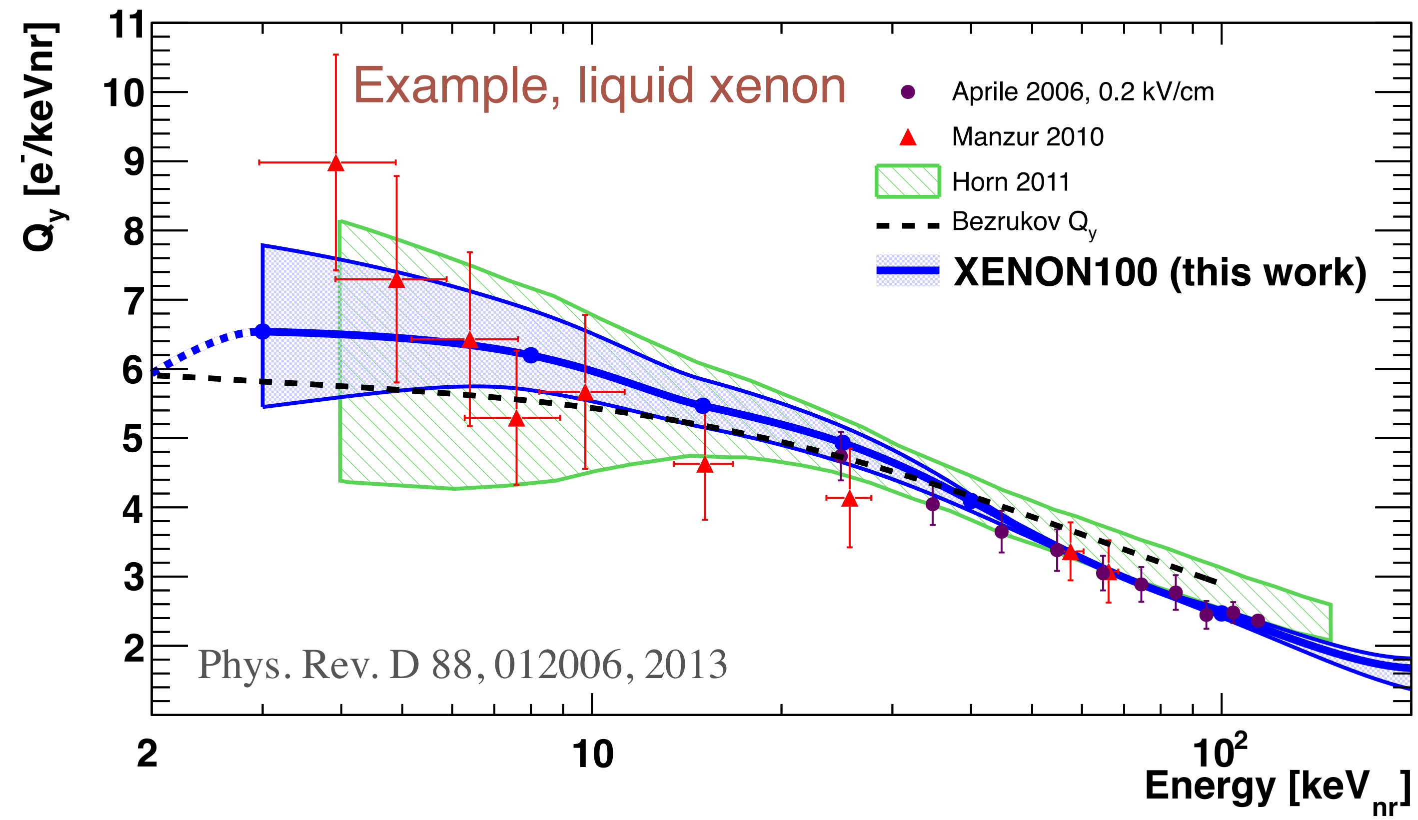

blue: indirect measurement, by data/MC comparison of AmBe neutron calibration data

Ionization Yield of Nuclear Recoils in Noble Liquids

- Charge yield as a function of the applied field
  - ➡ the dependance on the field is weak
  - ➡ the yield increases at low recoil energies - it is argued that this is due to the lower recombination rate expected from the drop in electronic stopping power at low energies
  - ➡ the increase allows the observation of xenon nuclear recoils down to a few keVr, improving the sensitivity for WIMP detection

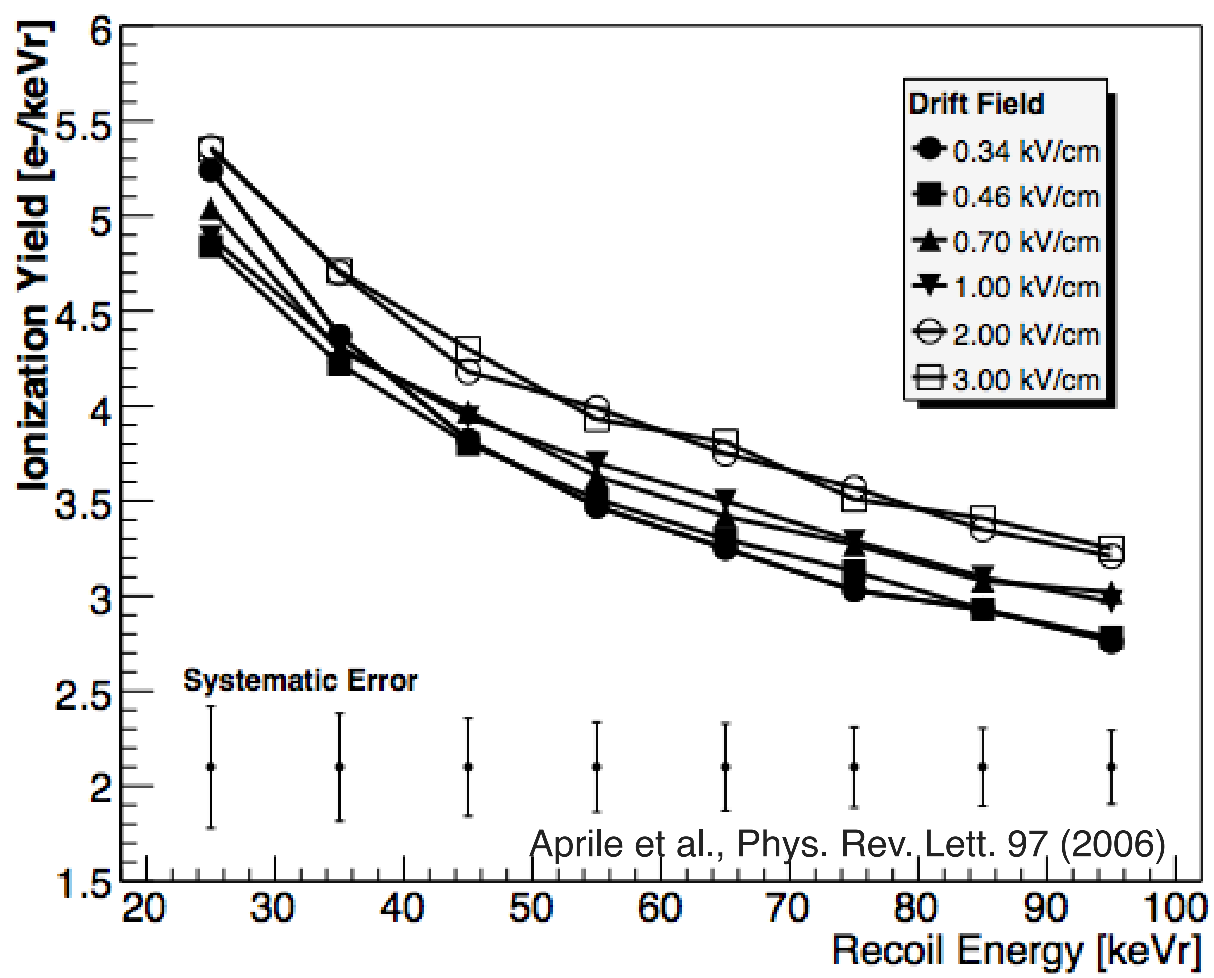

Aprile et al., Phys. Rev. Lett. 97 (2006)

Electron Attachment and Light Absorption

- To achieve a high collection efficiency for both ionization and scintillation signals, the concentration of impurities in the liquid has to be reduced and maintained to a level *below 1 part per 10^9 (part per billion, ppb) oxygen equivalent*
- The scintillation light is strongly reduced by the presence of water vapour
- The ionization signal requires both high liquid purity (in terms of substances with electronegative affinity, SF_6, N_2O, O_2, etc) and a high field (typically ~ kV/cm)
- Attenuation lengths of ~1 m for electrons and photons were already achieved > 1m and are necessary for ton-scale experiments

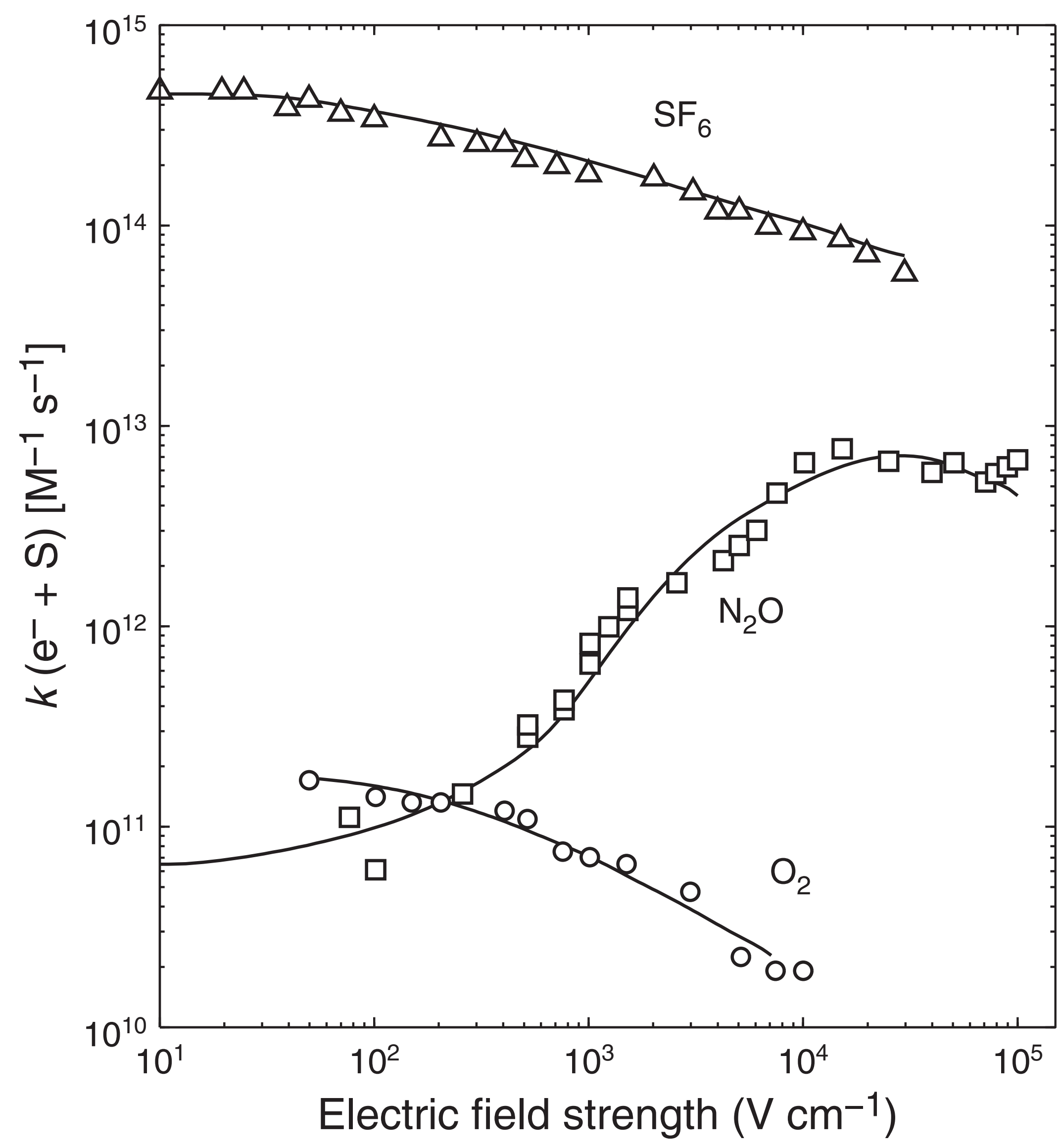

Fig. 21.4. Rate constant for the attachment of electrons in liquid xenon (T = 167 °K) to several solutes: (△) SF_6, (□) N_2O, (○) O_2 [174].

Particle discrimination

- Pulse shape of prompt scintillation signal (LAr)
  - ➡ the ratio of light from singlet and triplet depends on dE/dx (~ 10:1 for NRs:ERs)
- Charge versus light (LAr and LXe)
  - ➡ the recombination probability, and thus the S2-to-S1 ratio depends on dE/dx

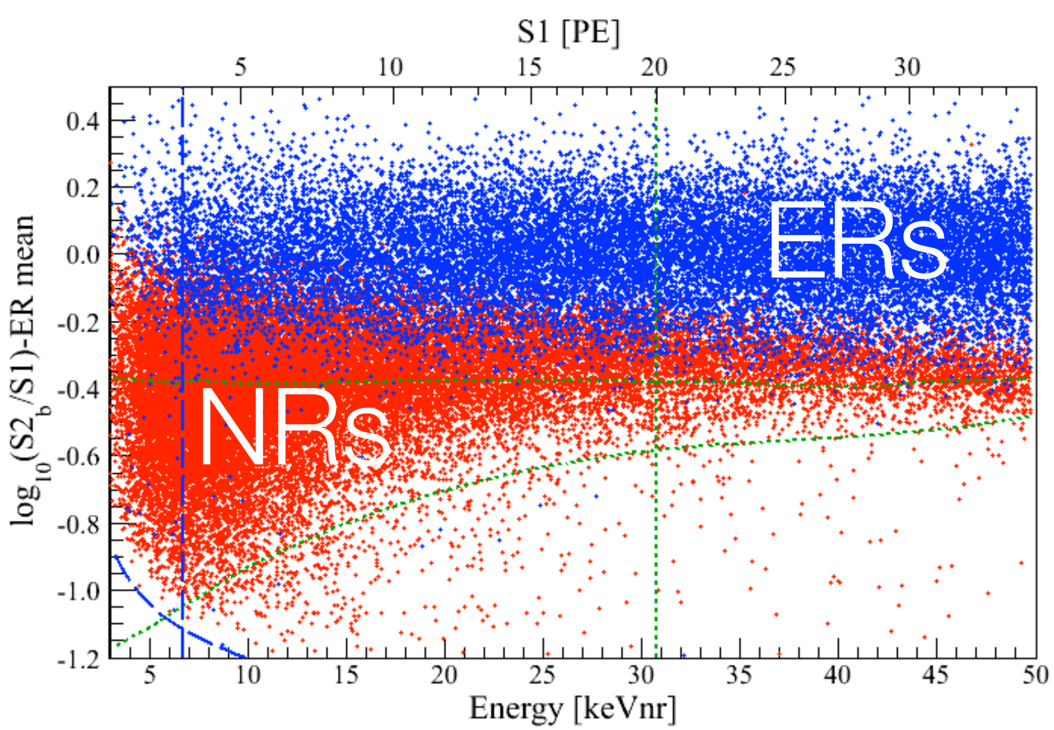

LXe (XENON100)

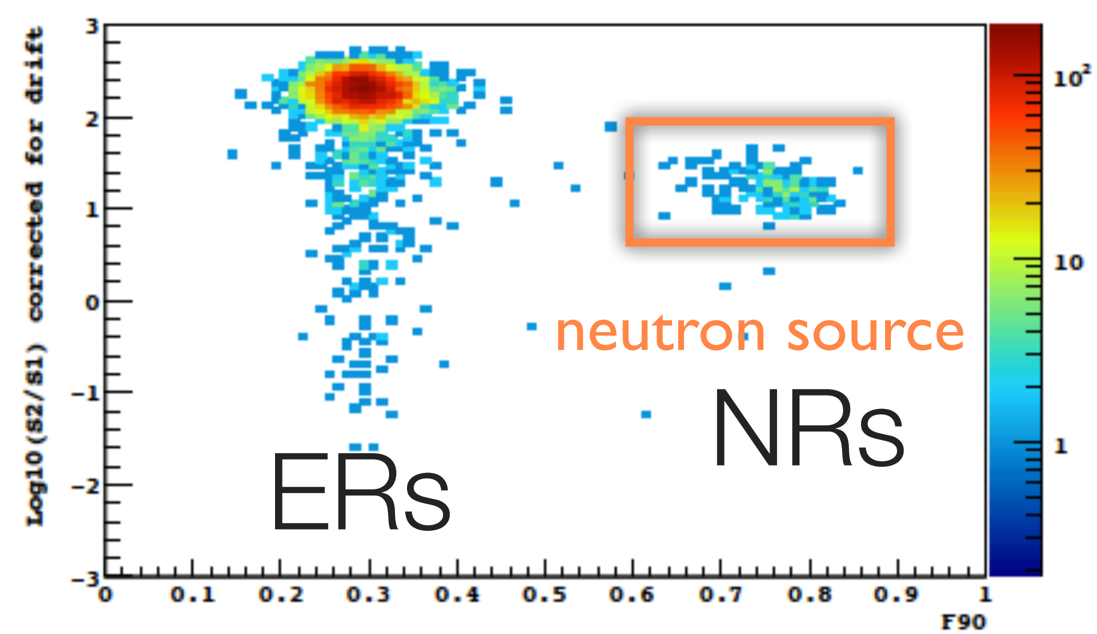

LAr (DarkSide-10)

Cryogenic Noble Liquids: some challenges

- Cryogenics: efficient, reliable and cost effective cooling systems
- Detector materials: compatible with low-radioactivity and purity requirements
- Intrinsic radioactivity: ^{39}Ar and ^{42}Ar in LAr, ^{85}Kr in LXe, radon emanation/diffusion

- **Light detection:**
  - ➡ efficient VUV PMTs, directly coupled to liquid (low T and high P capability, high purity), effective UV reflectors (also solid state Si devices are under study)
  - ➡ light can be absorbed by H_2O and O_2: continuous recirculation and purification
- **Charge detection:**
  - ➡ requires << 1ppb (O_2 equivalent) for e^--lifetime > 1 ms (commercial purifiers and continuous circulation)
  - ➡ electric fields ≥ 1 kV/cm required for maximum yield for MIPs; for alphas and NRs the field dependence is much weaker, challenge to detect a small charge in presence of HV

Single-phase noble liquid detectors

Instrumented LAr or LXe volume

Scintillation light in VUV region

PMT array

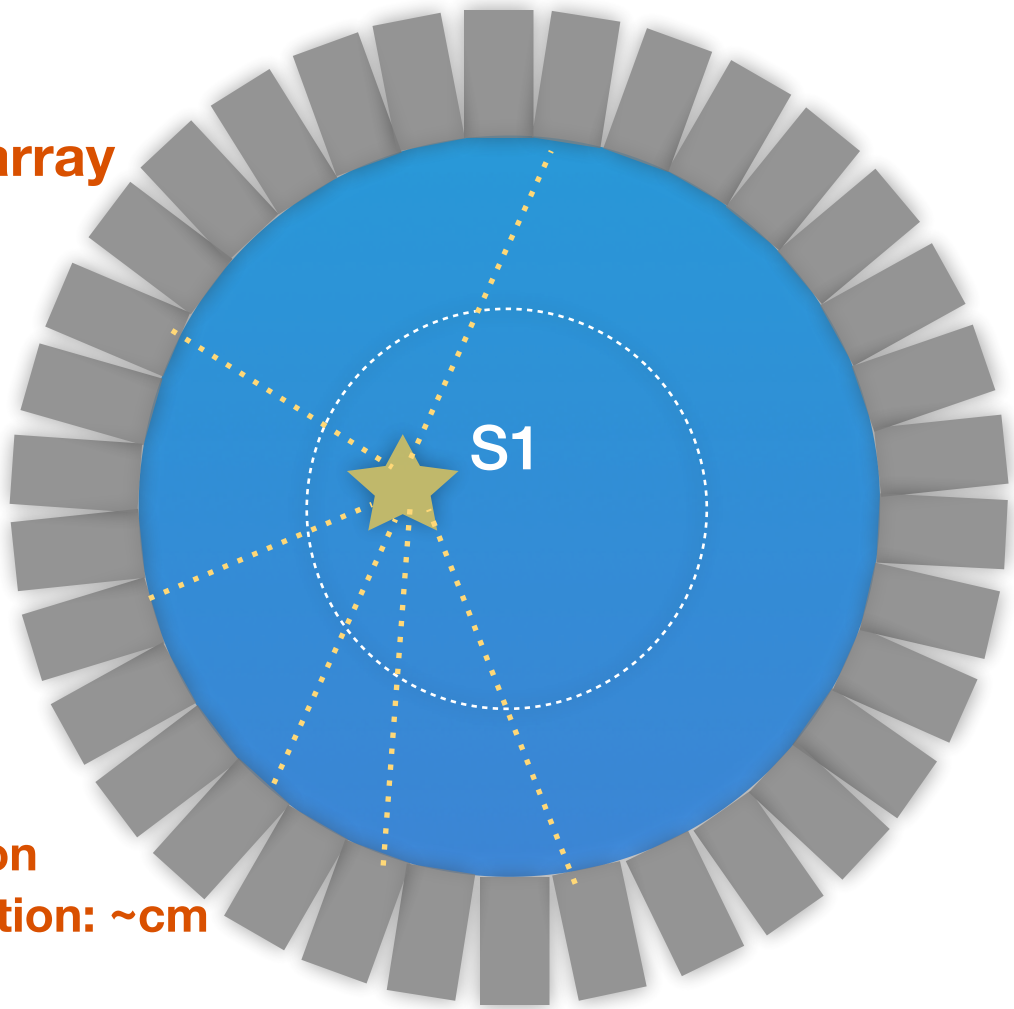

position resolution: ~cm

Xenon

XMASS at Kamioka, 832 kg

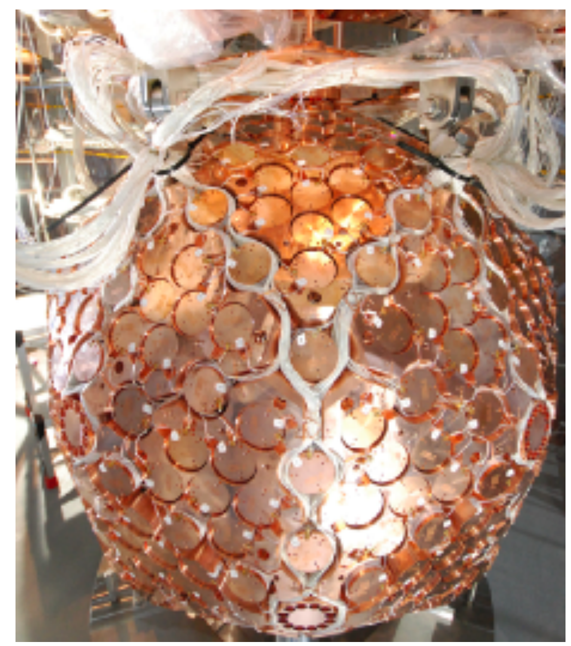

Refurbished, running since 2013
Results in 2016

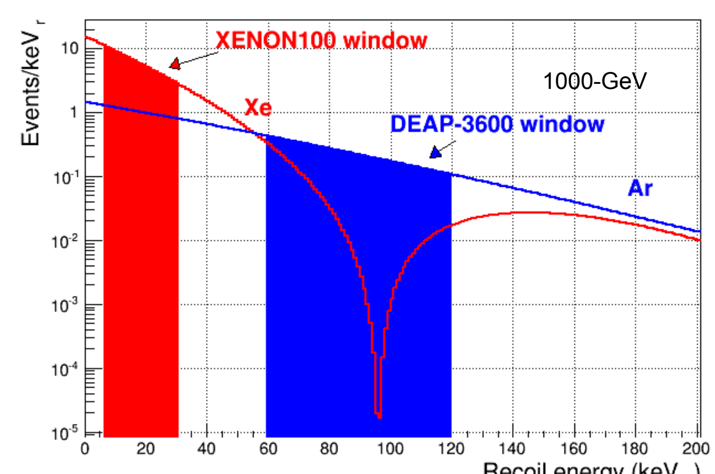

Argon

DEAP-3600 at SNOLAB, 3.6 t

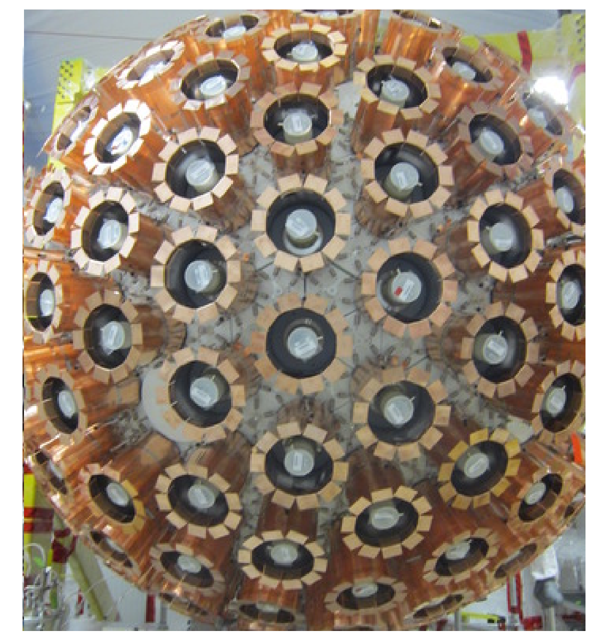

In commissioning
First data and results in late 2015 and early 2016
~ 1 x 10^{-46} cm^2 sensitivity, 3 yr run

The Double-Phase Detector Concept

- Particle interaction in the active volume produces *prompt scintillation light (S1)* and ionization electrons

- Electrons drift to interface (E= 0.53 kV/cm) where they are extracted and amplified in the gas. Detected as *proportional scintillation light (S2)*

    - $(S2/S1)_{WIMP} \ll (S2/S1)_{Gamma}$

    - 3-D position sensitive detector with particle ID

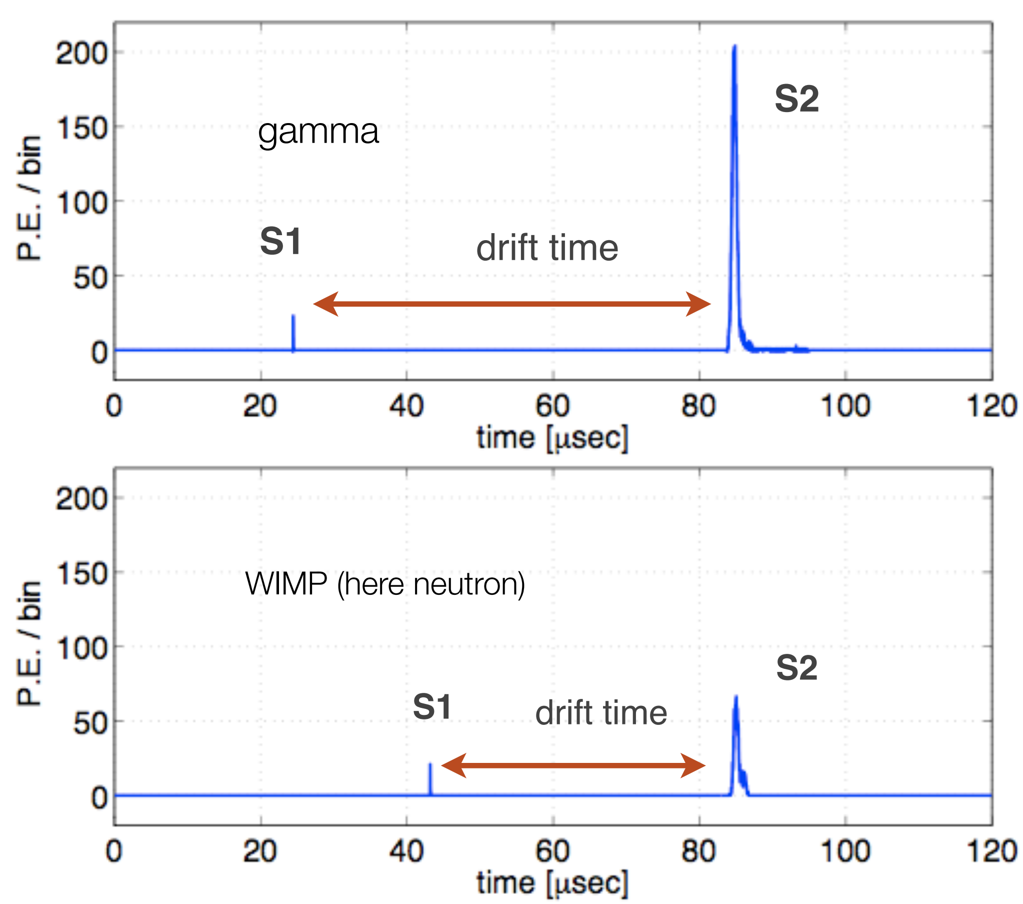

Xe (A=131); λ = 178 nm

position resolution:

<3mm in x-y; < 0.3 mm in z

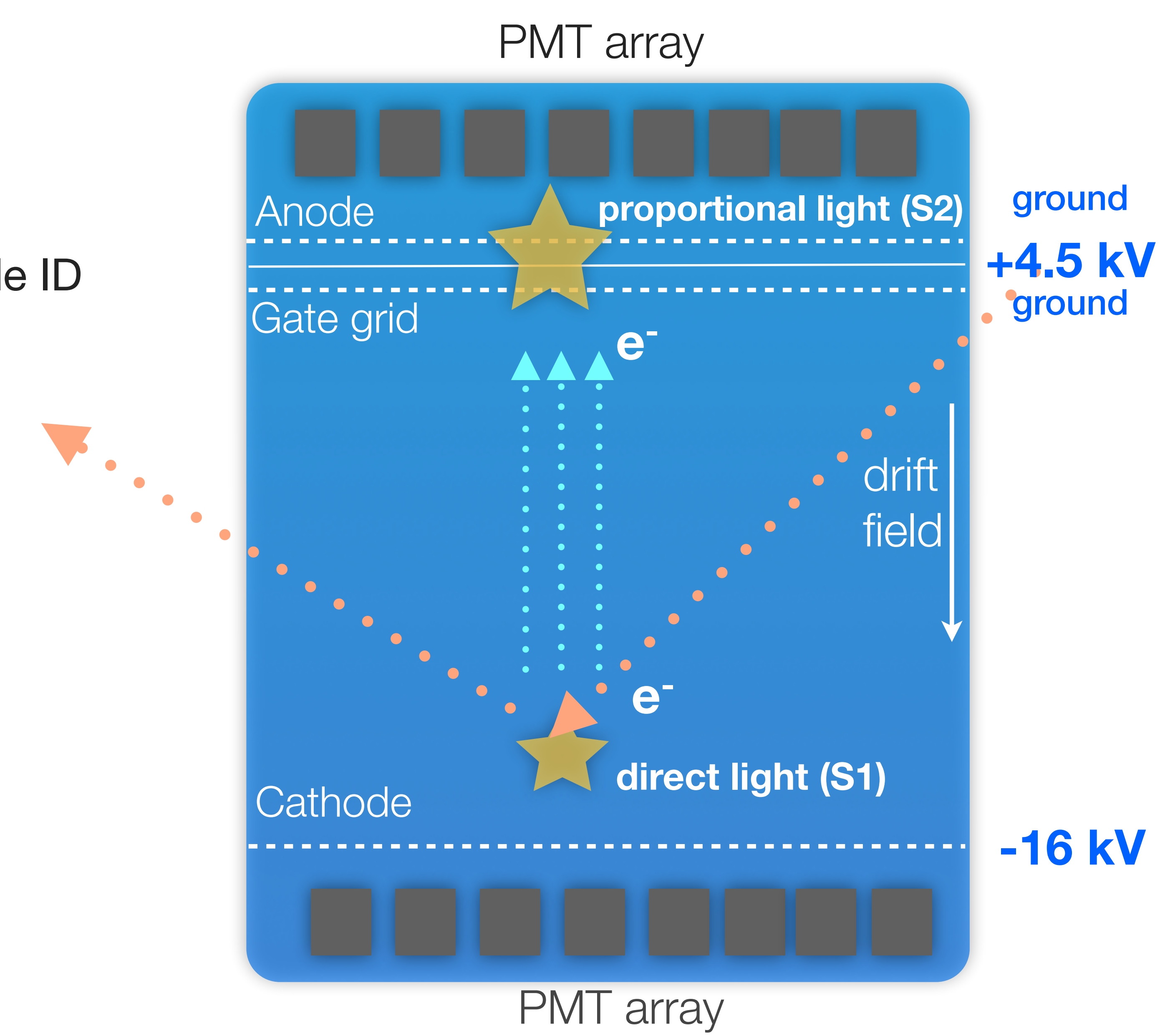

Overview: existing projects

DarkSide50 in LS shield at LNGS:

50 kg LAr (~33 kg fiducial), dual-phase, 38 PMTs taking science data

LUX: In water Cherenkov shield at SURF:

350 kg LXe (100 kg fiducial), dual-phase, 122 PMTs, second run started in 2015

XENON100 in conventional shield at LNGS:

161 kg LXe (~50 kg fiducial), dual-phase, 242 PMTs taking calibration data

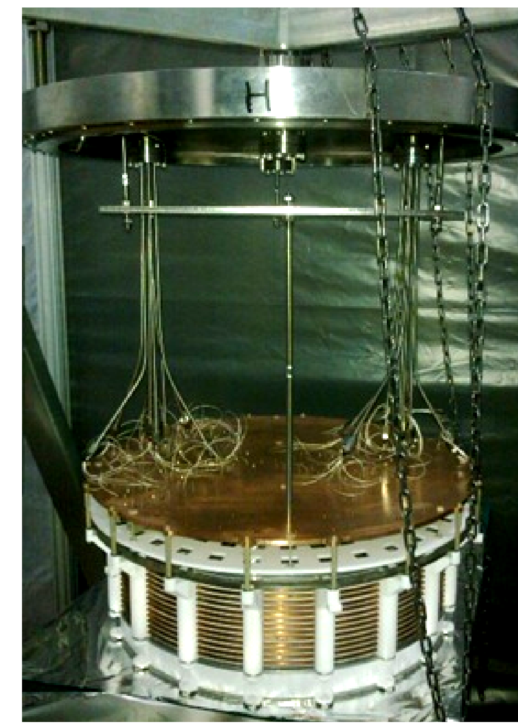

PandaX in conventional shield at CJPL:

stage I: 123 kg LXe (25 kg fiducial), dual-phase, 180 PMTs
stage II: 500 kg, running

Example: the XENON100 detector

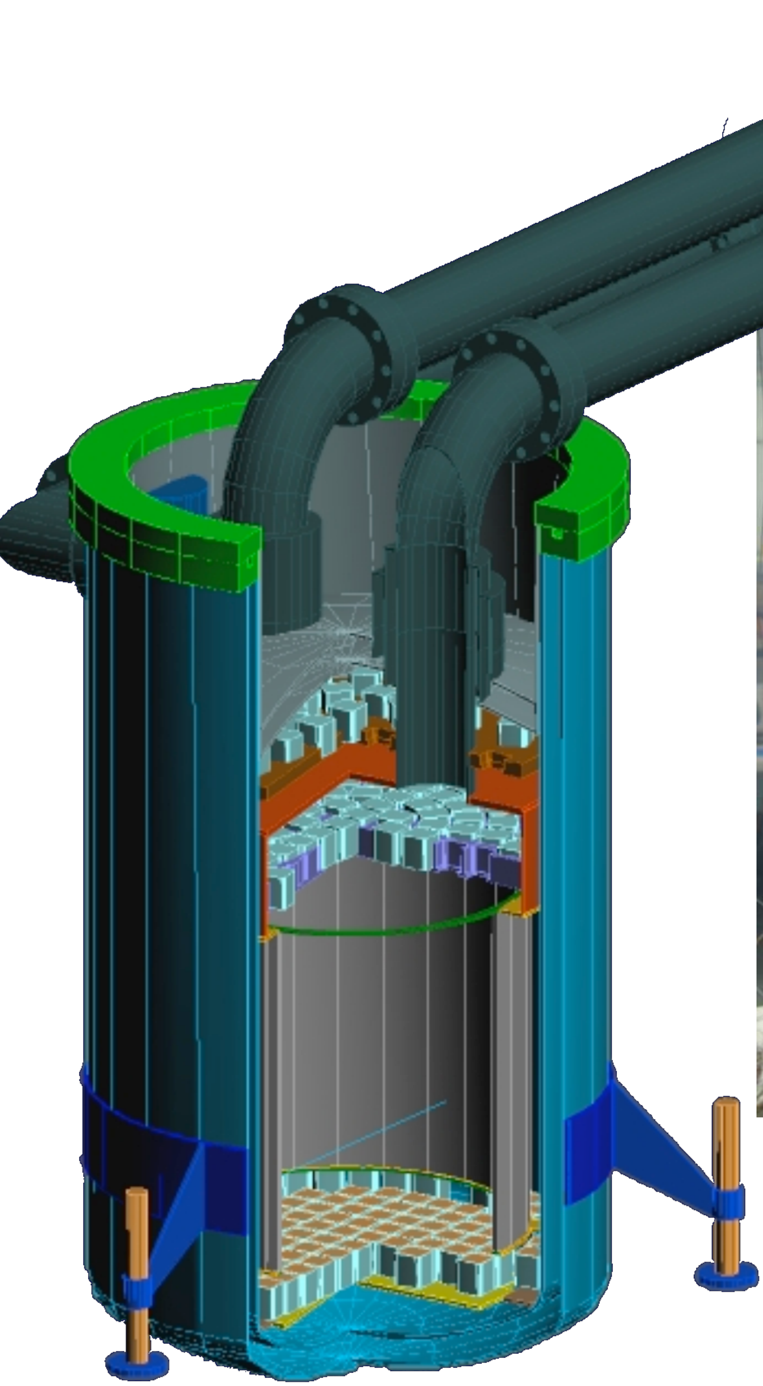

Instrument described in: Astroparticle Physics 35, 573-590, 2012

TPC with 30 cm drift x 30 cm diameter

161 kg ultra pure LXe (62 kg as target)

1” square PMTs with ~1 mBq (U/Th)

Requirements:

100 x less background than XENON10

10 x more fiducial mass than XENON10

Solutions:

Cryocooler and FTs outside shield

Materials screened for low radioactivity

LXe scintillator active veto system

Improved passive shield system

Dedicated Kr distillation column

The XENON100 detector design

Astropart.Phys. 35 (2012) 573-590

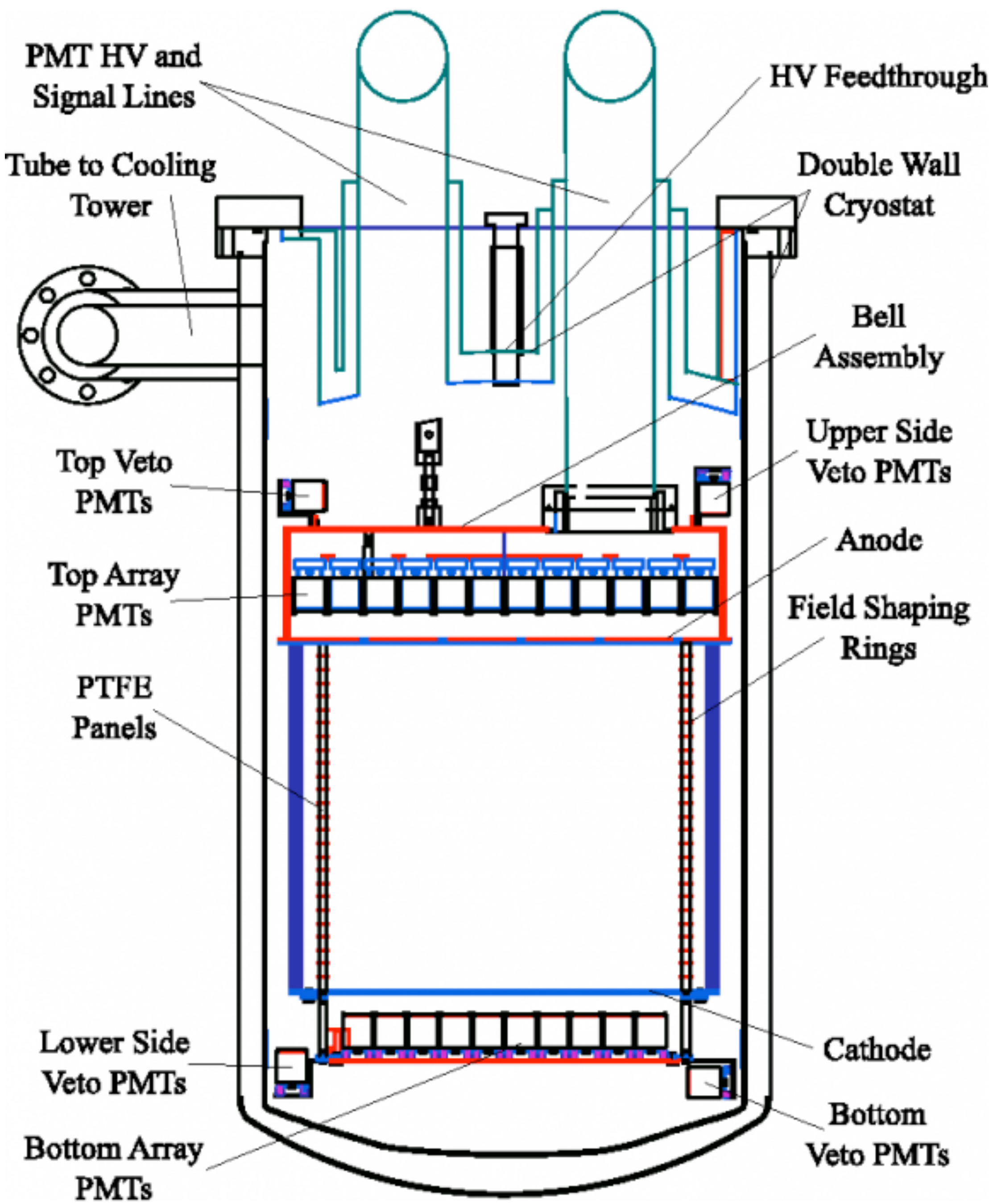

- TPC with 30.6 cm height, 15.3 cm radius, made of 24 interlocking teflon panels
- Drift field (0.53 kV/cm) generated between cathode on bottom (-16 kV) and grounded gate grid on top
- Anode at +4.5 kV between two grounded grids: extraction field of ≈ 12 kV
- Field shaping rings (40) for homogeneous drift field inside the TPC
- Liquid xenon shield (99kg), 4 cm thick, optically separated from the TPC
- 242 PMTs: 98 on top, 80 on bottom, 64 in the liquid xenon shield
- Because of the 1.69 refractive index of LXe, about 80% of the S1 signal is seen by the bottom PMT array

The photosensors

- 1-inch square R8520 Hamamatsu PMTs, optimized to work at LXe T and P, and of low-radioactivity (< 1 mBq/PMT in $^{238}U/^{232}Th$)
- Top array: 98 PMTs (23% quantum efficiency) in concentric circles to improve radial event position reconstruction, teflon holder
- Bottom array: 80 PMTs, closely packed, and of higher quantum efficiency (~ 33% at 178 nm), for efficient S1 light collection
- Liquid xenon veto: 64 PMTs, 23% quantum efficiency


top array

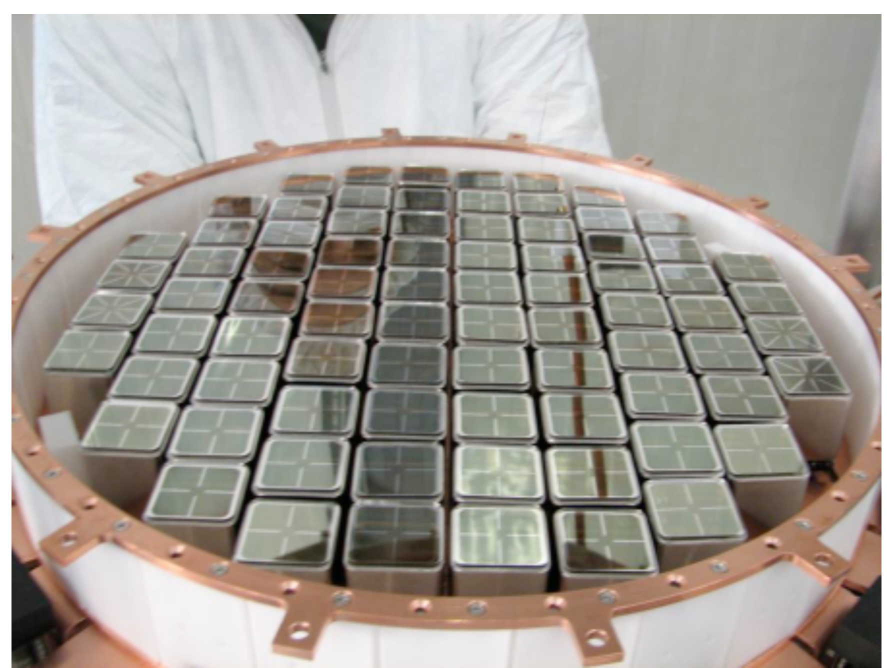
bottom array

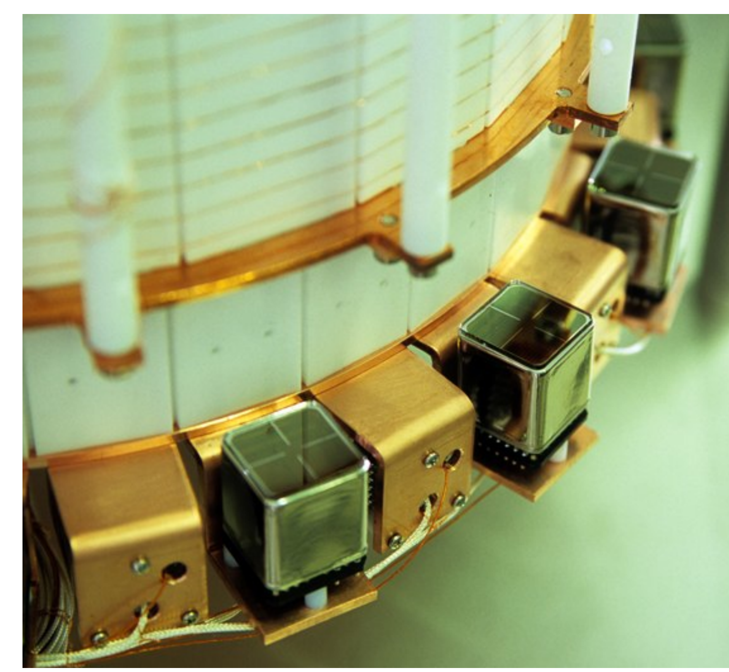
veto PMTs

Screening results in Astroparticle Physics 35, 43-49, 2011

Location and shield

- Gran Sasso Laboratory: shield against cosmic rays: 1.4 km of mountain
- Passive shield:
  ➡ 5 cm (2 tons) of Cu, 20 cm (1.6 tons) of PE, 20 cm (33 tons) of Pb, plus 20 cm water shield
- Detector housing is continuously purged with boil-off N_2, to maintain a radon level < 0.5 Bq/m^3
- All materials were screened with HPGe detectors at LNGS `JINST 6 P08010, 2011`

Screening results in Astroparticle Physics 35, 43-49, 2011

1 m

Example of a low-energy event

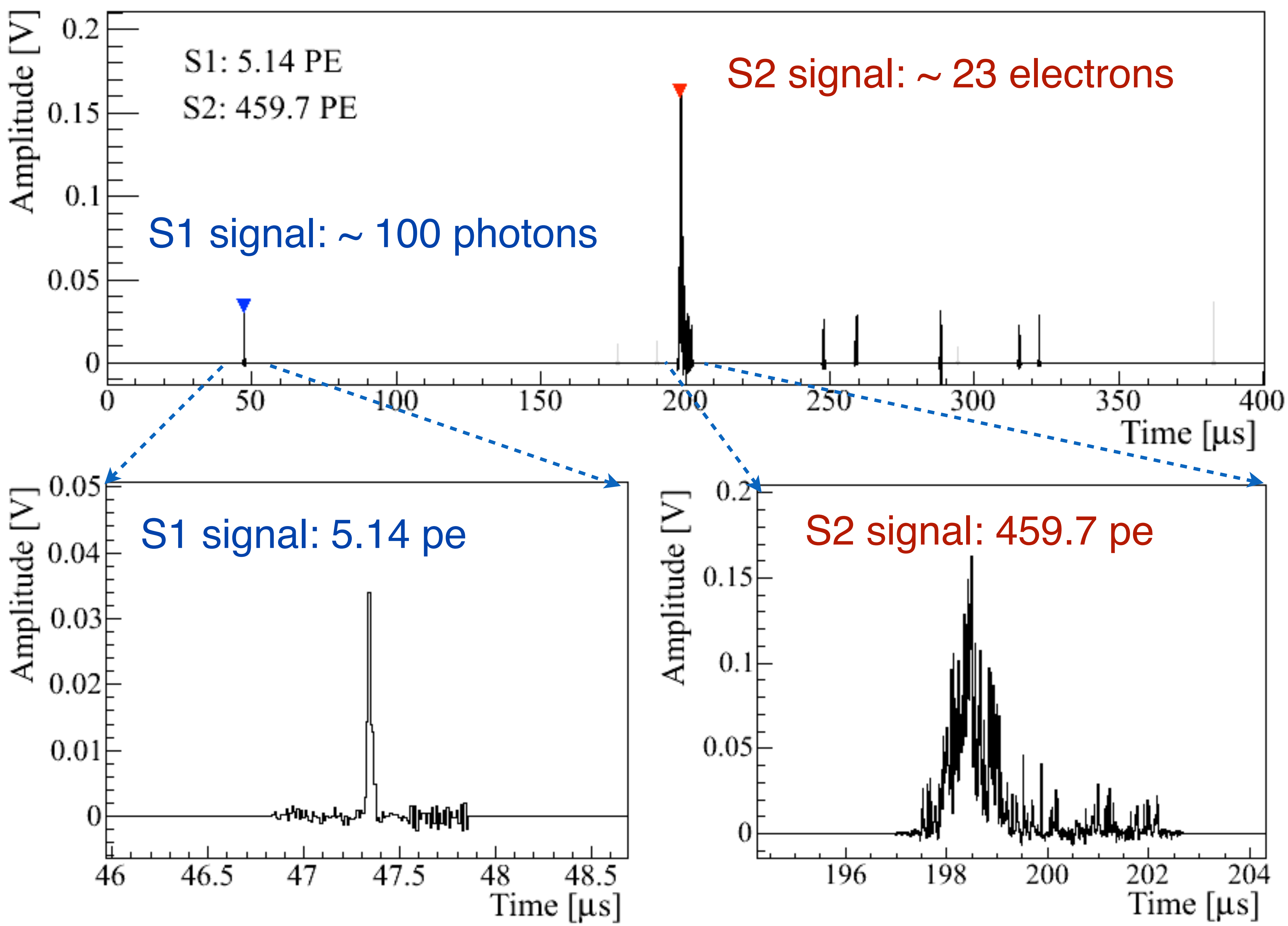

Example of a low energy (9 keV$_{nr}$) nuclear recoil

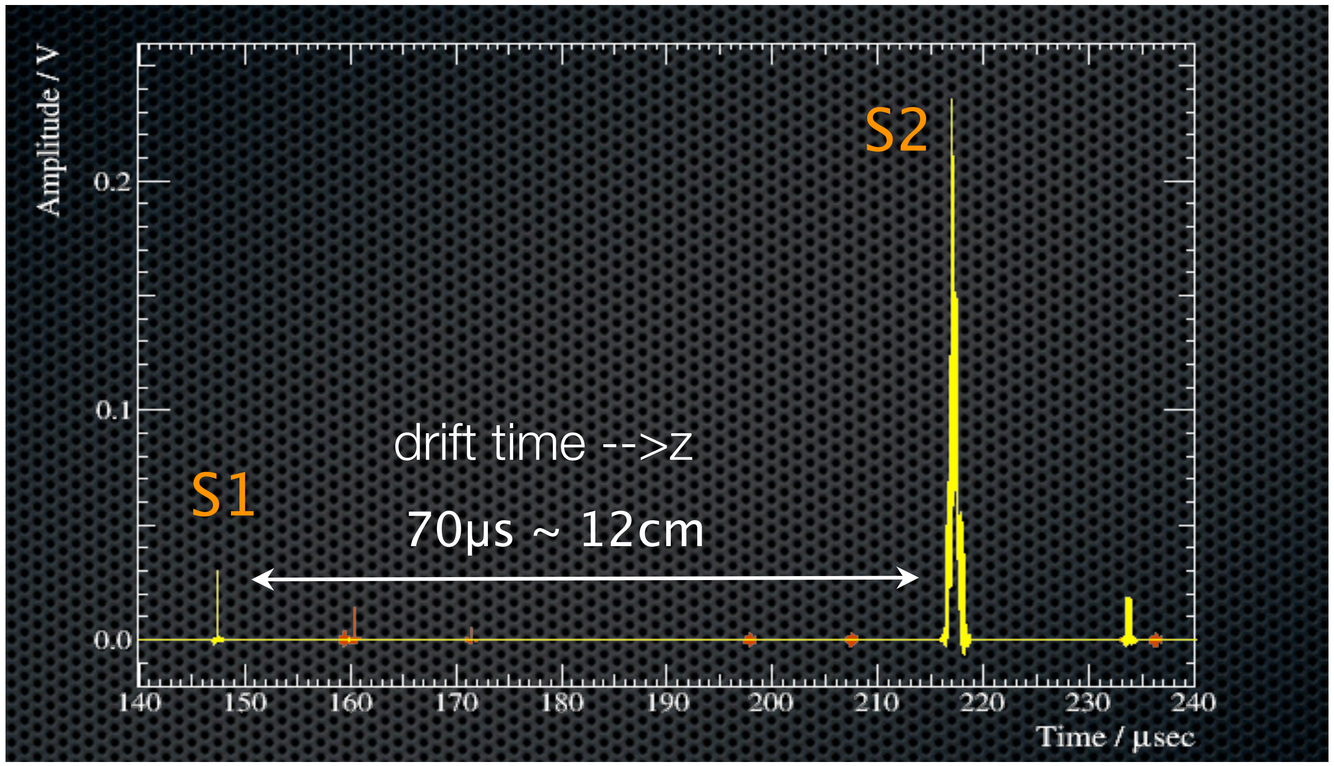

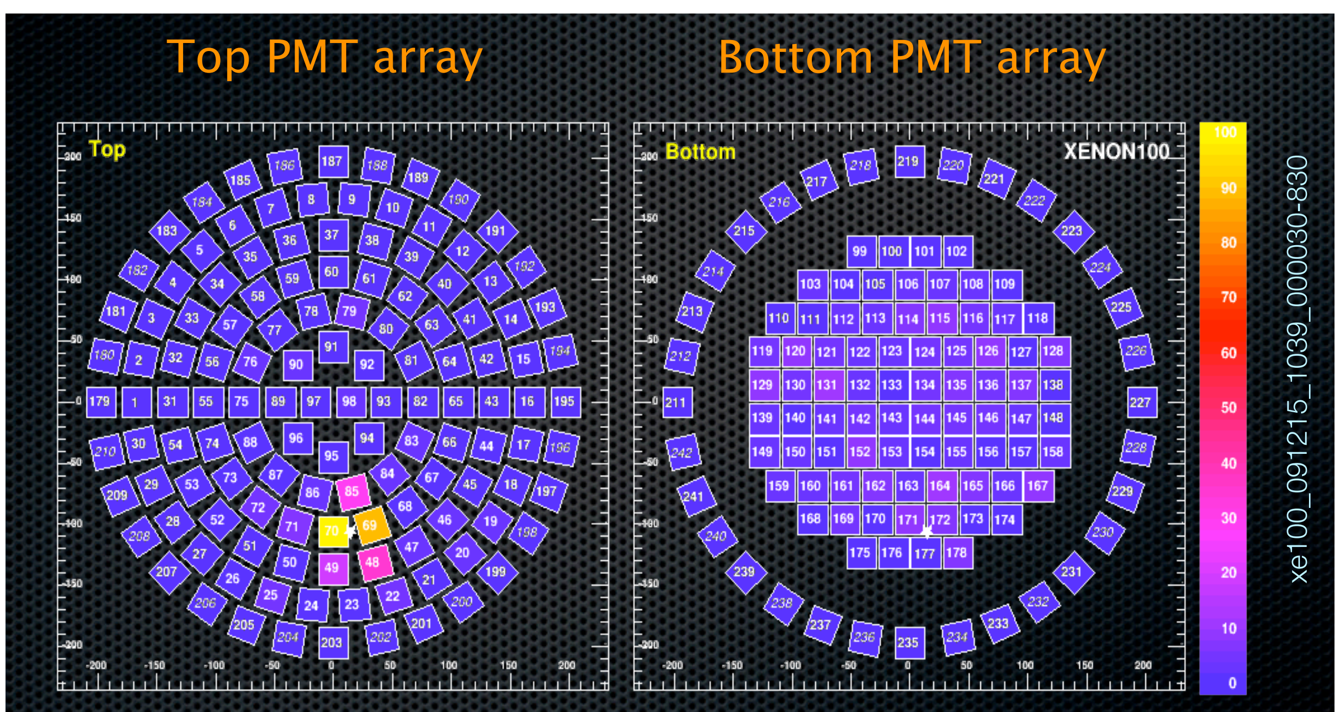

4 photoelectrons detected from about 100 S1 photons

645 photoelectrons detected from 32 ionization electrons which generated about 3000 S2 photons

the measured drift times gives the z-coordinate of the interaction

the measured PMT-hit-pattern in the top array provides the x-y-position of the interaction

The measured background in XENON100

- Data and MC (no MC tuning; before the active LXe veto cut)
- Region above ~ 1500 keV: saturation in the PMTs
- The background meets the design specifications:

➡ 100 times lower than in XENON10

XENON100 collaboration, arXiv:1101.3866, PRD 83, 082001 (2011)

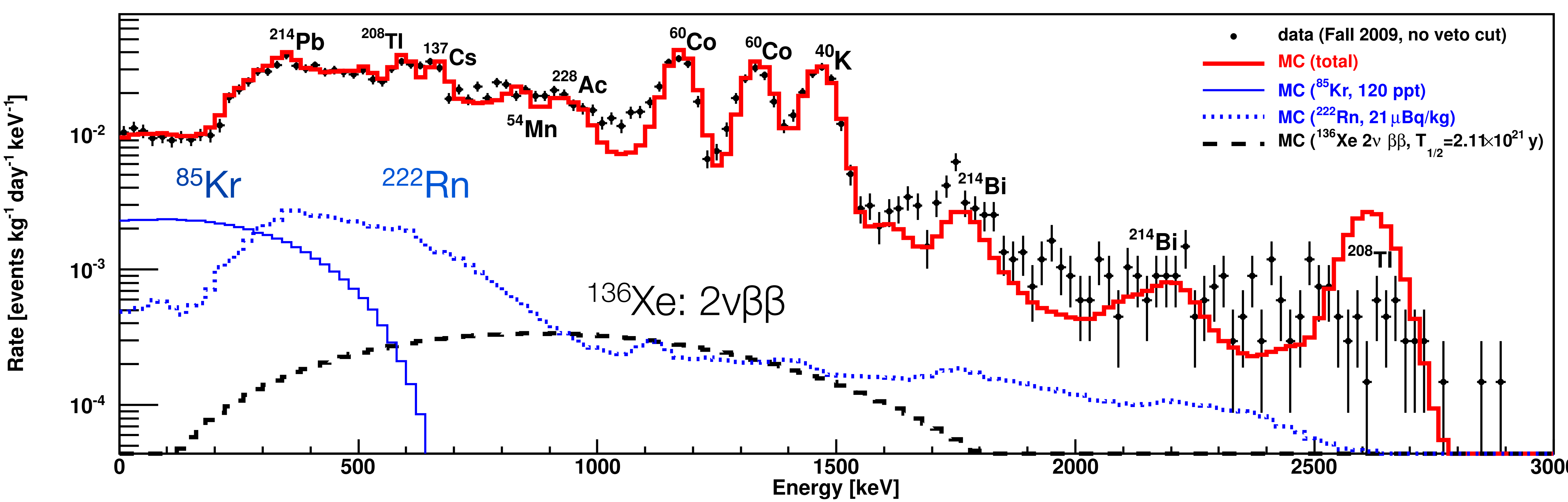

Calibration of ER and NR bands

- The electronic recoil (ER) band is calibrated with high energy gammas from ^{60}Co and ^{232}Th sources
- This data is also used to determine the background in the signal region due to low-energy Compton scatters
- The nuclear recoils band (NR) is calibrated with an AmBe neutron source
- Single scatters from elastic neutron-xenon collisions are used to define the expected WIMP signal region

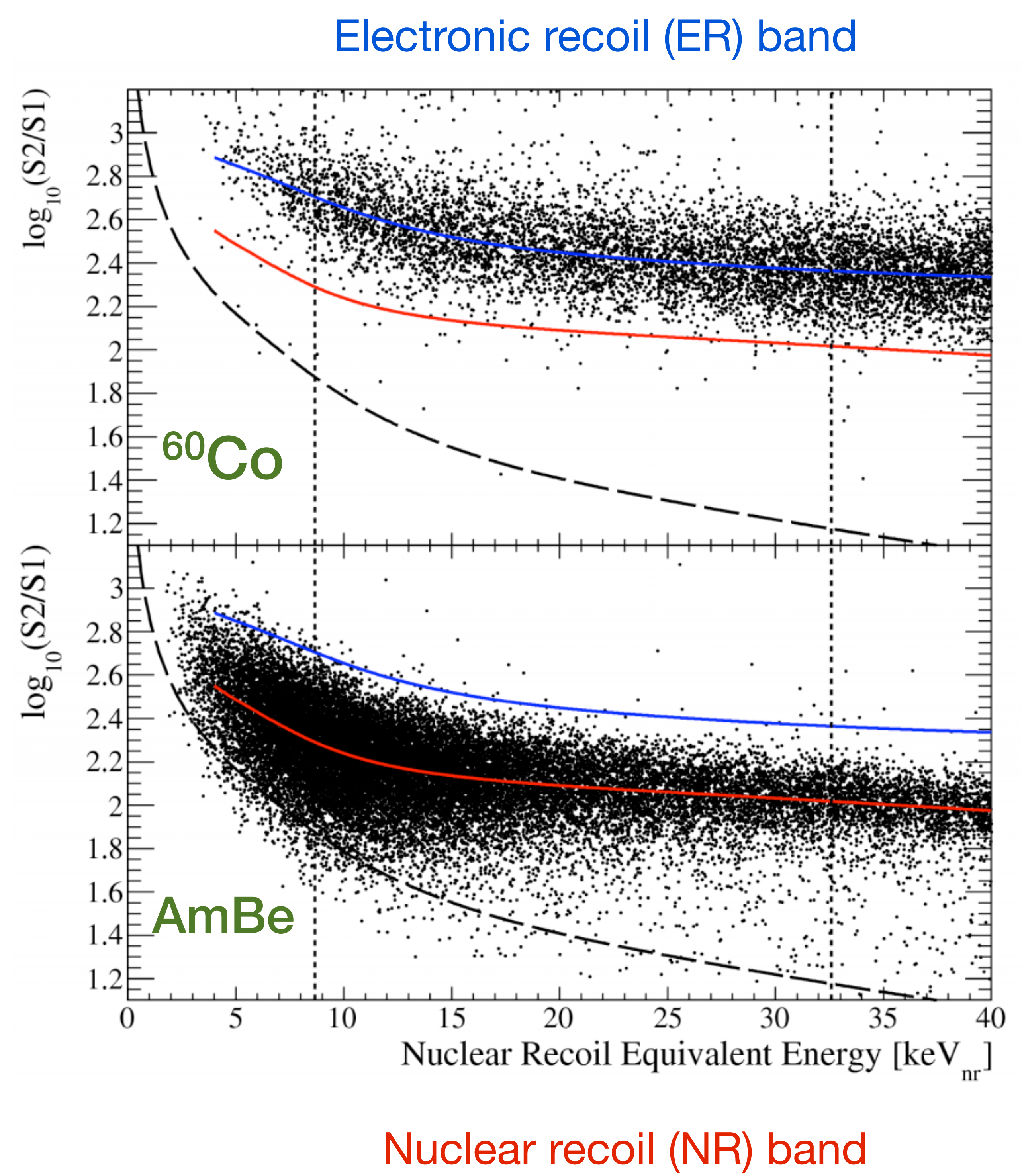

Nuclear recoils: data and MC

- Matching the AmBe data with MC simulations

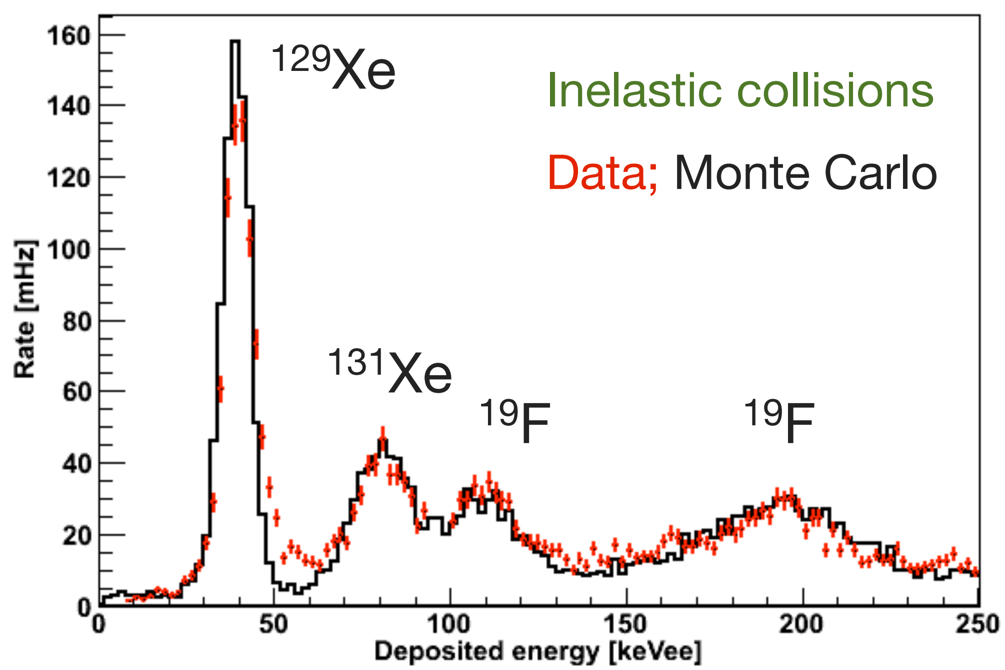

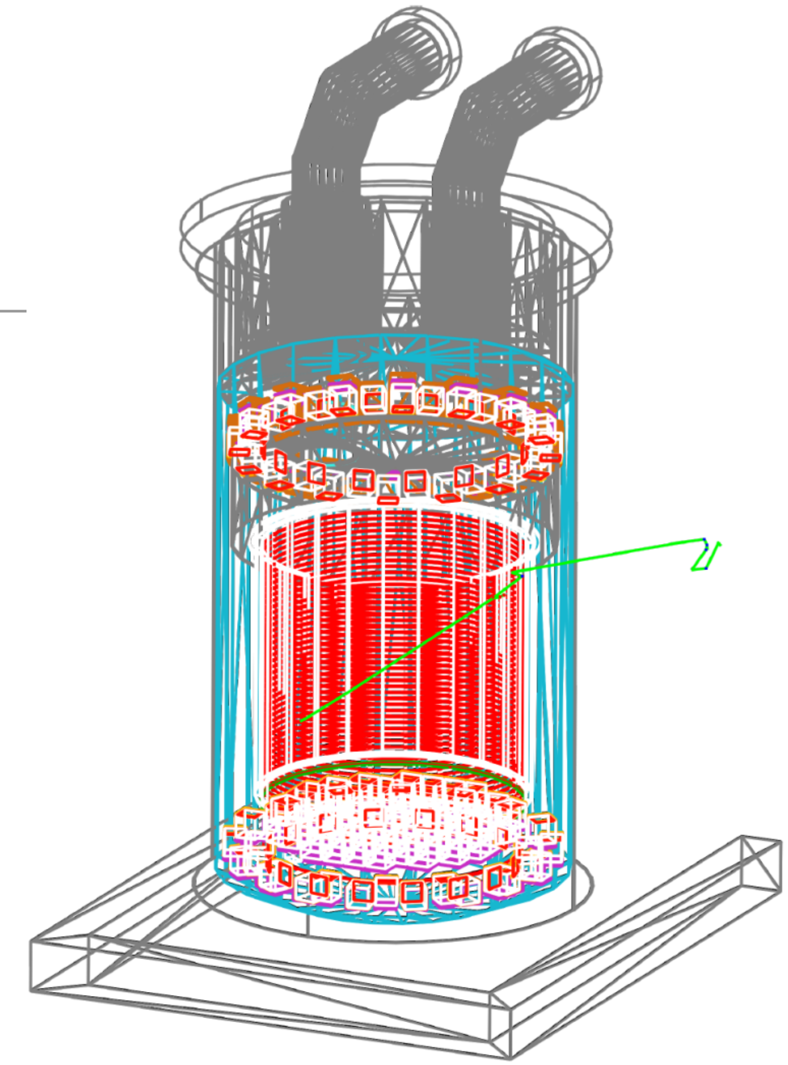

Elastic collisions, S2 versus S1

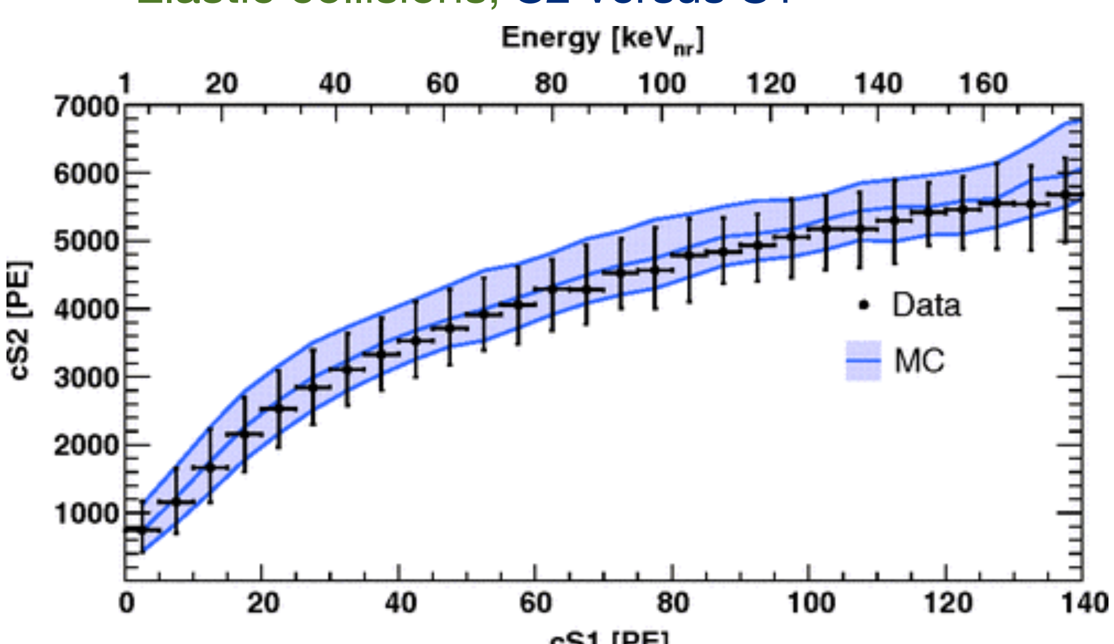

arXiv: 1304.1427

Elastic collisions, S2

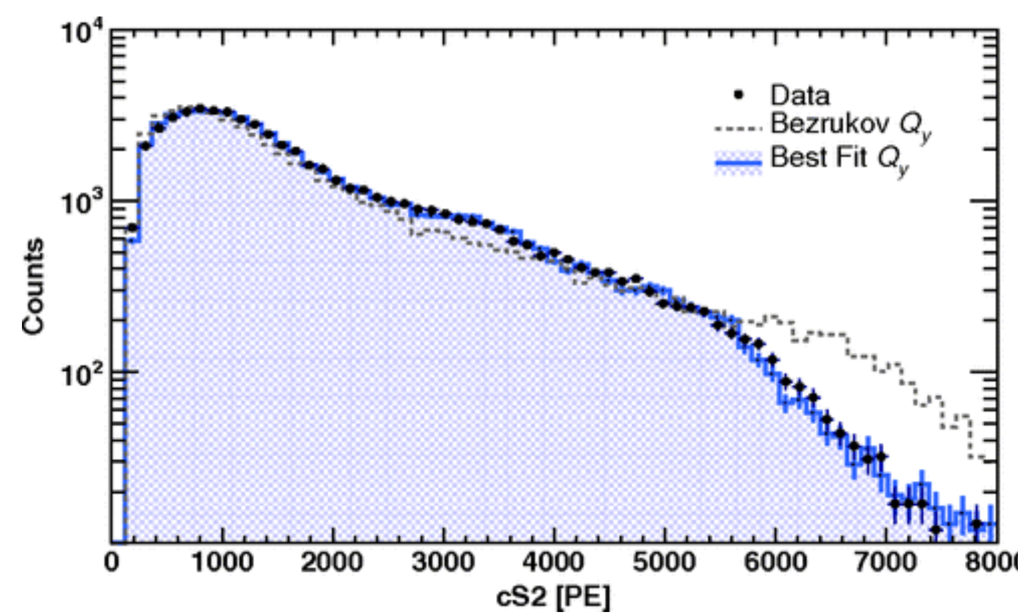

Background prediction for Run10

- Expected background in: 34 kg inner region, 224.6 live days, 99.75% rejection of electronic recoils
- Electronic recoil background:
  - 0.79±0.16 events
  - from ER calibration data, scaled to non-blinded ER band background data
- Nuclear recoil background
  - 0.17+0.12-0.07 events
  - from cosmogenic and radiogenic neutrons
- Total: 1.0±0.2 events

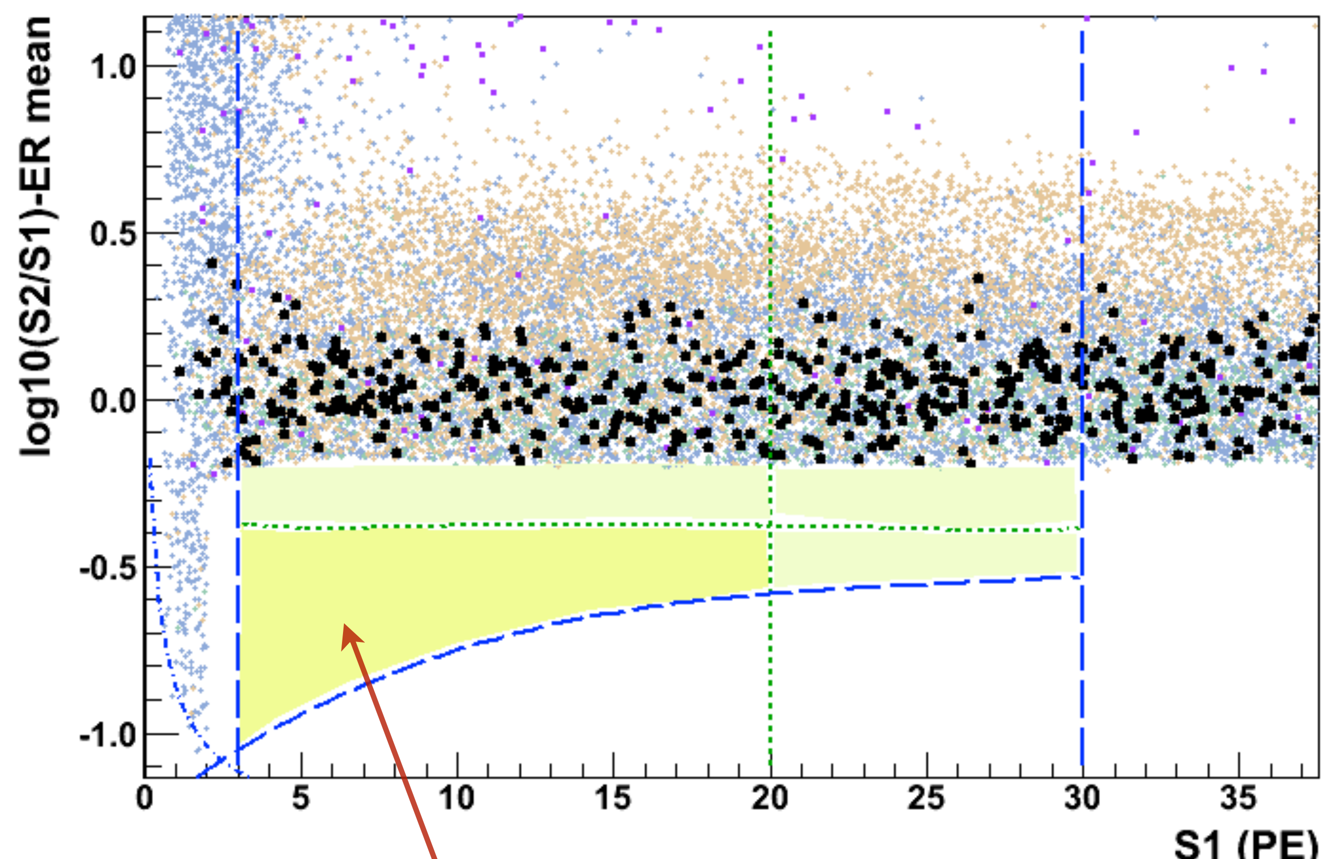

- *benchmark WIMP region (not used in PL analysis)*

Observed events after data unblinding

- Two events observed in signal region (there is a 26.4 % chance for upward fluctuation): at 7.1 keV$_{nr}$ (3.3 pe) and at 7.8 keV$_{nr}$ (3.8 pe)
- Both events at low S2/S1 with respect to NR calibration data
- Visual inspection: waveforms of high quality

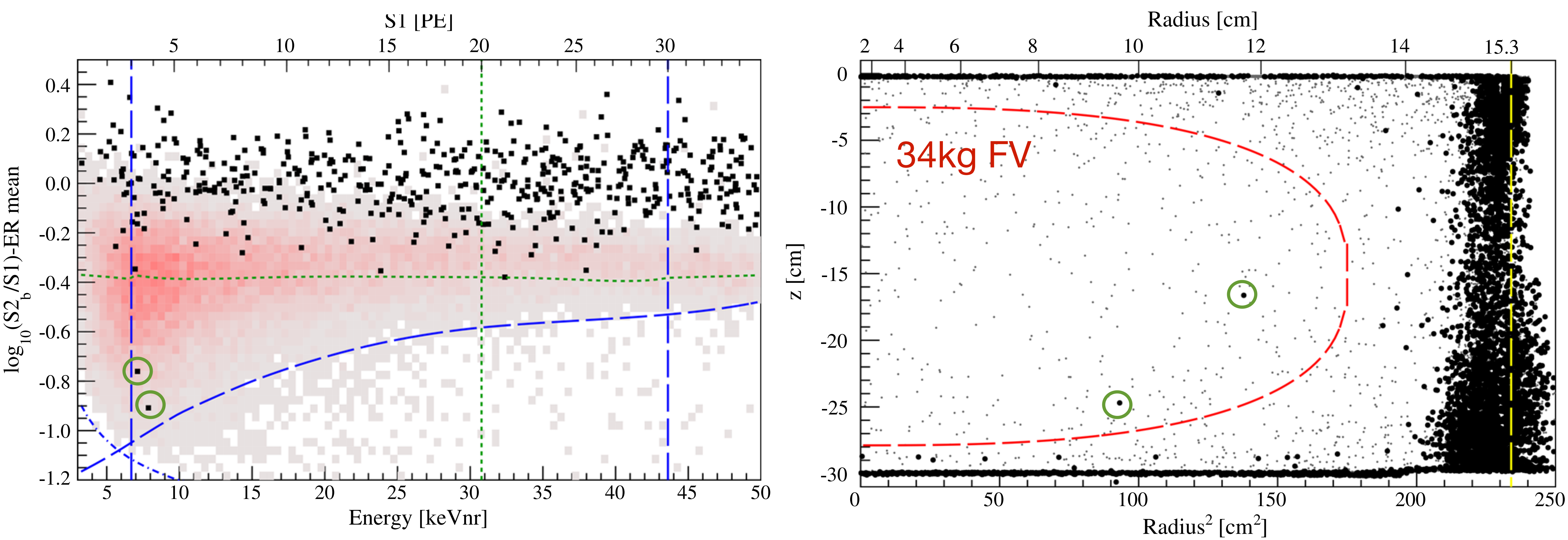

Predictions for light WIMPs

- How would signal claims of other experiments look like in XENON100's Run10 data?

WIMP with m_W = 8 GeV

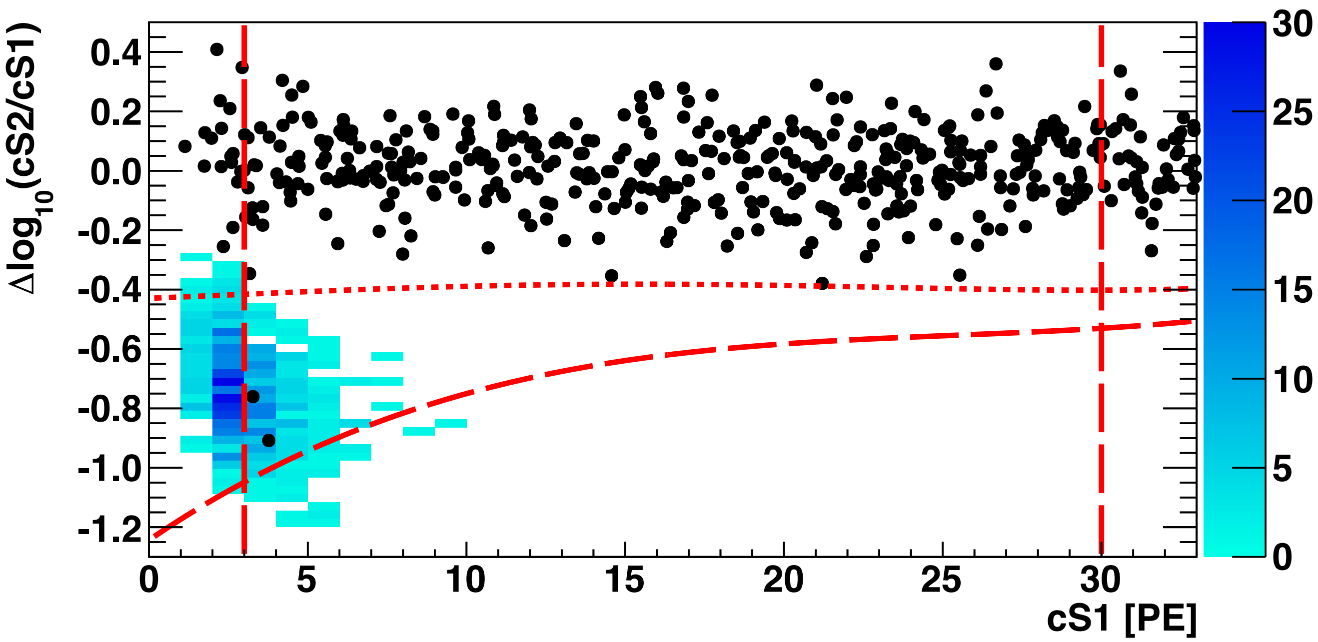

WIMP-nucleon cross section : 3 x 10^{-41} cm^2

WIMP with m_W = 25 GeV

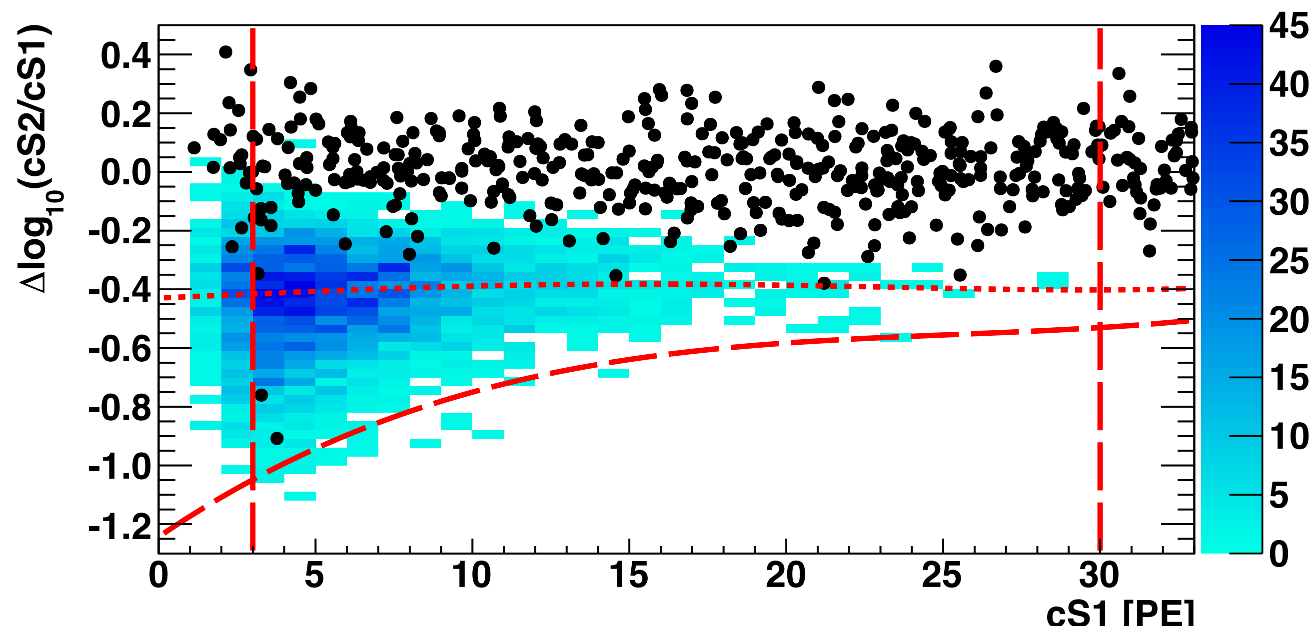

WIMP-nucleon cross section : 1.6 x 10^{-40} cm^2

XENON100 spin-independent results

- No evidence for WIMP interactions; region above thick blue line is excluded
- Upper limit on SI WIMP-nucleon cross section is 2x10^{-45} cm^2 at M_W = 55 GeV

PRL 109, 181301 (2012)

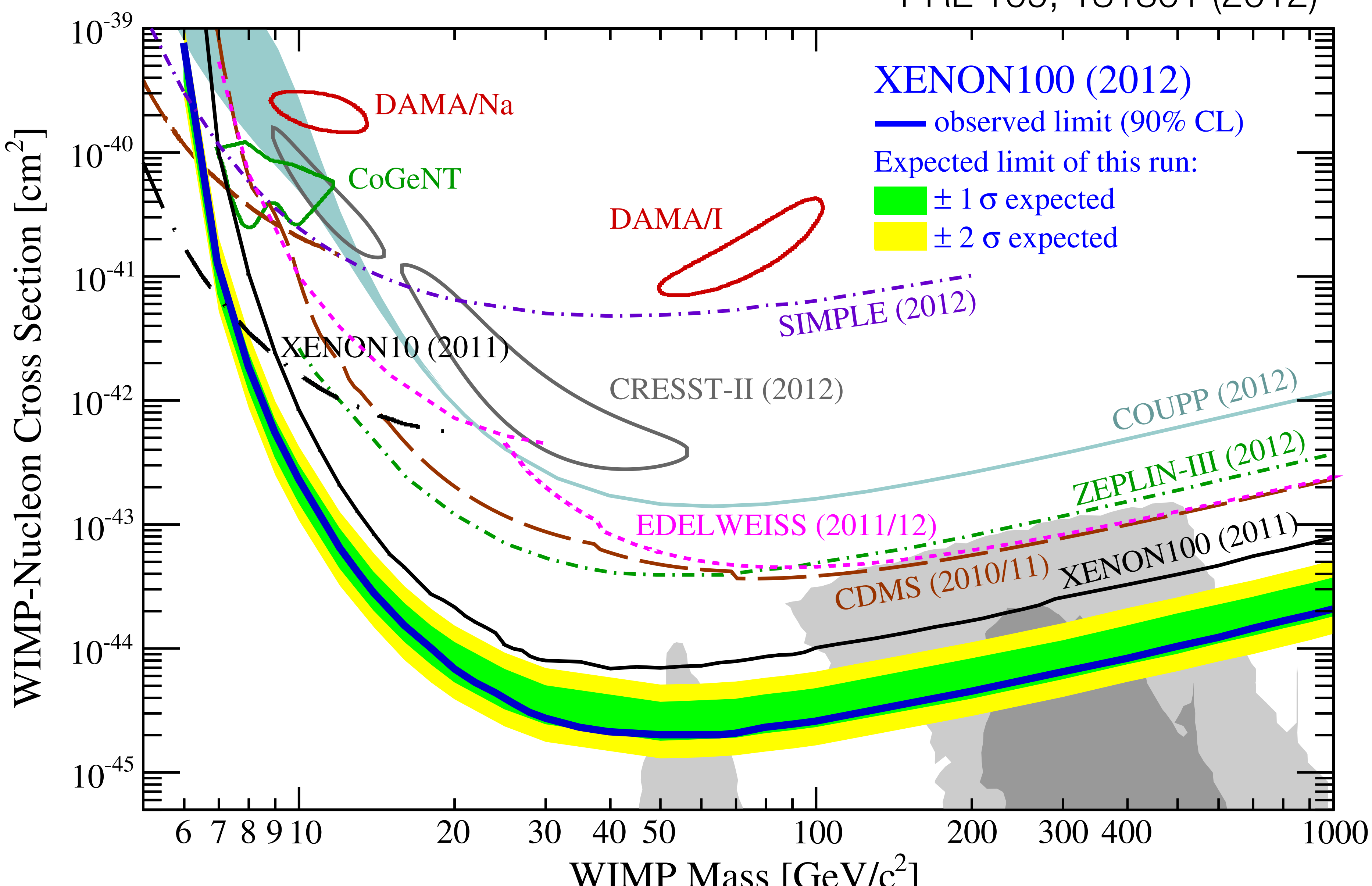

Vanilla Exclusion Plot

- **Assume we have detector of mass M, taking data for a period of time t**
- The total exposure will be **ε = M × t [kg days]**; nuclear recoils are detected above an energy threshold E_{th}, up to a chosen energy E_{max}. The **expected number of events n_{exp}** will be:

$$n_{exp} = \varepsilon \int_{E_{th}}^{E_{max}} \frac{dR}{dE_R} dE_R$$

⇒ cross sections for which $n_{exp} \geq 1$ can be probed by the experiment

- If ZERO events are observed, Poisson statistics implies that $n_{exp} \leq 2.3$ at 90% CL

=> exclusion plot in the cross section versus mass parameter space (assuming known local density)

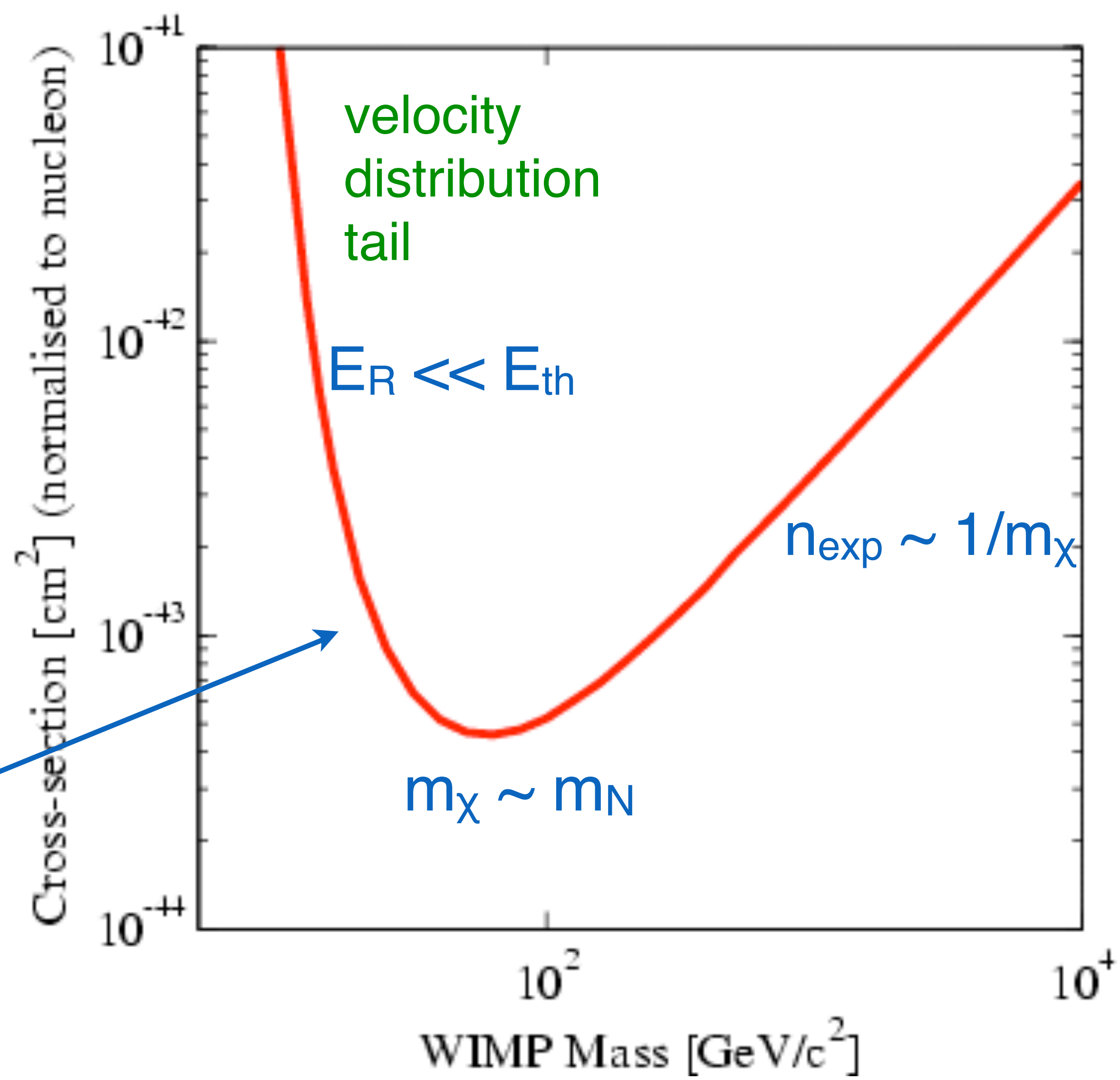

XENON100 spin-dependent results

- ^{129}Xe (spin-1/2) and ^{131}Xe (spin-3/2), two isotopes with $J \neq 0$ and abundance of 26.2% and 21.8% in XENON100

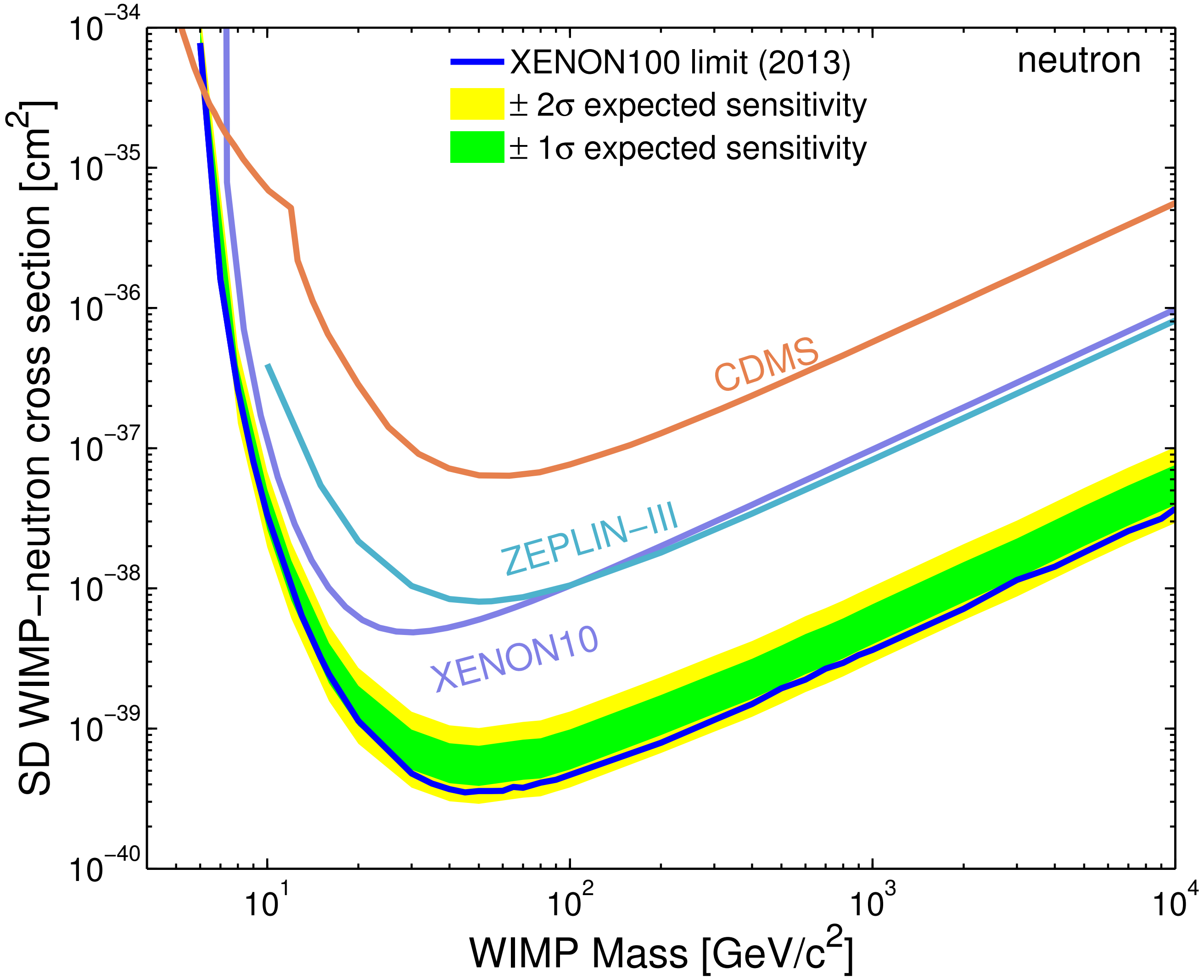

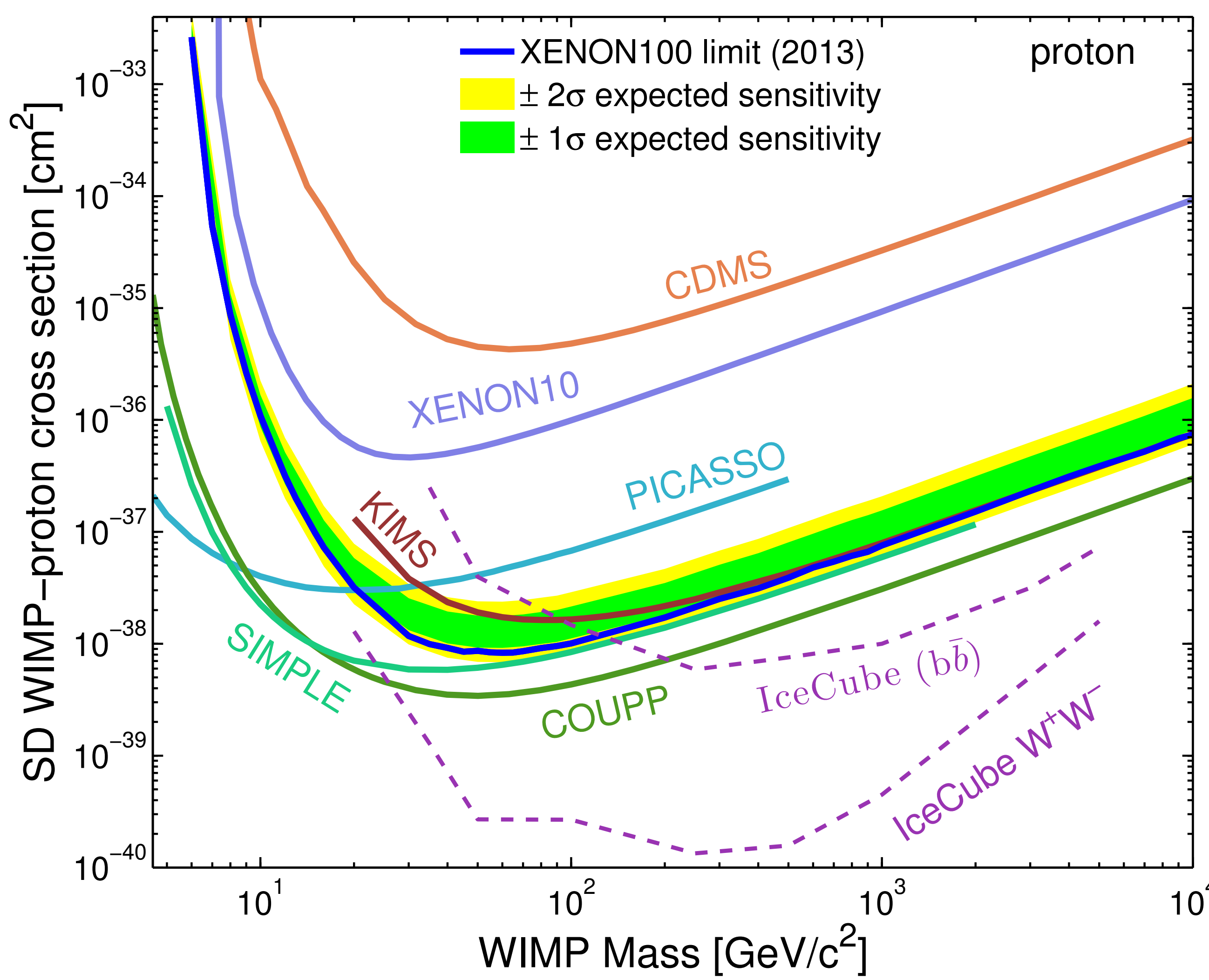

Phys.Rev.Lett. 111 (2013) 2, 021301

New XENON100 results

- Dark matter particles interacting with e^-
  - XENON100's ER background lower than DAMA modulation amplitude

➡ search for a signal above background in the ER spectrum

XENON collaboration, arXiv: 1507.07747, Science 349, 2015

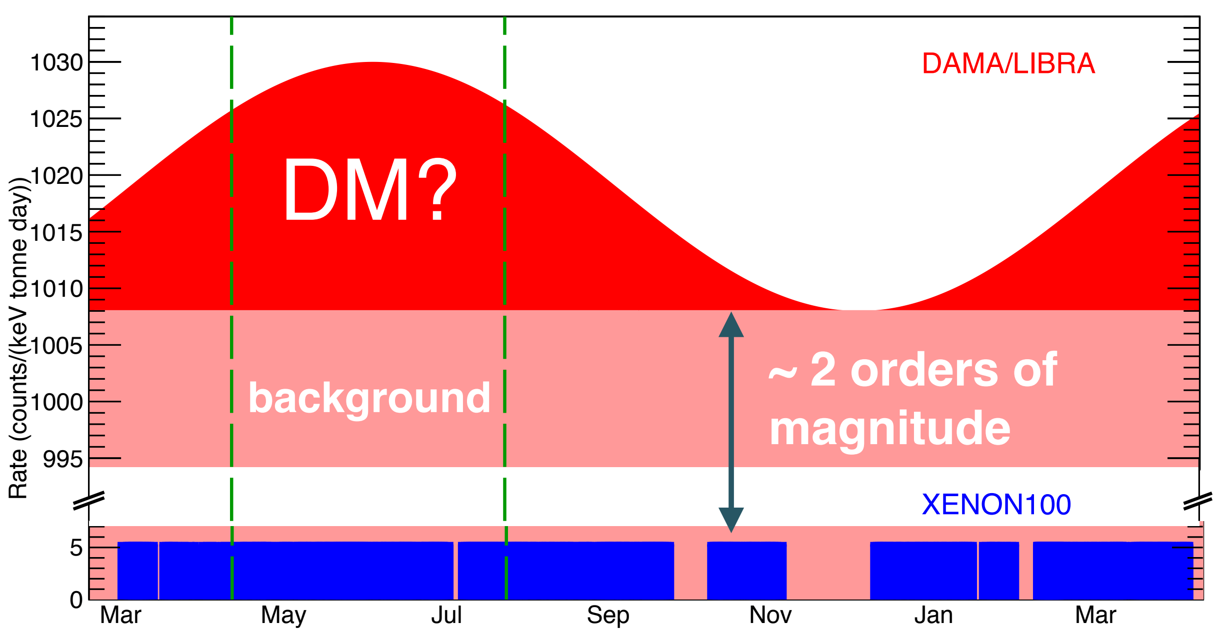

Consider the 70 days with the largest signal

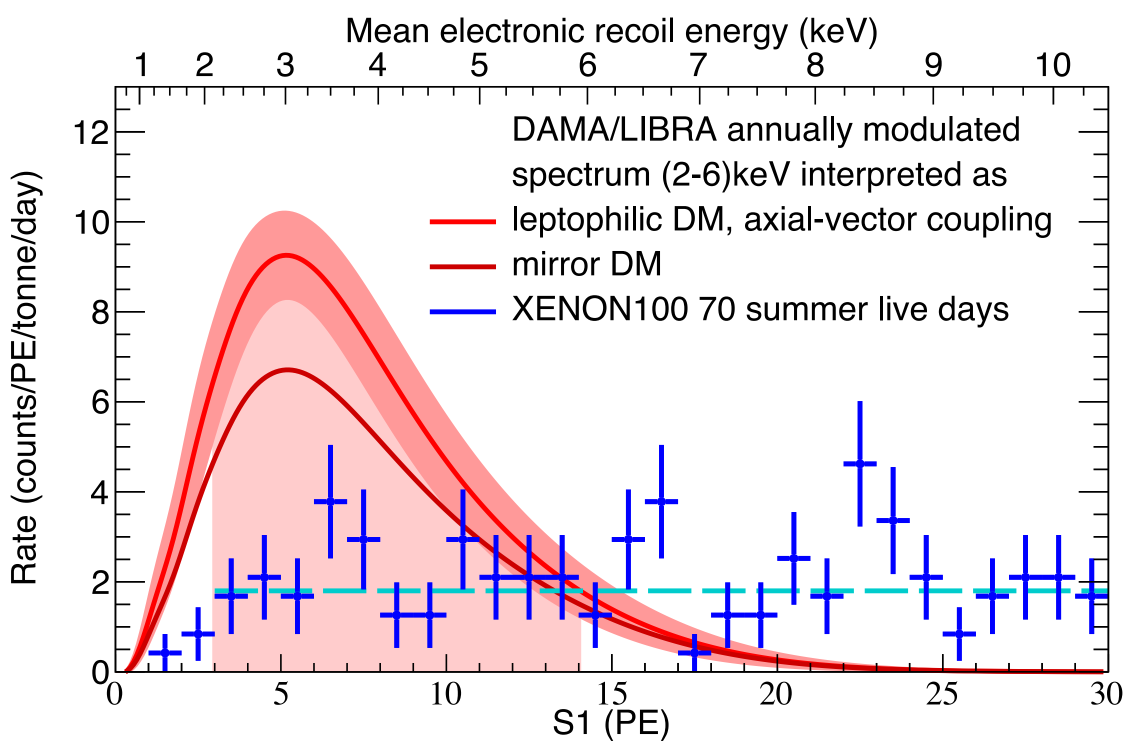

DAMA/LIBRA modulated spectrum as would be seen in XENON100 (for axial-vector WIMP-e^- scattering)

XENON100 excludes leptophilic models

- Dark matter particles interacting with e^-
    1. No evidence for a signal
    2. Exclude various leptophilic models as explanation for DAMA/LIBRA

XENON collaboration, arXiv: 1507.07747, Science 349, 2015

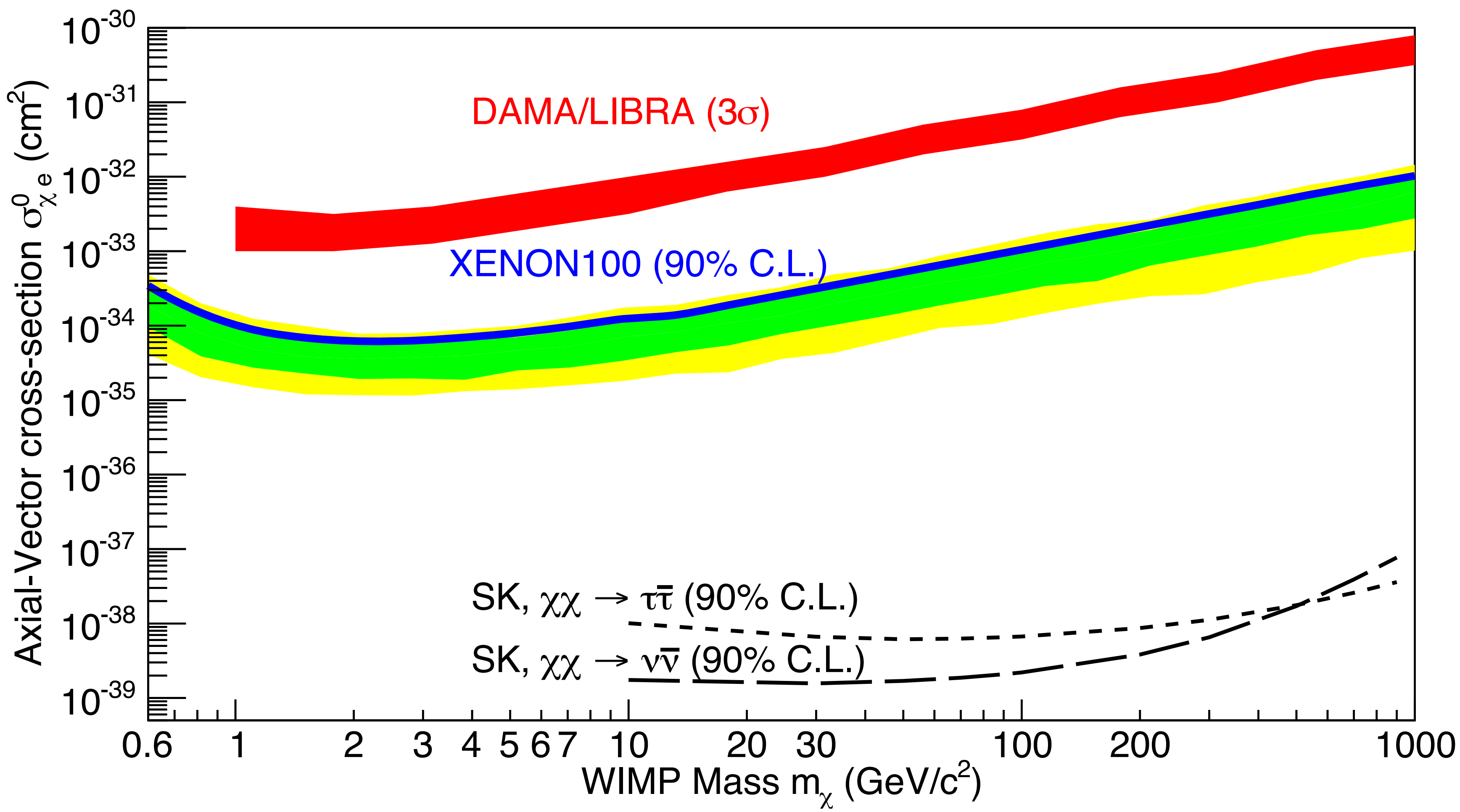

Liquefied noble gases recent results

DarkSide-50: factor 1.4 x 10^3 depletion of ^{39}Ar

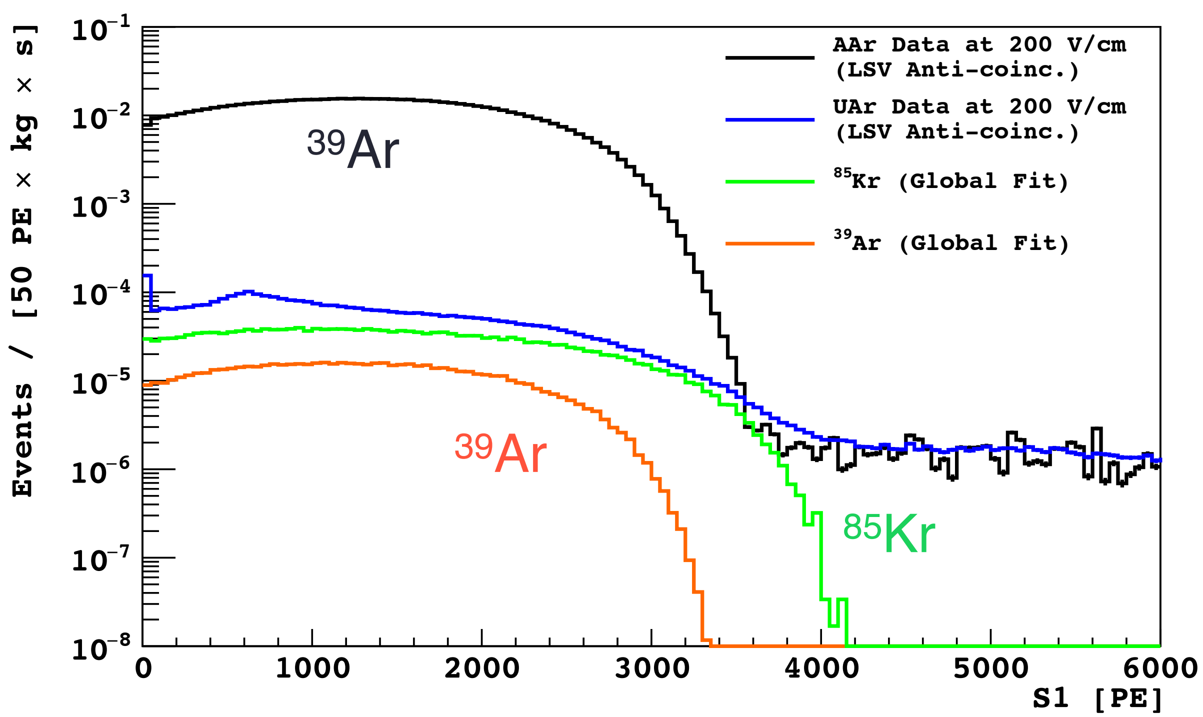

DarkSide-50, 70.9 live days, arXiv:1510.00702

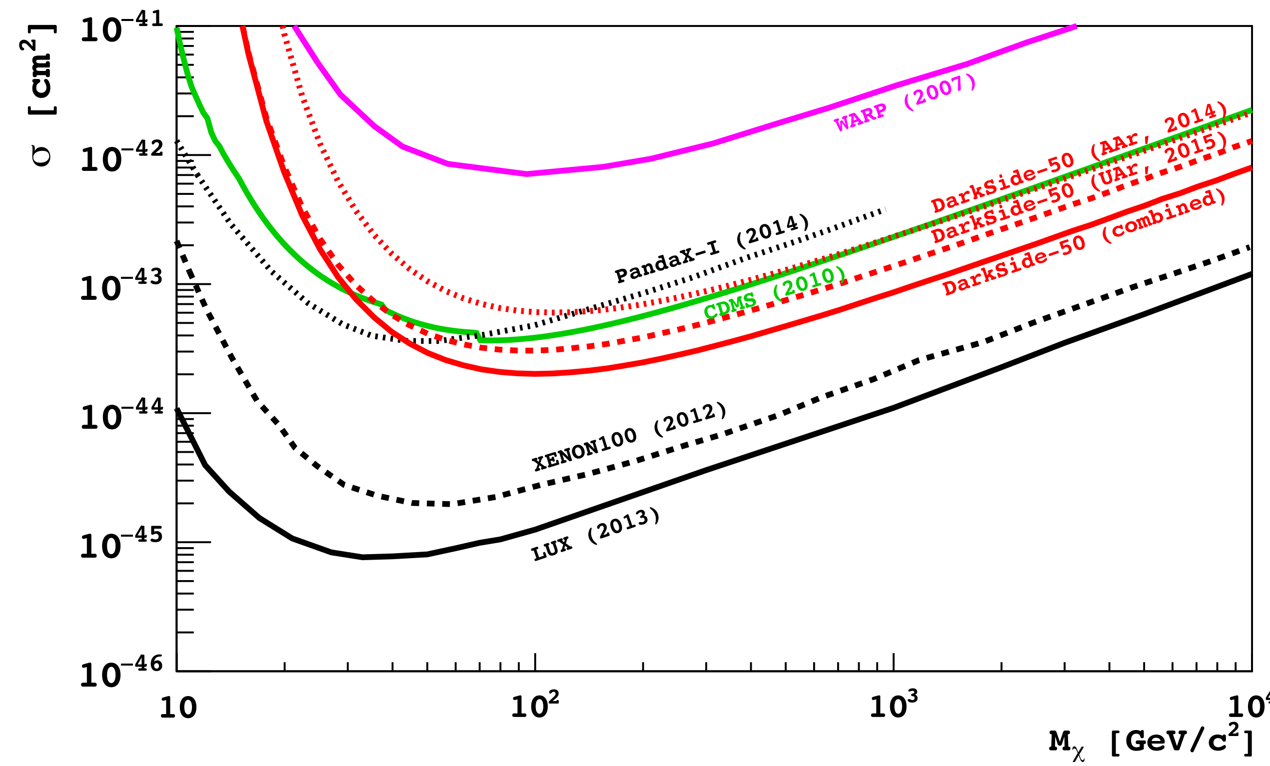

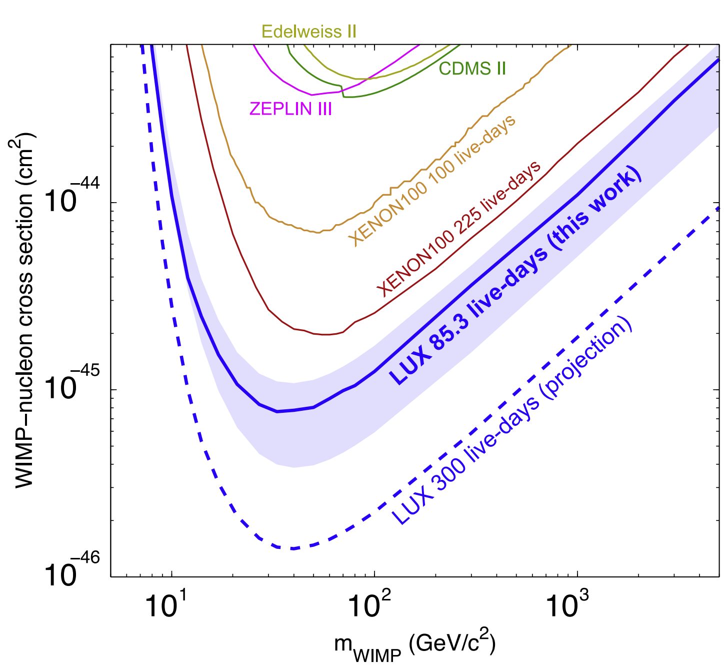

LUX 85.3 live-days, PRL 2014

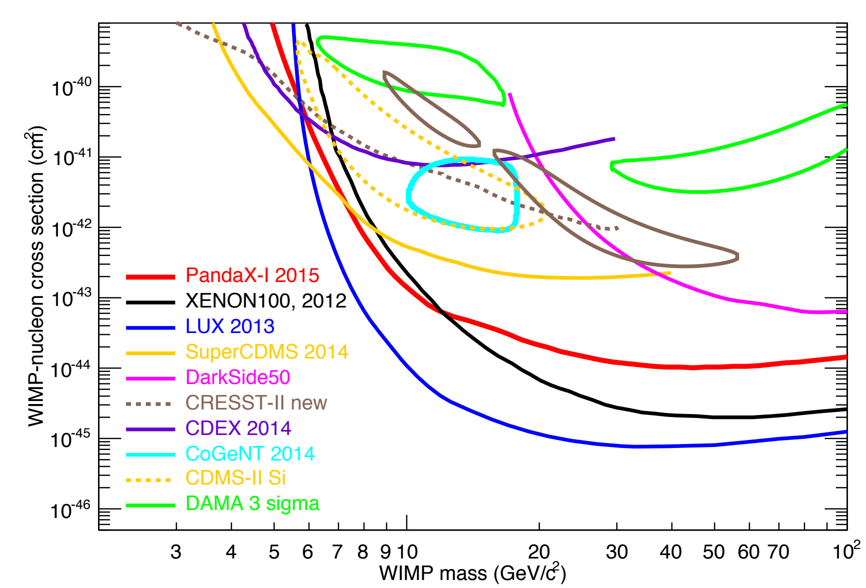

PandaX 80.1 live-days, arXiv 1505.00771

Future noble liquid detectors

- **Under construction: XENON1T/nT (3.3 t/ 7t LXe) at LNGS**
- Proposed LXe: LUX-ZEPLIN 7t *(approved)*, XMASS 5t LXe
- Proposed LAr: DarkSide 20 t LAr, DEAP 50 t LAr
- Design & R&D studies: DARWIN 30-50 t LXe; ARGO 300 t LAr


XENON1T: 3.3 t LXe

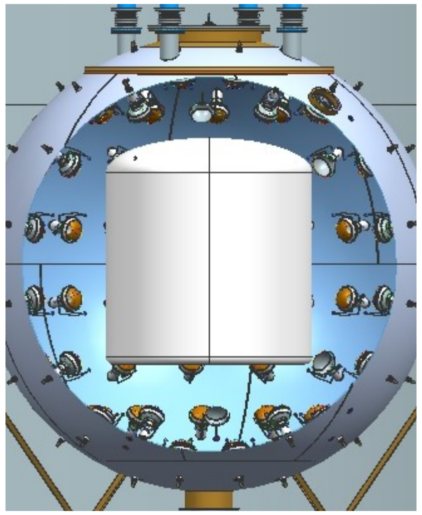
DarkSide: 20 t LAr

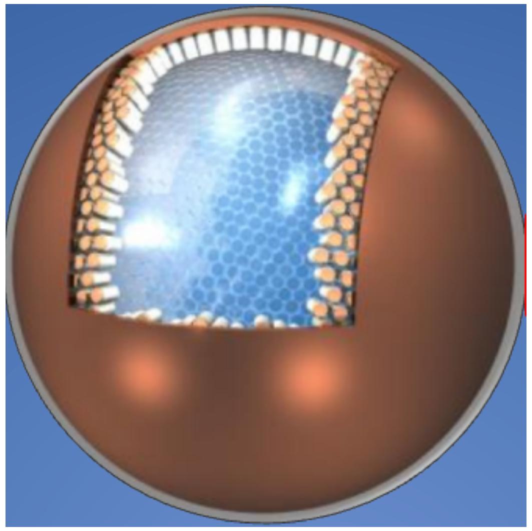
XMASS: 5t LXe

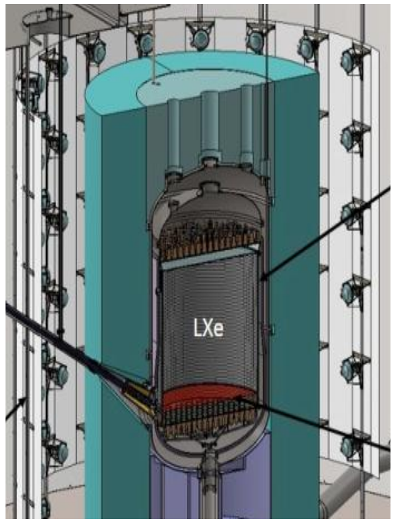

LZ: 7t LXe

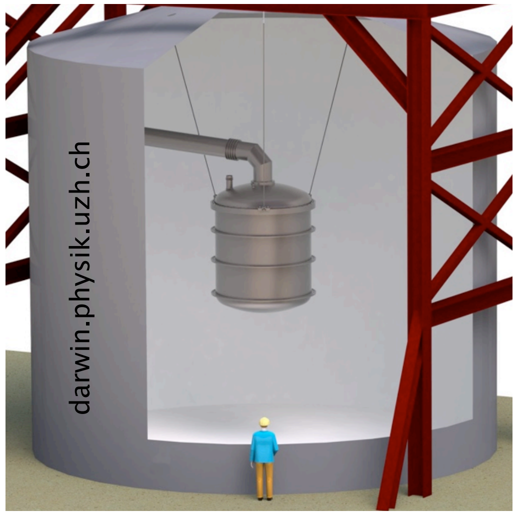

DARWIN: 50 t LXe

The XENON1T experiment

- Under construction at LNGS since autumn 2013; commissioning planned for late 2015
- Total (active) LXe mass: 3.3 t (2 t), 1 m electron drift, 248 3-inch PMTs in two arrays
- Background goal: 100 x lower than XENON100 ~ 5×10^{-2} events/(t d keV)

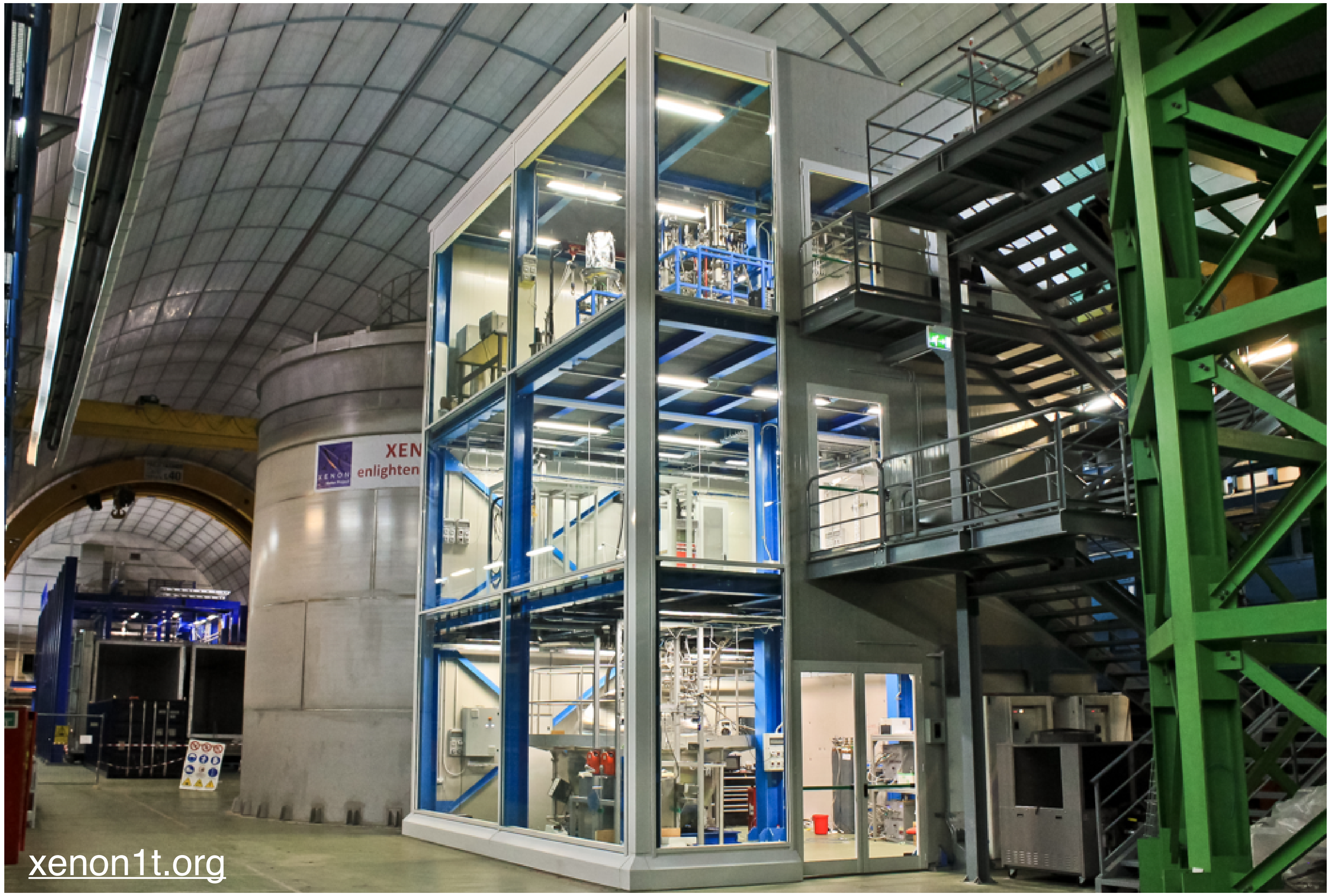

XENON1T: status of construction work

- Water Cherenkov shield built and instrumented
- Cryostat support, service building, electrical plant completed
- Several subsystems (cryostat, cryogenics, storage, purification, cables & fibres, pipes) installed and under commissioning underground





XENON1T: status of construction work

- Water Cherenkov shield built and instrumented

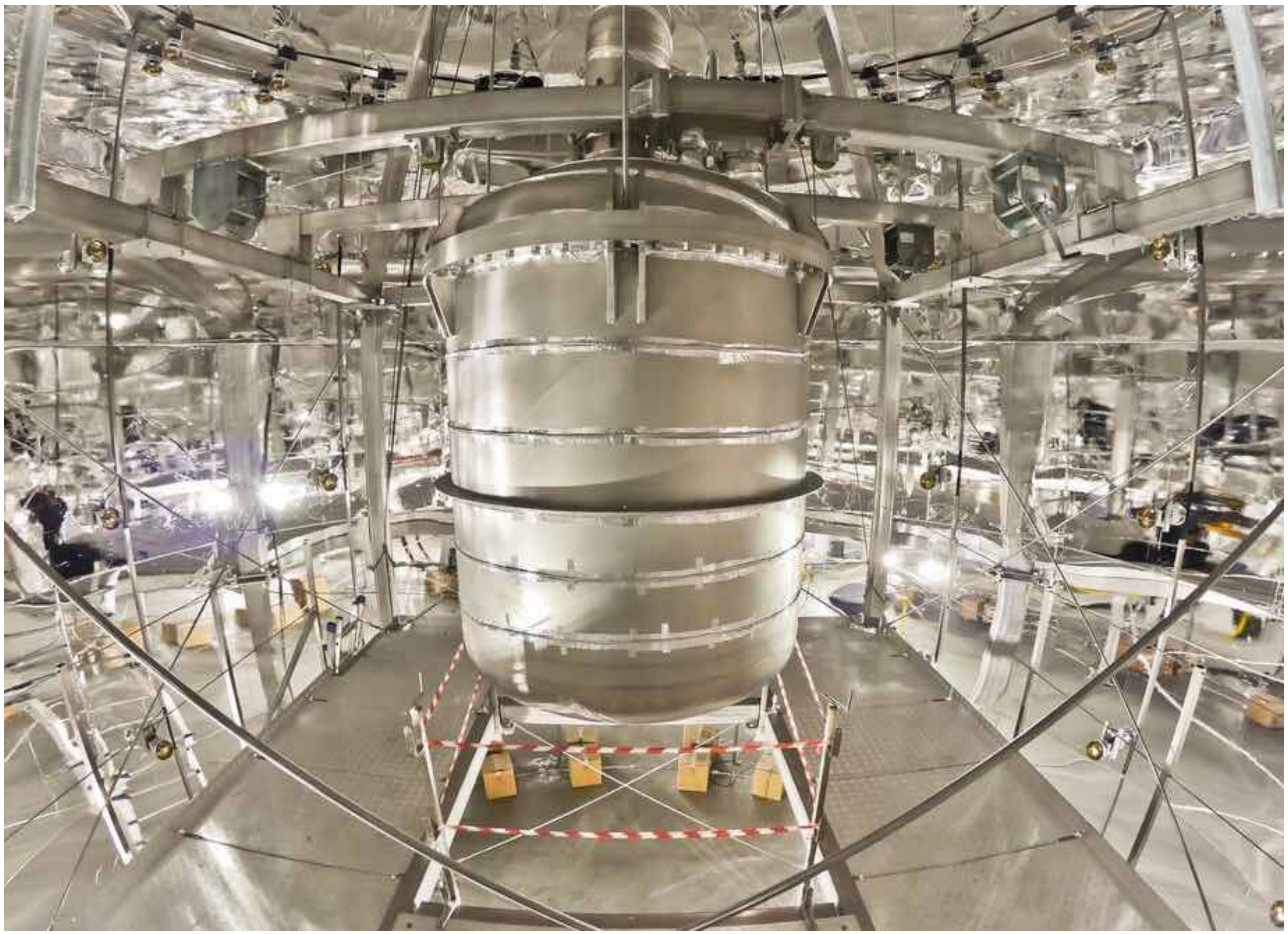

The XENON1T inner detector

- PMTs tested at cryogenic temperatures; arrays with electronics & cables assembled
- TPC assembly and cold tests completed; **installation at LNGS in October/November 2015**

The TPC

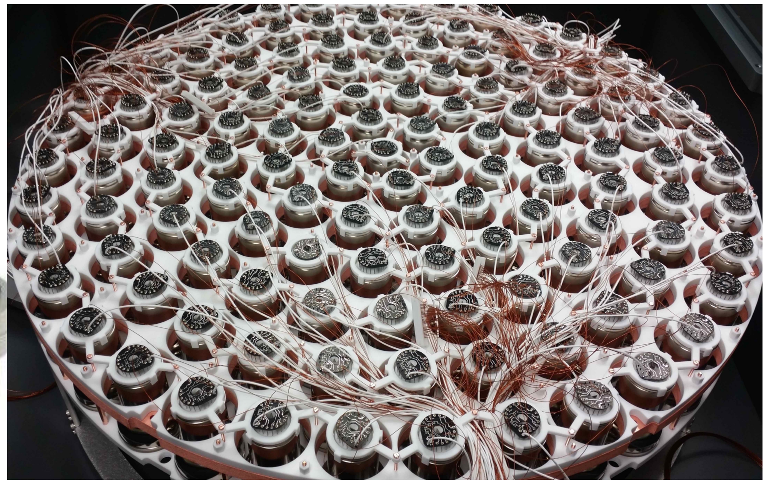

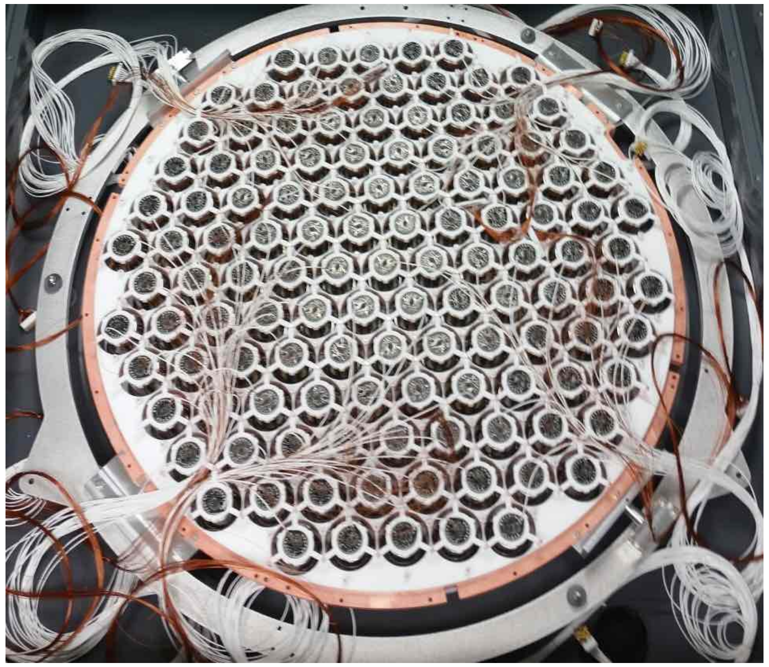

PMT array, bases & cables

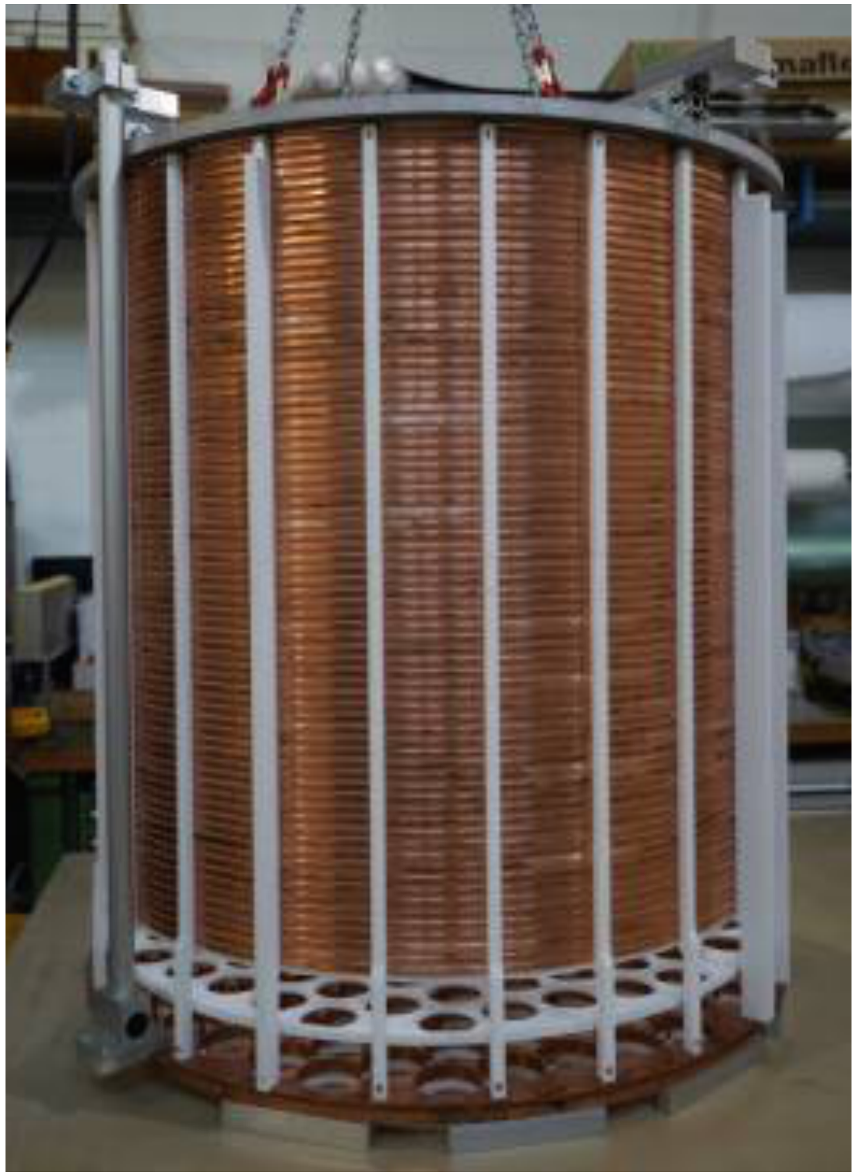

TPC assembly, cool down tests

The XENON1T inner detector

- PMTs tested at cryogenic temperatures; arrays assembled
- TPC assembly and cold tests completed; installation at LNGS in October/November 2015

The XENON1T field cage

Field cage in LNGS clean room
74 Cu field shaping rings

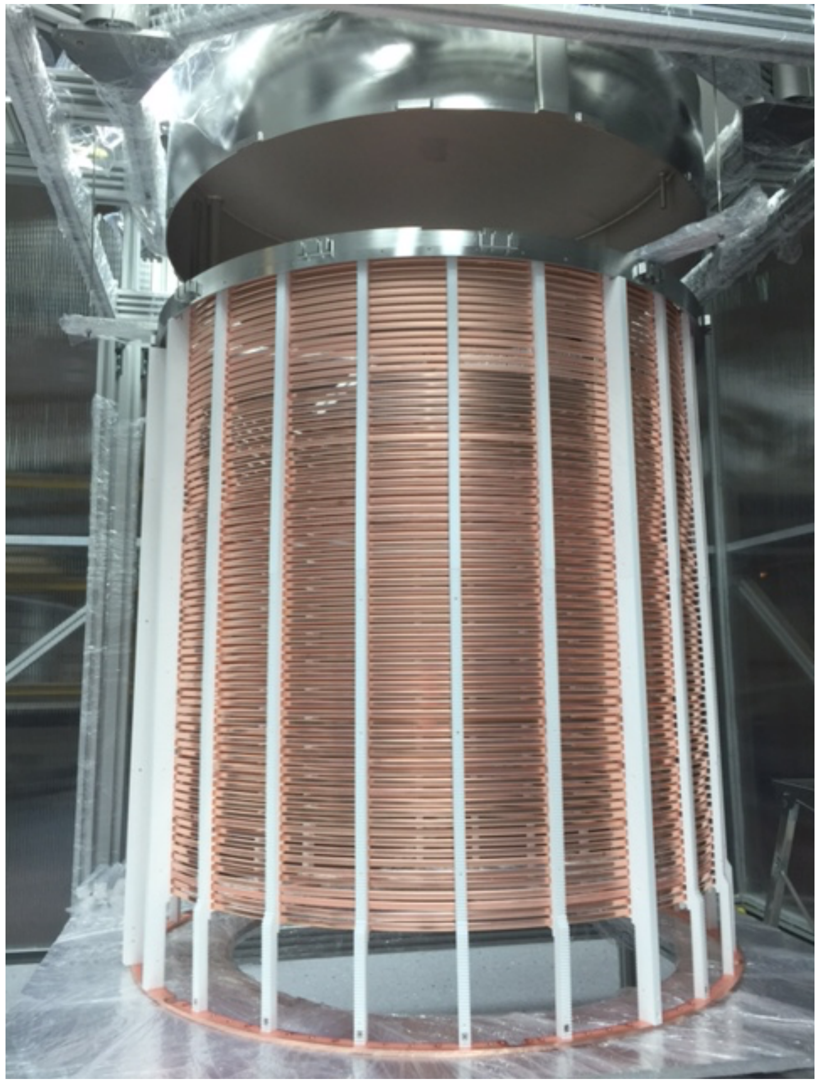

Field cage in LNGS clean room
Teflon panels for >98%
reflectivity of 175 nm VUV light

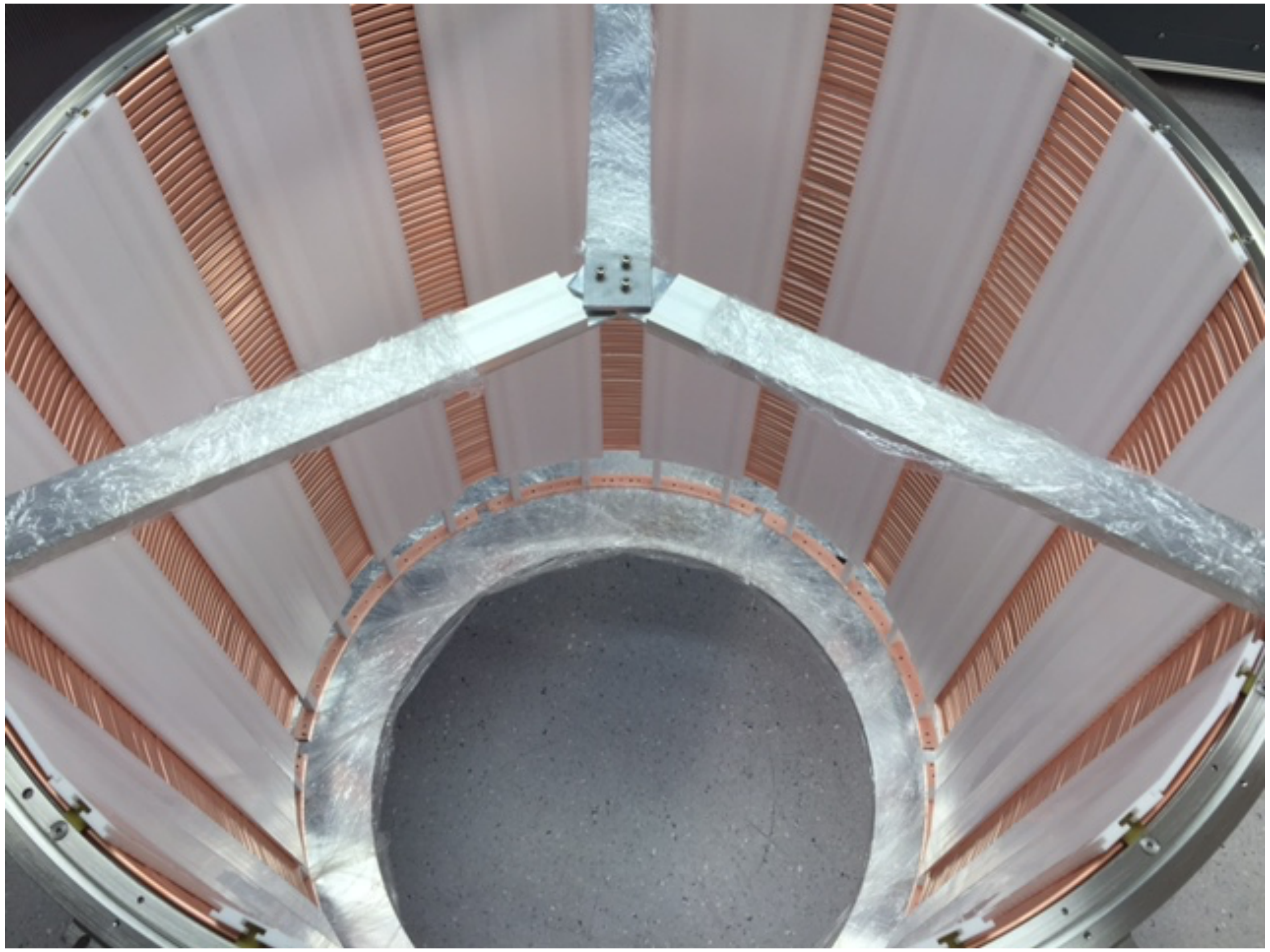

The XENON1T PMT arrays

Bottom PMT array
Close packing for efficient S1 light collection

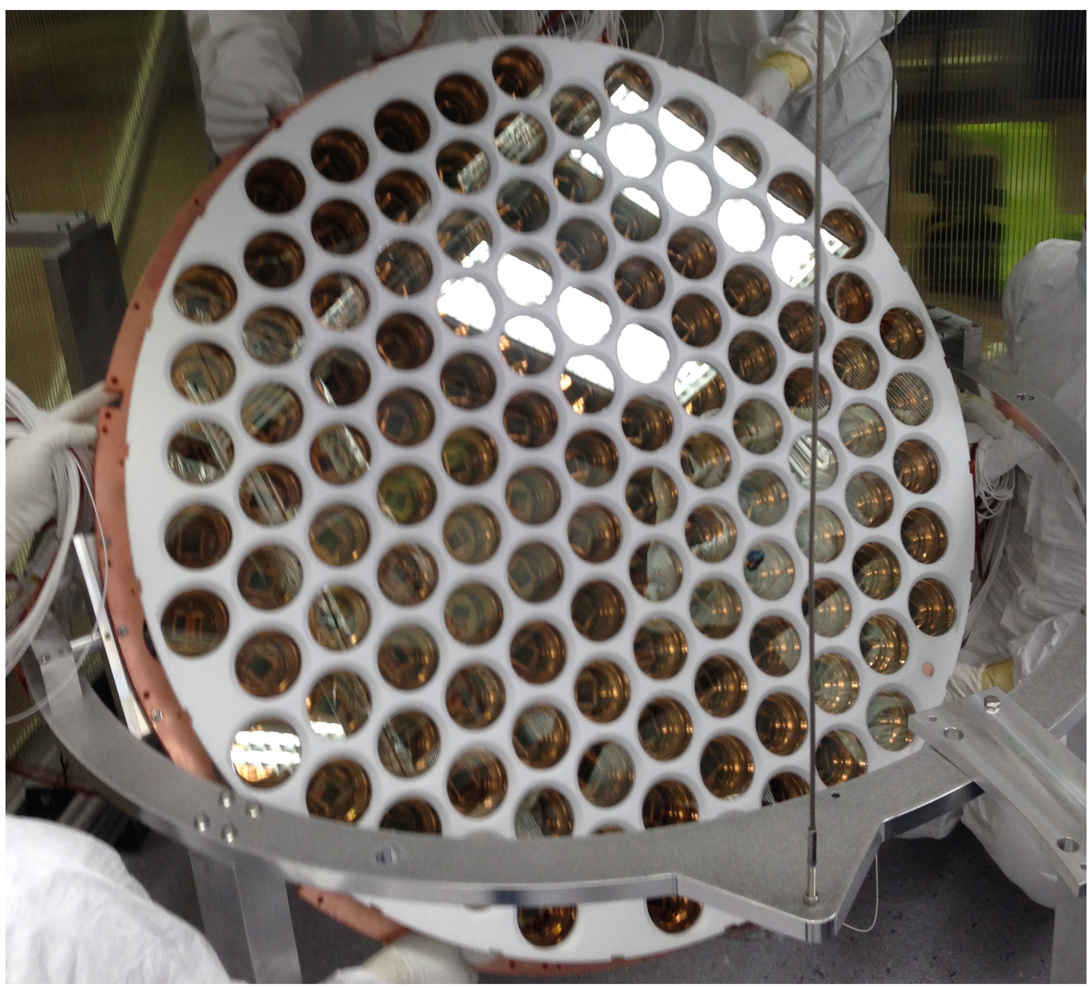

Top PMT array
Optimised for optimal position reconstruction (S2-based)

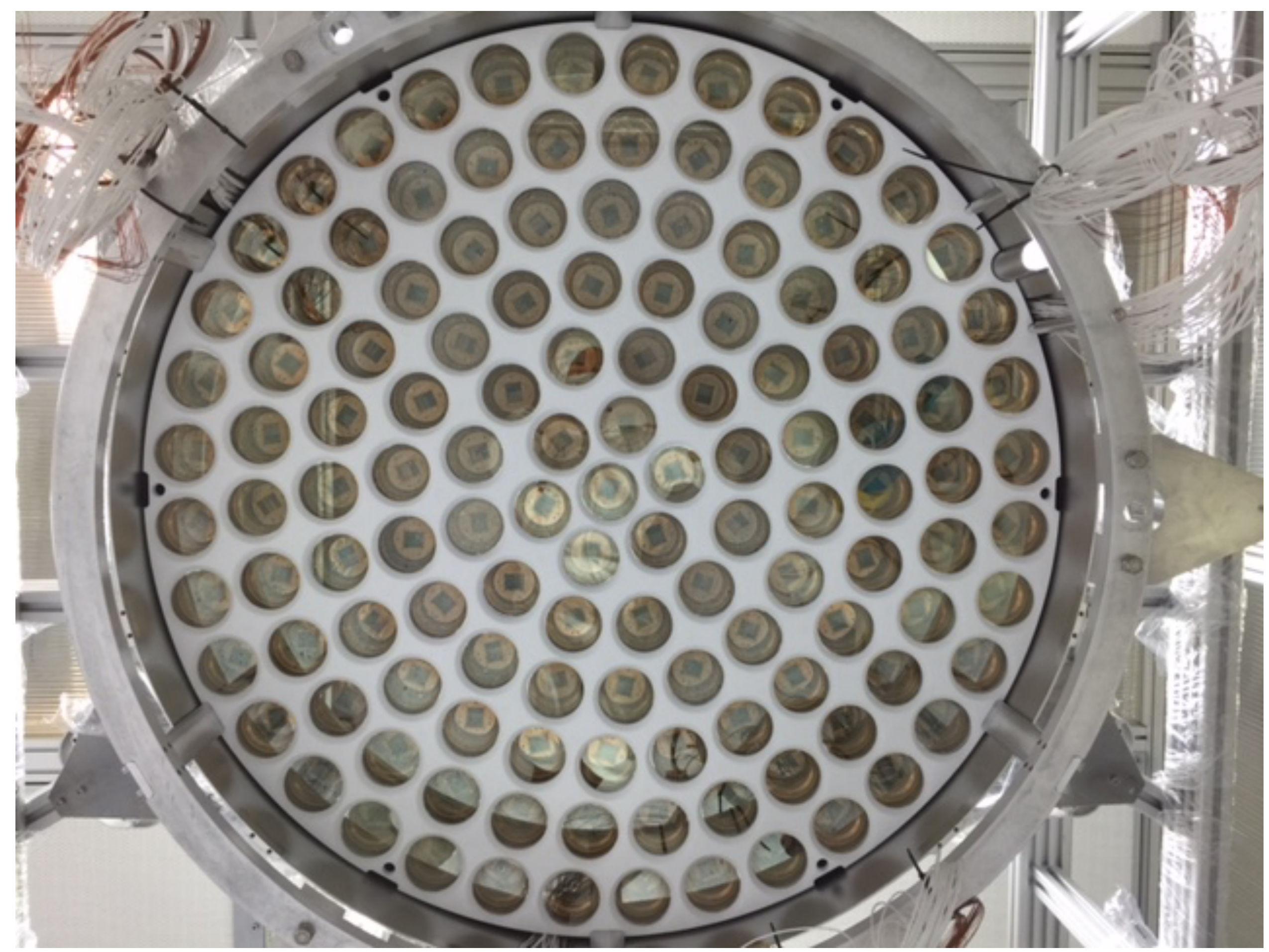

From XENON100 to XENON1T in numbers

	XENON100	XENON1T
Total LXe mass [kg]	161	3500
Background [dru]	5×10^{-3}	5×10^{-5}
^{222}Rn [μBq/kg]	~ 65	~ 1
^{nat}Kr [ppt]	~120	~0.2
e- drift [cm]	30	100
Cathode HV [kV]	-16	-100

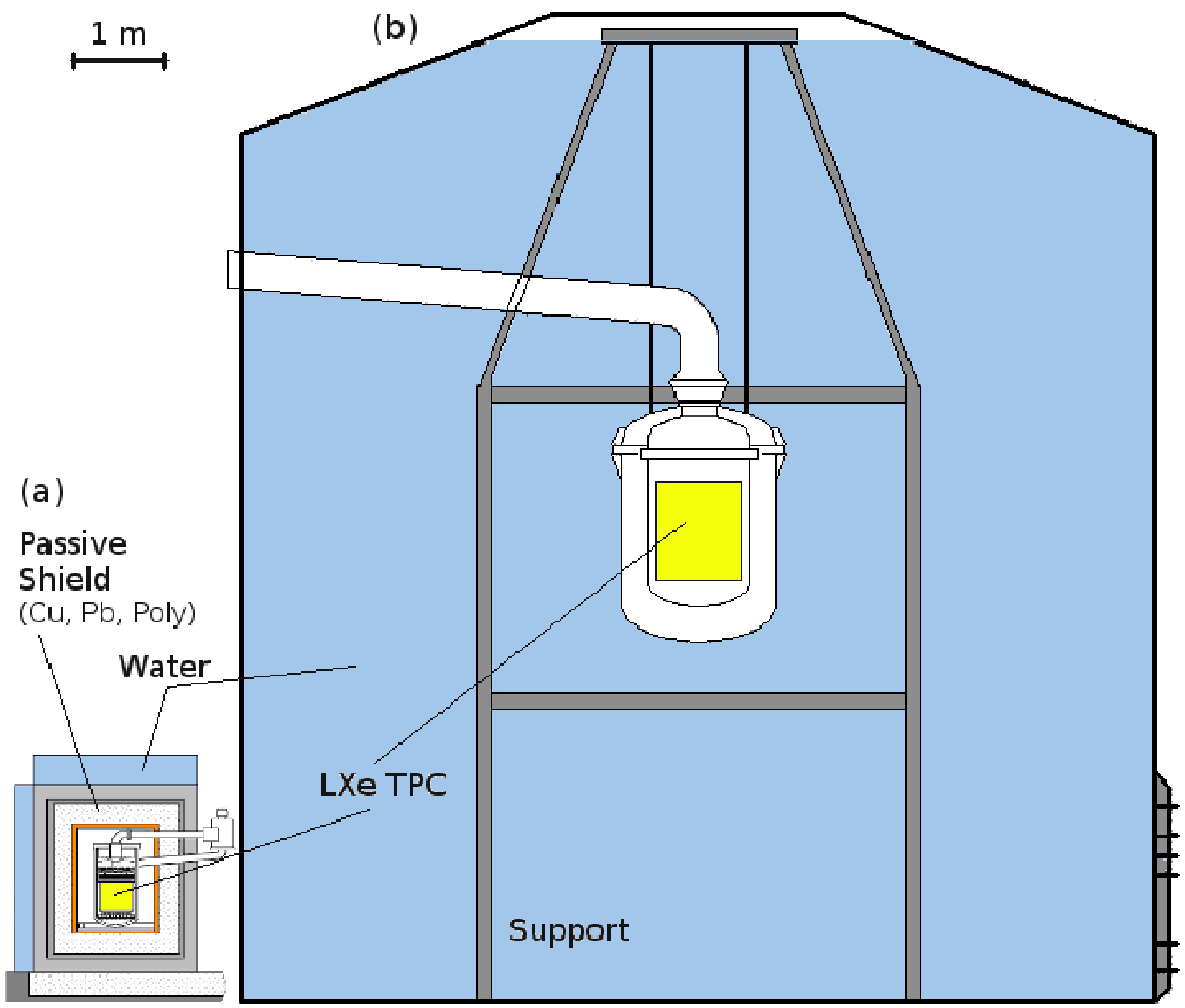

XENON1T background predictions

- Materials background: based on screening results for all detector components
- ^{85}Kr: 0.2 ppt of ^{nat}Kr with 2x10^{-11} ^{85}Kr; ^{222}Rn: 1 μBq/kg; ^{136}Xe double beta: 2.11x10^{21} y
- ER vs NR discrimination level: 99.75%; 40% acceptance for NRs
  - ➡ Total ERs: 0.3 events/year in 1 ton fiducial volume, [2-12] keV$_{ee}$
  - ➡ Total NRs: 0.2 events/year in 1 ton, [5-50] keV$_{nr}$ (muon-induced n-BG < 0.01 ev/year)

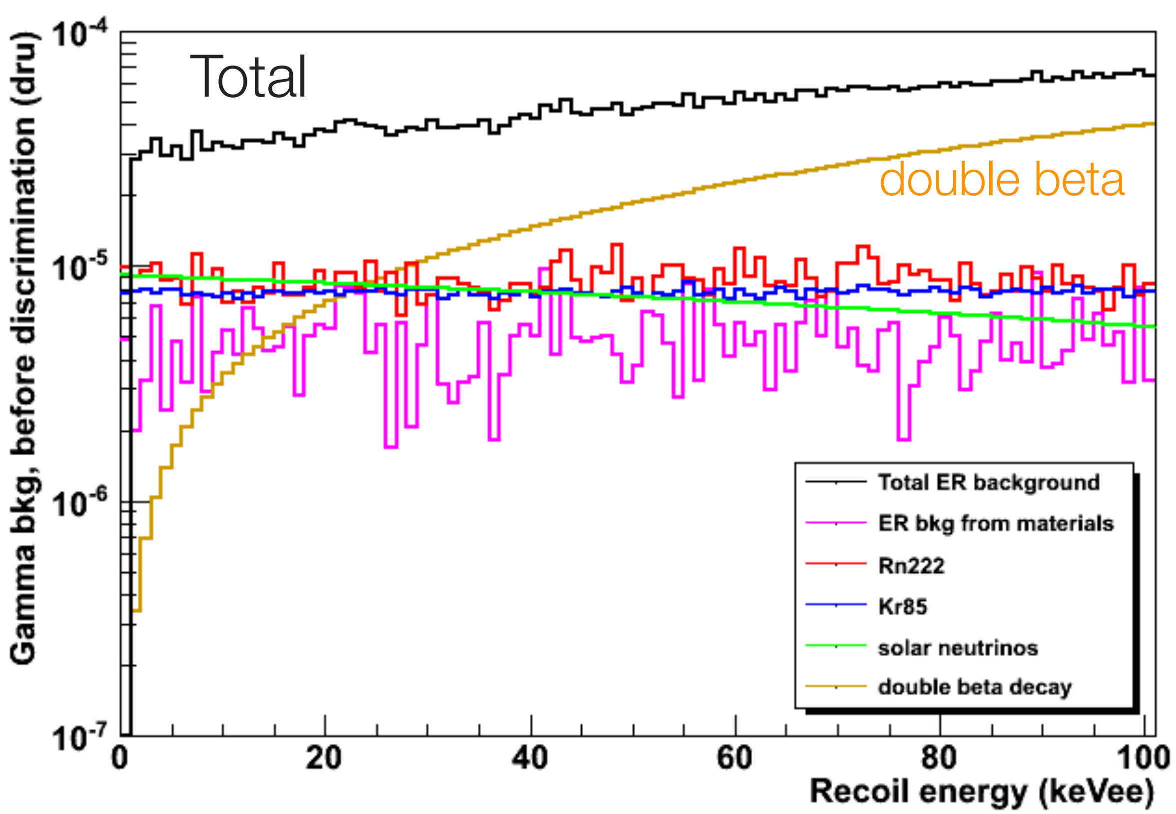

Background rate from various components

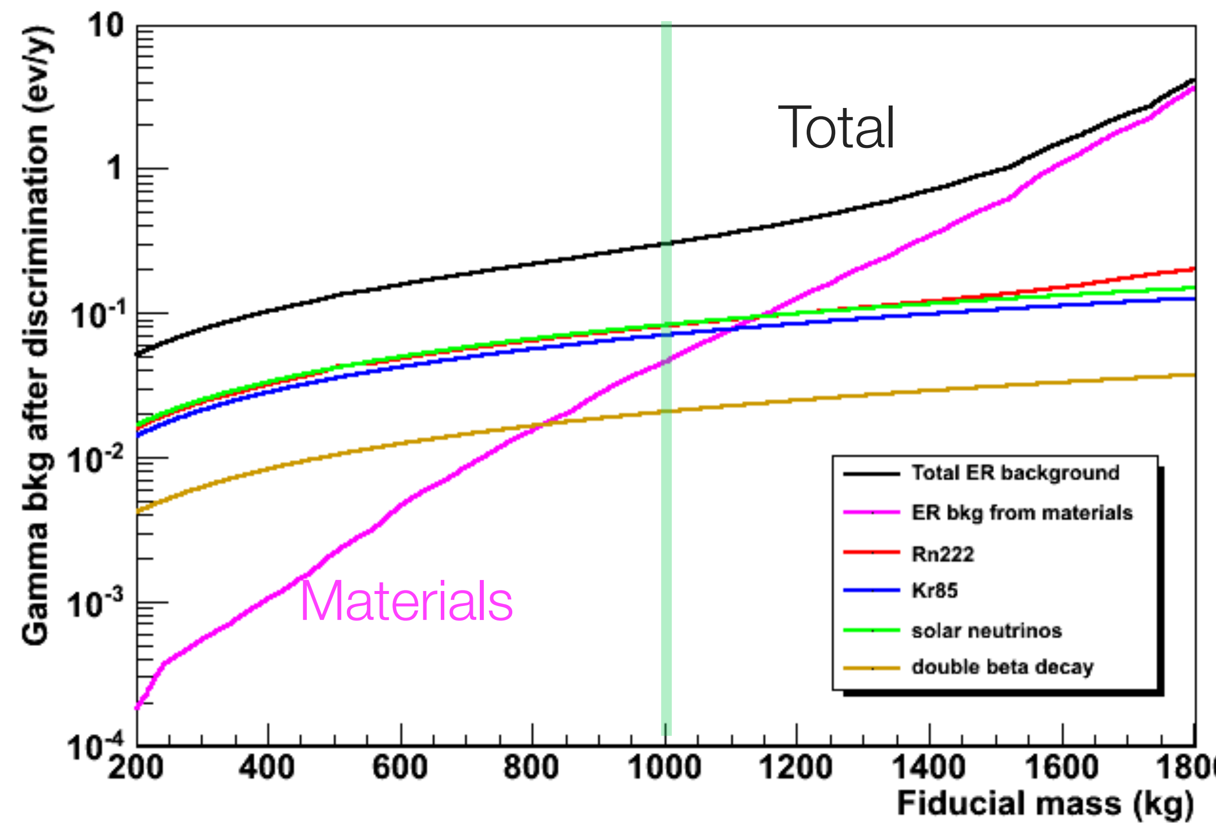

Background versus fiducial LXe mass

XENON1T backgrounds and WIMP sensitivity

Single scatters in 1 ton fiducial
99.75% S2/S1 discrimination
NR acceptance 40%
Light yield = 7.7 PE/keV at 0 field
L_{eff} = 0 below 1 keVnr

WIMP mass: 50 GeV
Fiducial LXe mass: 1 t
Sensitivity at 90% CL

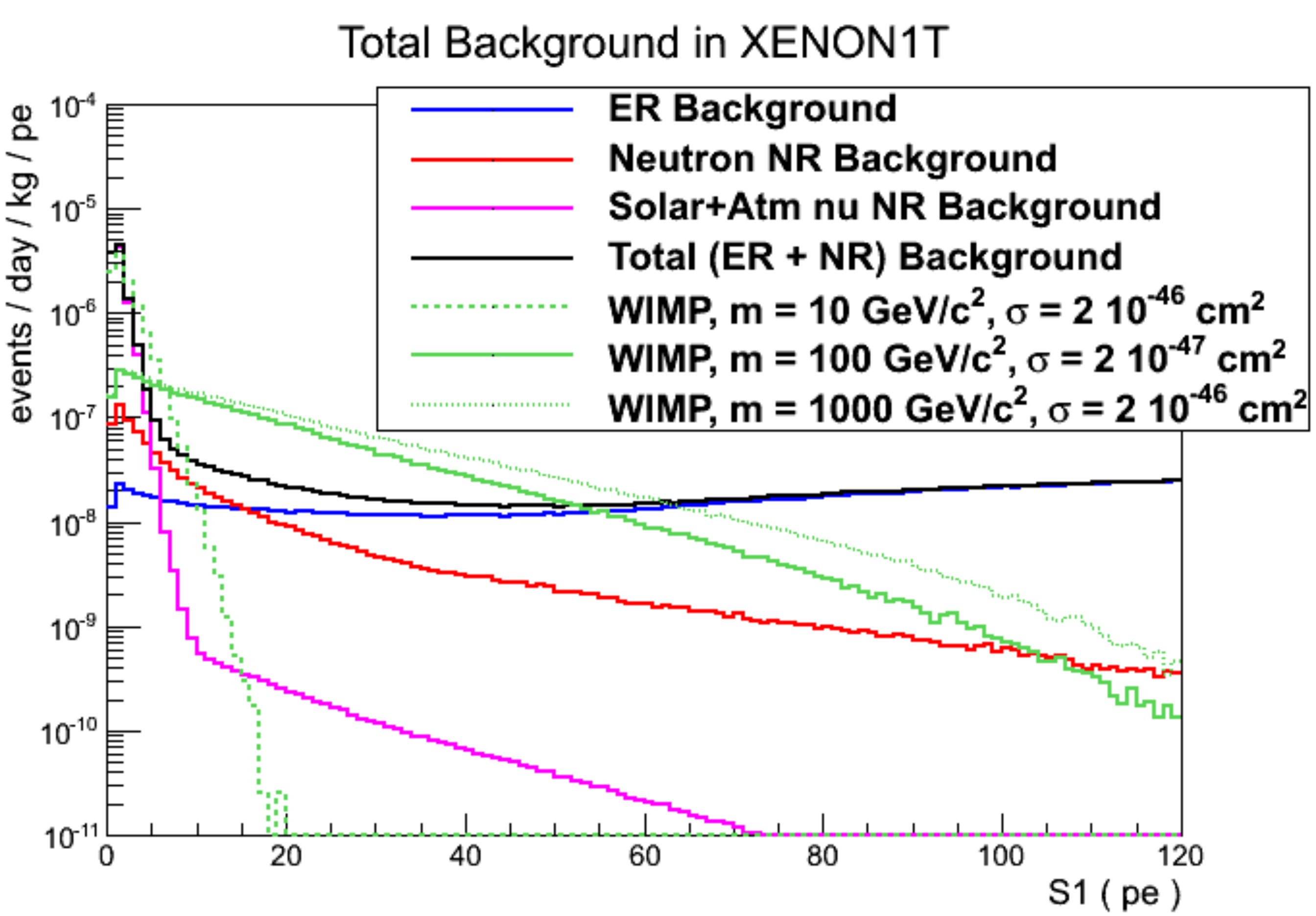

ER + NR backgrounds and WIMP spectra

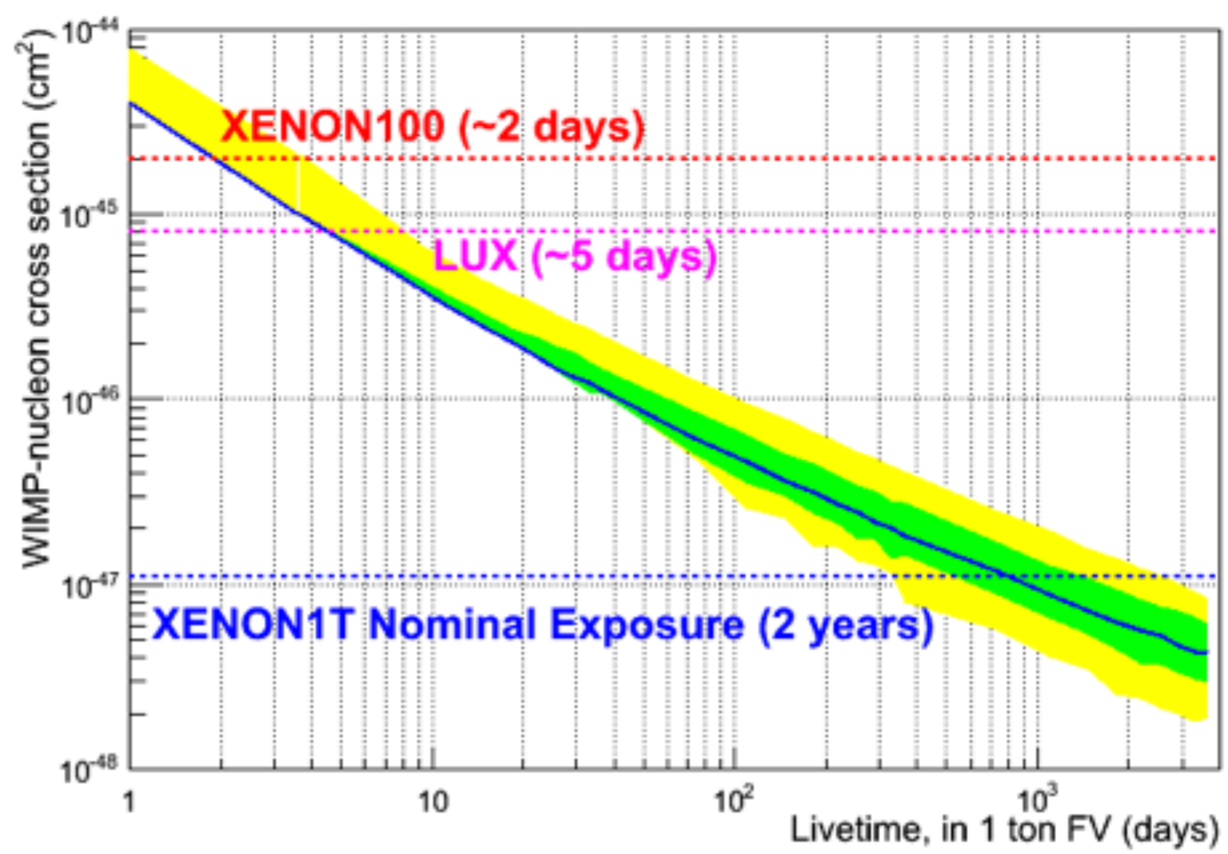

Sensitivity versus exposure (in 1 ton fiducial mass)

DARWIN-LXe TPC *baseline* concept

darwin-observatory.org

- 30-50 tons LXe in total
- ~ few x 10^3 photosensors
- >2 m drift length
- >2 m diameter TPC
- PTFE walls with Cu field shaping rings
- Background goal: dominated by neutrinos

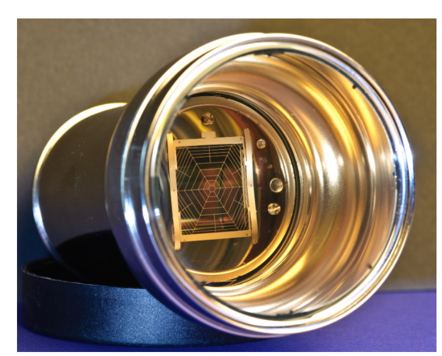

3-inch PMT, R11410-21

4-inch PMT

Science reach: WIMP physics with xenon

Probe WIMP-Xe interactions via:

- spin-independent elastic scattering: ^{124}Xe, ^{126}Xe, ^{128}Xe, ^{129}Xe, ^{130}Xe, ^{131}Xe, ^{132}Xe (26.9%), ^{134}Xe (10.4%), ^{136}Xe (8.9%)
- spin-dependent elastic scattering: ^{129}Xe (26.4%), ^{131}Xe (21.2%)
- inelastic WIMP-^{129}Xe and WIMP-^{131}Xe scatters $\chi +^{129,131} Xe \rightarrow \chi +^{129,131} Xe^* \rightarrow \chi +^{129,131} Xe + \gamma$

1 ns, 0.5 ns

40 keV, 80 keV

SI, elastic WIMP-nucleus

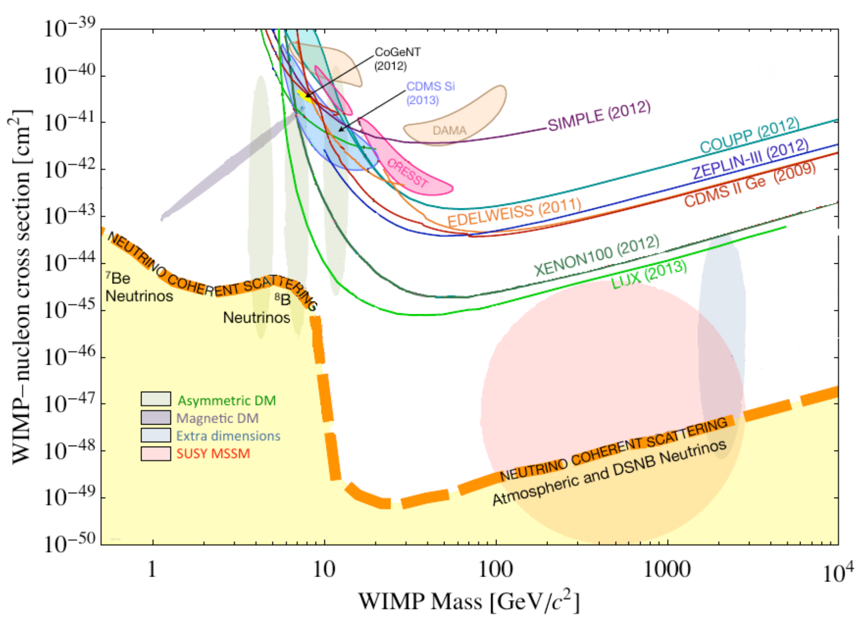

SD, elastic WIMP-nucleus

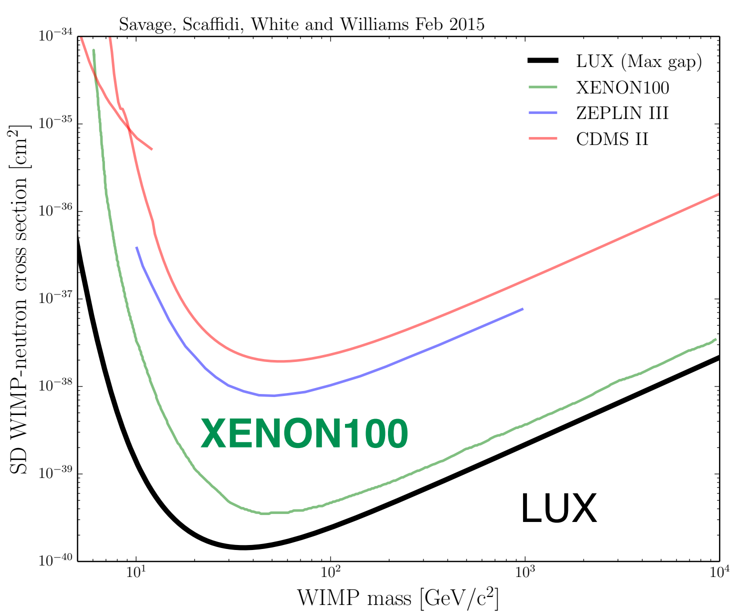

SD, inelastic WIMP-nucleus

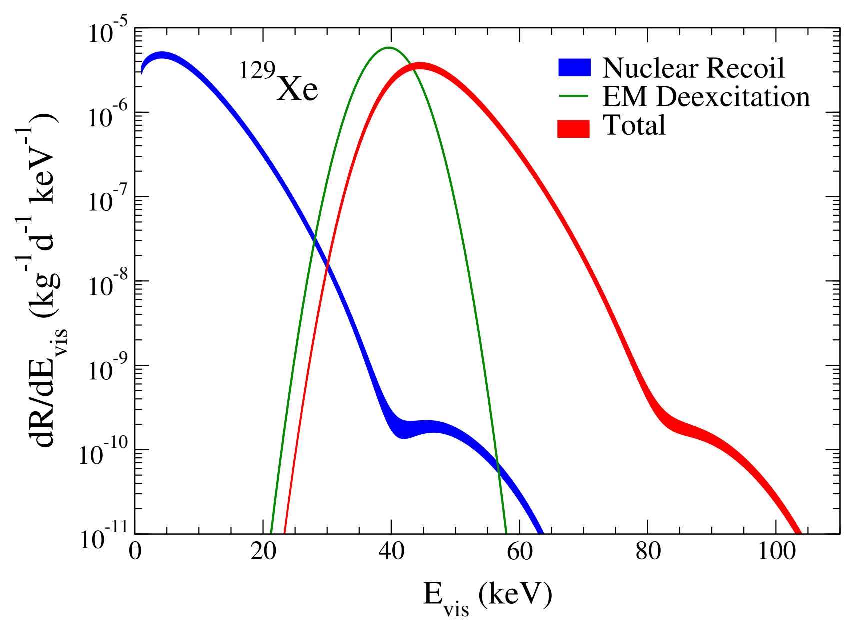

C. Savage et al, arXiv:1502.02667

L. Baudis et al, Phys. Rev. D 88, 115014 (2013)

Backgrounds: nuclear recoils

- **Radiogenic** goal: <7 x 10^{-4} events/(t y)
  - active LS veto around cryostat under study
- **Cosmogenic** (MC: 7.3 x 10^{-10} n/(cm^2 s) for E_n > 10 MeV)
  - <0.01 events/(t y) in XENON1T/nT shield
  - **<<0.003 events/(t y) in 14 m diameter water shield**
- **XENON1T muon veto performance must be improved by ~ a factor of 10 (very conservative)**
- Alternative: line the experimental hall with muon veto (multi-layered proportional tubes, as in Soudan Lab)

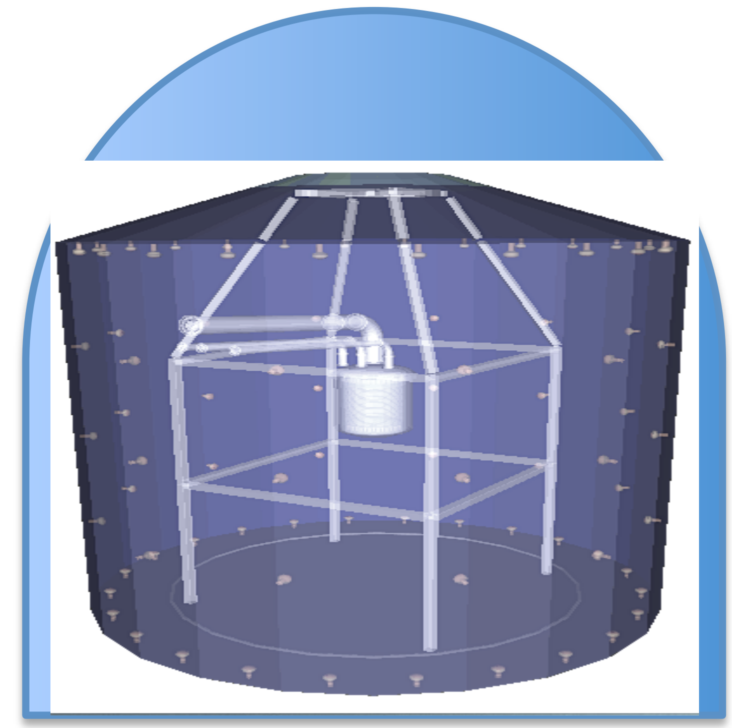

DARWIN-LXe in 14 m ø water Cherenkov shield

MC simulation for XENON1T

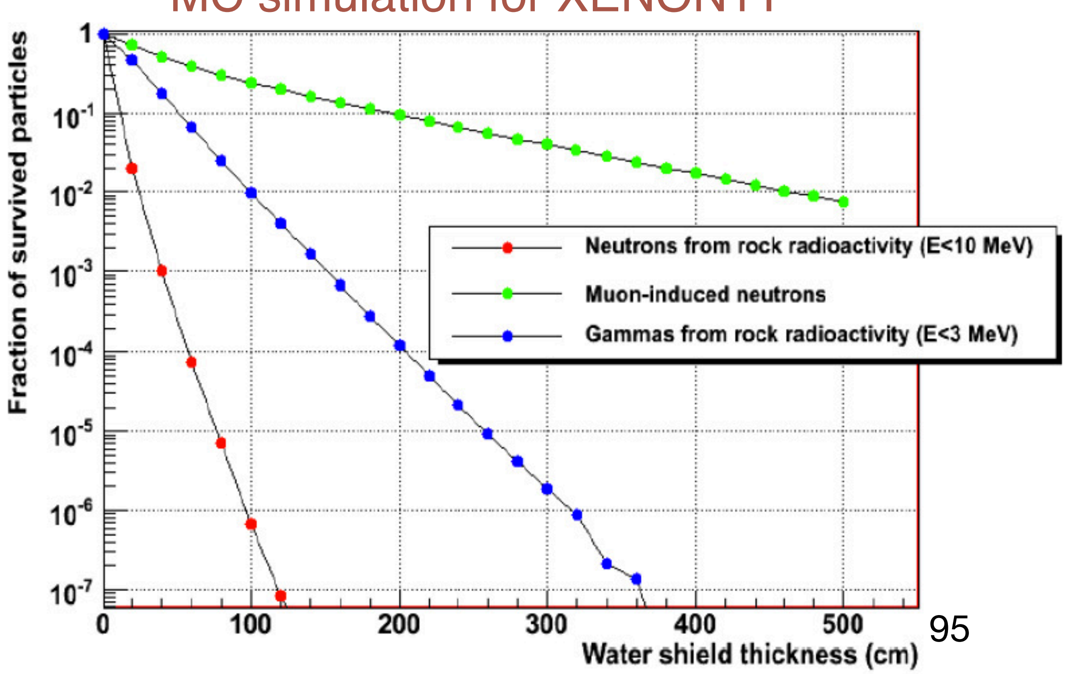

DARWIN backgrounds: electronic recoils

- Materials (cryostat, photosensors, TPC)
- ^{222}Rn in LXe: **0.1 μBq/kg (1 μBq/kg** => same background level as solar neutrinos)
- ^{nat}Kr in LXe: **0.1 ppt ^{nat}Kr (0.2 ppt ^{nat}Kr** => same background level as solar neutrinos)
- ^{136}Xe double beta decay
- Solar neutrinos (mostly pp, ^{7}Be)

Materials: strong self-shielding by dense LXe

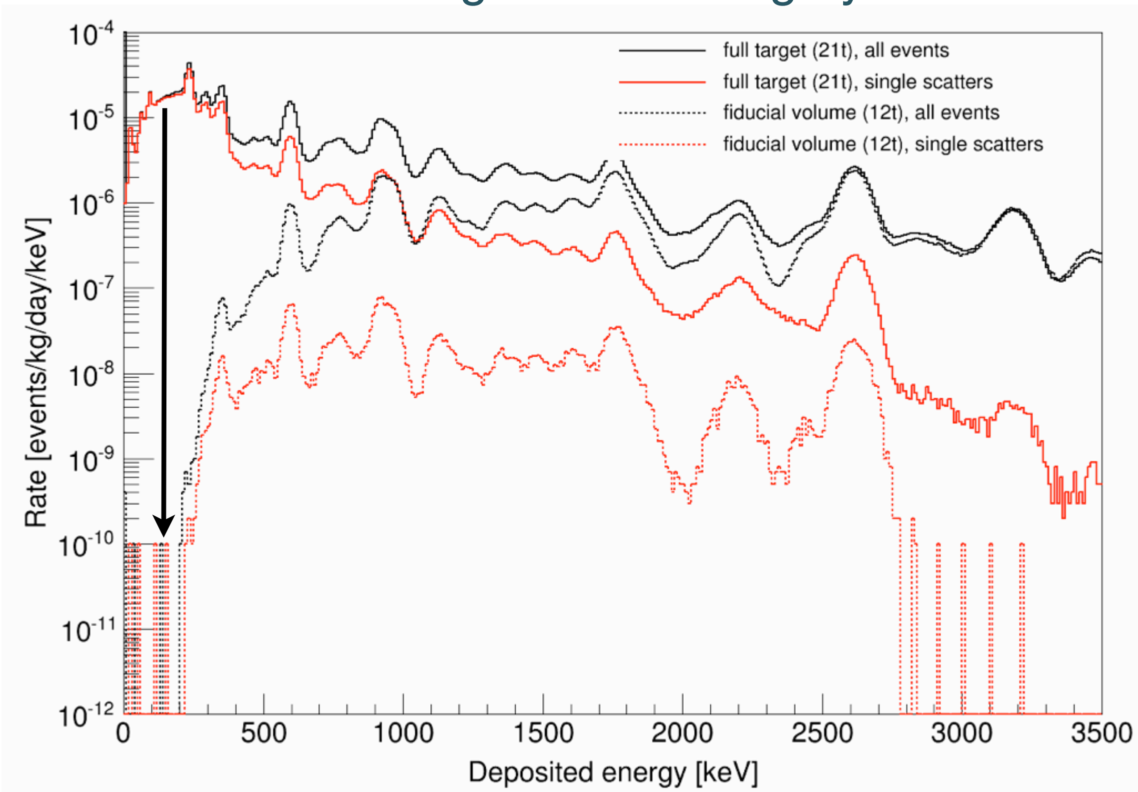

Channel	Before discr	After discr (99.98%)
pp + ^{7}Be neutrinos	95	0.488
Materials	1.4	0.007
^{85}Kr in LXe (0.1 ppt ^{nat}Kr)	40.4	0.192
^{222}Rn in LXe (0.1 μBq/kg)	9.9	0.047
^{136}Xe	56.1	0.036

1 t x yr exposure,
2-30 keVee

200 t x yr exposure
4-50 keVnr, 30% acceptance

DARWIN backgrounds: electronic recoils

- Materials (cryostat, photosensors, TPC)
- ^{222}Rn in LXe: **0.1 μBq/kg (1 μBq/kg** => same background level as solar neutrinos)
- ^{nat}Kr in LXe: **0.1 ppt ^{nat}Kr (0.2 ppt ^{nat}Kr** => same background level as solar neutrinos)
- ^{136}Xe double beta decay
- Solar neutrinos (mostly pp, ^{7}Be)

WIMPs and backgrounds

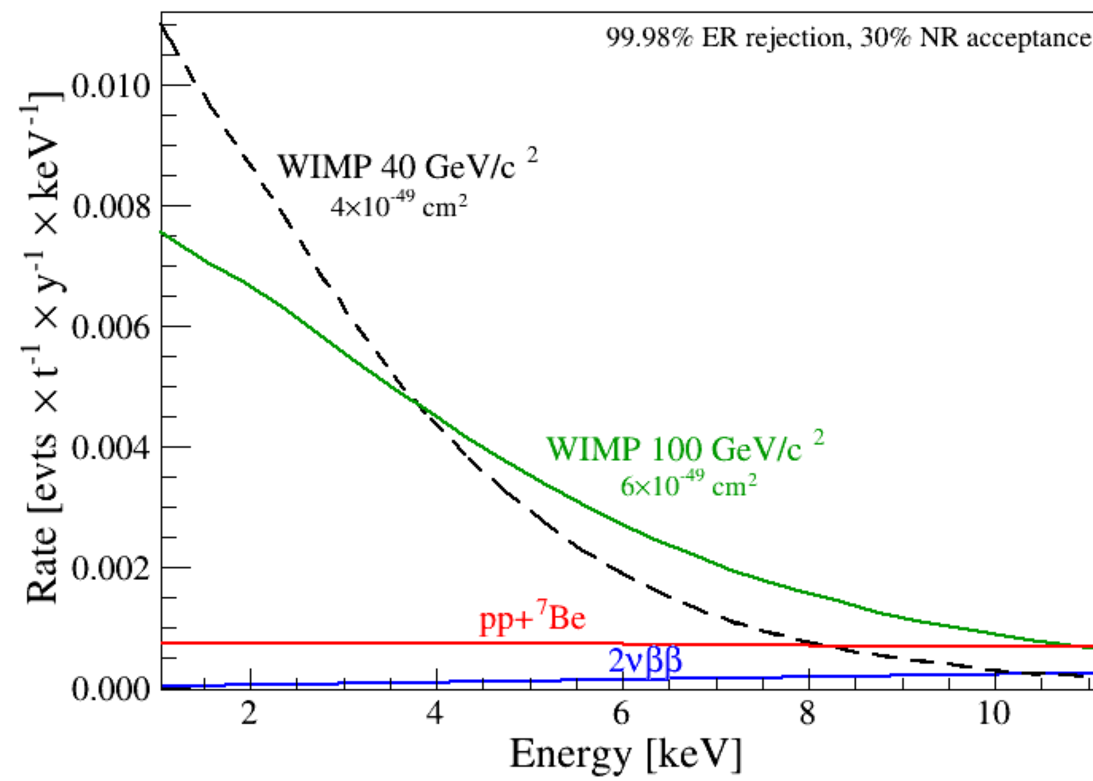

Channel	Before discr	After discr (99.98%)
pp + ^{7}Be neutrinos	95	0.488
Materials	1.4	0.007
^{85}Kr in LXe (0.1 ppt ^{nat}Kr)	40.4	0.192
^{222}Rn in LXe (0.1 μBq/kg)	9.9	0.047
^{136}Xe	56.1	0.036

1 t x yr exposure,
2-30 keVee

200 t x yr exposure
4-50 keVnr, 30% acceptance

WIMP physics: spectroscopy

- Capability to reconstruct the WIMP mass and cross section for various masses (**20, 100, 500 GeV/c²**) and a spin-independent cross section of 2×10^{-47} cm² (assuming different exposures)

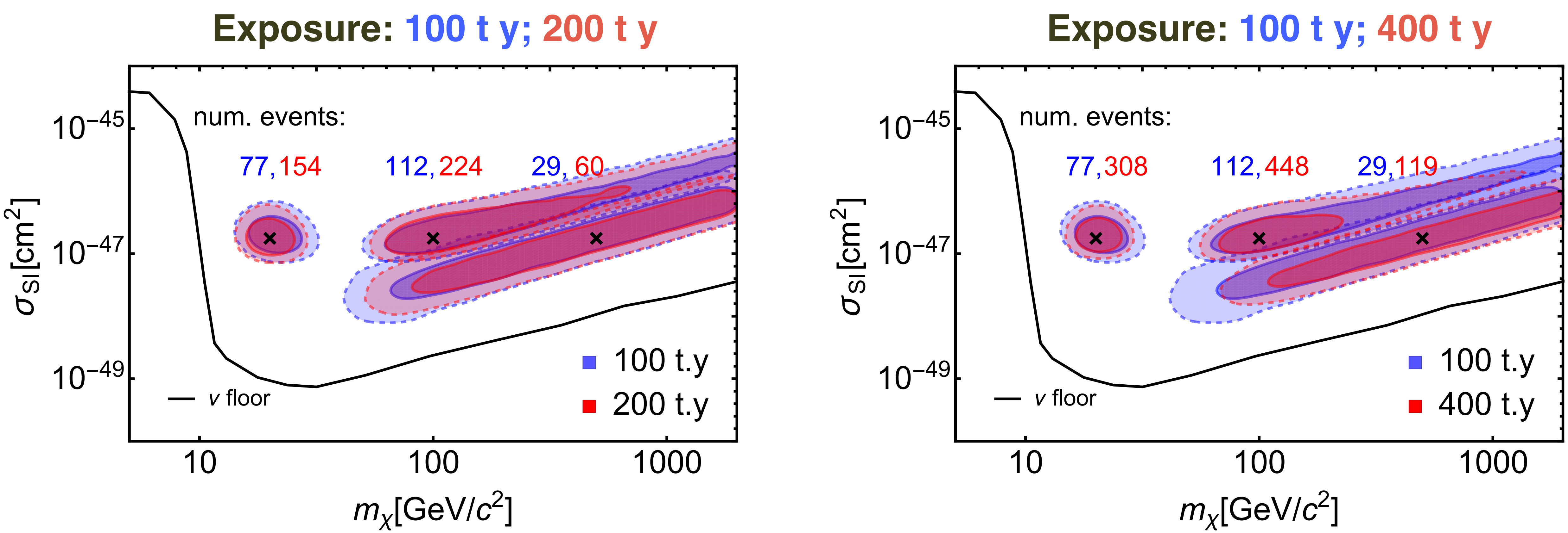

1 and 2 sigma credible regions after marginalizing the posterior probability distribution over:

$$v_{esc} = 544 \pm 40\,\mathrm{km/s}$$

$$v_0 = 220 \pm 20\,\mathrm{km/s}$$

$$\rho_\chi = 0.3 \pm 0.1\,\mathrm{GeV/cm^3}$$

Update: Newstead et al., PHYSICAL REVIEW D 88, 076011 (2013)

DARWIN WIMP sensitivity

- E = [5-35] keV_{nr}

99.98% discrimination, 30% NR acceptance, LY = 8 pe/keV at 122 keV

Spin-independent

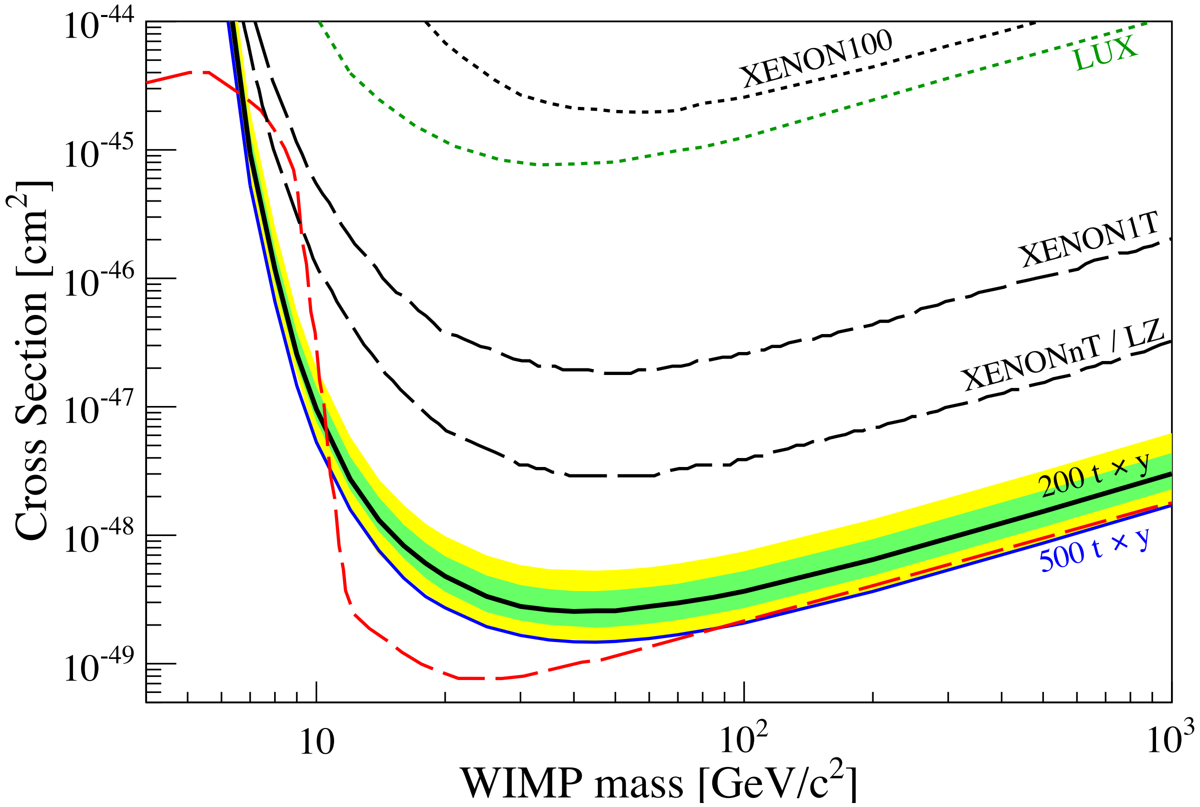

Spin-dependent

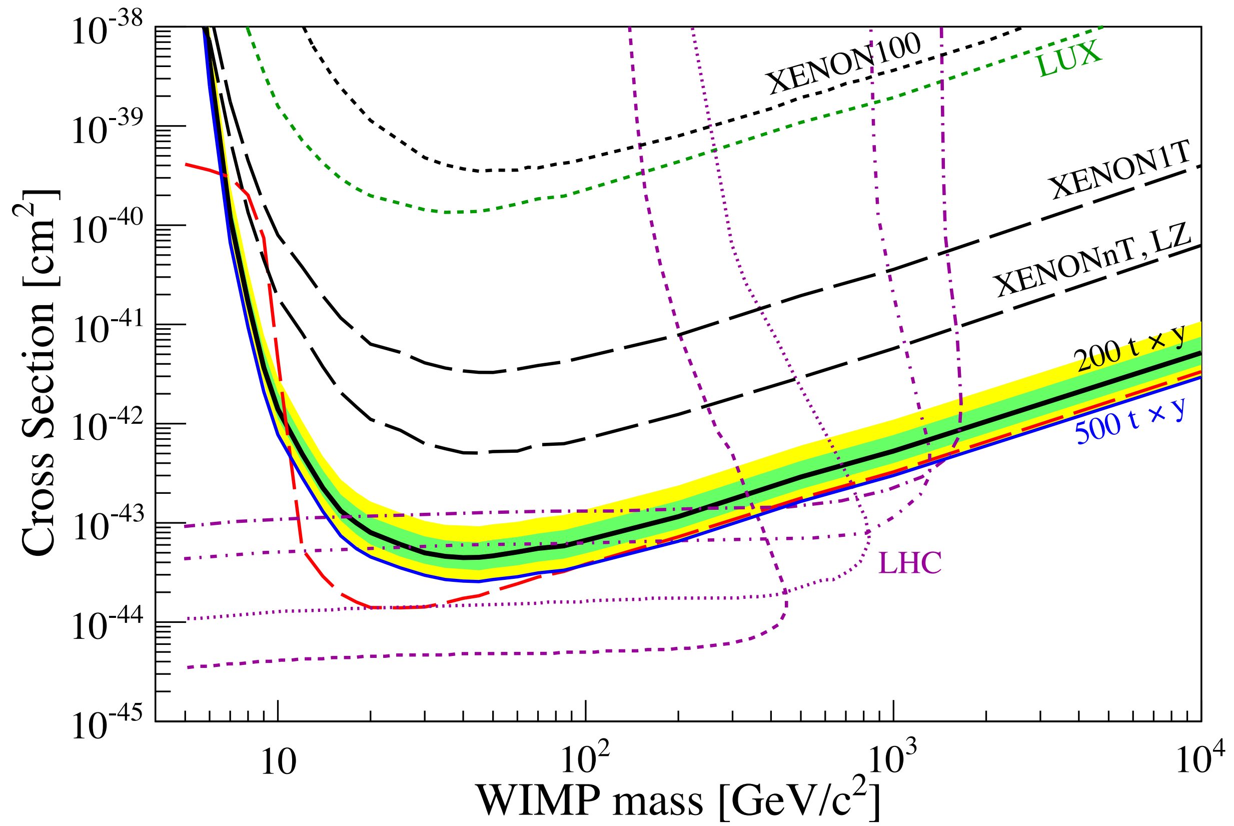

arXiv:1506.08309, JCAP 10 (2015) 016

Note: “nu floor” = 3-sigma detection line at 500 CNNS events above 4 keV

Accelerator searches

- **Minimal simplified DM model with only 4 variables: m_{DM}, M_{med}, g_{DM}, g_q**

- Here DM = Dirac fermion interacting with a vector or axial-vector mediator; equal-strength coupling to all active quark flavours

$$\sigma_{\mathrm{DD}} \propto \frac{g_{\mathrm{DM}}^2 g_q^2 \mu^2}{M_{\mathrm{med}}^4}$$

Spin independent

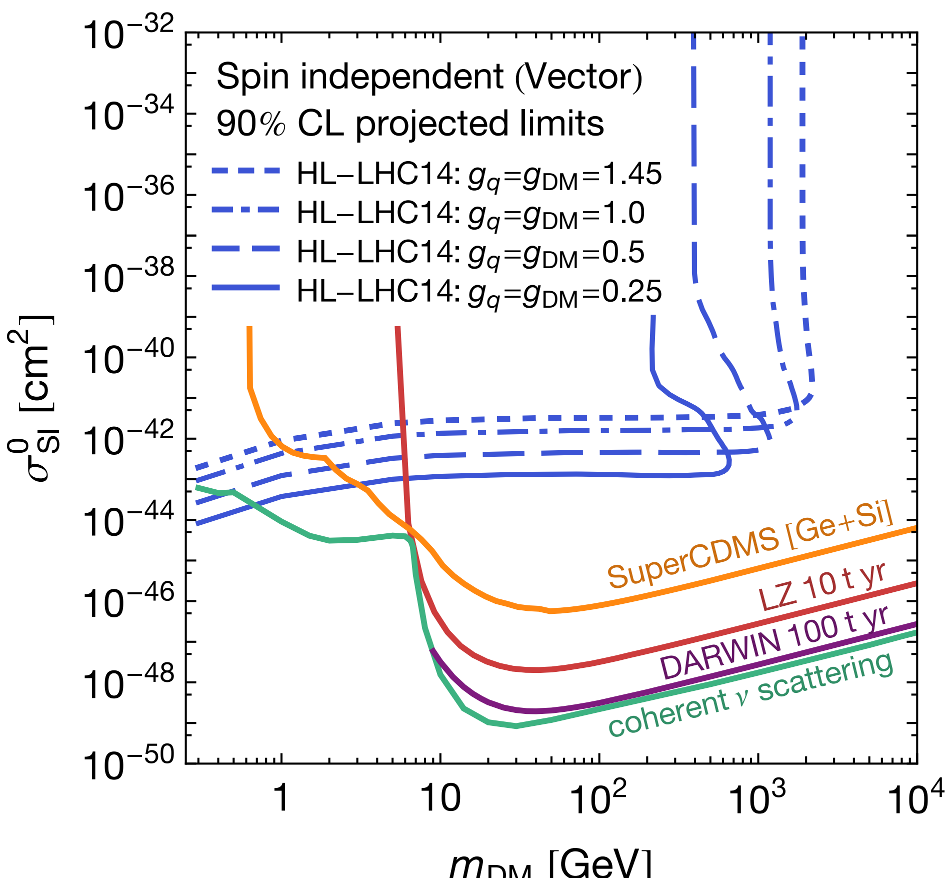

Spin dependent

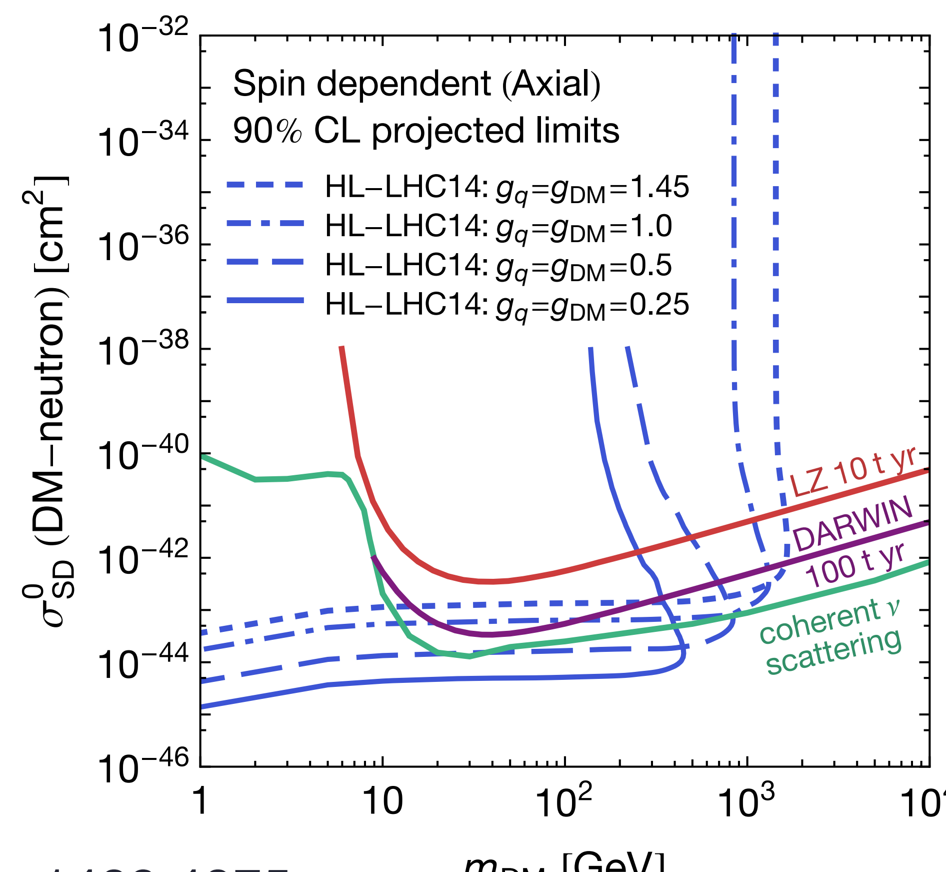

S. Malik et al., arXiv:1409.4075

Accelerator searches

- **Minimal simplified DM model with only 4 variables: m_{DM}, M_{med}, g_{DM}, gq**
- Here DM = Dirac fermion interacting with a vector or axial-vector mediator; equal-strength coupling to all active quark flavours

$$\sigma_{\mathrm{DD}} \propto \frac{g_{\mathrm{DM}}^2 g_q^2 \mu^2}{M_{\mathrm{med}}^4}$$

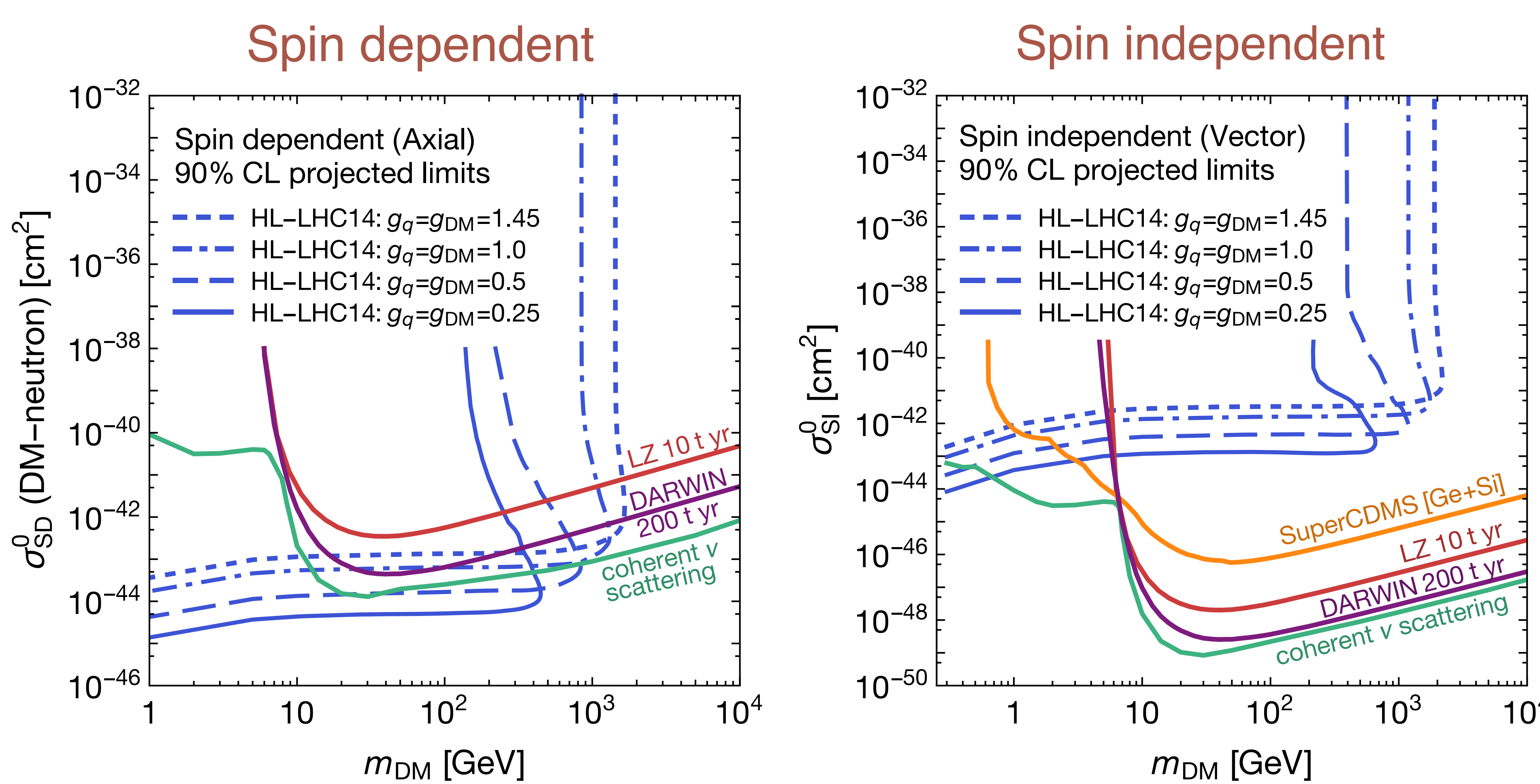

S. Malik et al., arXiv:1409.4075

WIMP-nucleon cross sections versus time

- About a factor of 10 increase every ~ 2 years
- Can we keep this rate of progress?

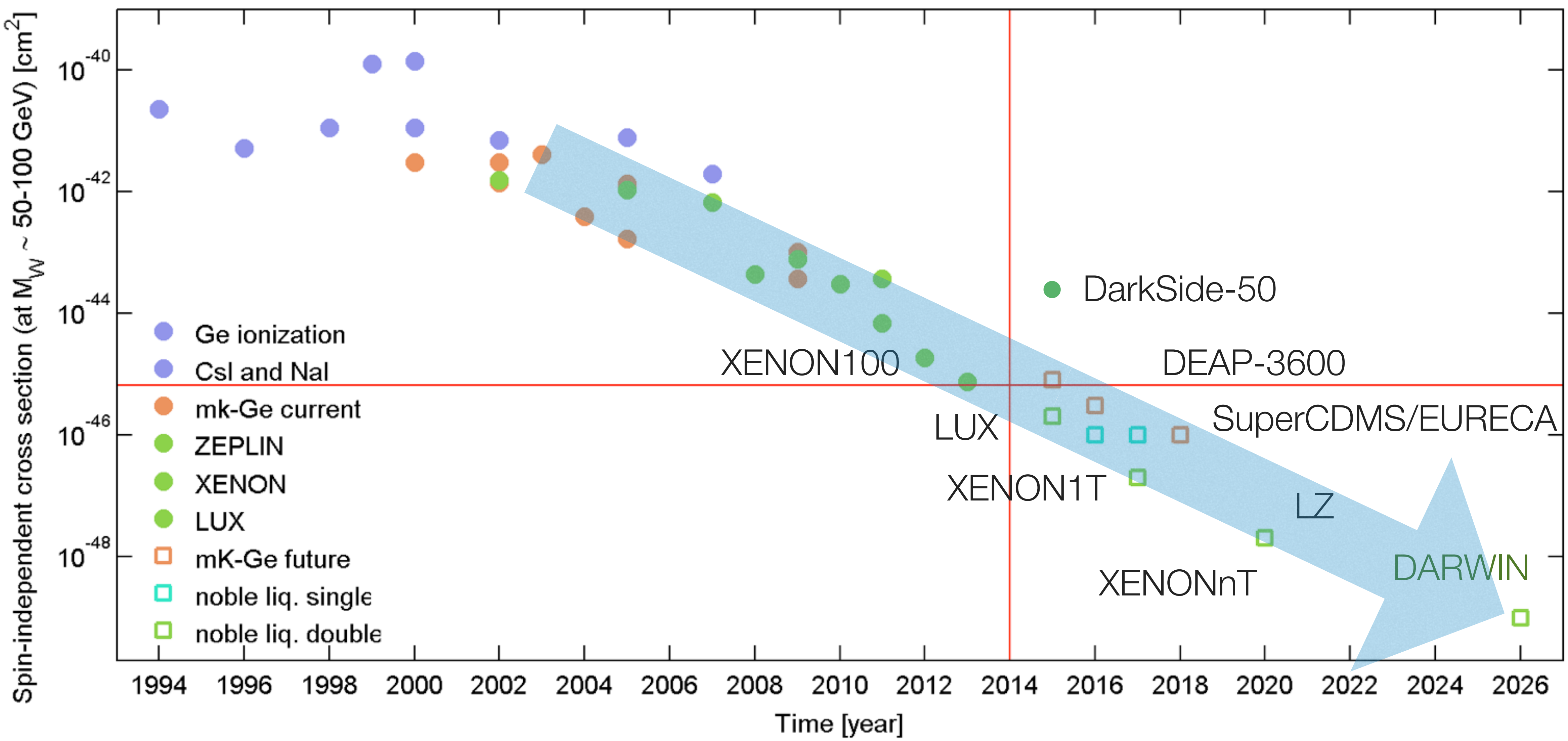

LB, Physics of the Dark Universe 4, 2014

Conclusions

Direct detection experiments have reached tremendous sensitivities

- probe cross sections down to 10^{-45} cm^2 at WIMP masses ~ 50 GeV
- probe particle masses below 10 GeV (new models)
- complementary with the LHC and with indirect searches
- test various other particle candidates

Excellent prospects for discovery

- increase in WIMP sensitivity by 2 orders of magnitude in the next few years
- reach neutrino background (measure neutrino-nucleus coherent scattering!) this/ next decade

The end

Of course, “the probability of success is difficult to estimate, but if we never search, the chance of success is zero”

G. Cocconi & P. Morrison, Nature, 1959

DARWIN technical challenge: backgrounds

- **ER dominance by solar neutrinos needs:**

  ➡low intrinsic levels of ^{85}Kr and ^{222}Rn

- **^{85}Kr: 0.1 ppt ^{nat}Kr (0.2 ppt ^{nat}Kr** => same background level as solar neutrinos)
  - **0.2 ppt is goal for XENON1T, factor 20 better than this already achieved by Münster group*: separation factor > 120000!)**

- **^{222}Rn: 0.1 µBq/kg (1 µBq/kg** => same background level as solar neutrinos)
  - **1 µBq/kg is goal for XENON1T): control Rn levels with low-emanation materials & cryogenic distillation (use different vapour pressure), adsorption**

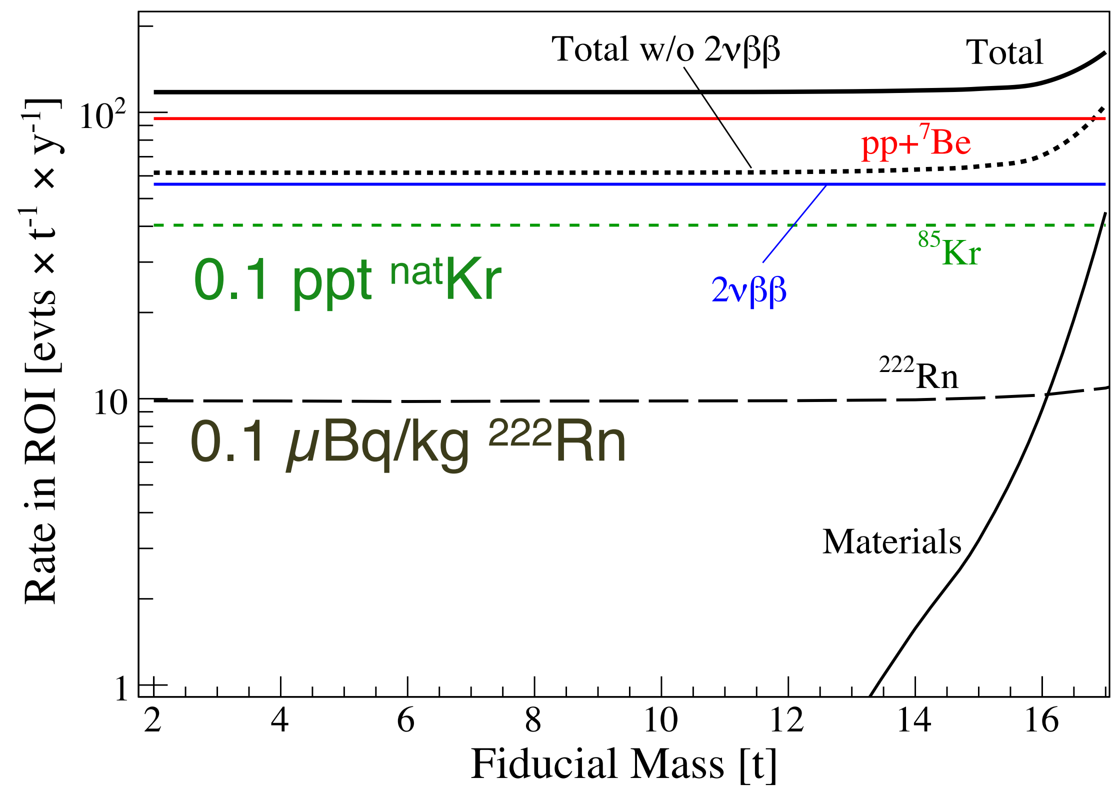

*Purified liquid out: ^{nat}Kr/Xe < 26e-15 = 26 ppq (90% CL); measured with MPIK RGMS system

Will directional information help?

- Yes, but mostly at low WIMP masses
- Directional detection techniques currently in R&D phase
- Would be very challenging to reach 10^{-48} - 10^{-49} cm^2 with these techniques

36.6 t yr exposure, 500 (solar) nu events

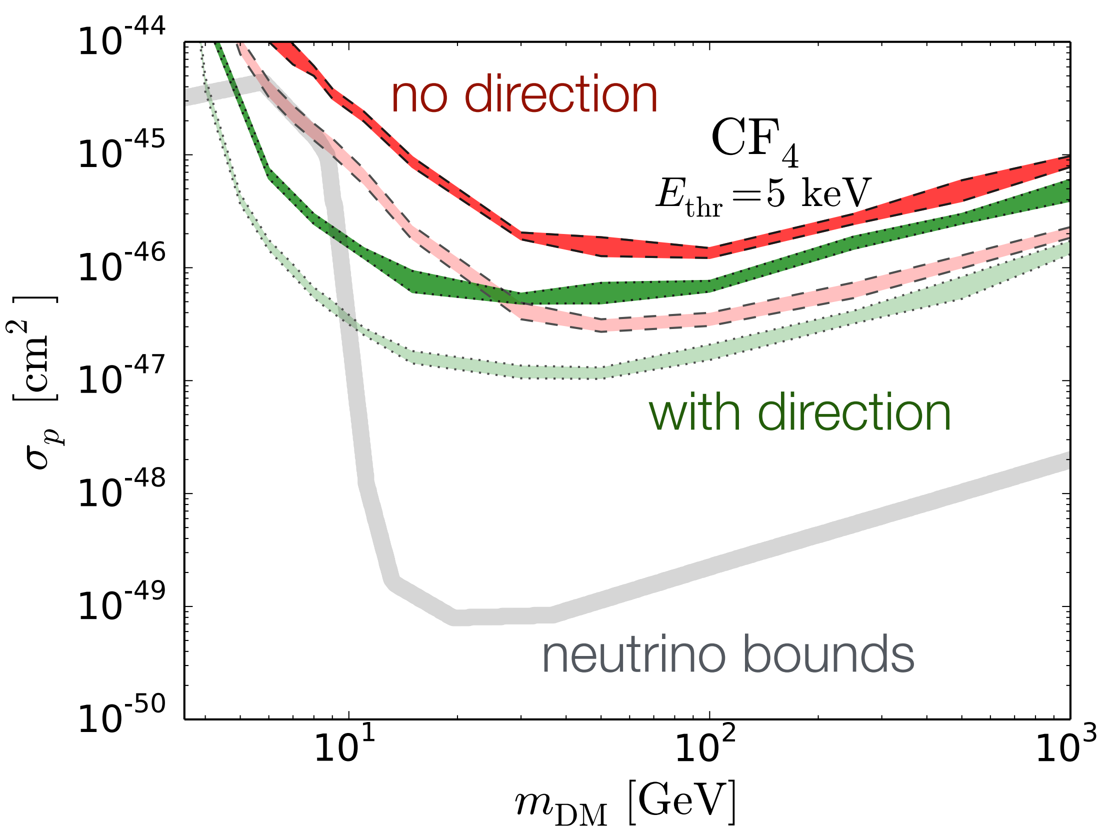

367 t yr exposure, 500 nu events

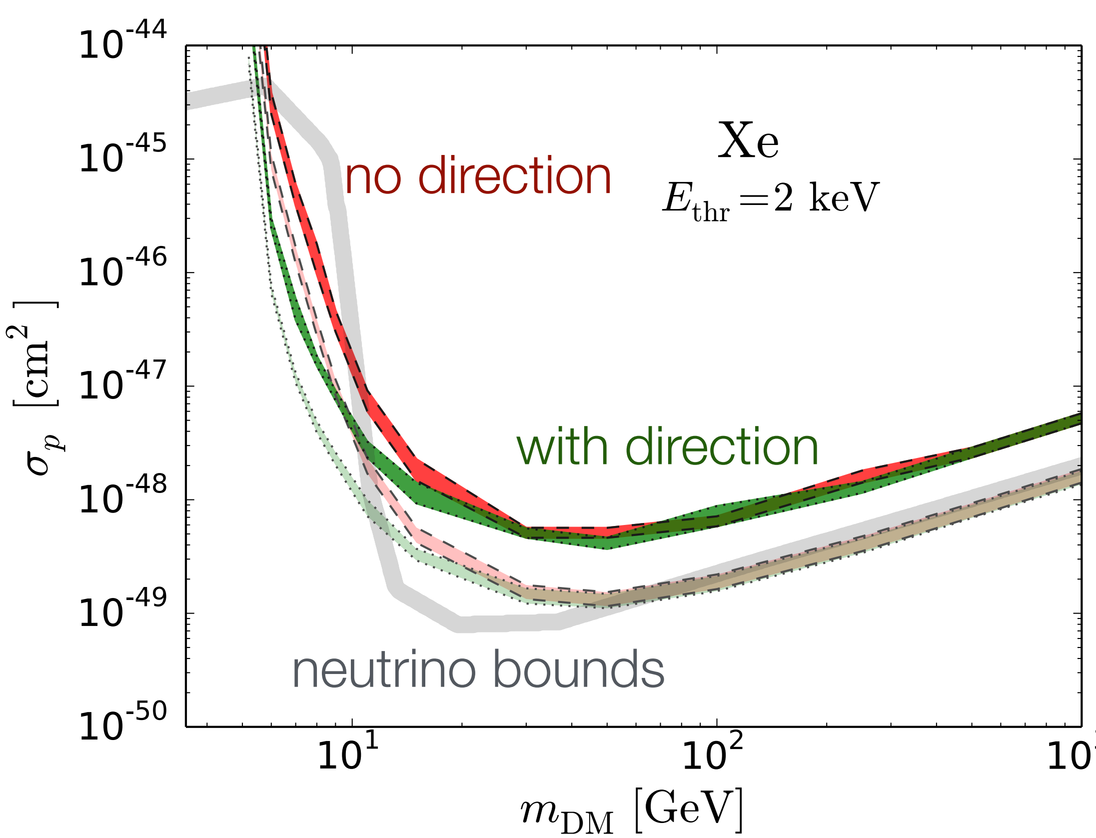

P. Grothaus, M. Fairbairn, J. Monroe, arXiv: 1406.5047

Complementarity DD, ID, LHC

CMSSM

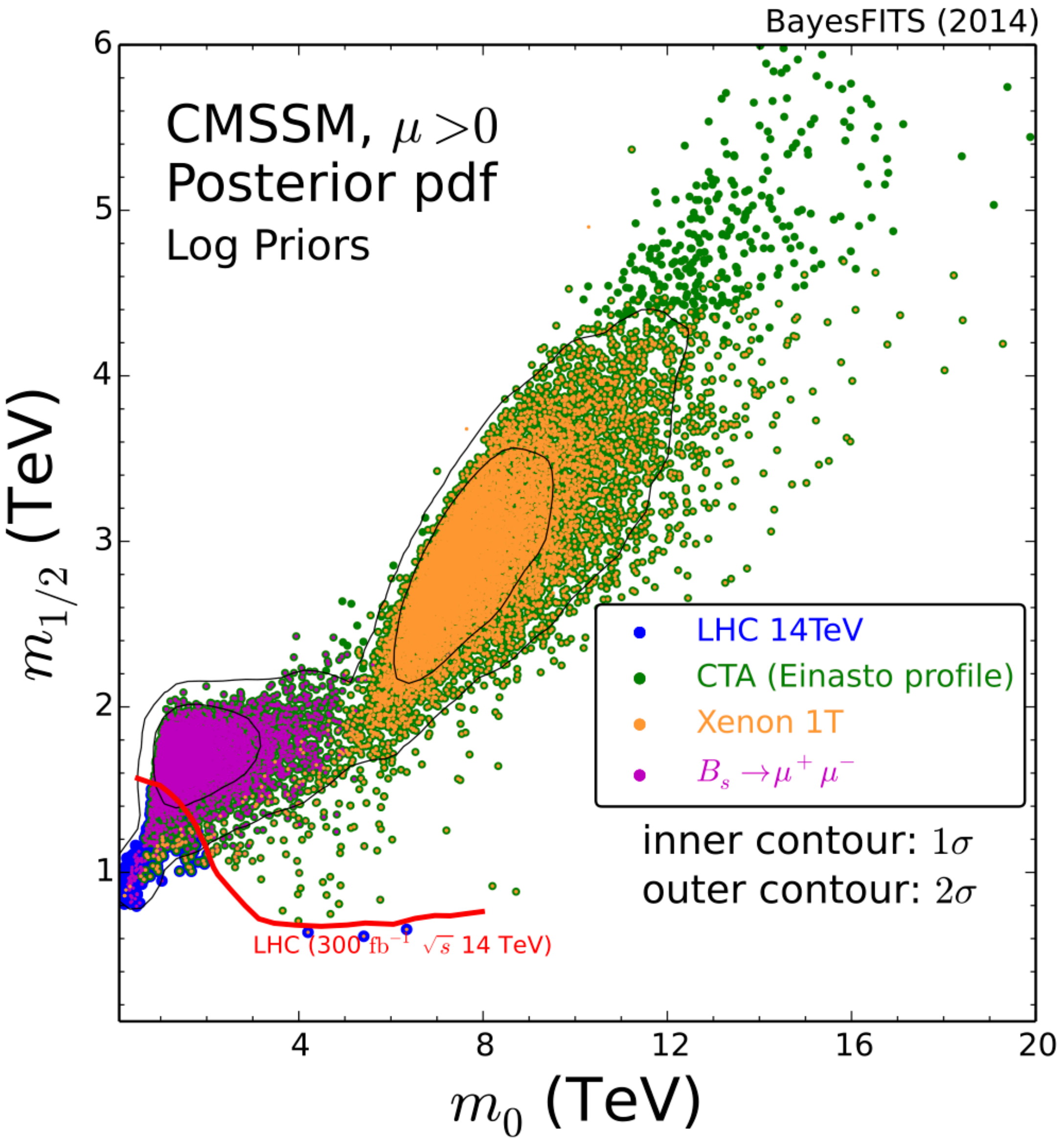

L. Rozkowski, Stockholm 2015

pMSSM

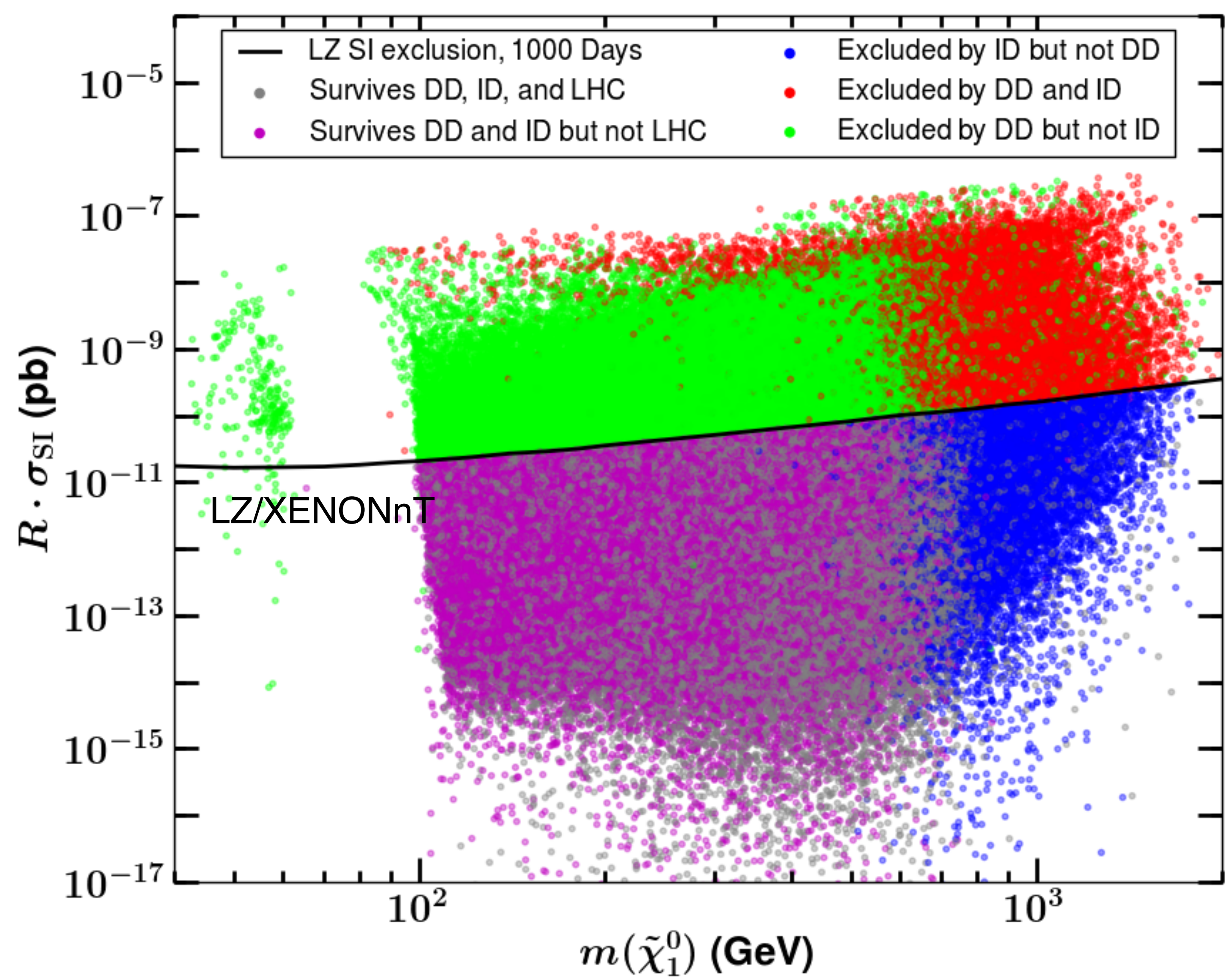

M. Cahill-Rowley, Phys.Rev. D91 (2015) 055011

Probing a modulation signal in XENON100

- Unbinned PL analysis of ER data assuming periodic signal hypothesis (L_1)

Acceptance

Background from known air leak

Modulation

$$f(t) = \epsilon(t)\left(C + Kt + A\cos\left(2\pi\frac{(t-\phi)}{P}\right)\right)$$

Normalized

$$\mathcal{L} = \left(\prod_{i=1}^{n}\tilde{f}(t_i)\right)\mathrm{Poiss}\left(n|N_{\mathrm{exp}}(E)\right)\underbrace{\mathcal{L}_\epsilon\mathcal{L}_K\mathcal{L}_E}_{\text{Constraint terms}}$$

Total observed events

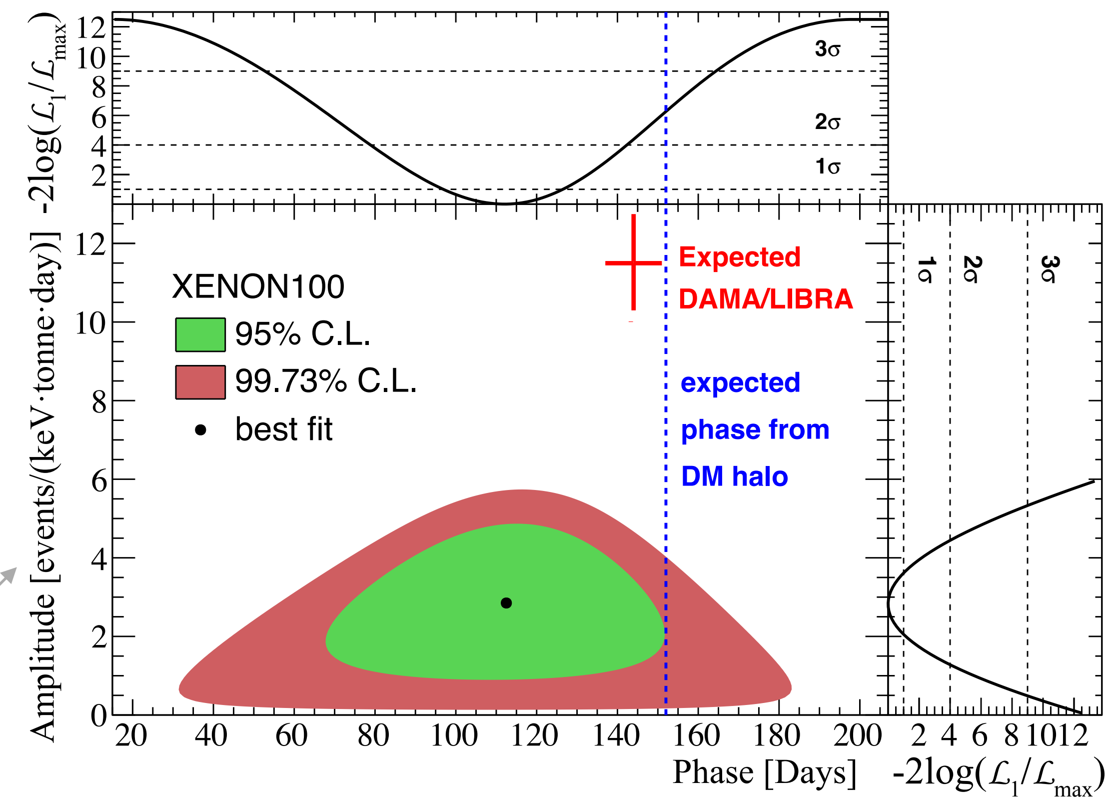

- Compare to maximum likelihood (L_{max}), fixing period to 1 year

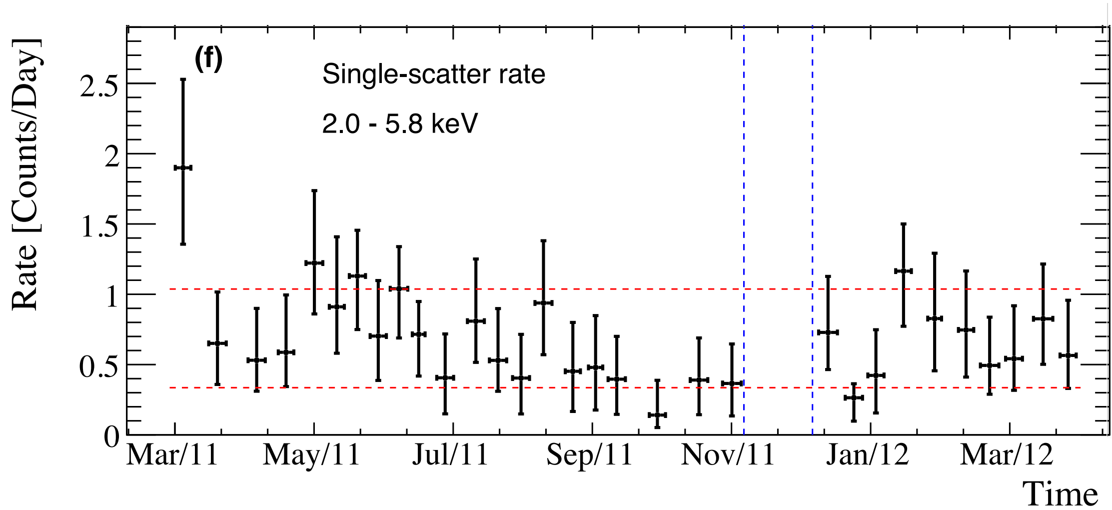

- Standard dark matter halo phase is disfavoured by 2.5-sigma

- Assuming V-A coupling of WIMPs to e^-, DAMA/LIBRA annual modulation is excluded at 4.8-sigma

Example: Solar axions with XENON100

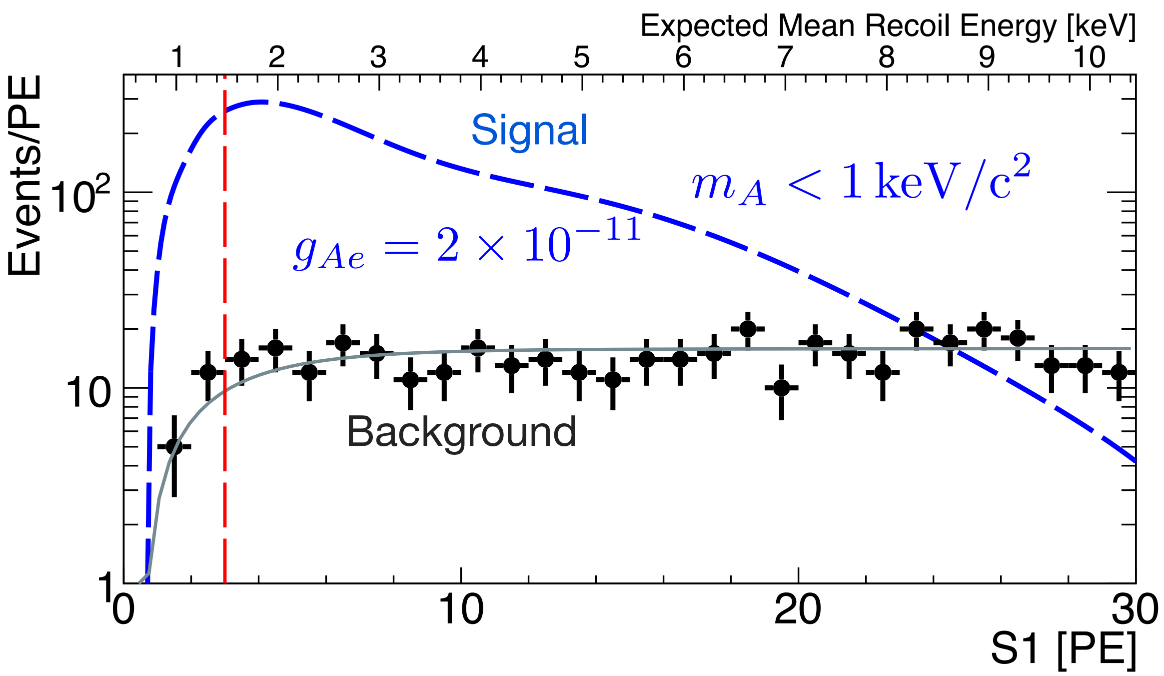

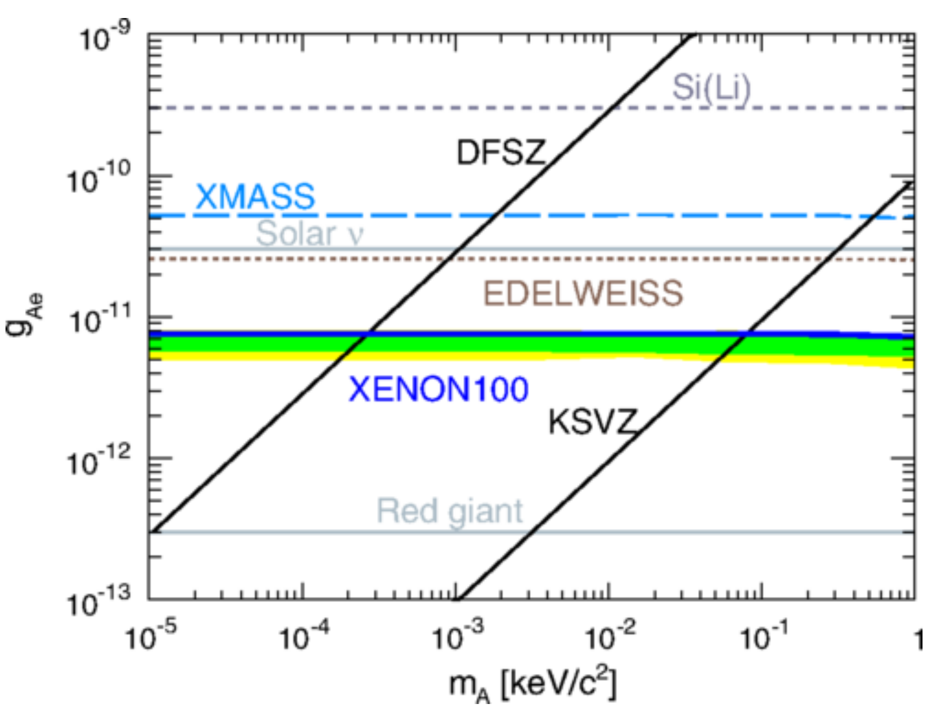

Look for solar axions via their couplings to electrons, g_{Ae}, through the axio-electric effect

$$\sigma_{Ae} = \sigma_{pe}(E_A)\frac{g_{Ae}^2}{\beta_A}\frac{3E_A^2}{16\pi\alpha_{em}m_e^2}\left(1-\frac{\beta_A^{2/3}}{3}\right)$$

$$\phi_A \propto g_{Ae}^2 \Longrightarrow R \propto g_{Ae}^4$$

- XEON100: based on 224.6 live days x 34 kg exposure; using the electronic-recoil spectrum, and measured light yield for low-energy ERs (LB et al., PRD 87, 2013; arXiv:1303.6891)

XENON, Phys. Rev. D 90, 062009 (2014)

Example: Galactic axion-like particles with XENON100

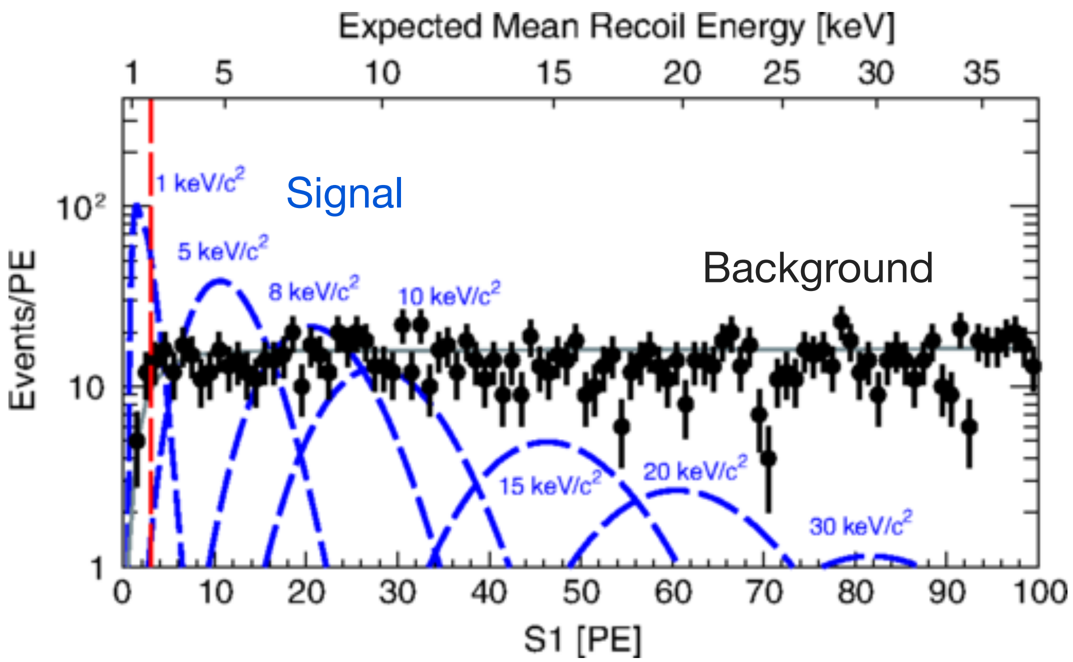

XENON, Phys. Rev. D 90, 062009 (2014)

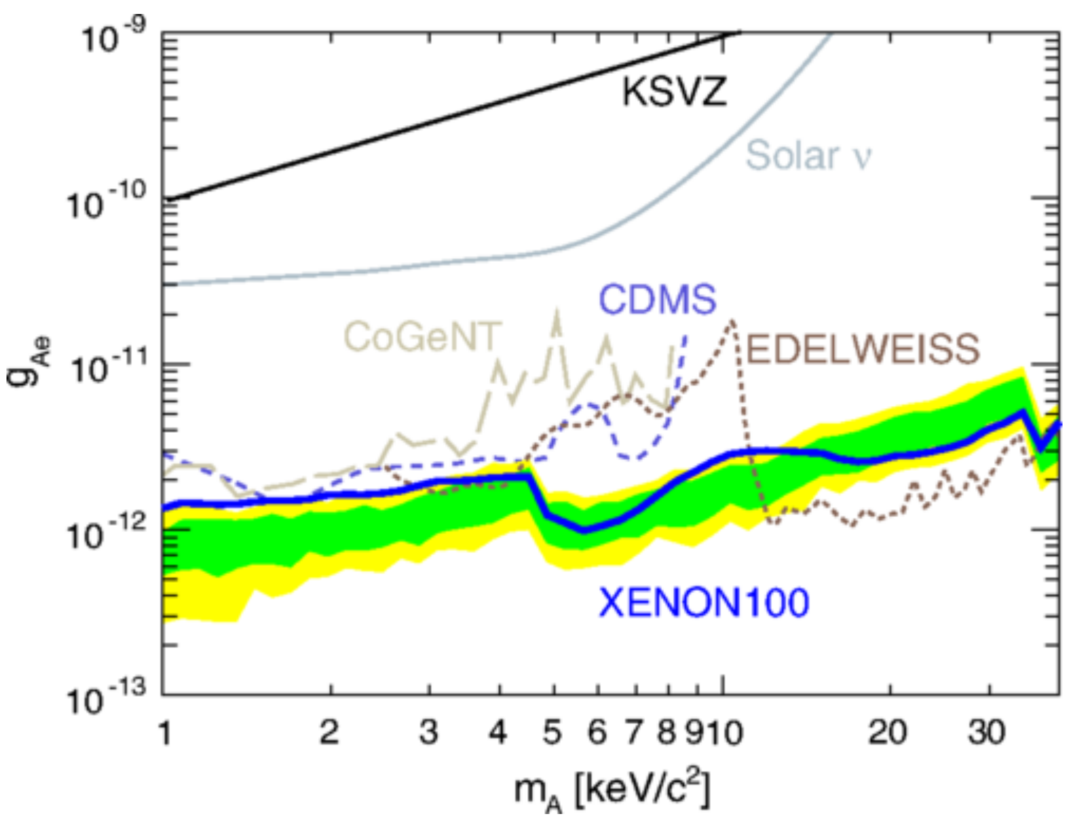

Look for ALPs via their couplings to electrons, g_{Ae}, through the axio-electric effect

Expect line feature at ALP mass

Assume $\rho_0 = 0.3\,\mathrm{GeV/cm^3}$

$$\phi_A = c\beta_A \times \frac{\rho_0}{m_A}$$

$$R \propto g_{Ae}^2$$

- XEON100: based on 224.6 live days x 34 kg exposure; using the electronic-recoil spectrum, and measured light yield for low-energy ERs (LB et al., PRD 87, 2013; arXiv:1303.6891)

XENON, Phys. Rev. D 90, 062009 (2014)

What is the origin of the DAMA signal?

Possible explanation: **a combination of neutrinos and muons**

Solar ^{8}B neutrino- and atmospheric muon-induced neutrons

Combined phase of muon and neutrino components: good fit to the data*

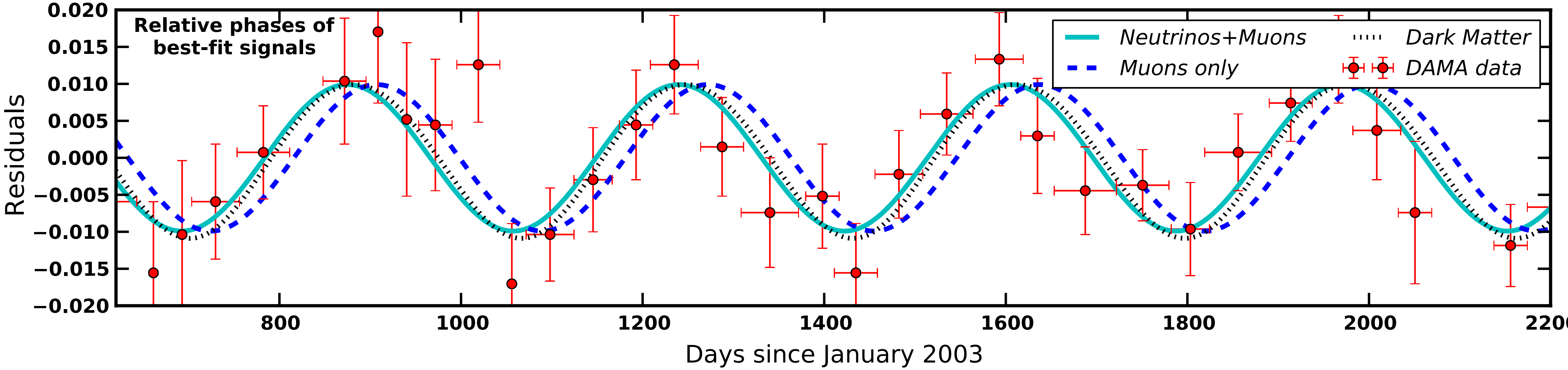

Jonathan Davis, PRL 113, 081302 (2014)

*Muons: flux correlated with T of atmosphere; period is ok but phase is 30 d too late
*Neutrinos: flux varies with the Sun-Earth distance; period is ok but phase peaks in early Jan

The DAMA/LIBRA Experiment

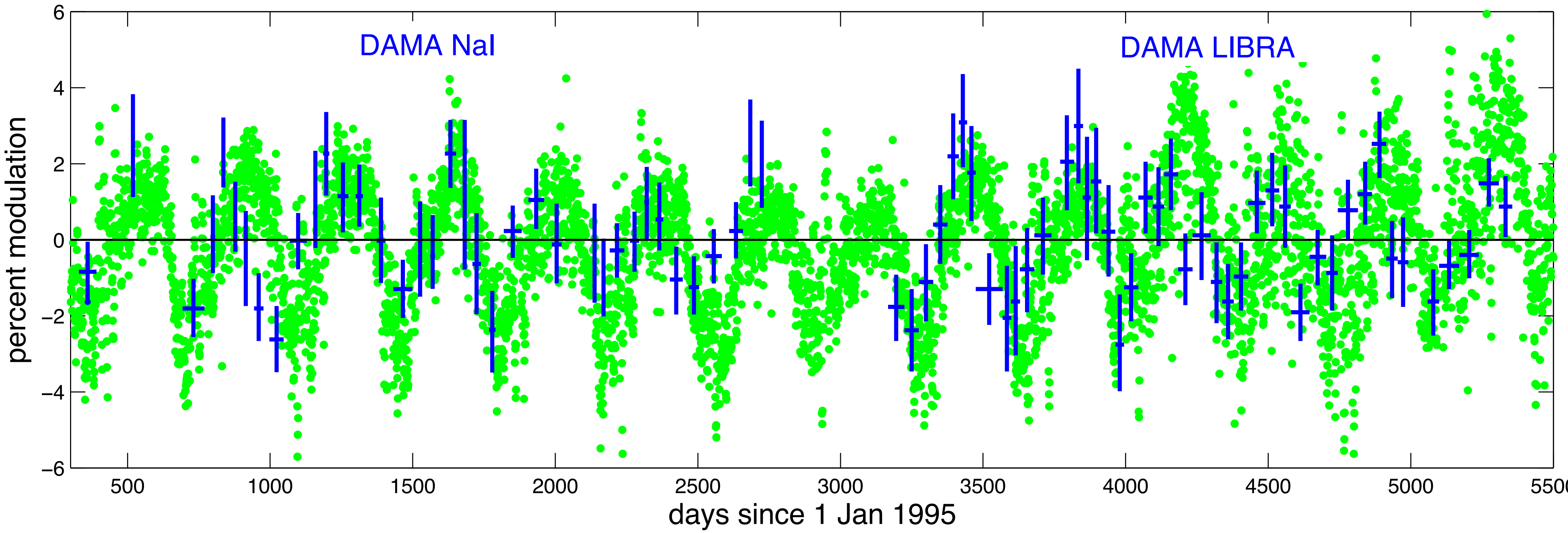

Figure 6: DAMA residuals (blue) and stratospheric temperature residuals $\Delta T_{eff}/T_{eff}$ (green), in percent from the respective baselines.

Kfir Blum, arXiv:1110.0857

The DAMA/LIBRA Experiment

- Annual modulation: significance is 9-sigma; 1 - 2% effect in bin count rate
- The effect appears only in lowest energy bins
- The origin of the time variation in the observed rate is still unclear
  - ➡ motion of the Earth-Sun system through the WIMP halo?
  - ➡ environmental effects?
  - ➡ other observables (muon flux, temperature, radon levels etc) vary with the season

see also David Nygren, arXiv:1102.0815 and Kfir Blum, arXiv:1110.0857